

*ELUCIDATING TCF7 AND TCF7L1
FUNCTIONS AND GENE REGULATORY
MECHANISMS IN MOUSE EMBRYONIC STEM
CELLS*

**ELUCIDATING TCF7 AND TCF7L1 FUNCTIONS AND
GENE REGULATORY MECHANISMS IN MOUSE
EMBRYONIC STEM CELLS**

BY

STEVEN MOREIRA, BSc (Honours)

A dissertation submitted to the School of Graduate Studies in
partial fulfilment of the requirements for the degree of Doctor of
Philosophy

McMaster University

Copyright© by Steven Moreira, December 2018

DESCRIPTIVE NOTE

DOCTOR OF PHILOSOPHY (2018) (Biochemistry and Biomedical Sciences)

McMaster University, Hamilton, Ontario Canada

TITLE: Elucidating TCF7 and TCF7L1 Functions and Gene Regulatory
Mechanisms in Mouse Embryonic Stem Cells

AUTHOR: Steven Moreira

SUPERVISOR: Dr. Bradley Doble

NUMBER OF PAGES: 272

LAY ABSTRACT

Stem cells are capable of giving rise to multiple different cell types and thus are able to generate all adult tissues. The identity of a cell is controlled by external signals that regulate internal programs encoded by our genes. The execution of the instructions in genetic programs is conducted by proteins called transcription factors that can turn different genes on or off, giving rise to distinct cell types. The T-Cell Factors and Lymphoid Enhancer Factor (TCF/LEFs) are a family of four transcription factors regulated by external signaling molecules called Wnts. By using the TCF/LEFs, Wnts establish gene outputs that determine the identity of cells throughout embryonic development and in adult tissues. However, the mechanisms used by this family of transcription factors to establish the programs controlling cellular identity remain poorly understood. Using genetically engineered mouse embryonic stem cells, we have uncovered new information about the mechanisms TCF/LEFs use to regulate gene function, identified programs controlled by TCF/LEFs, and discovered potential protein partners that work with TCF/LEFs to implement genetic programs. This thesis provides novel insights into the control of cell identity by the TCF/LEFs, which has implications for the numerous human diseases linked to abnormal Wnt-mediated signaling.

ABSTRACT

Wnt signaling regulates critical cellular interactions throughout normal development and directs cell fate decisions of stem cells. Previous work by our lab implicates β -catenin as an essential modulator of embryonic stem cell self-renewal and differentiation. Genetic studies in mice have demonstrated broad functional redundancies between the most downstream effectors of the Wnt signaling cascade, the T-cell factor / Lymphoid enhancer factor (TCF/LEF) family of transcription factors. Despite this, loss-of-function experiments suggest that β -catenin reinforces the pluripotent state by mediating a TCF switch in which repressive TCF7L1 is replaced with activating TCF7. However, these experiments do not account for potential confounding functional compensation by other TCF/LEF factors. As such, *I hypothesized that TCF7 and TCF7L1 are functionally redundant in mouse embryonic stem cells and bind a largely overlapping set of target genes and interacting proteins.*

In support of this notion, we demonstrated that both TCF7 and TCF7L1 were similarly able to restore the altered transcriptomic profile and differentiation deficits observed in mouse embryonic stem cells (mESCs) lacking all full-length TCF/LEFs. With the expectation that TCF7 and TCF7L1 recruit similar transcriptional co-regulators to a broadly overlapping set of target genes, we employed the unbiased techniques, ChIP-seq and BioID to test our hypothesis. We observed that regardless of the degree of Wnt signaling activity, TCF7L1 was more abundantly associated with chromatin than TCF7, and TCF7 and TCF7L1 regulate distinct target genes. We demonstrated that Wnt stimulation, simulated by GSK-3 inhibition, facilitates TCF7L1 interactions with transcriptional modulators such as the BAF and nuclear receptor co-repressor complexes, despite a reduction in TCF7L1 levels. Taken together, the work in this thesis provides new insights into the mechanisms of Wnt target gene regulation by the TCF/LEF factors.

ACKNOWLEDGEMENTS

First and foremost, I must thank my amazing supervisor Dr. Bradley Doble. I don't think I could've made it this far without him! Brad has been incredibly patient with me through this long journey of mine. When I began my graduate studies, I was unfocused and unsure of how to best carry out my project. But Brad allowed me to make mistakes and discover, under his guidance, how to think critically and troubleshoot any problem that came my way. Brad also encouraged me to use new techniques and technologies, which at times made me feel like the guinea pig, but in the end worked out for the best, as I got to learn and master many new cool things that will help me in the long term! Brad has also been instrumental in helping me hone my presentation skills and made me a much more confident public speaker. For all of this I am grateful, as I was able to learn a lot about science, but more importantly myself. I'll always appreciate Brad's open-door policy, in which he demonstrated that he knew pretty much everything when it came to science and technology. I wish you nothing but success in the future Brad!

Secondly, I would like to thank both of my committee members Dr. Juliet Daniel and Dr. Jonathan Draper for new perspectives and insights into my research and life over the past 7 years. I appreciate both of you for not giving me too much grief over my often-late reports or last-minute committee meetings! Thank you both for being a part of my graduate studies and I wish you both good luck!

I would also like to thank current and past members of the Doble lab. Dr. Kevin Kelly, thank you for making me feel welcomed and being so nice to me during my interview. You left too early!! Sweet Debbie Ng, thanks for training me for those first few months and helping me with BioID. Sujeivan Mahendram, thanks for being my partner in crime for the first two years as master's students, I'll always appreciate your company during those late nights in the lab. Enio Polena, I owe you a lot as your work in creating the QKOs was critical! I realized how efficiently you made the lab run after you left! Victor Gordon, thank you for counting all of those beating EBs so I didn't have too and thanks for letting me live with you! Caleb Seo, thanks for the last-minute help with experiments while I wrote my thesis! Smarth we still need to play ball sometime. To all the Doble lab undergrads that I have mentored and have helped me with my projects, thank you!

To my student and post-doc support team, thanks for keeping me sane and for all the fun times: Kyle, Ryan, Rami, Stefan, Lili, Sonam, Nick Holzapfel, Vicki, Brianna, Jen, Deanna, Diana, David, Derek, Nadeem, Ava, Neil, Yannick, Borko, Lucha, Brendan, Saleem, Rohan, J.H., J.B., Borhane, Mio, and Branavan. Thank you to my friends Tarek, Omar and Nick Green for the good times. A special thanks to Mohini Singh, Nick Yelle and Michelle Ly for being my thesis writing support team, encouraging me when I doubted myself or taking me out for some much-needed fun! Finally, another special thank you to Ana Vujovic for your support and reassuring me that I could finish, throughout the preparation of my thesis. Getting to know you this summer was nice and without your quirky sense of humour, I would have been much more stressed out!

To my family: Mom, Dad and Sophia. I did it! I wouldn't have even been able to have even started any of this without the support of my loving and amazing family. Thank you to my parents for your continued unwavering support. Mom and Dad, you help me in every way possible whether it is emotionally, financially, or making the best food. Although at times I let my stress get the better of me and I may not show it, I love and appreciate you both! Sophia thank you for being the best sister and supporting me through all the difficult times. I hope I have been there for you too!

TABLE OF CONTENTS

DESCRIPTIVE NOTE	III
LAY ABSTRACT	IV
ABSTRACT	V
ACKNOWLEDGEMENTS.....	VI
TABLE OF CONTENTS	VII
LIST OF TABLES.....	XI
LIST OF FIGURES.....	XII
LIST OF ABBREVIATIONS AND ACRONYMS.....	XV
LIST OF APPENDICES.....	XVII
CHAPTER 1 INTRODUCTION	18
1.0 PREAMBLE	18
1.1 THE WNT/ β -CATENIN SIGNALING PATHWAY.....	18
1.2 T-CELL FACTORS AND LYMPHOID ENHANCER FACTOR: THE NUCLEAR EFFECTORS OF THE WNT/ β -CATENIN PATHWAY .	22
1.3 THE ROLE OF WNT SIGNALING AND THE TCF/LEFs IN MOUSE DEVELOPMENT.....	29
1.3.0 <i>Wnt</i> signaling is required for primitive streak formation and gastrulation.....	29
1.3.1 <i>TCF/LEF</i> factors in mouse development	30
1.4 REGULATION OF EMBRYONIC STEM CELL PROPERTIES BY WNT SIGNALING AND THE TCF/LEF FACTORS.....	40
1.4.0 <i>Embryonic stem cells</i>	40
1.4.1 <i>Naïve and primed states of pluripotency</i>	41
1.4.2 <i>The core pluripotency transcriptional network</i>	43
1.4.3 <i>Wnt</i> signaling in ESC self-renewal and pluripotency	45
1.4.4 <i>TCF/LEF</i> regulation of ESC self-renewal and pluripotency.....	52
SUMMARY OF INTENT	61

CHAPTER 2.....	67
A SINGLE TCF TRANSCRIPTION FACTOR, REGARDLESS OF ITS ACTIVATION CAPACITY, IS SUFFICIENT FOR EFFECTIVE TRILINEAGE DIFFERENTIATION OF ES CELLS.....	67
PREAMBLE.....	67
SUMMARY.....	69
INTRODUCTION.....	71
RESULTS	73
GENERATION OF TCF/LEF QUADRUPLE-KNOCKOUT (QKO) MESC'S	73
QKO MESC'S DISPLAY ENHANCED SELF-RENEWAL.....	76
RE-EXPRESSION OF TCF7L1 OR TCF7 IN QKO MESC'S REVERTS THEM TO A WT-LIKE STATE	79
RE-EXPRESSION OF <i>TCF7</i> OR <i>TCF7L1</i> IN QKO MESC'S SIMILARLY RESCUE DIFFERENTIATION DEFICITS AND BIASES <i>IN VITRO</i> AND <i>IN VIVO</i>	87
DISCUSSION	95
EXPERIMENTAL PROCEDURES.....	100
REFERENCES.....	108
SUPPLEMENTAL INFORMATION.....	112
CHAPTER 3.....	126
TCF7L1 AND TCF7 DIFFERENTIALLY REGULATE SPECIFIC MOUSE ES CELL GENES IN RESPONSE TO GSK-3 INHIBITION.....	126
PREAMBLE.....	126
SUMMARY.....	128
INTRODUCTION.....	130
RESULTS	132

GENERATION OF mESC LINES WITH N-TERMINAL 3xFLAG TAGS KNOCKED INTO SINGLE COPIES OF ENDOGENOUS TCF7 AND TCF7L1 LOCI	132
NEITHER 3xFLAG-TCF7 NOR 3xFLAG-TCF7L1 PROTEIN LEVELS INVERSELY CORRELATE WITH NANOG PROTEIN EXPRESSION IN mESCs	134
CONSEQUENCES OF GSK-3 INHIBITION ON TCF7L1 AND TCF7 FUNCTION IN mESCs	137
EXAMINING GENOME-WIDE TCF7L1 AND TCF7 CHROMATIN OCCUPANCY	142
3xFLAG-TCF7L1 AND 3xFLAG-TCF7 DISPLAY DIFFERENTIAL CHROMATIN OCCUPANCY	148
TCF7L1 ACTS AS A TRANSCRIPTIONAL ACTIVATOR IN RESPONSE TO CHIR-MEDIATED GSK-3 INHIBITION	153
DISCUSSION	156
EXPERIMENTAL PROCEDURES.....	161
REFERENCES.....	163
SUPPLEMENTAL INFORMATION.....	165
CHAPTER 4.....	175
ENDOGENOUS BIOID ELUCIDATES TCF7L1 INTERACTOME MODULATION UPON GSK-3 INHIBITION IN MOUSE ESCS.....	175
PREAMBLE.....	175
SUMMARY.....	177
INTRODUCTION.....	179
RESULTS	180
INDUCIBLE AND ENDOGENOUS BIRA*-TCF7L1 BioID SYSTEMS	180
INDUCIBLE AND ENDOGENOUS TCF7L1 BioID SYSTEMS DEMONSTRATE BIOTINYLACTION OF PROTEINS <i>IN VIVO</i>	184
BioID-BASED ASSEMBLY OF THE TCF7L1 INTERACTOME.....	187
INDUCIBLE AND ENDOGENOUS BioID SCREENS DETECT SIMILAR, BUT DISTINCT, TCF7L1 INTERACTOMES.....	191
VALIDATION OF JMJD1C, SALL4, AND SMARCA4 INTERACTIONS WITH TCF7L1 IN mESCs.....	195
DISCUSSION	199

EXPERIMENTAL PROCEDURES	204
REFERENCES	207
SUPPLEMENTAL INFORMATION	212
CHAPTER 5 DISCUSSION	215
5.0 TCF/LEFs: SETTING THE STAGE FOR COMPLEX WNT TARGET GENE REGULATION	215
5.1 UNRAVELLING REDUNDANT FUNCTIONS OF THE ARCHITECTURAL TCF/LEF FACTORS.....	216
5.2 EMPHASIZING MECHANISMS OF TCF/LEF TARGET GENE SELECTION AND SPECIFICITY	221
5.3 TCF/LEFs FLICKING THE SWITCH ON WNT/ β -CATENIN SIGNALING.....	227
5.4 MOVING FORWARD WITH MECHANISMS OF TCF/LEF FUNCTION.....	235
5.5 CONCLUDING REMARKS	239
BIBLIOGRAPHY	243
APPENDICES	269
APPENDIX I: BioID PERFORMED ON ENDOGENOUS SINGLE COPY BIRA* TAGGED TCF7.....	269
APPENDIX II: GENERATION OF ENDOGENOUS SINGLE COPY FLUORESCENT PROTEIN TAGGED TCF7L1 AND TCF7	271

LIST OF TABLES

Chapter 2

TABLE S1. TALEN RVD AND CRISPR SGRNA SEQUENCES 117

TABLE S2. QUANTITATIVE RT-PCR PRIMERS 118

TABLE S3. LIF + SERUM CELL CYCLE CHI-SQUARED ANALYSIS (RELATED TO FIGURE 4) 120

TABLE S4. LIF + 2I CELL CYCLE CHI-SQUARED ANALYSIS (RELATED TO FIGURE 4) 121

LIST OF FIGURES**Chapter 1**

FIGURE 1. OVERVIEW OF THE WNT/ β -CATENIN SIGNALING PATHWAY. 21

FIGURE 2. OVERVIEW OF THE T-CELL FACTORS/LYMPHOID ENHANCER FACTOR STRUCTURE.
27

FIGURE 3. FORMATION OF A WNT ENHANCEOSOME AND CHROMATIN LOOPS. 28

FIGURE 4. SIGNALING PATHWAYS AND THEIR EFFECTS ON THE NAÏVE AND PRIMED PLURIPOTENT
STATES. 60

Chapter 2

FIGURE 1. QKO mESCs ARE VIABLE AND PROLIFERATIVE BUT DO NOT RESPOND APPROPRIATELY TO
WNT PATHWAY ACTIVATION. 75

FIGURE 2. QKO mESCs DISPLAY ENHANCED SELF-RENEWAL CAPACITY IN SERUM-CONTAINING AND
DEFINED SERUM-FREE MEDIA. 78

FIGURE 3. SINGLE COPY RE-EXPRESSION OF ENDOGENOUS TCF7 OR TCF7L1 IN QKO mESCs
DEMONSTRATES DIFFERENTIAL EFFECTS ON WNT/ β -CATENIN SIGNALING ACTIVITY. 82

FIGURE 4. RE-EXPRESSION OF TCF7 OR TCF7L1 IN QKO mESCs REVERTS THEIR WHOLE-GENOME
TRANSCRIPTIONAL PROFILE TO MORE RESEMBLE THAT OF WT mESCs. 86

FIGURE 5. QKO mESCs RE-EXPRESSING TCF7 OR TCF7L1 ARE RESCUED IN THEIR ABILITY TO
GENERATE MESODERM IN EB ASSAYS. 91

FIGURE 6. QKO mESCs RE-EXPRESSING TCF7 OR TCF7L1 ARE RESCUED IN THEIR ABILITY TO
GENERATE MESODERM IN TERATOMAS. 94

FIGURE S1, RELATED TO FIGURE 1 112

FIGURE S2, RELATED TO FIGURE 3 113

FIGURE S3, RELATED TO FIGURE 3A 114

FIGURE S4, RELATED TO FIGURE 3 115

FIGURE S5, RELATED TO FIGURE 6 116

Chapter 3

FIGURE 1. CHARACTERIZATION OF 3xFLAG-TCF7 AND 3xFLAG-TCF7L1 MESCLINES. 133

FIGURE 2. NEITHER TCF7L1 NOR TCF7 EXPRESSION INVERSELY CORRELATE WITH NANOG LEVELS
IN SELF-RENEWING AND DIFFERENTIATING MESCS. 136

FIGURE 3. GSK-3 INHIBITION PROMOTES ASSOCIATION OF B-CATENIN WITH 3xFLAG-TCF7 AND
3xFLAG-TCF7L1. 140

FIGURE 4. CHARACTERIZATION OF GENOMIC REGIONS BOUND BY 3xFLAG-TCF7L1 OR 3xFLAG-
TCF7 IN MESCS. 145

FIGURE 5. 3xFLAG-TCF7L1 AND 3xFLAG-TCF7 EXHIBIT DIFFERENTIAL OCCUPANCY AT WNT
TARGET AND PLURIPOTENCY-ASSOCIATED GENES. 151

FIGURE 6. *Id3* ACTIVATION IS MEDIATED BY CONVERSION OF TCF7L1 INTO A TRANSCRIPTIONAL
ACTIVATOR IN THE PRESENCE OF CHIR. 155

FIGURE S1, RELATED TO FIGURE 1 165

FIGURE S2, RELATED TO FIGURE 2 167

FIGURE S3, RELATED TO FIGURE 3 168

FIGURE S4, RELATED TO FIGURE 4 169

FIGURE S1 5, RELATED TO FIGURE 5 171

Chapter 4

FIGURE 1. BIRA*-P2A-TCF7L1 AND BIRA*-TCF7L1 EXPRESSION IN INDUCIBLE AND ENDOGENOUS BIOID SYSTEMS. 183

FIGURE 2. INDUCIBLE AND ENDOGENOUS TCF7L1 BIOID SYSTEMS DEMONSTRATE BIOTINYLATION OF PROTEINS IN VIVO. 186

FIGURE 3. PROTEINS BIOTINYLATED BY BIRA*-TCF7L1 IN INDUCIBLE AND ENDOGENOUS BIOID SYSTEMS IN THE PRESENCE AND ABSENCE OF CHIR. 190

FIGURE 4. INDUCIBLE AND ENDOGENOUS BIOID SCREENS DETECT SIMILAR, BUT DISTINCT, TCF7L1 INTERACTOMES. 194

FIGURE 5. VALIDATION OF JMJD1C, SALL4, AND SMARCA4 INTERACTIONS WITH TCF7L1 IN MESCs. 198

FIGURE S1, RELATED TO FIGURE 1 212

Chapter 5

FIGURE 1. MODEL OF TCF/LEF FUNCTIONS AND MECHANISMS OF WNT TARGET GENE REGULATION. 242

LIST OF ABBREVIATIONS AND ACRONYMS

AP	Alkaline Phosphatase
APC	Adenomatous Polyposis Coli
β -TrCP	β -Transducin repeats-Containing Protein
BMP	Bone Morphogenetic Protein
CBP	CREB-Binding Protein
cDNA	Complementary DNA
ChIP	Chromatin Immunoprecipitation
ChIP-seq	ChIP-sequencing
CK1	Casein Kinase 1
CRD	Context regulatory domain
DBD	DNA binding domain
DKO	Double Knockout
DMEM	Dulbecco's Modified Eagle Medium
DN or dn	Dominant-Negative
DNA	Deoxyribonucleic Acid
Dvl	Dishevelled
EB	Embryoid Body
EMT	Epithelial to Mesenchymal Transition
EpiSC	Epiblast Stem Cell
ERK	Extracellular signal-Regulated Kinase
ESC	Embryonic Stem Cell
FBS	Fetal Bovine Serum
FGF	Fibroblast Growth Factor
FL or fl	Full-Length
Fz or Fzd	Frizzled
GSK-3	Glycogen Synthase Kinase-3
HDAC	Histone Deacetylase
hESC	Human Embryonic Stem Cell
HMG	High Mobility Group
ICM	Inner Cell Mass
Id	Inhibitor of Differentiation
JAK	Janus Kinase
LIF	Leukaemia Inhibitory Factor
LRP	Low-density lipoprotein Receptor-related Protein
MAPK	Mitogen-Activated Protein Kinase

mEpiSC	Mouse Epiblast Stem Cell
mESC	Mouse Embryonic Stem Cell
MLL	Mixed Lineage Leukaemia
MMTV	Mouse Mammary Tumor Virus
OSN	OCT4 SOX2 NANOG
PS	Primitive Streak
PSC	Pluripotent Stem Cell
QKO	Quadruple Knockout
QT7	QKO rescued with 3xFLAG TCF7
QT7L1	QKO rescued with 3xFLAG TCF7L1
qRT-PCR	Quantitative Real-Time Polymerase Chain Reaction
RNA	Ribonucleic Acid
RNA-seq	RNA-sequencing
RT	Rosa TetOne
SEM	Standard Error of the Mean
STAT	Signal Transducer and Activator of Transcription
TCF/LEF	T-Cell Factor/Lymphoid Enhancer Factor
TGF- β	Transforming Growth Factor- β
TLE	Transducin Like-Enhancer of Split
WNT	Wingless-related MMTV Integration site
WRE	WNT Responsive Element

LIST OF APPENDICES

APPENDIX I: BIOID PERFORMED ON ENDOGENOUS SINGLE COPY BIRA* TAGGED TCF7 269

APPENDIX II: GENERATION OF ENDOGENOUS SINGLE COPY FLUORESCENT PROTEIN TAGGED TCF7L1
AND TCF7 271

CHAPTER 1 INTRODUCTION

1.0 Preamble

The research presented in this thesis was primarily inspired by the findings of Kelly *et al.* and Yi *et al.*, which triggered my interest in understanding the redundancy versus the specialized functions of the T-cell factor / Lymphoid enhancer factor (TCF/LEF) family of transcription factors. These two studies implicated β -catenin as an important regulator of the pluripotent state in embryonic stem cells (ESCs) and proposed that atypical or complex TCF/LEF mechanisms played an essential role in mediating β -catenin's nuclear functions. Yi *et al.* built on their original findings and demonstrated that Wnt/ β -catenin-mediated reinforcement of the pluripotent state employed a TCF/LEF switch in which repressive TCF7L1- β -catenin is replaced by activating TCF7- β -catenin complexes.

In this introductory chapter I provide an overview of the Wnt/ β -catenin signalling pathway and its downstream nuclear effectors, the TCF/LEFs. I then discuss the important roles Wnt/ β -catenin signalling and the TCF/LEFs play in embryonic development. Lastly, I discuss *in vitro* pluripotency, including the continuum of pluripotency, the core pluripotency transcriptional network and the effects of Wnt/ β -catenin signalling and the TCF/LEFs on the pluripotent state.

1.1 The Wnt/ β -catenin signaling pathway

Nusse and Varmus first described a proto-oncogene called *integration-1 (Int1)*, a homolog of *wingless (Wg)* in *Drosophila* (Nusse and Varmus, 1982; Rijsewijk *et al.*, 1987). Subsequent studies determined that *Int1* belonged to a highly conserved metazoan family of genes, now known as the wingless-type mouse mammary tumor virus (MMTV) integration site (Wnt) family (Nusse and Varmus, 2012).

The Wnts are a gene family of short-range secreted glycoproteins that initiate signaling pathways that play essential roles in embryonic development and adult tissue homeostasis (Grainger and Willert, 2018). Wnt proteins are post-translationally modified through palmitoylation by Porcupine, which is required for secretion and activity (Willert *et al.*, 2003). Mice and humans express 19 distinct Wnt genes in specific patterns throughout development, each capable of binding combinations of cell-surface receptors to initiate different signalling cascades in a context-specific manner (Grainger and Willert, 2018).

Non-canonical Wnt signaling pathways include the Wnt-planar cell polarity and Wnt-Ca²⁺ signaling cascades that regulate cell migration and polarity in tissue morphogenesis (Gómez-Orte *et al.*, 2013). However, this chapter will focus exclusively on the canonical Wnt/ β -catenin signaling pathway.

At the cell surface, activation of the Wnt/ β -catenin signaling pathway requires binding of Wnts to their cognate co-receptors, the 10 Frizzled (Fz or Fzd) seven-pass transmembrane receptors and the LDL receptor-related proteins 5 and 6 (LRP5 and LRP6) single-pass transmembrane receptors (Nusse and Clevers, 2017). Key to Wnt/ β -catenin signaling is the regulation of a cytoplasmic signalling pool of the protein β -catenin, which also serves as a junctional protein that binds E-cadherin at adherens junctions (Figure 1) (Peifer *et al.*, 1992). Cytosolic β -catenin levels are regulated by a destruction complex consisting of the scaffold protein Axin1/2, which interacts with β -catenin, Adenomatous Polyposis Coli (APC), Casein Kinase-1 α/δ (CK1 α/δ) and Glycogen Synthase Kinase-3 α/β (GSK-3 α/β) (Figure 1) (Nusse and Clevers, 2017). In the absence of a Wnt ligand, CK1 and GSK-3 sequentially phosphorylate β -catenin at a series of N-terminal Ser/Thr residues, known collectively as the phospho-degron motif, allowing the E3 ubiquitin ligase β -TrCP to bind and ubiquitinate β -catenin, thereby targeting it for subsequent

proteasomal degradation (Figure 1) (Kitagawa *et al.*, 1999; Liu *et al.*, 2002). Downstream of β -catenin, the main nuclear effectors of the Wnt/ β -catenin signaling cascade, the T-cell factor/Lymphoid Enhancer factor (TCF/LEF) family of transcription factors, serve to repress Wnt target genes in the absence of Wnt ligand, primarily through the Transducin-like enhancers of split (TLE) co-repressor family (Figure 1) (Brantjes *et al.*, 2001).

Upon Wnt ligand-initiated signal transduction, the intact destruction complex is recruited to LRP5/6, preventing ubiquitination of phosphorylated β -catenin. As a consequence, the destruction complex becomes saturated, allowing newly synthesized β -catenin to accumulate in the cytosol (Figure 1) (Li *et al.*, 2012). When a threshold level of β -catenin is reached, it translocates to the nucleus where it interacts with TCF/LEFs to derepress them and/or recruit co-activators through unclear mechanisms, initiating transcription of Wnt target genes (Figure 1) (Behrens *et al.*, 1996; Huber *et al.*, 1996).

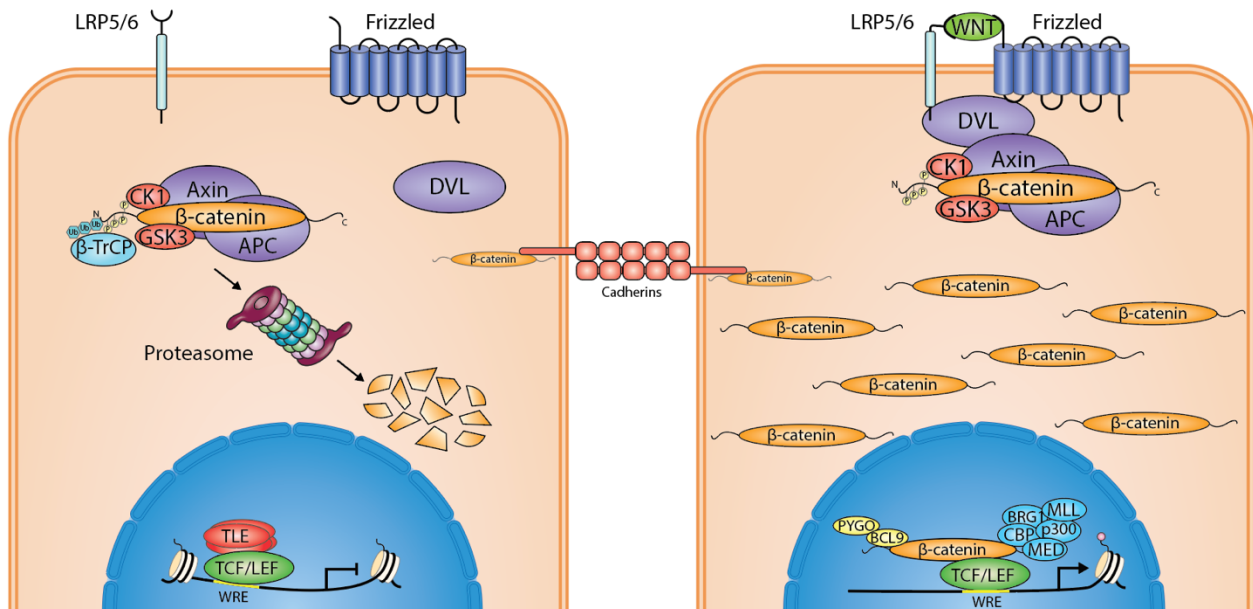


Figure 1. Overview of the Wnt/β-catenin signaling Pathway.

LEFT: In the absence of Wnt ligand, GSK-3, CK1, APC, and Axin bind β-catenin to form the ‘β-catenin destruction complex.’ GSK-3 and CK1 phosphorylate β-catenin, priming it for ubiquitination by β-TrCP and subsequent proteasomal degradation. In the nucleus, TCF/LEF factors are bound to the TLE co-repressors and repress Wnt target genes. *RIGHT:* In the presence of Wnt, Frizzled binds to Dishevelled (Dvl) leading to Axin recruitment together with the other components of the destruction complex. As a result, ubiquitination of β-catenin by β-TrCP is inhibited, saturating the destruction complex and allowing β-catenin to accumulate in the cytoplasm and then translocate to the nucleus, where it binds TCF/LEFs and recruits co-activators.

1.2 T-cell factors and Lymphoid enhancer factor: the nuclear effectors of the Wnt/ β -catenin pathway

The TCF/LEF family is a subset of the high-mobility group (HMG) of DNA-binding transcription factors. Although vertebrates possess four TCF/LEF family members, most invertebrate species express fewer members, but will minimally express at least a single TCF/LEF ortholog (Figure 2) (Cadigan and Waterman, 2012). T-cell factor 7 or TCF7 (*TCF7*) and Lymphoid enhancer factor 1 or LEF1 (*LEF1*) were first discovered in human T and B lymphocytes (Travis *et al.*, 1991; Waterman *et al.*, 1991; Van De Wetering *et al.*, 1991). T-cell factor 7-like 1 or TCF7L1 (*Tcf7l1*) and T-cell factor 7-like 2 or TCF7L2 (*Tcf7l2*) were subsequently identified in mouse embryos via low-stringency hybridization screens with probes from *Xenopus Tcf7l1* and human *TCF7* (Korinek *et al.*, 1998a). Each of these members possesses highly conserved regions, including an HMG box and adjacent small stretch of basic residues that together form the HMG DNA-binding domain (HMG DBD), a β -catenin-binding domain, and a TLE binding domain (Figure 2).

A striking feature of the HMG DBD is the ability to bind the minor groove of the DNA at target gene promoters or enhancers containing the consensus sequence (5'-SCTTTGATG-3'), also known as the Wnt-responsive element (WRE) (van de Wetering and Clevers, 1992; Van de Wetering *et al.*, 1997). Interestingly, a new TCF/LEF consensus sequence known as the negative regulatory element (NRE) has been identified as being necessary for TCF/LEF- β -catenin-mediated suppression of Wnt target genes (Kim *et al.*, 2017). This finding suggests that Wnt signaling promotes transcription of target genes through WREs and, in a context-dependent manner, fine-tunes their expression through the NRE. Binding of the TCF/LEFs induces a 90°-130° bend, promoting additional contacts between the basic tail (also the nuclear localization signal) and the positively charged DNA backbone, as well as distant interactions with transcriptional complexes

(Van Beest *et al.*, 2000; Giese *et al.*, 1992; Love *et al.*, 1995). Thus, TCF/LEFs are architectural proteins capable of organizing the chromatin and enabling long-range interactions between chromatin domains or transcriptional regulators.

Shortly after being identified as HMG domain-containing transcription factors, TCF/LEFs were identified as β -catenin interactors through a conserved N-terminal domain (Behrens *et al.*, 1996; Huber *et al.*, 1996). Upon Wnt activation, β -catenin recruits a plethora of transcriptional co-activators to TCF/LEF-occupied WREs (Figure 3).

Histone acetylation is an epigenetic modification associated with actively transcribed genes, preventing the compaction of nucleosomes (Mosimann *et al.*, 2009). Two histone acetyltransferases, CBP and p300, interact with the C-terminus of β -catenin, catalyzing widespread histone acetylation spanning up to 40kb surrounding WREs, thereby activating Wnt target genes (Hecht *et al.*, 2000; Parker *et al.*, 2008; Takemaru and Moon, 2000). Nucleosomes can also be regulated by the SWI/SNF family of ATPases that shuffle or disassemble nucleosomes, exposing transcription factor binding sites normally entangled around nucleosomes (Mosimann *et al.*, 2009). β -catenin, through its C-terminus, interacts with a SWI/SNF protein, SMARCA4, required for Wnt target gene activation (Barker *et al.*, 2001). Moreover, β -catenin C-terminal interactions recruit Mixed lineage leukaemia (MLL) complexes, which are histone methyltransferases that induce tri-methylation of H3K4, a mark associated with genes that are being actively transcribed (Mosimann *et al.*, 2009; Sierra *et al.*, 2006).

The N-terminus of β -catenin recruits Pygopus1/2 indirectly through interactions with BCL-9 or B9L, a complex essential for Wnt target gene activation (Valenta *et al.*, 2011). Pygopus1/2 is an epigenetic reader capable of binding all H3K4 methylated states, localizing transcriptional regulators to modified histones (Fiedler *et al.*, 2008). Pygopus and β -catenin recruit the Mediator

complex, essential for the recruitment the RNA polymerase II pre-initiation complex and Wnt target gene activation (Carrera *et al.*, 2008; Kim *et al.*, 2006). β -catenin is, therefore, critical in promoting an epigenetically active and open chromatin state, required for recruitment of RNA polymerase II to initiate Wnt target gene transcription.

In the absence of β -catenin, TCF/LEFs through their context-regulatory domains (CRD) as well as a portion of the HMG DBD, bind to the glutamine rich Q-domain at the N-terminus of the TLEs (Brantjes *et al.*, 2001; Daniels and Weis, 2005). A small motif in the CRD, present in all TCF/LEFS, has recently been shown to be essential for the LEF1 and TLE1 interaction (Figure 2) (Arce *et al.*, 2009).

TLEs are a family of co-repressors that tetramerize and exert their repressive functions by recruiting HDACs and binding nucleosomes, resulting in histone deacetylation, compaction of the chromatin, and subsequent transcriptional repression (Figure 3) (Ramakrishnan *et al.*, 2018). Structural studies discovered that upon Wnt activation, β -catenin binds to a secondary region on the TCF/LEFs that overlaps with the TLE binding site. Therefore, it was proposed that β -catenin displaced the TLEs (Daniels and Weis, 2005). Recently, this has been questioned, as subsequent work from the same group determined that the TCF/LEFs were able to bind both β -catenin and the TLEs simultaneously (Chodaparambil *et al.*, 2014). Proteomic studies revealed that regardless of the state of Wnt signaling, β -catenin co-activators including BCL9, B9L, and Pygopus1/2 interacted with TLEs and the TCF/LEFs (van Tienen *et al.*, 2017).

A study by the Bienz group has recently proposed an interesting mechanism of TLE regulation in lieu of the displacement model (Flack *et al.*, 2017). In the new model, Wnt-stabilized β -catenin-mediated derepression of the TCF/LEFs depends on TLE ubiquitination by the HECT E3 ubiquitin ligase, UBR5, and subsequent recruitment of an ATPase, VCP, a protein involved in

protein folding (Flack *et al.*, 2017). It was proposed that ubiquitination of TLE prevents binding to nucleosomes, allowing VCP to unfold the TLE tetramer, thereby disabling its repressive function (Chodaparambil *et al.*, 2014; Flack *et al.*, 2017). However, future experiments are necessary to determine whether the binding of β -catenin to TCF/LEFs triggers the unfolding of TLE tetramers.

The TCF/LEFs also have two domains that are dissimilar between family members; the context regulatory domain (CRD) and variable C-termini generated through extensive mRNA splicing and alternative promoter usage. Alternative promoters located in the second intron of *Tcf7* and *Lef1* and the fifth intron of *Tcf7l2* yield isoforms lacking the β -catenin-binding domain, whereas *Tcf7l1* has only a single promoter (Hovanes *et al.*, 2001; Vacik *et al.*, 2011; Van de Wetering *et al.*, 1996). These truncated TCF/LEF isoforms are potent suppressors of Wnt target genes and are therefore considered dominant-negative, competing with their full-length counterparts for binding to WREs (Hovanes *et al.*, 2000; Hsu *et al.*, 1998; Van de Wetering *et al.*, 1996).

Alternative splicing generates further TCF/LEF functional diversity. All TCF/LEFs undergo splicing of at least a single exon within the CRD (Duval *et al.*, 2000; Hovanes *et al.*, 2000; Salomonis *et al.*, 2010; Van de Wetering *et al.*, 1996). Further splicing occurs within the C-termini of all the TCF/LEFs, with the exception of *Tcf7l1* (Duval *et al.*, 2000; Hovanes *et al.*, 2000; Van de Wetering *et al.*, 1996). Notably, the so called ‘E-tail’ C-termini found only in TCF7 and TCF7L2, contain a cysteine-rich motif, termed the C-clamp, which provides additional binding specificity to Wnt target genes (Atcha *et al.*, 2003, 2007). The C-clamp binds and recognizes a RCCG motif, termed the helper site, that is variably spaced and oriented around WREs (Hoverter *et al.*, 2014). The consequence of this extensive structural diversity is that different TCF/LEF isoforms demonstrate differential regulation of Wnt target genes, as TCF7 and LEF1 are generally

thought to behave as activators, and TCF7L1 and TCF7L2 are thought to be repressors (Cadigan and Waterman, 2012). Adding to this complexity, all of the TCF/LEF factors contain WREs within their promoters and, therefore, have the ability to auto- and cross-regulate each other's expression (Hatzis *et al.*, 2008; Hovanes *et al.*, 2001; Li *et al.*, 2006; Solberg *et al.*, 2012).

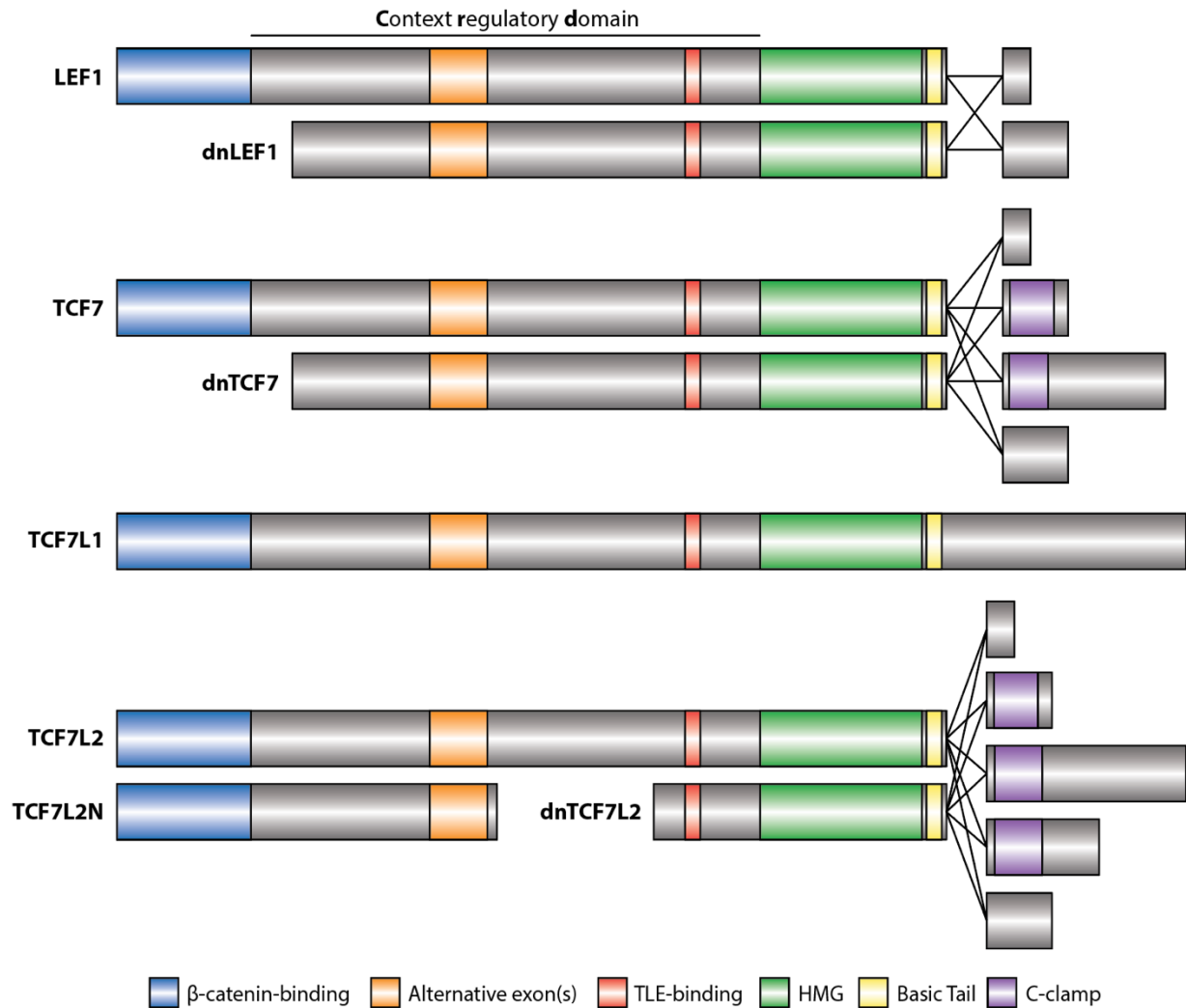


Figure 2. Overview of the T-Cell Factors/lymphoid Enhancer Factor structure.

Alternative promoter usage and splicing generate a variety of TCF/LEF isoforms. With the exception of dominant-negative isoforms encoded through alternative promoter usage, all TCF/LEF isoforms contain a β -catenin binding domain (Blue). Within the region with the least conservation, the context regulatory domain (CRD), all TCF/LEF proteins contain alternatively spliced exons (Orange) and a TLE binding domain (Red). Similarly, all TCF/LEFs contain a high mobility group (HMG) that confers DNA binding (Green), and a basic tail that serves as the nuclear localization signal (NLS) (Yellow). Alternative splicing at the C-terminus generates highly variable C-termini, some with E-tails containing an additional DNA binding domain called the cysteine-clamp or C-clamp (Purple).

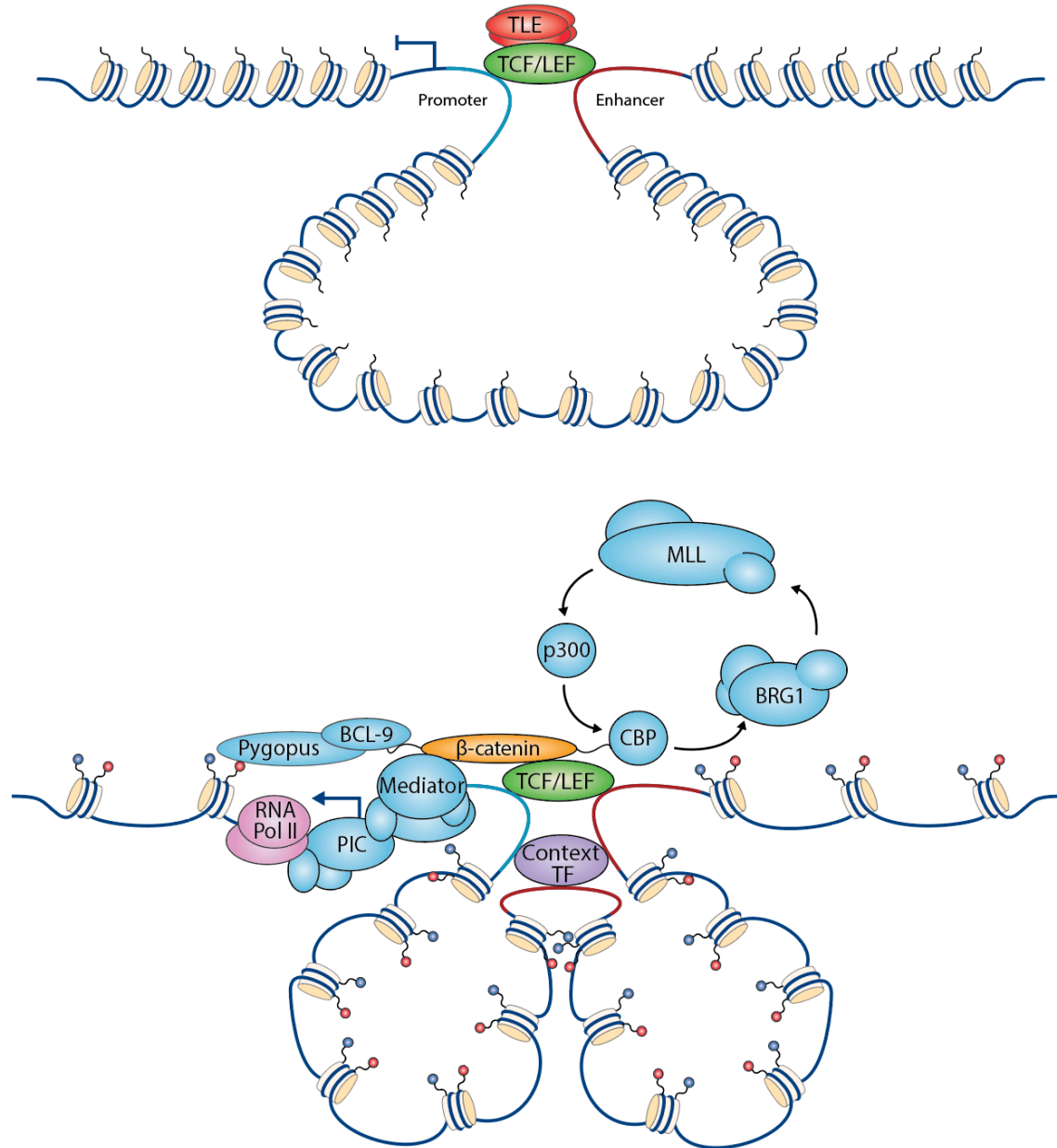


Figure 3. Formation of a Wnt Enhanceosome and chromatin loops.

Positioning of Wnt-responsive elements (WREs) at, or around, enhancers or promoters enables TCF/LEF factors to bind and bend the DNA, allowing distal DNA elements to come into close proximity. In the absence of β -catenin, this would permit TLE co-repressors to mediate widespread histone deacetylation through HDAC recruitment, promoting chromatin compaction at promoters and enhancers and repressing Wnt target genes. Binding of β -catenin, and subsequent recruitment of a plethora of transcriptional co-activators, allows for widespread histone shuffling and eviction, as well as acetylation and methylation of histones. This promotes an open chromatin structure that allows context-dependent transcription factor binding at additional enhancer elements in ‘super enhancers’ regulating Wnt target genes.

1.3 The role of Wnt signaling and the TCF/LEFs in mouse development

1.3.0 *Wnt signaling is required for primitive streak formation and gastrulation*

Perhaps the most critical developmental stage is gastrulation, a morphogenetic process initiating the formation of mesoderm and the organization of the embryo into the three germ layers: ectoderm, endoderm and mesoderm. Gastrulation begins in the mouse after implantation at embryonic day 6.5 (E6.5) and is marked by the formation of a specialized transient structure called the primitive streak (PS) (Ang and Behringer, 2002; Rivera-pérez *et al.*, 2014). The PS first appears when epiblast cells located at the proximal egg cylinder ingress and undergo an epithelial to a mesenchymal transition (EMT), facilitating their migration from the proximal to the distal ends of the epiblast, establishing the anterior-posterior axis of the embryo, as well as bilaterally forming the mesodermal wings (Ang and Behringer, 2002; Rivera-pérez *et al.*, 2014).

As the PS elongates, the anterior and middle regions form axial, cardiac, lateral plate and paraxial mesoderm, as well as structures that are crucial in mesodermal patterning such as the node (Ang and Behringer, 2002; Rivera-pérez *et al.*, 2014). In particular, the node is a crucial structure as it gives rise to progeny located in the midline of all three germ layers; the ectodermal floor plate, the mesodermal notochord and gut endoderm (Ang and Behringer, 2002).

In preimplantation embryos, Wnt signaling is not required, as *Lrp5/6*- and *Porcn*-null mice only begin to display defects at the onset of PS formation (Biechele *et al.*, 2013; Kelly, 2004). TCF/LEF reporter activity is first detected around E6.0 in the proximal epiblast of an implanted embryo, marking the initiation of the PS. TCF/LEF activity continues to demarcate the PS as it elongates distally (Currier *et al.*, 2010; Maretto *et al.*, 2003).

In support of a crucial role for Wnt signaling in PS formation and gastrulation, *Wnt3* knockout mice are unable to form the PS and do not undergo gastrulation (Kelly, 2004; Liu *et al.*,

1999). *Wnt3a*-null mice also fail to form posterior mesoderm and caudal structures, indicating that *Wnt3a* is necessary for the maintenance and function of the PS (Takada *et al.*, 1994). A critical target of *Wnt3a* and the TCF/LEFs is *T* (*Brachyury*), and *T* mutant mice recapitulate the *Wnt3a* null mouse phenotype (Galceran *et al.*, 2001; Yamaguchi *et al.*, 1999). Downstream of the Wnt ligands and co-receptors, β -catenin-null embryos also demonstrate an inability to gastrulate and initiate PS formation (Haegel *et al.*, 1995; Huelsken *et al.*, 2000).

1.3.1 TCF/LEF factors in mouse development

Spatio-temporal regulation of the TCF/LEF factors can allow for a single factor, or multiple factors, to be dynamically expressed in a context-dependent manner, in response to exceedingly coordinated and complex extrinsic, as well as intrinsic factors, including Wnt signaling itself. Specific roles for a single TCF/LEF factor can be imparted by their unique expression under highly specific contexts or cell lineages. Adding a layer to this complexity, TCF/LEF factors, whose effects differ depending on the state of Wnt signaling, have the ability to bind each other's enhancers and promoters, auto- and cross-regulating one another's expression. Therefore, perturbation of the levels of a single TCF/LEF factor can have implications on the levels of other, or multiple, TCF/LEF family members. Moreover, TCF/LEFs share highly conserved functional domains such as the HMG DNA-binding, TLE-binding, and β -catenin-binding domains, which suggests that they all have the capacity to broadly function in a similar manner. This does not preclude a single TCF/LEF from binding context-dependent co-factors to mediate regulation of distinct Wnt target genes. Due to these complex dynamics, studying the TCF/LEF factors has made it difficult to interpret their functions. The TCF/LEF mutant mice discussed below have highlighted the roles individual TCF/LEF factors play in mouse development, as well as the functional overlap among family members.

Tcf7ll

Tcf7ll is abundantly expressed at E6.5 throughout the embryo proper, with levels beginning to decline at E7.5, becoming restricted to the anterior portion of the embryo (Korinek *et al.*, 1998a). *Tcf7ll* expression is lower at the posterior of the embryo and the PS, suggesting that other TCF/LEF factors may be required for PS progression (Korinek *et al.*, 1998a). By E8.5 *Tcf7ll* remains highly abundant at the anterior neuroectoderm and is barely expressed in the posterior of the embryo and PS (Korinek *et al.*, 1998a). *Tcf7ll* is undetectable by E10.5 and thereafter (Korinek *et al.*, 1998a). The expression of *Tcf7ll* suggests that it may facilitate early patterning of the embryo and mediate Wnt signaling during early gastrulation, primitive streak, and AP axis formation events.

In support of this, *Tcf7ll* knockout mice are distinct in that they are the only TCF/LEF single-gene knockout that is embryonic lethal, with no intact embryos recovered past E9.5 (Merrill *et al.*, 2004). The earliest defects observed in *Tcf7ll* null embryos were expansions of the PS at E7.5 (Merrill *et al.*, 2004). *Tcf7ll* mutant embryos presented with mild to severe morphological defects after gastrulation at E8.5 (Merrill *et al.*, 2004). Backcrossing to produce congenic C57BL/6 *Tcf7ll* mutant mice resulted in null mice with uniformly severe phenotypes, suggesting that the mixed genetic background of the initial knockout mice produced the variable defects (Hoffman *et al.*, 2013). *Tcf7ll* mutant mice with milder phenotypes displayed duplicated neural folds, resulting in multiple neural grooves as well as an extra row of somites and enlarged hearts (Merrill *et al.*, 2004). Severely affected *Tcf7ll* null embryos lacked neural folds, somites, and hearts, however they contained multiple neural grooves (Merrill *et al.*, 2004).

All *Tcf7ll* mutant mice demonstrated anterior truncations and neural patterning defects, reminiscent of those observed upon ectopic Wnt signaling activation (Fossat *et al.*, 2011; Merrill *et al.*, 2004). *Tcf7ll* null embryos lacked forebrain structures with forebrain marker expression

being significantly reduced (Merrill *et al.*, 2004). Expression of midbrain markers was expanded, whereas hindbrain marker expression was reduced and restricted (Merrill *et al.*, 2004). These findings implicate TCF7L1-mediated regulation of Wnt target genes in neural patterning required for specifying the forebrain and proper development of caudal regions of the brain.

In addition to neural patterning defects, severely affected *Tcf7l1* knockout embryos also displayed mesodermal patterning defects, including missing paraxial and lateral mesodermal structures such as somites and the heart (Merrill *et al.*, 2004). During PS progression, specialized cells at the anterior PS form the axial mesoderm, giving rise to the node and notochord, which are responsible for further patterning and formation of paraxial and lateral mesodermal structures (Beddington and Robertson, 1999; Rivera-pérez *et al.*, 2014). *Tcf7l1* null embryos exhibited duplicated nodes and expanded abnormal notochord-like structures, with increased expression of the node markers (and Wnt target genes) *FoxA2* and *Brachyury* (Merrill *et al.*, 2004; Morrison *et al.*, 2016; Sinner *et al.*, 2004; Yamaguchi *et al.*, 1999). Visualization of these two markers earlier in PS formation, revealed expanded and ectopic *FoxA2* and kinked *Brachyury* expression (Merrill *et al.*, 2004). Also, at this stage a lateral mesodermal marker was diminished (Merrill *et al.*, 2004). Together, these results suggested that TCF7L1 does not play a role in mesoderm specification but may restrict axial mesoderm formation or, conversely, promote lateral mesoderm formation.

To determine whether the defects observed in mice lacking *Tcf7l1* were the result of lost non-redundant TCF7L1-activation or -repression of Wnt targets, the activity of a TCF/LEF reporter, TOPGal, was examined in *Tcf7l1* null embryos (Merrill *et al.*, 2004). TOPGal expression was observed in the PS and the node of both wildtype and *Tcf7l1* mutant embryos to the same extent. As TOPGal activity was maintained, this suggested that TCF7L1 functions primarily as a non-redundant repressor of genes that requires other transcription factors for transactivation during gastrulation and early development of the mouse (Merrill *et al.*, 2004). Another possibility is that

other TCF/LEFs, that are not normally expressed, become upregulated in response to Wnt signaling or other cues, mediating appropriate repression or activation of Wnt target genes at this early stage.

In preimplantation mouse embryos, *Tcf7l1* is expressed throughout the epiblast before PS initiation, but its expression becomes reduced near the site of PS initiation (Hoffman *et al.*, 2013). Conversely, *Nanog* becomes upregulated during initiation of the PS at the posterior of the embryo proper (Hoffman *et al.*, 2013). *Tcf7l1* null embryos display prolonged and expanded expression of *Oct4* and *Nanog* in the epiblast. Furthermore, in *Tcf7l1* deficient embryos, *Nanog* levels become significantly upregulated and expands to anterior regions of the embryo during the initiation and progression of the PS (Hoffman *et al.*, 2013). This suggests that TCF7L1 facilitates epiblast development by dynamically regulating pluripotency factors during PS progression.

In support of this, in *Tcf7l1* knockout embryos, mesoderm specification became decoupled from PS formation, as *Prickle1*, a marker of PS morphology, was expressed in the absence of the mesodermal and PS marker, *Brachyury* (Hoffman *et al.*, 2013). *Brachyury* expression was observed later in *Tcf7l1* null embryos, suggesting an eventual compensation conferred by another TCF/LEFs (Hoffman *et al.*, 2013). Intriguingly, TCF7L1's function in accelerating epiblast development and coupling of PS formation to mesoderm specification does not appear to require β -catenin, as *dnTcf7l1* knock-in embryos demonstrated coordinated expression of *Prickle1* and *Brachyury* as well as appropriate downregulation of *Oct4* and *Nanog* expression (Hoffman *et al.*, 2013).

Unlike *Tcf7l1* null mice, *dnTcf7l1* knock-in embryos are viable up to E11.5 with normal morphology through E9.0 (Wu *et al.*, 2012). This suggests that TCF7L1 repressor functions are crucial for PS formation and subsequent gastrulation, as other TCF/LEFs are not expressed. In

response to a Wnt signal, it is likely that other TCF/LEFs are upregulated and compensate for the lack of the TCF7L1- β -catenin interaction.

The TCF7L1- β -catenin interaction is required later on in mouse development as *dnTcf7l1* mutant mice display numerous defects, such as exencephaly, edema, open eyelids, forelimb oligodactyly, and they eventually succumb to haemorrhaging and vascular integrity defects (Wu *et al.*, 2012). In the forelimbs, the TCF7L1- β -catenin interaction is necessary for posterior digit formation (Wu *et al.*, 2012). In the eyelid, a reduction in readout from the TCF/LEF reporter, BATGal, was observed in *dnTcf7l1* knock-in embryos (Wu *et al.*, 2012). Overexpression of TCF7L1 in the eyelid, demonstrated that cells with high levels of TCF7L1 did not activate the BATGal reporter and displayed reduced LEF1 levels (Wu *et al.*, 2012). A feedback loop was proposed in which β -catenin-mediated derepression of TCF7L1 allowed for an upregulation of *Lef1*. Subsequently, LEF1- β -catenin complexes could activate Wnt target genes (Wu *et al.*, 2012). Strikingly, mice with a single *dnTcf7l1* allele are healthy and viable, suggesting that TCF7L1 is required primarily as a repressor or that other TCF/LEFs can compensate for its inability to be activated by β -catenin (Shy *et al.*, 2013). In mice containing two *dnTcf7l1* alleles, the other TCF/LEF factors may be unable to displace DNA-bound dnTcf7l1, resulting in constitutive repression of Wnt target genes. The single-copy *dnTcf7l1* findings suggest that derepression of *Tcf7l1* involves β -catenin-mediated regulation of TCF7L1 levels.

Tcf7

Tcf7 is most abundantly expressed in the posterior of E7.5 mouse embryos, with expression being highest in the germ layer corresponding to mesoderm, followed by lower expression in the ectoderm (Oosterwegel *et al.*, 1993). Both *Tcf7* and *Lef1* are abundantly expressed in the PS of E8.5 embryos (Galceran *et al.*, 1999). Moreover, at later developmental stages, *Tcf7* was expressed

in the cortex of the adrenal gland (Oosterwegel *et al.*, 1993). Given the extensive overlap between *Tcf7* and *Lef1* expression, it is likely that mutant mice demonstrate relatively minor defects as a result of functional compensation by either factor.

Indeed, *Tcf7* knockout mice are healthy, fertile and have normal lifespans (Verbeek *et al.*, 1995). However, the thymus of *Tcf7* null mice was significantly reduced in size, with a severe reduction in the number of total thymocytes that progressively worsened with age (Verbeek *et al.*, 1995). Similarly, the lymph nodes and spleens also demonstrated reduced thymocyte numbers (Verbeek *et al.*, 1995). Thymocyte lineage commitment follows an ordered progression, which can be tracked using surface markers such as CD8, CD4, and CD3 (Verbeek *et al.*, 1995). *Tcf7* null thymocytes demonstrated a blockade in the transition from CD8-positive immature thymocytes to CD4/CD8 double-positive thymocytes (Verbeek *et al.*, 1995).

In adult mice, *Tcf7* expression is restricted to lymphoid lineages, with the highest *Tcf7* levels found in pre-thymocytes (Travis *et al.*, 1991; van de Wetering *et al.*, 1991). Low level *Tcf7* expression is also observed in the epithelial cells of the intestinal crypts and is upregulated in intestinal adenomas (Gregorieff *et al.*, 2005). Autopsies of adult *Tcf7* mutant mice of various ages revealed the formation of mammary gland adenomas and intestinal polyp-like neoplasms (Roose *et al.*, 1999). Together, these findings suggest that TCF7 has a specific role in thymocyte maturation and behaves as a tumor suppressor in mammary and intestinal tissues.

Lef1

Lef1 and *Tcf7* are expressed in similar patterns at the onset of gastrulation, in the mesoderm layer at the posterior of the mouse embryo (Galceran *et al.*, 1999; Oosterwegel *et al.*, 1993). However, at this early stage, *Lef1* is expressed at higher levels (Galceran *et al.*, 1999; Oosterwegel *et al.*, 1993). At E9.5, expression of both *Tcf7* and *Lef1* was observed in the forelimb bud and at the posterior and lateral mesoderm (Galceran *et al.*, 1999; Oosterwegel *et al.*, 1993). Both genes

were also expressed in the neural crest, pharyngeal arches, lung bud, thymus, tooth bud and kidneys at later developmental stages (Oosterwegel *et al.*, 1993). In the central nervous system, *Tcf7* was specifically expressed in meninges surrounding the spinal cord, whereas *Lef1* was exclusively observed in the brain (Oosterwegel *et al.*, 1993). Furthermore, *Lef1* was exclusively expressed in the cochlea (Oosterwegel *et al.*, 1993).

Lef1 null mice are born at mendelian ratios but die within a few weeks after birth (van Genderon *et al.*, 1994). These mice had pointed snouts and were significantly smaller than wildtype mice (van Genderon *et al.*, 1994). The most obvious phenotype was a lack of hair and whiskers, corresponding to a significant reduction in the number of follicles, despite normal initiation of hair follicle formation (van Genderon *et al.*, 1994). The skin of *Lef1* null mice displayed defects in dermal fat and lacked melanin (van Genderon *et al.*, 1994). *Lef1* knockout mice also lacked incisors and molar teeth, despite being able to initiate the formation of the ectoderm-derived tooth bud at E12 (van Genderon *et al.*, 1994). Subsequent examination of odontogenesis, revealed an arrest of *Lef1* null teeth at the bud stage (van Genderon *et al.*, 1994). FGF4 has been identified as a critical downstream target of LEF1 in tooth development (Kratochwil *et al.*, 2002). Interestingly, *Lef1* is expressed in developing mammary buds at E13.5 and *Lef1* null mice displayed a severe reduction in the number of mammary buds (van Genderon *et al.*, 1994). In the brain, *Lef1* was abundantly expressed in the mesencephalon, diencephalon, and hippocampus (Galceran *et al.*, 2000; van Genderon *et al.*, 1994). Specifically, *Lef1* was expressed in a region in which the trigeminal nerve sensory neurons are formed (van Genderon *et al.*, 1994). *Lef1* deficient mice display a lack of dentate gyrus granule cells of the hippocampus (Galceran *et al.*, 2000). Furthermore, trigeminal nerve sensory neurons were not detected in postnatal *Lef1* mutant mice (van Genderon *et al.*, 1994). In adult mice, *Lef1* expression is limited to the lymphoid lineage (Travis *et al.*, 1991). However, unlike *Tcf7*, *Lef1* is expressed in pro- and pre-B cells and is detected

at all stages of thymocyte differentiation (Travis *et al.*, 1991). *Lef1* null pro-B lymphocytes demonstrate proliferation defects and increased apoptosis (Reya *et al.*, 2000). Together, these studies suggest that LEF1 plays an important role in the regulation of tissues requiring cooperative interactions between ectoderm and mesoderm as well as B lymphocyte maturation.

Tcf7l2

Tcf7l2 expression is not detected during early mouse development at E6.5 (Korinek *et al.*, 1998a). *Tcf7l2* expression first arises at E10.5 in the roof of the diencephalon and anterior of the mesencephalon of the central nervous system (Korinek *et al.*, 1998a). At later stages of mouse development, *Tcf7l2* remained most abundantly expressed in the central nervous system, specifically in the roof of the mesencephalon, dorsal thalamus, and the di-telencephalic junction (Chodelkova *et al.*, 2018; Korinek *et al.*, 1998a). Low level *Tcf7l2* expression was also detected in the intestinal epithelium (Barker *et al.*, 1999; Korinek *et al.*, 1998a). This suggests that TCF7L2 may play crucial roles in the development of the central nervous system and intestines.

Tcf7l2 deficient mice are born at mendelian ratios but die after 24 hours as a result of defects in the organization of the small intestine (Korinek *et al.*, 1998b). The lumen of the small intestine is normally filled with villi, formed from non-proliferative differentiated epithelial cells, whereas the intervillus region, which forms the intestinal crypts, houses multipotent progenitors and stem cells capable of self-renewal (Clevers *et al.*, 2014). *Tcf7l2* null mice displayed a reduction in the number of villi and cells in the intervillus of the small intestine (Korinek *et al.*, 1998b). Specifically, enteroendocrine and enterocytes were absent or reduced in *Tcf7l2* null small intestines, suggesting a defect in the stem cell compartment from which they are derived (Korinek *et al.*, 1998b). Further interrogation of the structure of the small intestine in *Tcf7l2* deficient mice, revealed that cells of the intervillus did not demonstrate distinguishing features of the intervillus crypt cells, but instead resembled that of the differentiated villus cells (Korinek *et al.*, 1998b). Cell

cycle analysis initially revealed numerous proliferating cells early in development of the small intestine, which later became exhausted, demonstrated by the absence of proliferative cells in intervilli of *Tcf7l2* null small intestines (Korinek *et al.*, 1998b). Thus, TCF7L2 plays a crucial role in the maintenance, but not the establishment, of the stem cell compartment of the small intestine.

TCF/LEF double knockout mice reveal functional redundancies

Given that *Tcf7* and *Lef1* are similarly expressed throughout the PS and at the posterior of the embryo, it is not surprising that these two factors demonstrate functional overlap. *Lef1/Tcf7* compound knockout mice are distinct from single knockout mice, as they are embryonic lethal (Galceran *et al.*, 1999). *Lef1/Tcf7* null embryos display defects in the caudal region, forelimb bud, telencephalon, and somites (Galceran *et al.*, 1999). Examination of specific mesodermal and neural markers also revealed the formation of multiple neural tubes at the expense of paraxial mesoderm posterior to the forelimb in *Lef1/Tcf7* null embryos, similar to *Wnt3a* mutant embryos (Galceran *et al.*, 1999). The forelimb bud and mid/hindbrain marker *Engrailed1*, which is also a Wnt1 target, was absent in the forelimb bud but was normally expressed in the mid/hindbrain (Danielian and McMahon, 1996; Galceran *et al.*, 1999). Maintenance of *Engrailed1* expression in the central nervous system suggests that TCF7L1 or TCF7L2, which are primarily expressed in the brain during early mouse development, mediate the activation of *Engrailed1* by Wnt1.

Although *Lef1/Tcf7* null mice revealed a high degree of functional redundancy between both family members, this may not be unexpected based on their overlapping expression during early mouse development. The generation of *Tcf7/Tcf7l2* deficient mice demonstrated a surprising amount of functional overlap between two TCF/LEF factors that are not generally co-expressed throughout mouse development. *Tcf7/Tcf7l2* null embryos are embryonic lethal, displaying caudal defects similar to that of *Lef1/Tcf7* deficient mice (Gregorieff *et al.*, 2004).

Specifically, *Tcf7/Tcf7l2* null embryos displayed neural tube branching and lacked genital tubercle, hindgut, and the entire posterior, including hindlimbs and tail (Gregorieff *et al.*, 2004). Moreover, *Tcf7/Tcf7l2* mutant embryos displayed an anteriorization of the gastro-intestinal tract, as the duodenum underwent a homeotic transformation into a second stomach (Gregorieff *et al.*, 2004). Unlike *Lef1/Tcf7* knockout mice, paraxial mesoderm was unaffected, as somites were formed in *Tcf7/Tcf7l2* deficient mice (Gregorieff *et al.*, 2004).

The hair follicle has provided unique insights into the differential utilization and distribution of the TCF/LEF factors. TCF7L1 and TCF7L2 are both expressed in multipotent hair follicle stem cells located in the bulge of the outer root sheath of the hair follicle (DasGupta and Fuchs, 1999). As hair follicle stem cells differentiate into transiently amplifying matrix precursor cells and eventually hair, expression of both TCF7L1 and TCF7L2 is downregulated, and conversely, both *Lef1* expression and Wnt activity are upregulated (DasGupta and Fuchs, 1999). Conditional ablation of *Tcf7l1/Tcf7l2* in the skin revealed redundant roles of both factors in maintenance of hair follicle stem cells, as these mice had very thin epidermis and arrested hair follicle homeostasis (Nguyen *et al.*, 2009). Conversely, conditional overexpression of *dnLef1* in the hair follicle repressed hair follicle differentiation, whereas *Tcf7l1* overexpression promoted bulge and stem cell features (Merrill *et al.*, 2001). TCF7L1/ TCF7L2 are thought to repress hair follicle lineage-specifying genes through the repressive actions of the TLEs, whereas LEF1- β -catenin interactions mediate the activation of these genes (Lien *et al.*, 2014).

Taken together, these studies highlight the specific functions of individual TCF/LEF factors in mouse development as well as the functional overlap among family members, which likely arise from context-dependent differential expression of the TCF/LEFs, co-factor usage and target gene selection.

1.4 Regulation of Embryonic Stem Cell Properties by Wnt signaling and the TCF/LEF factors

1.4.0 Embryonic stem cells

Pluripotency describes a unique state of cellular potential characterized by an ability to form all three germ layers, through a process of cellular differentiation, into the diverse cell types that comprise the embryo. The pluripotent state can be defined by several functional assays including; differentiation into the three germ layers spontaneously *in vitro* by the formation of embryoid bodies; formation of teratomas comprising all three germ layers in syngeneic or immunocompromised mice; chimaera formation and germline transmission through blastocyst injection; or the most stringent test, tetraploid complementation, described below. The first untransformed source of pluripotent cell lines were mouse embryonic stem cells (mESCs) generated from pre-implantation mouse embryos by Evans and Kauffman as well as by Gail Martin (Evans and Kaufman, 1981; Martin, 1981).

Although the Evans/Kauffmann and Martin mESC lines differed, with one derived from whole blastocysts and the other from the inner cell mass (ICM), respectively, both lines demonstrated the ability to be serially passaged *in vitro* without losing their ability to differentiate into all three germ layers in teratomas (Evans and Kaufman, 1981; Martin, 1981).

Tetraploid complementation assays would later reveal that entirely ESC-derived mice could be generated by injecting mESCs into tetraploid blastocysts, definitively demonstrating the pluripotent potential of mESCs and their utility in generating genetically modified mouse strains (Nagy *et al.*, 1993). 17 years later, human embryonic stem cells (hESCs) were derived by Jamie Thomson from isolated ICMs of human *in vitro* fertilized embryos and similarly demonstrated an ability to be cultured for several months, while retaining their pluripotent capacity to form

teratomas consisting of all three germ layers (Thomson *et al.*, 1998). Both mouse and human ESCs have been instrumental in understanding developmental and differentiation processes.

1.4.1 Naïve and primed states of pluripotency

Pluripotency is a transient property of epiblast cells of the early embryo, but pluripotent cells can be derived at various early developmental stages *in vitro* by coaxing cells to self-renew indefinitely through the supplementation of exogenous signaling factors. Mouse ESCs were initially established *in vitro* by culturing them on a supportive layer of mitotically inactivated mouse fibroblast feeder cells in the presence of fetal bovine serum (FBS) (Evans and Kaufman, 1981; Martin, 1981). Efforts by Austin Smith's group would later identify Leukemia Inhibitory Factor (LIF), which activates the JAK-STAT3 pathway, as sufficient to allow mESCs to self-renew in the absence of feeders, without compromising pluripotency (Niwa *et al.*, 1998; Smith *et al.*, 1988). Recently, the transcription factor TFCP2L1 was identified as being a crucial mediator of LIF-dependent pluripotency (Martello *et al.*, 2013). Smith's group would then define the first serum- and feeder-free medium for the culture of mESCs, which combined Bone Morphogenetic Protein 4 (BMP4) with LIF (Ying *et al.*, 2003).

Although they were derived in a manner similar to that used for mESCs, hESC maintenance cannot be sustained with mESC medium formulations. Instead hESC medium requires supplementation with Fibroblast Growth Factor 2 (FGF2), Transforming Growth Factor- β (TGF- β)/Activin A, and a synthetic serum-replacement (Vallier *et al.*, 2005; Xu *et al.*, 2005a, 2005b). The differences between mouse and human ESCs were initially attributed to unknown genetic differences between species. However, the derivation of pluripotent cells from post-implantation mouse epiblasts (mEpiSCs), which like hESCs depended on FGF and TGF- β /Activin signaling to promote their self-renewal in a pluripotent state, suggested the existence of alternative pluripotent states (Brons *et al.*, 2007; Tesar *et al.*, 2007). Like hESCs, mEpiSCs can also be derived directly

from pre-implantation mouse embryos (Najm *et al.*, 2011). Moreover, ESCs can be converted into EpiSCs through culture in FGF/Activin, however conversion of EpiSCs into ESCs requires ectopic expression of an ancillary pluripotency associated transcription factor, *Klf4* (Guo *et al.*, 2009).

Although EpiSCs are capable of differentiating into all 3 germ layers *in vitro* and can form teratomas, they display distinct expression signatures and epigenetic features resembling that of hESC (Brons *et al.*, 2007; Tesar *et al.*, 2007). Mouse ESCs and EpiSCs express the core pluripotency factors *Oct4 (Pou5f1)*, *Sox2*, and *Nanog*, whereas ancillary pluripotency promoting transcription factors such as *Rex1*, *Klf4*, *Tbx3*, *Stella (Dppa3)* and *Esrrb* are highly expressed in mESCs, but not mEpiSCs (Festuccia *et al.*, 2012; Tesar *et al.*, 2007). Furthermore, mEpiSCs demonstrated elevated levels of lineage-specifying genes such as *Otx2*, *FoxA2*, and *Sox17*, suggesting that mEpiSCs are primed for lineage specification (Tesar *et al.*, 2007). This priming is thought to occur at enhancers associated with differentiation-associated genes, which are epigenetically repressed in ESCs and converted to an epigenetically active state in EpiSCs (Factor *et al.*, 2014). Although mESCs are readily capable of contributing to mouse chimeras when injected or aggregated with a pre-implantation blastocyst, no chimeras were observed with mEpiSCs (Brons *et al.*, 2007; Tesar *et al.*, 2007; Wood *et al.*, 1993). However, mEpiSCs derived from post-implantation embryos or mESCs, readily form chimeras when injected into post-implantation embryos, whereas mESCs injected into post-implantation embryos do not (Huang *et al.*, 2012).

These studies indicate that mESCs lie upstream of the more developmentally advanced and differentiation-primed mEpiSCs and hESCs. Thus, mESCs represent the “naïve”, whereas mEpiSCs and hESCs represent the “primed” pluripotent states, each relying on distinct signaling cues for self-renewal (Figure 4). Notably, hESCs are thought to be less primed, as they express elevated levels of NANOG as well as REX1, which is not expressed in mEpiSCs (Chia *et al.*,

2010). Multiple pluripotent states also exist *in vivo*, as single-cell transcriptome analyses have revealed that mESCs closely resemble the epiblast of E4.5 blastocysts, whereas EpiSCs are similar to epiblasts of late-PS stage embryos (Boroviak *et al.*, 2014; Kojima *et al.*, 2014). Furthermore, culture of mouse epiblast explants and hESCs in FGF2 and IWR1, an inhibitor that stabilizes the β -catenin destruction complex, allowed for the generation of a novel pluripotent-state with distinct epigenetic and transcriptional profiles, called region-selective pluripotent stem cells (rsPSCs) (Wu *et al.*, 2015). Importantly, both naïve and primed pluripotent cells exhibit heterogeneity, with subpopulations that display unique transcriptional and epigenetic profiles, leading to biased developmental potentials (Hayashi *et al.*, 2008; Hough *et al.*, 2014; Kumar *et al.*, 2014; Tsakiridis *et al.*, 2014).

1.4.2 The core pluripotency transcriptional network

Although pluripotency clearly exists in different states with unique characteristics, it is broadly governed by an extended interconnected pluripotency gene regulatory network established by a core set of core transcription factors, OCT4, SOX2, and NANOG. OCT4 is expressed in the epiblast and is essential for the establishment of pluripotency in the embryo as well as in ESCs (Nichols *et al.*, 1998; Niwa *et al.*, 2000). Similarly, SOX2 is required for pluripotency in the epiblast and ESCs (Avilion *et al.*, 2003; Masui *et al.*, 2007). Ectopic expression of *Oct4* is able to rescue ES cells from differentiation caused by the loss of *Sox2*, suggesting that *Sox2* regulates *Oct4* expression (Masui *et al.*, 2007). While the deletion of *Oct4* or *Sox2* promotes the differentiation of the epiblast into trophectoderm, overexpression of OCT4 or SOX2 leads to the differentiation into mesendoderm and neural ectoderm, respectively, implying that OCT4 and SOX2 levels need to be tightly regulated in order to promote the pluripotent state (Niwa *et al.*, 2000; Zhao *et al.*, 2004).

Conversely, overexpression of Nanog in ESCs is capable of promoting self-renewal and the pluripotent state independently of LIF (Chambers *et al.*, 2003; Mitsui *et al.*, 2003). NANOG deficient embryos fail to generate an epiblast and ESCs lacking NANOG demonstrate an increased propensity to differentiate, suggesting that NANOG is important in the acquisition and maintenance of pluripotency (Chambers *et al.*, 2003; Mitsui *et al.*, 2003). However, NANOG has been shown to be dispensable for ESC self-renewal and pluripotency, with downregulation of NANOG predisposing, but not marking lineage commitment, suggesting instead that NANOG stabilizes the pluripotent state (Chambers *et al.*, 2007).

OCT4 and SOX2 upregulate the expression of each other as well as *Nanog*, co-operatively binding as heterodimers at enhancer or promoter elements, thereby forming an interconnected feedforward regulatory loop (Chew *et al.*, 2005; Mitsui *et al.*, 2003; Rodda *et al.*, 2005). Analysis of the global distribution of OCT4, SOX2 and NANOG in both mouse and human ESCs revealed that these factors co-occupy a largely overlapping set of pluripotency-associated target genes, including their own promoters (Boyer *et al.*, 2005; Chen *et al.*, 2008; Kim *et al.*, 2008; Loh *et al.*, 2006; Marson *et al.*, 2008). Gene expression analyses undertaken after perturbation of the core transcription factors OCT4, SOX2, or NANOG revealed that co-occupied target genes were both active and repressed genes, implying context-specific regulation by OCT4, SOX2, and NANOG (Boyer *et al.*, 2005; Chen *et al.*, 2008; Kim *et al.*, 2008; Loh *et al.*, 2006). Transcriptionally active target genes were associated with chromatin remodelling, epigenetic modification of histones, and maintenance of ESC self-renewal, and included OCT4, SOX2, and NANOG themselves, as well as ancillary transcription factors belonging to the pluripotency network (Boyer *et al.*, 2005; Kim *et al.*, 2008; Loh *et al.*, 2006). Conversely, transcriptionally repressed genes bound by the core pluripotency transcription factors were related to differentiation and lineage commitment in the mammalian early embryo (Boyer *et al.*, 2005; Kim *et al.*, 2008; Loh *et al.*, 2006). Additionally,

the extrinsic pathways that promote self-renewal such as FGF2, TGF- β , LIF and BMP4 have all been shown to integrate their pathway specific transcription factors together with OCT4 to promote and maintain the expression of *Oct4*, *Sox2*, and *Nanog* (Chen *et al.*, 2008; Xu *et al.*, 2008).

Tight regulation of OCT4, SOX2, and NANOG expression is required for maintenance of the pluripotent state but can be buffered by ancillary pluripotency-related genes, whereas fluctuations in OCT4, SOX2, and NANOG in response to differentiation cues, or lineage-specific transcription factors, are required for specification of the three germ layers. Nanog suppression is required for differentiation to both neurectoderm and mesendoderm (Thomson *et al.*, 2011). However, OCT4 expression levels are maintained, and SOX2 is reduced, in mesendodermal differentiation (Thomson *et al.*, 2011). Conversely, SOX2 expression is maintained during neurectoderm specification and OCT4 is repressed (Thomson *et al.*, 2011). Intriguingly, OCT4 occupancy has been shown to be rearranged through interactions with OTX2, in response to activation of pathways associated with primed pluripotency such as FGF2 or TGF- β . Instead of binding *cis*-regulatory regions of pluripotency genes, it is recruited onto to enhancers related to early developmental and differentiation genes (Buecker *et al.*, 2014; Factor *et al.*, 2014). Taken together, these studies suggest that the core pluripotency transcription factors bind to enhancer/promoters of genes crucial for the maintenance of the pluripotent state as well as for lineage commitment, promoting or suppressing their expression in response to context-dependent extracellular signaling cues.

1.4.3 Wnt signaling in ESC self-renewal and pluripotency

Given the crucial role of Wnt signaling in the formation of the PS and mammalian gastrulation, it is no surprise that Wnt signaling also regulates the pluripotent state. The first indication that Wnt signaling could enhance self-renewal was revealed when treatment of mESCs and hESCs with recombinant Wnt3a, Wnt3a-conditioned medium, or BIO, a GSK-3 inhibitor, in

the absence of exogenous LIF, was shown to promote self-renewal and pluripotency (Sato *et al.*, 2004b). However, Wnt3a-conditioned medium appeared to be most effective, as it did not have the off-target effects of BIO, and was much more potent than recombinant Wnt3a, presumably due to synergism with low levels of LIF in the conditioned medium.

Synergism between Wnt and LIF signaling has been observed via ectopic expression of β -catenin, which reduces the dose of LIF required for mESC maintenance and allows mESC growth on C-STO feeders in the absence of exogenous LIF, which is otherwise required to support mESC expansion (Hao *et al.*, 2006; Ogawa *et al.*, 2006). Conversely, many groups have also suggested that Wnt signalling is dispensable for the maintenance of the pluripotent state. *β -catenin* null mESCs express pluripotency associated genes and readily self-renew in the presence of LIF and serum, (Lyashenko *et al.*, 2011; Wagner *et al.*, 2010; Wray *et al.*, 2011). Furthermore, rigorous culture of hESCs in a feeder-free system revealed that supplementation with Wnt3a was unable to promote long-term self-renewal, as hESCs gradually differentiated (Dravid *et al.*, 2005).

Wnt reporter activity is absent in self-renewing hESCs and is elevated upon their differentiation (Davidson *et al.*, 2012). Inhibition of endogenous Wnt signaling in hESCs, by using the inhibitor XAV-939, a Tankyrase inhibitor that stabilizes Axin2, had no effects on self-renewal, whereas Wnt3a treatment elevated transcripts of mesodermal lineage markers (Davidson *et al.*, 2012). Moreover, sorting of hESCs based on endogenous Wnt signaling leads to distinct lineage commitment (Blauwkamp *et al.*, 2012). These contradicting studies point to a potentially limited role for Wnt signaling in the regulation of the pluripotent state.

Counter-intuitively, a definitive role for Wnt signaling in mESC self-renewal was demonstrated by studies examining the FGF signaling pathway. FGF4 is a secreted growth factor that activates the MEK/ERK signaling cascade, facilitating mESC lineage commitment by

transitioning them to a primed state, where they are susceptible to additional lineage specifying signals (Kunath *et al.*, 2007; Lanner *et al.*, 2010; Stavridis *et al.*, 2007). Both *Fgf4* and *Erk2* null mESCs display compromised differentiation toward neural and mesendodermal lineages (Kunath *et al.*, 2007; Stavridis *et al.*, 2007).

Austin Smith and colleagues demonstrated that inhibitors SU5402 or PD184352, which inhibit FGF receptor tyrosine kinases and the MEK/ERK cascade, respectively, in combination with LIF, replaced the requirement for serum/BMP4 in promoting long-term mESC self-renewal (Ying *et al.*, 2008). However, mESCs survived poorly at clonal density when cultured in defined medium with the inhibitors alone (Ying *et al.*, 2008). As BIO-mediated GSK-3 inhibition appeared to stimulate short-term self-renewal of mESCs, Smith's group examined the effects of a more selective GSK-3 inhibitor, CHIR09921 (CHIR), determining that in the absence of LIF and serum, treatment with CHIR enhanced short-term self-renewal (Ying *et al.*, 2008). CHIR was then combined with a more potent MEK/ERK inhibitor, PD0325901 (PD), a cocktail known collectively as "2i", which enabled robust self-renewal and maintenance of pluripotency in mESCs in the absence of exogenous factors (Ying *et al.*, 2008).

Mechanistically, PD has been shown to prevent ERK-dependent phosphorylation and subsequent degradation of KLF2, an essential ancillary pluripotency transcription factor in 2i (Yeo *et al.*, 2014). CHIR functions through stabilized β -catenin, as *β -catenin* mutant mESCs were unable to self-renew in 2i (Faunes *et al.*, 2013; Lyashenko *et al.*, 2011; Wray *et al.*, 2011). Importantly, 2i medium, when supplemented with LIF, has allowed for the derivation of pluripotent stem cells from strains of mice as well as rats, which had been impossible with previous media formulations (Nichols and Smith, 2009; Wray *et al.*, 2010). Furthermore, recent culture conditions that support the derivation of naïve pluripotent hESCs from blastocysts or pre-existing 'primed' hESC lines, all employ 2i in combination with LIF, as well as additional inhibitors,

ectopic expression of ancillary pluripotent transcription factors, and in some cases FGF/Activin (Gafni *et al.*, 2013; Guo *et al.*, 2016; Hanna *et al.*, 2010; Takashima *et al.*, 2015; Theunissen *et al.*, 2014; Ware *et al.*, 2014).

At the transcript level, 2i significantly reduces the expression of genes associated with mesoderm and ectoderm lineages, in comparison to conventional serum and LIF (Marks *et al.*, 2012). This is a consequence of increased transcriptional pausing of RNA pol II and a reduction in the repressive histone mark H3K27me3 at these silenced genes, concomitantly reducing the number of lineage-specifying genes transcriptional poised with the bivalent histone marks H3K4me3 and H3K27me3 (Marks *et al.*, 2012). Additionally, the pluripotent state is stabilized in mESCs cultured in 2i, as the expression of ancillary pluripotent transcription factors such as *Klf2*, *Stella*, *Esrrb*, and *Tfcp2l1* is increased (Galonska *et al.*, 2015; Marks *et al.*, 2012; Martello *et al.*, 2012; Yeo *et al.*, 2014). In line with this, mESCs cultured in 2i exhibit a more uniform expression of the core pluripotent factors OCT4, SOX2, and NANOG, whose binding undergoes a rapid and widespread reorganization upon the transition from LIF and serum to 2i conditions (Galonska *et al.*, 2015; Silva *et al.*, 2009; Wray *et al.*, 2010). In 2i, distal enhancer sites displayed differential OCT4, SOX2, and NANOG binding and activity, and were enriched for TCF/LEF motifs (Galonska *et al.*, 2015). Therefore, these studies comparing mESCs cultured in 2i vs conventional LIF and serum suggested that conventional mESCs grown in LIF and serum represent a more developmentally advanced state, whereas mESCs captured in 2i represented the naïve ‘ground state’ of pluripotency.

In the naïve pluripotent state, endogenous Wnt signaling clearly reinforces self-renewal and pluripotency, as addition of IWP2, an inhibitor of Porcupine, an essential factor required for Wnt secretion, promoted the conversion of mESCs and naïve hESCs into mEpiSCs and primed hESCs (ten Berge *et al.*, 2011; Xu *et al.*, 2016). Strikingly, localized Wnt signals have been shown

to promote asymmetric cell divisions in mESCs, with the proximal daughter cell self-renewing and the distal cell differentiating (Habib *et al.*, 2013). Furthermore, treatment of mESCs with Wnt3a is sufficient to prevent their differentiation into EpiSCs. However, this has not been tested in naïve hESCs (ten Berge *et al.*, 2011; Xu *et al.*, 2016).

On the other hand, as was already discussed for conventional hESCs above, in the primed state, Wnt signaling appears to promote differentiation (Davidson *et al.*, 2012). Similar to primed hESCs, endogenous Wnt signaling promotes differentiation in mouse EpiSCs, whereas inhibition of endogenous Wnt signals via IWP2 or XAV, or β -catenin deletion, prevents mEpiSC specification into early lineages and also blocks hESC differentiation (Greber *et al.*, 2010; Kurek *et al.*, 2015; Sumi *et al.*, 2013).

Differentiation mediated by endogenous Wnt signals is thought to occur in a specific subpopulation of mouse EpiSCs that reversibly expresses markers of early PS formation, which confers a mesendodermal differentiation bias (Tsakiridis *et al.*, 2014). β -catenin is not required for the transition of naïve mESCs to primed mEpiSCs (Sumi *et al.*, 2013; Wray *et al.*, 2011). Given the requirement for β -catenin in the self-renewal of mESCs in 2i, this potentially suggests that conventionally cultured β -catenin knockout mESCs are in a primed pluripotent state. Indeed, *β -catenin* null mESCs express lower levels of OCT4 and NANOG and display higher levels of differentiation even when cultured in the ground state with LIF + 2i (Faunes *et al.*, 2013).

Although understanding ESC self-renewal is important for developing strategies aimed at growing large numbers of them for regenerative medicine purposes, the ultimate goal is to direct differentiation into specific developmental lineages. Much like its role in the embryo, Wnt signaling has been implicated in the formation of PS-like structures and mesendodermal lineage commitment during the differentiation of ESCs *in vitro*. This role for Wnt signaling was first

demonstrated in mESCs expressing reporters for two genes crucial for PS formation *FoxA2* and *T*, in which treatment with Wnt and Activin in serum-free conditions, promoted a posterior primitive streak identity (Gadue *et al.*, 2006). Similarly, spontaneous differentiation of mESCs as embryoid bodies revealed localized activation of a Wnt reporter coupled with induction of an EMT as well as expression of PS and mesendodermal markers (ten Berge *et al.*, 2008). In hESCs, β -catenin is required in order for cooperative Wnt and Activin signals to induce the expression of PS markers (Funa *et al.*, 2015). β -catenin is recruited to regulatory regions upstream of PS genes by OCT4, resulting in upregulation of their expression in cooperation with SMAD2/3 downstream of Activin signaling (Funa *et al.*, 2015). Thus, establishing a PS transcriptional programme requires inputs from Wnt and Activin signaling, followed by cooperative transcriptional activation by β -catenin and SMAD2/3.

As PS formation is required for mesendodermal specification in embryogenesis, it is not surprising that in mESCs, Wnt signaling is involved in the regulation mesendodermal lineage commitment. Prolonged culture of mESCs in Wnt3a-conditioned medium, the GSK-3 inhibitor LY2090314, or ectopic expression of Wnt3a results in activation of mesendodermal as well as primitive endoderm markers and biased differentiation towards these lineages (Bakre *et al.*, 2007; Price *et al.*, 2013). PS formation and gastrulation requires β -catenin downstream of Wnt signaling, consequently β -catenin null mESCs display an inability to differentiate into mesendodermal lineages *in vitro* (Lyashenko *et al.*, 2011; Wagner *et al.*, 2010). β -catenin's junctional role was determined to be required for endoderm specification, as ectopic expression of a β -catenin mutant lacking its C-terminal transactivation domain, in *β -catenin* mutant mESCs, was able to restore endodermal differentiation (Lyashenko *et al.*, 2011). However, β -catenin's N-terminus has been shown to mediate reading of epigenetic modified histones through interactions with BCL9 and

Pygopus, which could be critical in the regulation of endoderm-specifying genes (Kramps *et al.*, 2002; Valenta *et al.*, 2011). In support of this, BCL9 is required for maximal *Nanog* expression in mESCs, with NANOG and β -catenin activating PS genes during differentiation (Faunes *et al.*, 2013; Trott and Arias, 2013). The C-terminal β -catenin mutant was incapable of rescuing *T* expression, indicating that β -catenin's C-terminal transcriptional activity is necessary for mesoderm differentiation (Lyashenko *et al.*, 2011).

In addition to mesendodermal differentiation defects observed upon genetic deletion of Wnt signaling components, various developmental ectodermal abnormalities are observed upon ablation of *Tcf7l1* and *Wnt1* (McMahon and Bradley, 1990; Merrill *et al.*, 2004). In ESCs similar perturbations in Wnt signaling cause neurectodermal lineage commitment deficiencies, as *Apc* or GSK-3 deficient mESCs, which both display elevated levels of β -catenin, display severe neurectodermal differentiation defects, retaining expression of pluripotency genes such as *Oct4* and *Nanog* in *in vitro* assays and in teratomas (Doble *et al.*, 2007; Kielman *et al.*, 2002). This neurectodermal blockade in response to elevated Wnt signaling is β -catenin-dependent, but TCF/LEF-independent, as knockdown of β -catenin in GSK-3 null mESCs efficiently restored neurectodermal differentiation, whereas overexpression of dnTCF7L2, which effectively reduced activation of Wnt target genes, was unable to do so (Kelly *et al.*, 2011). Elevated β -catenin levels are thought to reinforce self-renewal at the expense of neurectodermal differentiation by binding OCT4, increasing transactivation of auxiliary transcription factors belonging to the pluripotent network (Kelly *et al.*, 2011). The potential for atypical mechanisms or compensation in the regulation of target genes by the TCF/LEFs, were not addressed in this study. Interestingly, neurectodermal differentiation is similarly inhibited by genetic ablation of *β -catenin* in mESCs,

with ectopic expression of a C-terminal β -catenin mutant in β -catenin knockout mESCs restoring differentiation (Lyashenko *et al.*, 2011).

Collectively, these studies clearly implicate Wnt signaling in the regulation of self-renewal and differentiation of ES cells. Pluripotency appears to represent a spectrum of developmental states requiring an intricate balance and fine-tuning of Wnt signaling to promote self-renewal of ES cells along the spectrum. Furthermore, these studies highlight the context-dependent outcomes that arise from crosstalk between different extrinsic lineage specifying cues and Wnt signaling.

1.4.4 TCF/LEF regulation of ESC self-renewal and pluripotency

As the TCF/LEF factors are the best characterized effectors downstream of β -catenin, there has been concerted focus on understanding how these factors function to mediate regulation of ESC self-renewal and differentiation via Wnt signaling. All of the TCF/LEF factors are expressed at the transcript and protein level in undifferentiated ES cells and demonstrate differential binding and transactivation of the Wnt target genes *Axin2*, *Cdx1*, and *T* (Kelly *et al.*, 2011; Pereira *et al.*, 2006; Sierra *et al.*, 2018; Wallmen *et al.*, 2012; Wöhrle *et al.*, 2007). As mESCs exit the pluripotent state and differentiate, TCF/LEF activity increases, as measured by reporter activity (Chatterjee *et al.*, 2015). Despite studies implicating all four TCF/LEF factors as crucial regulators of pluripotency downstream of Wnt signaling, TCF7L1 has been the most extensively characterized family member in ESCs.

Tcf7l1

In undifferentiated conventionally cultured mESCs and hESCs, *Tcf7l1* is the most abundantly expressed TCF/LEF factor at the transcript level (Pereira *et al.*, 2006; Sierra *et al.*, 2018). TCF7L1 was first implicated as a negative regulator of the pluripotent state after *Tcf7l1* null mESCs displayed increased proliferation and delayed differentiation (Pereira *et al.*, 2006). TCF7L1 was shown to directly bind and repress the *Nanog* promoter, explaining the delay in

differentiation, which was attributed to elevated *Nanog* transcript and protein levels (Pereira *et al.*, 2006). Interestingly, two different alternatively spliced *Tcf7l1* isoforms are expressed in mESCs, but knockdown of either isoform similarly delays differentiation (Salomonis *et al.*, 2010). These studies suggest that TCF7L1 is required for efficient differentiation of mESCs. In support of this, TCF7L1 is required for rapid transition into the primed pluripotent state, at which point mESCs become sensitized to Wnt-mediated specification of mesendodermal differentiation (Hoffman *et al.*, 2013). Despite TCF7L1 being dispensable for neurectodermal differentiation, overexpression of *Tcf7l1* in *Apc* mutant mESCs is able to partially restore neurectodermal differentiation (Atlasi *et al.*, 2013). Conversely, TCF7L1 is dispensable for endodermal differentiation, as *Tcf7l1* null mESCs no longer require active Wnt signals to initiate endodermal lineage specification (Morrison *et al.*, 2016). Combined, these studies show a crucial role for TCF7L1 in the regulation of mESC self-renewal and pluripotency.

Significant insights into understanding the mechanisms of TCF7L1 regulation of the pluripotent state came from examination of TCF7L1's chromatin occupation, which revealed a large degree of overlap with OCT4, SOX2, and NANOG, with all four factors co-occupying the promoters of many pluripotency-associated genes, including *Oct4*, *Sox2*, *Nanog*, and *Tcf7l1* (Cole *et al.*, 2008; Marson *et al.*, 2008; Tam *et al.*, 2008). This co-occupancy of OCT4, SOX2, NANOG and TCF7L1 is thought to occur at super-enhancers conferring enhanced responsiveness of genes involved in cell identity to signaling cues (Hnisz *et al.*, 2015).

Further breakthroughs were made via the transcriptional profiling of *Tcf7l1* null mESCs, which revealed that ablation of *Tcf7l1* had opposing transcriptional effects compared to knockdown of *Oct4* and *Nanog* (Yi *et al.*, 2008, 2011). Similarly, knockdown of *Tcf7l1* in mESCs caused an upregulation in *Oct4*, *Sox2*, *Nanog* and other pluripotency-associated genes (Cole *et al.*, 2008; Salomonis *et al.*, 2010; Tam *et al.*, 2008). TLE2 was found to co-occupy many TCF7L1

bound sites, suggesting TLE-mediated target gene repression in the absence of Wnt stimulation (Tam *et al.*, 2008). Intriguingly, gene expression profiling of mESCs treated with Wnt3a demonstrated a correlation between genes activated upon Wnt stimulation or loss of *Tcf7l1*, suggesting that Wnt signaling promotes the pluripotent state through TCF7L1- β -catenin transcriptional activation complexes (Cole *et al.*, 2008; Yi *et al.*, 2011). Collectively, these studies suggest that TCF7L1 is an integral component of the core pluripotent transcriptional network, acting as a rheostat to fine-tune network output, promoting self-renewal or lineage commitment, depending on the state of Wnt signaling.

However, subsequent studies from the groups of Austin Smith and Bradley Merrill proposed that Wnt-stabilized β -catenin primarily functioned to suppress TCF7L1-mediated repression. This was based on the finding that activation of the Wnt pathway was required for TCF7L1-overexpressing mESCs to self-renew (Wray *et al.*, 2011; Yi *et al.*, 2011). Examining global gene expression changes revealed that *Tcf7l1* deletion and Wnt3a stimulation similarly upregulated a common set of pluripotency-associated genes, independent of increased *Nanog* (Yi *et al.*, 2011). Moreover, *dnTcf7l1* knock-in mESCs displayed a partial inability to self-renew in response to Wnt3a or GSK-3 inhibition (Wray *et al.*, 2011; Yi *et al.*, 2011). By contrast, loss of *Tcf7l1* in mESCs alleviated the requirement for GSK-3 inhibition when mESCs were cultured in the pluripotent ground state with 2i medium (Wray *et al.*, 2011; Yi *et al.*, 2011).

Derepression of TCF7L1 does not require the transactivating C-terminus of β -catenin, implying that activating TCF7L1- β -catenin complexes are not required for Wnt stimulation of self-renewal (Wray *et al.*, 2011). In mESCs, TCF7L1 is unable to activate a TCF/LEF reporter, even in the presence of β -catenin, further supporting an inability of TCF7L1 to serve as a Wnt-responsive transcriptional activator (Yi *et al.*, 2011). Wnt-stabilized β -catenin mediated

derepression of TCF7L1 has been linked to the upregulation of *Esrrb* (Martello *et al.*, 2012). ESRRB was required for the enhancement of self-renewal elicited by GSK-3 inhibition, and overexpression of ESRRB was able to substitute for CHIR in 2i medium (Martello *et al.*, 2012). Despite the identification of *Esrrb* as a target downstream of β -catenin-dependent TCF7L1 derepression, the precise mechanisms of derepression remain poorly understood.

Part of the derepression mechanism is the regulation of *Tcf7l1* itself, at both the transcript and protein levels. Regulation of *Tcf7l1* transcript and protein levels was first observed in *Apc* mutant mESCs, which displayed significantly reduced *Tcf7l1* transcript and TCF7L1 protein levels (Atlasi *et al.*, 2013). Similarly, *Tcf7l1* transcript and protein expression levels were also reduced in wildtype mESCs treated with Wnt3a-conditioned medium or a GSK-3 inhibitor (Atlasi *et al.*, 2013). In response to Wnt signaling, a reduction in the histone marks H3K4me3 and H3Ac was observed near the *Tcf7l1* transcriptional start site, suggesting Wnt-dependent epigenetic regulation of *Tcf7l1* expression (Atlasi *et al.*, 2013). Upstream of this epigenetic regulation, c-MYC was shown to mediate the downregulation of *Tcf7l1* in response to GSK-3 inhibition (Morrison *et al.*, 2016). Moreover, profiling the expression of microRNAs revealed that mmu-miR-211 was specifically upregulated upon Wnt signaling activation, and when overexpressed, was able to post-transcriptionally reduce TCF7L1 protein levels (Atlasi *et al.*, 2013). Additional post-transcriptional regulation of *Tcf7l1* transcript is facilitated by the microRNA processor DGCR8, which directs splicing of *Tcf7l1* into the long and short isoforms (Cirera-Salinas *et al.*, 2017). Interestingly, the two isoforms demonstrated opposing effects on self-renewal and differentiation, as the short TCF7L1 isoform, promoted, whereas the long TCF7L1 isoform, inhibited, exit from the pluripotent state (Cirera-Salinas *et al.*, 2017).

Combined, these studies suggest that *Tcf7l1* is regulated at both the transcript and post-transcriptional levels. However, none of these studies demonstrated a specific role for β -catenin in

this regulation. A study by Merrill's group provided a breakthrough, describing β -catenin-dependent regulation of TCF7L1 DNA binding and protein stability (Shy *et al.*, 2013). β -catenin binding to TCF7L1 was shown to mediate the removal of TCF7L1 from Wnt target genes, targeting it for β -catenin-directed proteasomal degradation (Morrison *et al.*, 2016; Shy *et al.*, 2013).

A recent study in hESCs challenges the notion that Wnt-stabilized β -catenin primarily functions through the derepression of TCF7L1, rather it suggests that β -catenin-TCF7L1 complexes are capable of activating Wnt target genes. The p53 family has been shown to be necessary for mesendodermal specification by enabling SMAD2/3 occupancy at mesendodermal genes downstream of Activin/Nodal (Wang *et al.*, 2017).

Strikingly, TCF7L1 was the most abundant TCF/LEF factor at mesendodermal genes and TCF7L1- β -catenin and SMAD2/3 complexes were shown to cooperatively bind and activate mesendodermal genes (Wang *et al.*, 2017). *Wnt3* and its coreceptor *Fzd1* were direct p53 target genes, suggesting that p53 coordinates Wnt and Activin signaling in order to promote mesendodermal specification in hESCs (Wang *et al.*, 2017). Similarly, examination of the distribution of TCF7L1 and β -catenin on the chromatin revealed that both factors bind an overlapping set of genes corresponding to PS formation (Sierra *et al.*, 2018). Conversely, contradicting its role in mESCs, TCF7L1 displayed minimal overlap with OCT4 and NANOG in hESCs, presumably highlighting the different roles Wnt plays in the regulation of the naïve vs primed pluripotent states (Sierra *et al.*, 2018). Moreover, TCF7L1 gain- and loss-of-function studies led to the conclusion that TCF7L1 promotes the pluripotent state by suppressing genes involved in PS formation (Sierra *et al.*, 2018). However, this study did not determine the effects of Wnt activation on TCF7L1, and therefore TCF7L1 could potentially be converted to an activator through β -catenin interactions, promoting PS gene expression and formation.

Tcf7

In mESCs and hESCs, *Tcf7* is the second and third most abundant expressed TCF/LEF member, respectively, at the transcript level (Pereira *et al.*, 2006; Sierra *et al.*, 2018). Several experiments by Yi *et al.* indicated that TCF7 could be playing important roles in the regulation of pluripotency in mESCs. Firstly, it was observed that stimulation with Wnt3a was able to activate a group of genes regardless of the presence of TCF7L1 and instead were elevated to higher levels in the absence of TCF7L1 (Yi *et al.*, 2011). Secondly, the partial inability of *dnTcf7l1* knock-in mESCs to self-renew in response to Wnt activation indicated that other TCF/LEFs could be crucial for Wnt-mediated reinforcement of self-renewal (Yi *et al.*, 2011). In support of this, knockdown of *Tcf7* in wildtype mESCs and *dnTcf7l1* knock-ins decreased Wnt3a-mediated self-renewal (Yi *et al.*, 2011). Similarly, *Tcf7* knockdown reduced the expression of self-renewal genes stimulated by Wnt3a in wildtype, *Tcf7l1* knockout, and *dnTcf7l1* knock-in mESCs. Furthermore, β -catenin occupancy was reduced at pluripotency-associated genes by ablation of *Tcf7l1* and was further reduced by subsequent knockdown of *Tcf7* (Yi *et al.*, 2011). Despite this, OCT4 occupancy was increased in *Tcf7l1* null mESCs, suggesting that the β -catenin-OCT4 interaction was facilitated by TCF7L1 (Yi *et al.*, 2011). Collectively, these experiments suggest the requirement for potential TCF/LEF switching in response to Wnt stimulation, in which β -catenin-mediated derepression of TCF7L1 allows for the subsequent activation of target genes by β -catenin-TCF7 complexes.

Challenging this mechanism, a recent study disrupting β -catenin-TCF transcriptional activity, using iCRT3, an inhibitor that prevents interactions between β -catenin and TCF7 or TCF7L2 specifically, increased the expression of pluripotency-associated genes in medium containing LIF and serum and promoted their retention during differentiation (Chatterjee *et al.*, 2015). Similar to *Tcf7l1* ablation, knockdown of *Tcf7* was shown to prevent mESC differentiation, and was associated with increased levels of *Nanog* in conditions promoting self-renewal or

differentiation (Chatterjee *et al.*, 2015). Strikingly, substitution of CHIR with iCRT3 is able to maintain ground state pluripotency (Saj *et al.*, 2017). A comparison of the global genomic distributions of TCF7 and TCF711 revealed a minimal overlap, with TCF7 associating with cell-cycle related genes (De Jaime-Soguero *et al.*, 2017). Wnt stimulation of mESCs reduced their proliferation and lengthened the G1 phase, as a result of upregulated cell cycle genes by β -catenin-TCF7 complexes (De Jaime-Soguero *et al.*, 2017). Taken together, these studies contradict the findings by Yi *et al.*, suggesting that TCF7 regulates a unique set of target genes, promoting differentiation and reducing mESC proliferation. One explanation could be that deletion of *Tcf711* liberates previously occupied target genes, allowing TCF7 and other TCF/LEF factors to substitute for TCF7L1 function in the pluripotent state.

Lef1 and Tcf712

Unlike, *Tcf711* and *Tcf7*, the functional roles of *Lef1* and *Tcf712* have been underappreciated and significantly less characterized in mESCs. At the transcript level, *Lef1* and *Tcf712* are the 3rd and 4th most abundant TCF/LEF family members in mESCs cultured in LIF and serum, respectively (Pereira *et al.*, 2006). However, in undifferentiated conventional hESCs, *TCF7L2* is the second most abundant transcript, whereas *LEF1* is the least abundantly expressed family member (Sierra *et al.*, 2018). Interestingly, in mESCs, *Lef1* expression requires β -catenin-mediated derepression of TCF7L1 at an enhancer element (Wu *et al.*, 2012). Functionally, LEF1 activates, whereas TCF7L2 represses, a TCF/LEF reporter in mESCs, even in the presence of β -catenin (Yi *et al.*, 2011). Besides the inability of dnTCF7L2 to restore neuroectodermal differentiation, despite effectively repressing detectable TCF activity in GSK-3 knockout mESCs, and the potential enhancement of self-renewal by iCRT3 via inhibition of TCF7L2- β -catenin interactions, nothing else is known of a potential role for TCF7L2 in the pluripotent state (Chatterjee *et al.*, 2015; Kelly *et al.*, 2011).

On the other hand, ectopic expression of *Lef1* has been shown to promote the expression of pluripotency-associated factors including *Oct4* and *Nanog*, whereas *Lef1* knockdown has been shown to cause differentiation (Huang and Qin, 2010). Conversely, *Lef1* expression is downregulated by both PD and LIF in serum-free conditions and overexpression of *Lef1* has been shown to promote differentiation (Ye *et al.*, 2017). Furthermore, knockdown of *Lef1* partially alleviates the requirement for PD in the ground state (Ye *et al.*, 2017). These conflicting studies could potentially be explained by differences in pluripotent states due to differing culture conditions/practices. In hESCs, treatment with Wnt3a promotes mesendodermal differentiation. This induces a significant overlap in LEF1 and β -catenin occupancy at enhancers of mesendodermal genes, as determined by ChIP-seq (Estarás *et al.*, 2014). RNA pol II and transcription are paused at these genes despite LEF1- β -catenin-mediated formation of chromatin loops through interactions with Cohesin (Estarás *et al.*, 2014). Stimulation with Activin, and subsequent recruitment of SMAD2/3 to these mesendodermal genes, allows RNA pol II to escape the pause and proceed with productive transcript elongation (Estarás *et al.*, 2014). Taken together, these studies suggest that LEF1 and TCF7L2 are underappreciated in ESC biology, and their effects on the pluripotent states warrant further investigation.

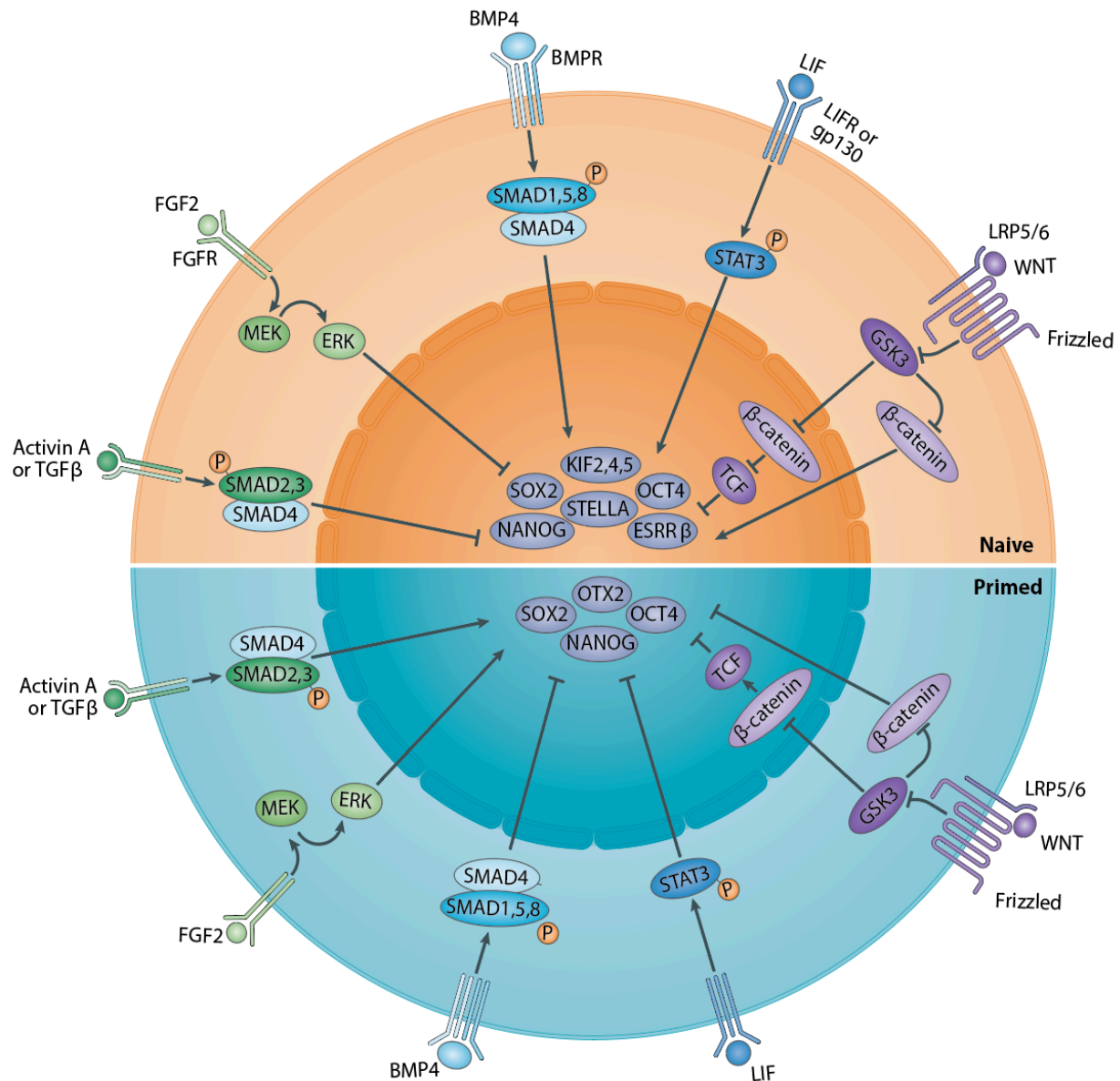


Figure 4. Signaling pathways and their effects on the naïve and primed pluripotent states.

The pathways discussed above have differential effects on the pluripotent state by influencing the core and ancillary pluripotent networks of transcription factors. Each signaling pathway has opposing effects on the naïve versus primed pluripotent states. For example, the Wnt signaling pathway in the naïve pluripotent state derepresses the repressive effects of the TCF/LEFs on the pluripotent network of transcription factors, thereby promoting self-renewal of cells in the naïve pluripotent state. Conversely, in the primed pluripotent state, activation of the Wnt signaling pathway causes β-catenin-TCF/LEF complexes to inhibit the pluripotent network of transcription factors and to promote the activation of lineage commitment genes, stimulating differentiation. Adapted from Weinberger *Nat Rev Mol Cell Biol* 2018.

SUMMARY OF INTENT

Appropriate spatio-temporal regulation of the Wnt/ β -catenin signaling cascade is essential throughout mammalian development and adult stem cell homeostasis. During development, the four members of the TCF/LEF family display distinct expression patterns, but there are regions of overlapping expression, with more than one factor being co-expressed in any given cell type (Korinek *et al.*, 1998a; Oosterwegel *et al.*, 1993). Genetic ablation of individual TCF/LEF factors in mice has demonstrated that specific knockouts produce markedly different phenotypes (van Genderon *et al.*, 1994; Korinek *et al.*, 1998b; Merrill *et al.*, 2004; Verbeek *et al.*, 1995). However, mouse studies of TCF/LEF double mutants develop much more severe embryonic lethal phenotypes, suggesting functional redundancy between TCF/LEF family members (Galceran *et al.*, 1999; Gregorieff *et al.*, 2004). *Tcf7l1* knockout mice are unique in that they are the only single gene TCF/LEF mutants that cause embryonic lethality (Merrill *et al.*, 2004). This can be explained by the fact that *Tcf7l1* transcripts are significantly more abundant than those of the other factors in mouse embryonic stem cells, with *Tcf7* transcripts being the next most abundant (Pereira *et al.*, 2006).

Our lab has played a key role in demonstrating that stimulation of the Wnt/ β -catenin pathway enhances ESC pluripotency. We have shown that mESCs devoid of GSK-3 display extremely elevated levels TCF- β -catenin signaling and a profound inability to differentiate into the three germ layers (Doble *et al.*, 2007). The effect of GSK-3 ablation on mESC biology was subsequently determined to rely on β -catenin through a mechanism independent of conventional TCF-mediated gene activation (Kelly *et al.*, 2011). Subsequent to our studies, TCF7L1 was shown to bind, in association with OCT4, SOX2, and NANOG, to genes related to maintenance of the pluripotent state and lineage commitment, acting as a transcriptional repressor to fine-tune their expression (Cole *et al.*, 2008; Marson *et al.*, 2008; Tam *et al.*, 2008; Yi *et al.*, 2008). Loss of *Tcf7l1*

led to an upregulation of these OCT4-, SOX2-, and NANOG-associated self-renewal and differentiation genes, which significantly correlated with genes upregulated upon Wnt3a treatment of mESCs (Cole *et al.*, 2008; Yi *et al.*, 2011).

This suggested that TCF7L1 behaved conventionally, repressing target genes in complex with a TLE corepressor and activating these genes upon Wnt-mediated stabilization of β -catenin. Conversely, derepression of TCF7L1 has been shown to be essential for the self-renewal enhancing effects of GSK-3 inhibition (Wray *et al.*, 2011). This derepression, is thought to employ a TCF switch between “repressive” TCF7L1 and “activating” TCF7, thereby activating Wnt/ β -catenin target genes and promoting the pluripotent state (Yi *et al.*, 2011). However, these experiments do not account for potential confounding functional compensation by other TCF/LEF factors. How TCF7L1 and TCF7 could be functioning differently to regulate the pluripotent state, despite the broad functional redundancies observed in TCF/LEF double-mutant mice, coupled with their similar functional domains, prompted me to ask a series of fundamental questions:

- 1) What is the degree of functional redundancy between TCF7 and TCF7L1 in mouse ES cells?
- 2) In mESCs, do TCF7 and TCF7L1 occupy the same Wnt Responsive Elements on the chromatin and how does Wnt activation effect their occupancy?
- 3) In mESCs, what proteins do TCF7 and TCF7L1 interact with, and what effect does Wnt stimulation have on these interactions?

Determining the degree of functional overlap between TCF7 and TCF7L1 would have important implications for understanding the role of Wnt signaling in cell fate decisions as well as cancer. Moreover, identifying TCF7- and TCF7L1-bound co-factors and target genes would help to determine whether a switch between repressive TCF7L1 and activating TCF7 is a universal mechanism for Wnt target gene activation. Importantly, this would provide insights into

mechanisms of TCF/LEF transcriptional regulation, both in the absence and presence of Wnt activation. Based upon this knowledge, **I hypothesize that both TCF7 and TCF7L1 will demonstrate functional redundancy by binding a largely overlapping set of target genes and interacting proteins.**

If this hypothesis holds true, in the absence and presence of a Wnt signal, both TCF7 and TCF7L1 should be able to bind similar epigenetic modulators and chromatin remodelers to regulate an overlapping set of target genes, imparting similar effects on maintenance of the pluripotent state and differentiation in mouse embryonic stem cells. To address my hypothesis, I devised the following specific objectives:

- 1) Investigate the phenotype of mESCs where all 4 TCF/LEF factors have been knocked-out and determine whether re-introduction of TCF7 or TCF7L1 at their endogenous loci can revert the phenotype to one more similar to wild-type.
- 2) Identify the TCF7 and TCF7L1 “targetome” through CHIP-seq and the effects of Wnt activation on target gene occupancy.
- 3) Identify the TCF7 and TCF7L1 “interactome” through BioID and elucidate the effects of Wnt activation on TCF7 and TCF7L1 protein interactions.

Through the implementation of CRISPR-Cas9 technology we were able to target and genetically ablate all four full-length TCF/LEF factors in mESCs, referred to as TCF/LEF **quadruple knockouts (QKOs)** (Chapter 2). These QKO mESCs demonstrated negligible activation of a TCF reporter and displayed enhanced self-renewal despite their proliferation being unaffected. Furthermore, QKO mESCs displayed delayed, neuroectoderm-biased, differentiation with defects in mesendoderm commitment, as assessed by embryoid bodies and teratomas. Importantly, re-introduction of 3xFLAG-tagged TCF7 or TCF7L1 at their endogenous loci using TALEN-facilitated homologous recombination, was able to rescue mesendodermal differentiation, despite

the differential TCF reporter transactivation capacities observed in each type of rescued cell line. Re-expression of either TCF7 or TCF7L1 resulted in similar global transcriptional changes and similarly reverted the transcriptome of QKO mESCs to resemble that of wildtype mESCs. This revealed that a switch between TCF7 and TCF7L1 was not an absolute requirement for Wnt target gene activation in mESCs. Overall, these results suggest that a single TCF/LEF factor, regardless of its reporter activation capability, is sufficient to appropriately regulate Wnt target genes and mediate effective trilineage differentiation of mESCs.

Following this body of work, we next sought to identify TCF7 and TCF7L1 target genes and the influence of Wnt stimulation on occupancy of TCF7 and TCF7L1 at these targets, by using chromatin immunoprecipitation followed by next-generation sequencing (ChIP-seq) (Chapter 3). To facilitate a true comparison between TCF7 and TCF7L1 ChIP-seq datasets, we created 3xFLAG-tag knock-ins at the endogenous loci of both genes using TALEN-facilitated homologous recombination in wildtype mESCs. TCF7L1 was more abundant than TCF7 at Wnt target genes and was much more highly expressed at the protein level in self-renewing and differentiating mESCs. Surprisingly, we found that neither TCF7 nor TCF7L1 negatively correlated with NANOG protein levels in self-renewing or differentiating mESCs. Mouse ES cells display peak activation of the Wnt signaling pathway 14 hours after the administration of the GSK-3 inhibitor CHIR, and TCF7L1 remains the most abundant TCF factor and binds more β -catenin than TCF7. ChIP-seq analysis of both TCF7 and TCF7L1 revealed distinct binding patterns, with minimal overlap in occupancy, in the absence and presence of CHIR. Furthermore, with and without CHIR, TCF7L1 was more abundantly associated with chromatin than TCF7, associating with genes related to maintenance of the pluripotent state. TCF7L1 remained highly associated with *Id3*, and *Id3* expression was responsive to GSK-3 inhibition in QKO mESCs rescued with TCF7L1. This

suggests that TCF7L1 predominantly mediates the effects of CHIR on the enhancement of mESC self-renewal and may be activating expression of pluripotency-associated genes.

As few TCF/LEF protein interactions have been described in the literature, other than the TLEs and β -catenin. We next identified putative TCF7L1 and TCF7 protein-protein interactions by using an unbiased technique, BioID, which is based on proximity-dependent biotinylation. This technique employs the use of a promiscuous biotin ligase mutant, BirA*, which is coupled to a bait protein, allowing for biotin labelling of vicinal proteins within a small radius.

Unfortunately, due to the low abundance of TCF7 in mESCs, we were unable to identify putative TCF7-interacting proteins. We introduced BirA* to the N-terminus of endogenous *Tcf7l1* and compared our BioID data from this approach with a doxycycline-inducible BirA*-TCF7L1 expression cassette overexpressed at the *Rosa26* locus. We identified 146 putative TCF7L1-proximal proteins in differentiating mESCs, consisting of predominantly epigenetic/transcription factors, in both BioID datasets and determined the effect of Wnt signaling activation on the Tcf7l1 interactome, by administering CHIR. Our study suggests that, despite the overexpression system being more likely to identify more false-positive hits, both BioID systems are capable of detecting important TCF/LEF transcriptional co-regulators. Importantly, there was a significant overlap in the biotinylated proteins identified by using both BioID systems, with the inducible system detecting more proximal proteins. Interestingly, treatment with CHIR caused an increase in detectable TCF7L1-proximal proteins despite reducing TCF7L1 protein levels. We validated the TCF7L1-interacting proteins, JMJD1C, SALL4 and SMARCA4 using proximity ligation and co-IP assays in self-renewing mESCs.

Overall, this thesis has advanced our understanding of the mechanisms that govern TCF/LEF-mediated Wnt target gene regulation by providing novel insights into the functional interplay between TCFs, the targets they bind, and the epigenetic modulators they use, as well as

the effects of Wnt activation on all of these properties. We have accomplished the following: 1) We identified a functional redundancy between two opposing TCFs, TCF7 and TCF7L1, which similarly restored the transcriptome and differentiation defects observed in cells lacking all four full-length TCF/LEF family members (Chapter 2); 2) We discovered minimal overlap in TCF7 and TCF7L1 genomic occupancy, with and without GSK-3 inhibition, with TCF7L1 being the most prevalent chromatin-associated TCF/LEF factor in either condition, suggesting that TCF7L1 may function as an activator in mediating the effects of Wnt signaling in mESCs (Chapter 3); and 3) We have employed BioID to identify numerous novel putative TCF7L1-interacting epigenetic/transcription factor proteins which were, surprisingly, enriched in the presence of CHIR.

In summary, these findings expand on TCF/LEF mechanisms of transcriptional regulation of Wnt target genes and suggest that TCF7L1 is not simply removed from chromatin in response to Wnt stimuli. In the future, the new information we have obtained through our studies could be used to develop novel drugs and therapies for use in regenerative medicine or Wnt-associated diseases such as cancer.

CHAPTER 2

A SINGLE TCF TRANSCRIPTION FACTOR, REGARDLESS OF ITS ACTIVATION CAPACITY, IS SUFFICIENT FOR EFFECTIVE TRILINEAGE DIFFERENTIATION OF ES CELLS

Preamble

This chapter is an original published article. It is presented in its published format.

“This research was originally published in Cell Reports. Steven Moreira, Enio Polena, Victor Gordon, Solen Abdulla, Sujeivan Mahendram, Jiayi Cao, Alexandre Blais, Geoffrey A. Wood, Anna Dvorkin-Gheva, and Bradley W. Doble. A Single TCF Transcription Factor, regardless of its Activation Capacity, is Sufficient for Effective Trilineage Differentiation of ES Cells. <https://doi.org/10.1016/j.celrep.2017.08.043>. © 2017 The Authors. Published by Elsevier Inc.”

Together Dr. Bradley Doble and I, conceived the study, designed experiments and wrote the paper. Enio Polena and I, generated the TCF/LEF CRISPRs as well as the QKO and TCF7/TCF7L1 rescue cell lines. Victor Gordon and Jiayi Cao provided technical assistance with *in vitro* differentiation assays. Solen Abdulla provided technical assistance with sanger sequencing, cloning and qRT-PCR. Sujeivan Mahendram generated the TCF7 TALENs and targeting construct. Dr. Alexandre Blais and Dr. Anna Dvorkin-Gheva provided technical assistance with RNA-seq data analyses and visualization. Dr. Geoffrey A. Wood provided technical assistance with interpretation of the teratomas. This body of work was designed to create a system that enabled the study of a single TCF/LEF transcription factor family without the confounding compensations provided by the other members. Importantly this work demonstrated that TCF7 and TCF7L1 typically thought to behave opposingly downstream of active Wnt signals in mESCs, were both able to rescue the differentiation defects and restore transcriptional changes observed in QKOs lacking all full-length TCF/LEF factors.

**A single TCF transcription factor, regardless of
its activation capacity, is sufficient for
effective trilineage differentiation of ES cells**

Steven Moreira¹, Enio Polena¹, Victor Gordon¹, Solen Abdulla¹, Sujeivan Mahendram¹,
Jiayi Cao¹, Alexandre Blais³, Geoffrey A. Wood⁴, Anna Dvorkin-Gheva² and Bradley W. Doble^{1*}

1. Department of Biochemistry and Biomedical Sciences, Stem Cell and Cancer Research Institute,
Michael G. DeGroote School of Medicine, McMaster University, Hamilton, ON L8N 3Z5,
Canada.

2. Department of Pathology, McMaster University, Hamilton, ON L8N 3Z5, Canada.

3. Ottawa Institute of Systems Biology, Department of Biochemistry, Microbiology, and
Immunology, and Department of Cellular and Molecular Medicine, Faculty of Medicine,
University of Ottawa, Ottawa, ON K1H 8M5, Canada

4. Department of Pathobiology, Ontario Veterinary College, University of Guelph, Guelph, ON
N1G 2W1, Canada.

*Correspondence:

dobleb@mcmaster.ca

Summary

Co-expression and cross-regulation of the four TCF/LEFs render their redundant and unique functions ambiguous. Here, we describe quadruple-knockout (QKO) mouse ES cells lacking all full-length TCF/LEFs and cell lines rescued with TCF7 or TCF7L1. QKO cells self-renew, despite gene expression patterns that differ significantly from WT, and display delayed, neurectoderm-biased, embryoid body (EB) differentiation. QKO EBs have no contracting cardiomyocytes and differentiate poorly into mesendoderm, but readily generate neuronal cells. QKO cells and TCF7L1-rescued cells cannot efficiently activate TCF reporters, whereas TCF7-rescued cells exhibit significant reporter responsiveness. Surprisingly, despite dramatically different transactivation capacities, re-expression of TCF7L1 or TCF7 in QKO cells restores their tri-lineage differentiation ability, with similar lineage marker expression patterns and beating cardiomyocyte frequencies observed in EBs. Both factors also similarly affect the transcriptome of QKO cells. Our data reveal that a single TCF, regardless of its activation capacity, is sufficient for effective trilineage differentiation of ES cells.

Highlights

- Self-renewal and proliferation of WT and QKO mESCs are identical in media containing LIF
- Long-term QKO EBs and teratomas lack mesoderm and display very low levels of endoderm
- Cancer, cell cycle and metabolism genesets are enriched in QKO vs WT RNA expression data
- QKO mESC gene expression and function are reverted to WT-like in TCF7 or TCF7L1 knockins

eTOC Blurb

Moreira *et al.* describe the generation and characterization of mouse ES cells lacking all four full-length TCF/LEF factors. By using re-expression of epitope-tagged endogenous TCF/LEFs, they reveal surprising redundancies in the abilities of “activating” and “repressive” TCFs to rescue the differentiation deficits of the quadruple-knockout cells.

INTRODUCTION

Activation of the Wnt/ β -catenin signaling pathway is one of the cellular responses that can be initiated when a Wnt ligand binds cell surface receptors (Yu and Virshup, 2014; Saito-Diaz, *et al.*, 2013; Logan and Nusse, 2004). β -catenin, originally identified as an intercellular junction protein, is the key mediator of Wnt/ β -catenin signaling, in which the ultimate outcome of ligand-initiated signal transduction depends on stabilized β -catenin's binding to the N-termini of DNA-bound T-cell factor (TCF) / lymphoid enhancer factor (LEF) transcription factors, thereby activating transcription of target genes (Cadigan and Waterman, 2012). In the absence of a Wnt signal, the signaling pool of β -catenin is constitutively degraded by a multi-protein destruction complex in which β -catenin's phosphorylation by glycogen synthase kinase-3 (GSK-3) primes it for proteosomal destruction (MacDonald, *et al.*, 2009).

The Wnt/ β -catenin pathway is required for the induction and patterning of endoderm and mesoderm during gastrulation, which can be mimicked during *in vitro* differentiation of ES cells (Baillie-Johnson, *et al.*, 2015). Our understanding of the cell context-specific nuclear events regulated by TCF/LEFs in these differentiation processes is limited.

There are four TCF/LEF genes in vertebrates: *TCF7*, *TCF7L1*, *TCF7L2* and *LEF1* (Arce, *et al.*, 2006). *TCF7L1* is the predominant TCF/LEF expressed in undifferentiated mouse embryonic stem cells (mESCs) (Pereira, *et al.*, 2006), although all TCF/LEFs are detectable by western blot analyses of mESC lysates (Wallmen, *et al.*, 2012; Kelly, *et al.*, 2011a). *TCF7L1* appears to function as a constitutive transcriptional repressor in most contexts via its interaction with co-repressors (Atlasi, *et al.*, 2013; Shy, *et al.*, 2013; Merrill, 2012; Solberg, *et al.*, 2012; Wu, *et al.*, 2012). In ES cells, *TCF7L1* is part of an extended network of transcription factors regulating pluripotency, where it negatively regulates the transcription of *Nanog* and mediates the transition

from naïve to primed pluripotent states (Hoffman, *et al.*, 2013; Cole, *et al.*, 2008; Pereira, *et al.*, 2006).

TCF7L1 has been shown to be essential for the self-renewal enhancing effects of the GSK-3 inhibitor CHIR99021 (or Wnt3a stimulation) in pluripotent mESCs (Wray, *et al.*, 2011; Yi, *et al.*, 2011). TCF7L1^{ΔN/ΔN} mESC lines that express TCF7L1 lacking its N-terminal β-catenin binding domain display defects in their ability to self-renew in response to Wnt3a stimulation or GSK-3 inhibition (Wray, *et al.*, 2011; Yi, *et al.*, 2011). Thus, direct interactions between β-catenin and TCF7L1 are required to stimulate mESC self-renewal.

Wnt/β-catenin target gene activation has been proposed to employ a TCF switch mechanism in which repressive TCF7L1 is replaced by activating TCF7 (Yi, *et al.*, 2011). This may arise through the promotion of TCF7L1 degradation upon β-catenin binding, which attenuates target gene repression (Morrison, *et al.*, 2016; Shy, *et al.*, 2013), thereby providing an opportunity for TCF7 occupation of liberated binding sites. Down-regulation of TCF7L1 in mESCs treated with CHIR99021 has also been reported to occur at the transcriptional level through c-Myc-mediated repression (Morrison, *et al.*, 2016).

Although LEF1 is expressed at very low levels in undifferentiated mESCs, when overexpressed in the presence of stabilized β-catenin, it robustly activates reporter activity (Yi, *et al.*, 2011). Moreover, ectopic expression of LEF1 has been reported to have a positive effect on the self-renewal of mESCs, and siRNA-mediated knockdown of LEF1 was shown to promote mESC differentiation (Huang and Qin, 2010). TCF7L2, also expressed at low levels in undifferentiated mESCs, behaves more similarly to TCF7L1, in that it represses TCF reporter activity, even in the presence of stabilized beta-catenin (Yi, *et al.*, 2011).

It has been difficult to assess the unique roles of the TCF/LEF factors and the mechanisms through which they work in mammalian cells. During mouse development, each TCF/LEF displays a distinct expression pattern, but there is often an overlap between regions of TCF/LEF expression, and it is common for more than one TCF/LEF to be co-expressed in any given cell. Also, the various TCF/LEFs cross-regulate each other at the transcriptional level.

To gain a better understanding of the function of individual TCF/LEF factors in the absence of confounding contributions of co-expressed TCF/LEFs, we used a mESC model in which we genetically ablated all full-length TCF/LEFs. Our data reveal a surprising redundancy in the function of “repressive” TCF7L1 and “activating” TCF7, providing new insights into the mechanism through which these factors function.

RESULTS

Generation of TCF/LEF Quadruple-knockout (QKO) mESCs

We employed CRISPR/Cas9 methodology to knock out all four full-length TCF/LEF factors (Figure 1A) in wild-type E14TG2a mESCs (WT). Null alleles were characterized by Sanger sequencing (Figure 1B). We confirmed loss of all TCF/LEF protein expression by using western blot analysis (Figure 1C and S1). We induced LEF1 expression by removing LIF for 48 hours so that we could more readily detect the WT LEF1 control. The morphology of QKO mESCs did not differ greatly from that of WT cells in standard serum- and LIF-supplemented medium (S+L), but after LIF withdrawal for 48 hours, the QKO colonies remained compact and highly refractile, whereas WT colonies tended to flatten out (Figure 1D). As expected, QKO mESCs did not display TCF/LEF reporter activity when treated with Wnt3a-conditioned medium or the GSK-3 inhibitor CHIR99021 (CHIR), a Wnt mimetic (Figure 1E). QKO cells were also unresponsive to CHIR in qRT-PCR-based assays testing the expression of well-characterized Wnt/ β -catenin target genes

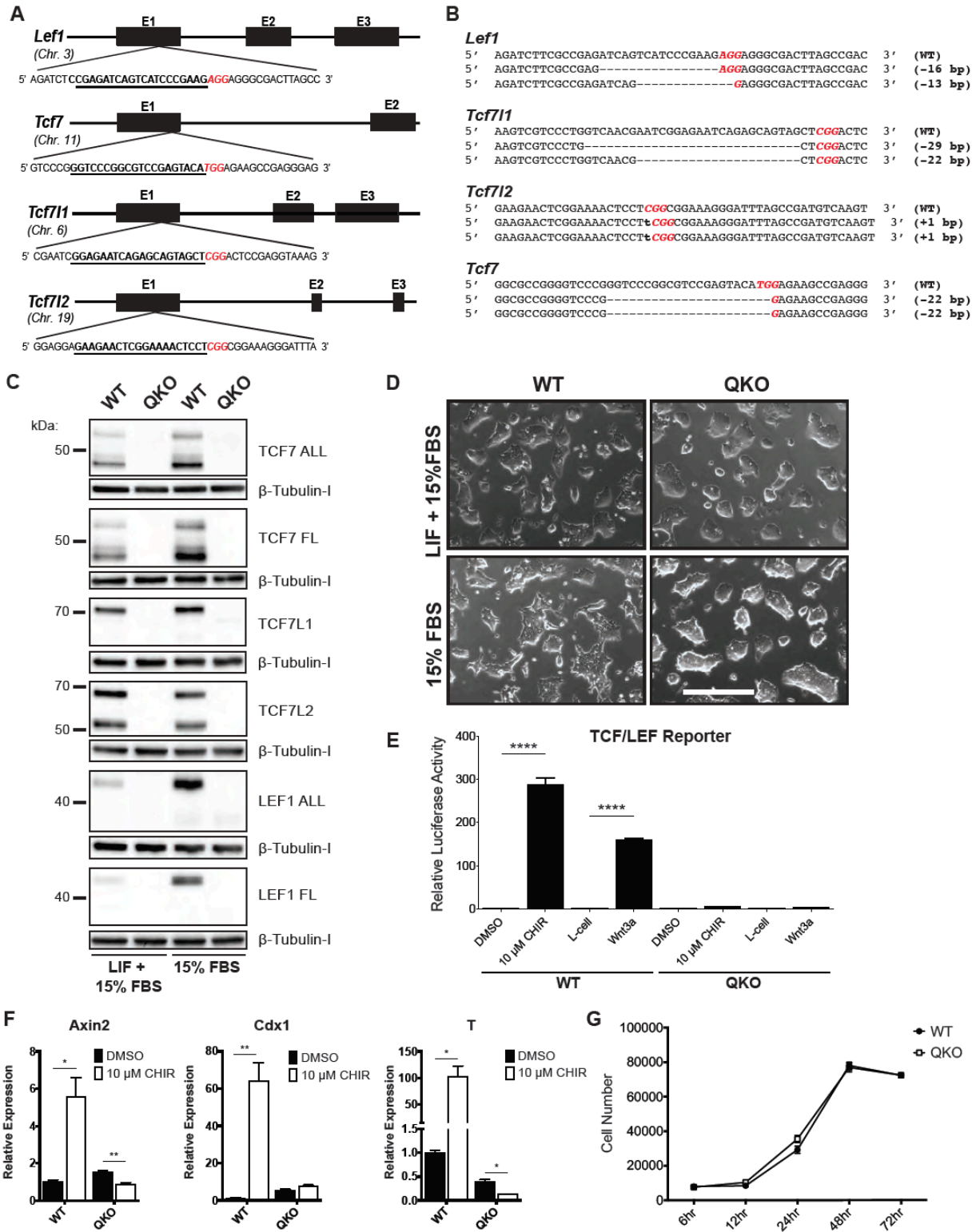


Figure 1. QKO mESCs are viable and proliferative but do not respond appropriately to Wnt pathway activation. (A) Diagram of targeted TCF/LEF loci. CRISPR sgRNA sequences are underlined, and PAM sites are red. (B) Biallelic sequences of TCF/LEF indels in QKO cells. (C) Western blots for all TCF/LEFs in WT and QKO lysates from cells maintained 48h in 15% FBS±LIF. (D) Morphology of WT and QKO mESCs maintained 48h in 15% FBS±LIF. Bar=400 µm. (E) TCF reporter assays for WT and QKO cells treated with 10 µM CHIR or Wnt3a-CM for 24 hours. Bars represent the mean of 3 independent experiments ±SEM, normalized to vehicle-treated WT cells. ****, $P < 0.0001$; one-way ANOVA. (F) qRT-PCR analyses of Axin2, Cdx1, and Brachyury relative transcript levels in WT and QKO cells treated with 10 µM CHIR or DMSO control for 48 hours. Bars = mean of 3 independent experiments ±SEM, normalized to vehicle-treated WT cells. *, $P < 0.05$, **, $P < 0.01$; unpaired Student's t-test. (G) CyQuant cell proliferation assay for WT and QKO cells maintained in 15%FBS + LIF. Dots represent the mean of 3 independent experiments.

Axin2, *Cdx1* and *T* (Figure 1F). Despite their inability to respond to activators of Wnt/ β -catenin signaling, QKO cell proliferation curves were virtually indistinguishable from WT curves in standard S+L medium (Figure 1G).

QKO mESCs Display Enhanced Self-renewal

We addressed the self-renewal capacity of QKO mESCs by assaying the number of alkaline-phosphatase-positive (AP⁺) colonies arising from cells plated at clonal densities in standard and defined medium conditions (Figs 2A, 2B). There was no distinguishable difference in the number of colonies generated by WT or QKO mESCs in S+L medium after 5 days, but when cultured in the absence of LIF, QKO mESCs retained a higher percentage of AP⁺ colonies and colonies with partial AP positivity (mixed) (Figure 2A). The QKO colonies were also noticeably larger in diameter than WT colonies in the serum-only condition (Figure 2A, 2C). The increased self-renewal of QKO mESCs was most apparent when they were maintained for 6 days in defined N2B27 medium alone, or in N2B27 supplemented with the MEK inhibitor PD0325901 (PD). The WT cells produced approximately 450 colonies in PD conditions, and almost half of these were AP⁻ or partially AP⁺ (mixed), whereas the QKO mESCs generated approximately 650 colonies, most of which were AP⁺ (Figure 2B). In the 2i conditions, the QKO colonies were not significantly larger than WT colonies. The WT and QKO mESCs responded similarly to CHIR alone, yielding far fewer colonies in these conditions (Figure 2B). In defined N2B27 medium alone, the QKO mESCs yielded approximately 250 colonies, with the majority AP⁺ or mixed, whereas less than 100 WT colonies survived in N2B27 alone and over half of these were mixed or AP⁻ (Figure 2B). Western blot analyses examining the pluripotency markers, Oct4, Sox2 and Nanog (Figure 2D) supported our colony formation assay results. In most of the conditions that would be expected to permit differentiation of WT mESCs (15% FBS, N2B27, N2B27 + CHIR or N2B27 + PD), higher levels of Nanog and Sox2 proteins were observed in QKO vs WT samples (Figure 2D). This was

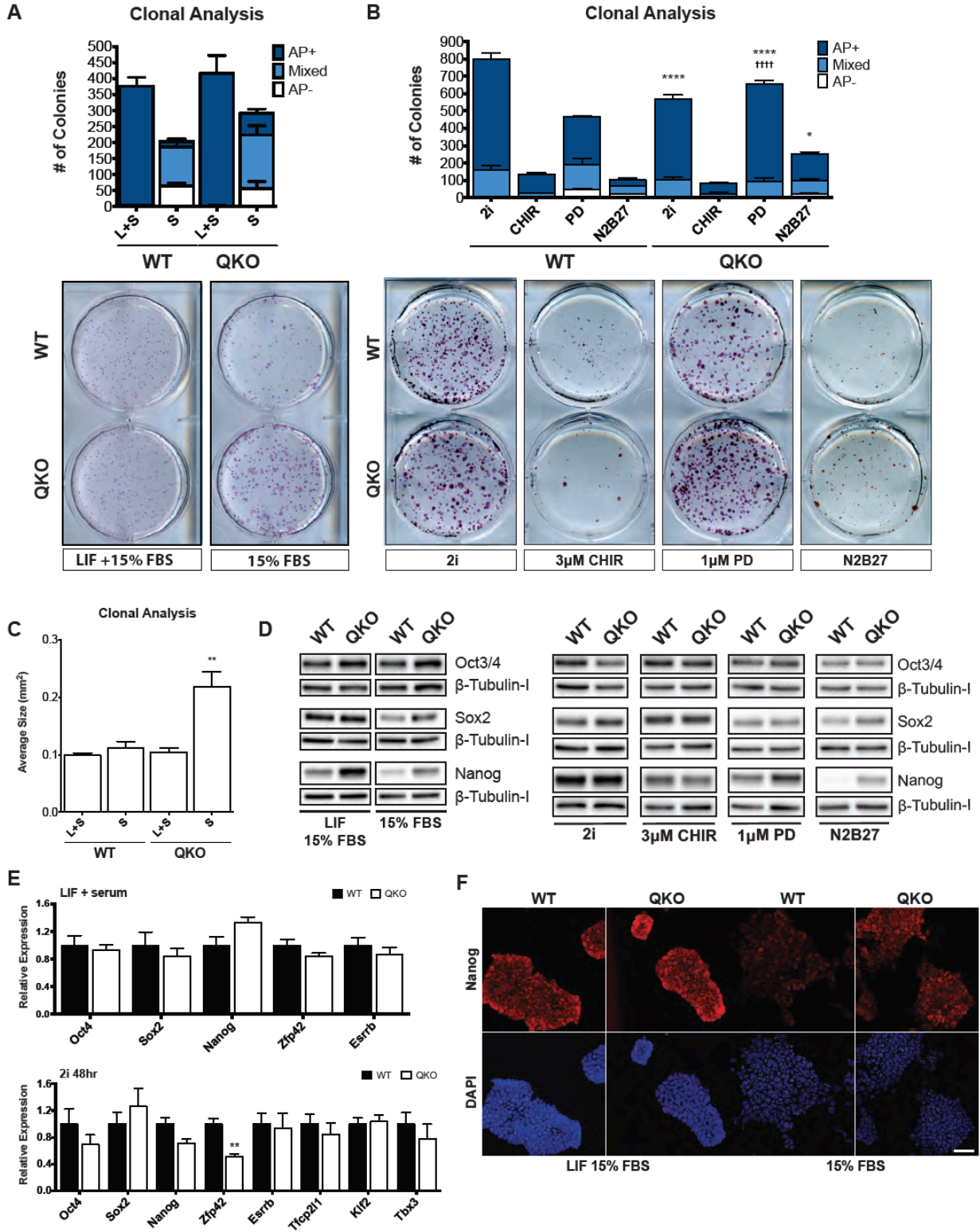


Figure 2. QKO mESCs display enhanced self-renewal capacity in serum-containing and defined serum-free media. (A) Alkaline phosphatase staining of WT and QKO mESCs cultured at clonal density in 15%FBS ± LIF for 5 days. Top: Histogram showing the number of undifferentiated (AP+, round, compact colonies), mixed (AP+) and differentiated (AP-) colonies formed from 600 plated cells. Bars = mean of 3 independent experiments ±SEM. Bottom: Representative images showing AP staining of WT and QKO colonies. (B) Alkaline phosphatase staining of WT and QKO mESCs cultured at clonal density in 2i, 3 μM CHIR, 1 μM PD, or N2B27 alone after 6 days. Top: Histogram showing the number of undifferentiated (AP+, round, compact colonies), mixed (AP+) and differentiated (AP-) colonies formed from 1000 plated cells. Bars = mean of 3 independent experiments ±SEM. AP+: *, P < 0.05, ****, P < 0.0001; Mixed: N.S.; AP-: ††††, P < 0.0001; two-way ANOVA's were performed comparing QKO to WT for each condition separately. Bottom: Representative images showing AP staining of WT and QKO colonies. (C) Average size of colonies corresponding to the AP stains performed on WT and QKO mESCs cultured for 5 Days in 15% FBS ± LIF. Bars = mean of 3 independent experiments ±SEM. **, P < 0.01. (D) Western blot analyses for pluripotency markers Oct4, Sox2 and Nanog in lysates from WT or QKO mESCs maintained in serum-containing or defined serum-free media for 48 hours, as indicated. (E) qRT-PCR analyses of the relative transcript levels for pluripotency markers in WT and QKO mESCs maintained in serum-containing or defined serum-free media for 48 hours, as indicated. Bars represent the mean of 3 independent experiments ±SEM. **, P < 0.01; unpaired Student's t-test. (F) Immunofluorescence analysis of Nanog and DAPI in WT and QKO mESCs maintained in 15% FBS ± LIF for 48hours. Scale bar represents 50 μM.

most apparent in the comparisons conducted in 15% FBS medium and N2B27 medium. No clear difference between the Sox2 or Nanog levels in WT and QKO mESCs was observed in samples obtained from cells maintained in N2B27 + CHIR (Figure 2D). Oct4 levels did not appear to be considerably different between WT and QKO mESCs at the 48-hour time point, in any of the conditions tested.

Quantitative RT-PCR analyses of a panel of pluripotency markers revealed no significant differences between WT and QKO mESCs maintained in LIF + serum for 48 hours, but there was a significant, yet minor (approx. 2-fold), decrease in the expression of the naïve pluripotent stem cell marker *Zfp42* in QKO vs WT mESCs maintained in N2B27 + 2i (Figure 2E). The increased retention of pluripotent mESC traits in differentiation-promoting conditions was also reflected in immunocytochemical analysis of colonies stained for the pluripotency marker Nanog (Figure 2F).

Re-expression of TCF7L1 or TCF7 in QKO mESCs reverts them to a WT-like state

We used a TALEN-facilitated knock-in approach to re-introduce a single-copy of 3xFLAG-tagged TCF7 and TCF7L1 into their endogenous loci (Figure S3A). We will refer to the TCF7- and TCF7L1-rescued clones as QT7 and QT7L1, respectively. The expression of 3xFLAG-tagged TCF7 and TCF7L1 was confirmed by western blotting in standard medium (L+S) and medium lacking LIF (Figure 3A and S4). Surprisingly, despite single-copy rescue expected to yield 50% of WT levels of each factor, protein levels of 3xFlag-tagged TCF7 and TCF7L1 were approximately 20% and 25% of the levels detected in WT mESCs, respectively (Figure 3A and Table S3).

TCF7 was expressed at lower levels than TCF7L1 (approximately 5-fold) in standard media (Fig 3A and Table S3), in agreement with previously published transcript expression data (Pereira, *et al.*, 2006). The higher level of TCF7L1 expression correlated with a stronger reversion of the QT7L1 cells towards a WT phenotype, as assessed by western blot analyses of Oct4, Sox2

and Nanog in differentiation-inducing conditions (Figure S3B, S3C). This return to a WT-like state was most notable in the QT7L1 cells when examining Nanog protein levels in 15% FBS (no LIF) and defined N2B27 medium lacking inhibitors (Figure S3B, S3C).

Re-expression of TCF7, but not TCF7L1, restored the ability of QKO mESCs to respond to CHIR and Wnt3a treatments, as determined by a luciferase-based reporter assay of TCF/LEF function, although the response was considerably less than that observed with WT mESCs (Figure 3B). This is consistent with the primarily repressive role of TCF7L1 in most cell types. Of three TCF/LEF target genes known to be upregulated by CHIR treatment of WT mESCs, *Axin2*, *Cdx2* and *T*, only *T* was appreciably upregulated in a TCF/LEF-specific manner, and this upregulation was specific to the TCF7-rescued cell lines (Figure 3C).

Western blot analyses of QT7L1 and QT7 cell lines in defined media revealed that, in all tested conditions, TCF7L1 was expressed at higher levels than TCF7 (Figure S3D). Interestingly, in the 2i condition, the levels of TCF7L1 in WT and QT7L1 cell lines were similar, with slightly more TCF7L1 expressed in the QT7L1 line despite its single-copy expression (Figure S3D). In response to 10 μ M CHIR treatment for 48 hours in standard S+L medium, levels of TCF7L1 protein were reduced, whereas levels of TCF7 were increased (Figure S3E). By using primers that only detected WT or repaired TCF7 or TCF7L1 transcripts in qRT-PCR assays, we did not detect a change in the levels of expression of either repaired allele upon treatment with CHIR for 48 hours, whereas in WT cells, clear differences in these transcript levels upon CHIR treatment (up for TCF7 and down for TCF7L1) were observed. Similar changes in the protein levels of TCF7 and TCF7L1 were observed in WT cells treated with CHIR, but in these cells, in contrast to the rescued cells, we also detected concomitant parallel changes in transcript levels (Figure S3E). This points to the involvement of TCF/LEF cross-regulation at the level of transcription. The changes in protein levels observed in Figure S3E are likely due to post-transcriptional regulation of TCF7

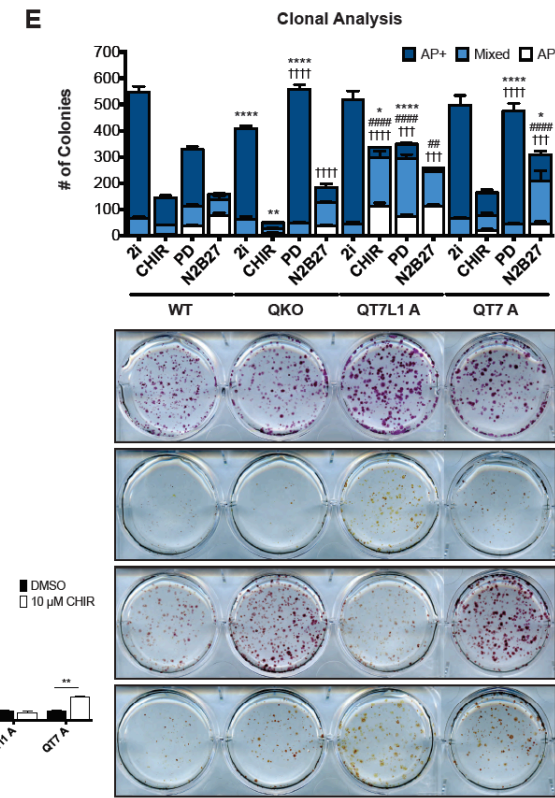
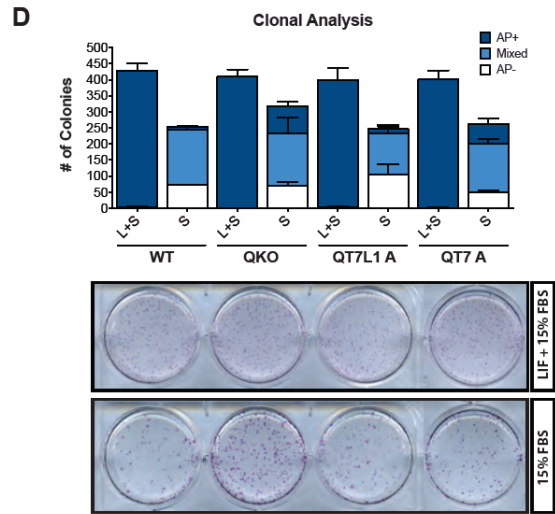
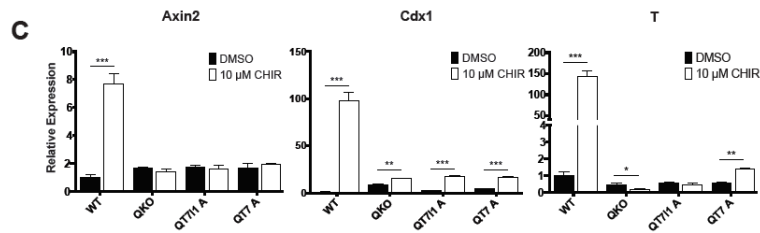
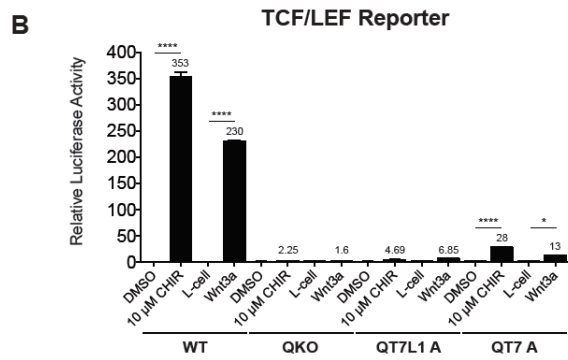
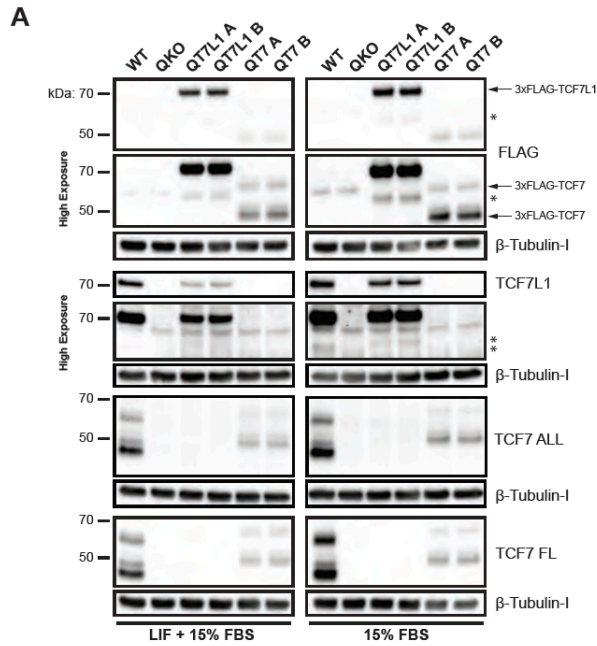


Figure 3. Single copy re-expression of endogenous TCF7 or TCF7L1 in QKO mESCs demonstrates differential effects on Wnt/ β -catenin signalling activity. (A) Western blot analysis of WT, QKO, QT7 and QT7L1 cells maintained in 15%FBS \pm LIF for 48 hours. Protein lysates were probed with antibodies against TCF7, TCF7L1, FLAG and β -tubulin (loading control), as indicated. (B) TCF reporter assays for WT, QKO, QT7, and QT7L1 cells treated with 10 μ M CHIR or Wnt3a-CM for 24 hours. Bars = mean of 3 independent experiments \pm SEM, normalized to vehicle-treated WT cells. *, $P < 0.05$; ****, $P < 0.0001$; one-way ANOVA. (C) qRT-PCR analyses of Axin2, Cdx1, and Brachyury relative transcript levels in WT, QKO, QT7 and QT7L1 cells treated with 10 μ M CHIR or DMSO control for 48 hours. Bars = mean of 3 independent experiments \pm SEM, normalized to vehicle-treated WT cells. *, $P < 0.05$, **, $P < 0.01$; ***, $P < 0.001$; unpaired Student's *t*-test. (D) Alkaline phosphatase staining of WT, QKO, QT7, and QT7L1 mESCs cultured at clonal density in 15%FBS \pm LIF for 5 days. Top: Histogram showing the number of undifferentiated (AP+, round, compact colonies), mixed (AP+) and differentiated (AP-) colonies formed from 600 cells. Bars = mean of 3 independent experiments \pm SEM. Bottom: Representative images showing AP staining of WT, QKO, QT7, and QT7L1 colonies. (E) Alkaline phosphatase staining of WT, QKO, QT7 and QT7L1 mESCs cultured at clonal density in 2i, 3 μ M CHIR, 1 μ M PD, or N2B27 alone after 6 days. Top: Histogram showing the number of undifferentiated (AP+, round, compact colonies), mixed (AP+) and differentiated (AP-) colonies formed from 1000 plated cells. Bars = mean of 3 independent experiments \pm SEM. AP+: *, $P < 0.05$, **, $P < 0.01$, ****, $P < 0.0001$; Mixed: ##, $P < 0.01$, #####, $P < 0.0001$; AP-: †††, $P < 0.001$, ††††, $P < 0.0001$; two-way ANOVA's were performed comparing QKO, QT7 and QT7L1 to WT controls for each condition separately. Bottom: Representative images showing AP staining of WT, QKO, QT7 and QT7L1 colonies.

and TCF7L1 levels in the rescued QKO cells, and a combination of transcriptional and post-transcriptional regulation in WT cells.

We used colony formation assays to evaluate the self-renewal properties of QT7 and QT7L1 cells. Both yielded fewer undifferentiated (AP⁺) clones than QKO mESCs after five days in LIF-free medium, although QT7L1 colony counts were more similar to WT, and QT7 counts were between WT and QKO counts (Figure 3D). This could be a reflection of the protein levels of TCF7 being less than TCF7L1 in these conditions due to differential gene expression, which would be augmented by the low-level single-copy expression of TCF7 we observed in standard mESC medium (Figure 3A) In defined conditions, whereas the QT7 cell line behaved very similarly to the QKO cell line in all conditions, as observed in serum-containing media, the QT7L1 line displayed differentiation profiles that differed from those of WT cells. Although the total number of colonies for QT7L1 cells in CHIR, PD and N2B27 conditions were greater than those observed for WT cells, a lesser proportion were AP⁺ (Figure 3E).

To evaluate global changes in gene expression arising from the loss of all TCF/LEF factors, and upon rescue with re-expression of TCF7 or TCF7L1, we used RNA-seq analysis. To examine the distribution of the samples, we performed principal component analysis. As shown in Figure 4A, the samples, each comprising two independent biological replicates, clearly segregated based on their experimental group, with QKO and QT7L1 samples exhibiting tighter clustering within their groups. Hierarchical clustering supported that WT samples were most closely related to the QT7 and QT7L1 samples, and most distantly related to the QKO samples (Figure 4B). It is notable that the majority of genes that were significantly differentially expressed between the WT and QKO samples were down-regulated in the QKO samples, which was somewhat unexpected given that, in the absence of Wnt signaling, the TCF/LEF factors are thought to function as repressors. Gene set enrichment analyses revealed three large interconnected clusters of gene sets that were

enriched in QKO samples vs WT samples, which could be broadly categorized as being functionally related to metabolism, cancer, and the cell cycle (Fig 4C, Tables S4 and S5). The enrichment of these gene sets in QKO samples was lost when either TCF7 or TCF7L1 was reintroduced into the cells, supporting a redundant role for these factors.

We also used qRT-PCR to quantify the relative expression of several pluripotency-associated genes, as well as one of the genes that was relatively abundant in undifferentiated mESCs and was significantly upregulated in QKO vs WT mESCs in our RNA-seq analysis, namely, *Id3* (Figure S4A). In S+L medium, there were minimal significant changes detected in the expression of pluripotency markers, and any observed changes were less than 2-fold, findings that were in accordance with our RNA-seq data. We also verified that in these conditions *Id3* expression was significantly upregulated (approx. 3-fold) in QKO mESCs and observed that its levels were reduced to WT levels in QT7L1 cells, but not QT7 cells. In 2i medium, most pluripotency markers were not differentially expressed between the various cell types. The two exceptions were *Zfp42* and *Dppa3*, with relative transcript levels (compared to WT) reduced by approximately 2-fold in the QKO, QT7, and QT7L1 mESCs. Surprisingly, in 2i conditions, *Id3* transcript levels were significantly lower than WT in QKO, QT7L1 and QT7 mESCs, suggesting that the increase in *Id3* expression observed in S+L conditions required a serum factor and/or LIF. It should be noted that although the transcript expression of *Zfp42* and *Dppa3* was reduced in QKO mESCs in 2i medium, these cells displayed similar (2i), or enhanced (PD), self-renewal compared to WT mESCs in serum-free conditions (Figure 2B).

We were intrigued by the strong representation of cell cycle genesets in our GSEA and examined the cell cycles of WT, QKO and rescued cell lines, despite no obvious differences in the growth curves of WT and QKO mESCs (Figure 1G). We analyzed the cell cycle parameters of WT, QKO, QT7 and QT7L1 cells by using Invitrogen's Click-iT EdU 488 Flow Cytometry, with

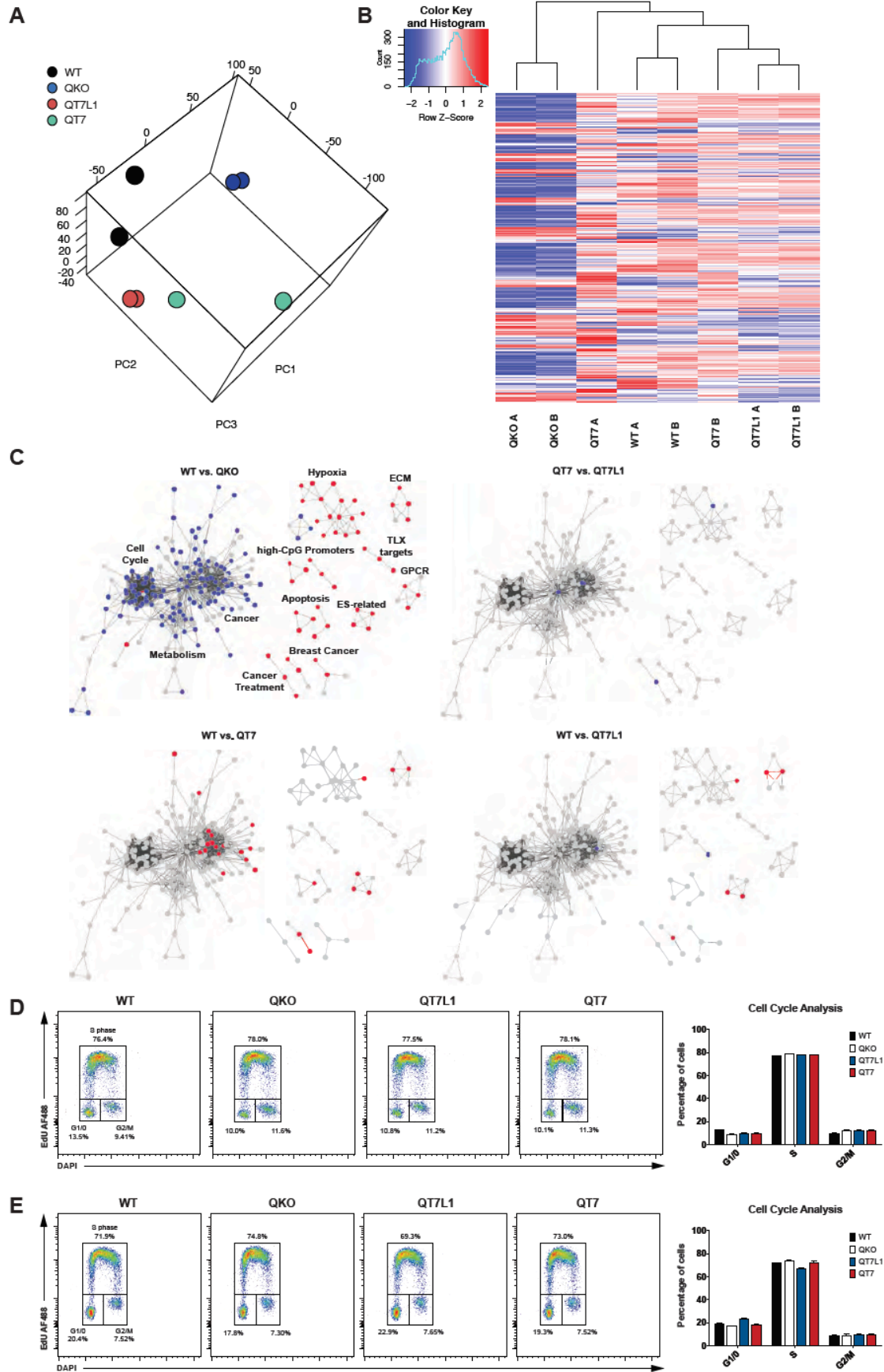


Figure 4. Re-expression of TCF7 or TCF7L1 in QKO mESCs reverts their whole-genome transcriptional profile to more resemble that of WT mESCs. (A) Principal component analysis on the transcriptional changes in WT, QKO, QT7L1 and QT7 maintained for 48 hours in 15%FBS + LIF. Each data point represents an independent biological replicate. (B) Hierarchical clustering of differentially expressed genes with at least a 2 fold change in any WT, QKO, QT7L1, or QT7 comparison. Dendrograms indicating the clustering relationships are shown above the heat map. (C) Gene set enrichment analyses on the transcriptional changes in WT, QKO, QT7L1 and QT7, maintained for 48 hours in 15%FBS + LIF, using the C2 collection of published genesets. Each dot represents a geneset, with multiple genesets clustered into networks based on connectivity. Red dots represent genesets enriched in the first group, while blue dots represent genesets enriched in the second group. (D) Cell cycle analysis performed on WTs, QKOs, QT7L1s and QT7s cultured for 48 hours in serum + LIF, stained with EdU and DAPI. LEFT: Representative flow cytometry profiles for an individual experiment following EdU and DAPI staining. RIGHT: Graph of the proportion of cells in G1/0, S, and G2/M phases of the cell cycle. Bars represent the mean of three independent experiments \pm SEM. (E) Cell cycle analysis performed on WTs, QKOs, QT7L1s and QT7s cultured for 48 hours in defined serum-free media supplemented with LIF+2i, stained with EdU and DAPI. LEFT: Representative flow cytometry profiles for an individual experiment following EdU and DAPI staining. RIGHT: Graph of the proportion of cells in G1/0, S, and G2/M phases of the cell cycle. Bars represent the mean of three independent experiments \pm SEM.

cells grown in fully-defined serum-free or S+L medium. Intriguingly, the results for cells grown in the two conditions are quite different. The QKO, QT7L1 and QT7 cell lines display shortened G1/0 and lengthened G2/M, compared to WT, in S+L conditions. In the LIF+2i conditions, all cell lines except for the QT7L1 line have essentially identical cell cycle profiles. The QT7L1 line, in LIF+2i, has a lengthened G1/0 phase and a shortened S phase. Chi-square analysis of cell cycle phase distributions indicated that the most pronounced of the observed cell cycle differences are statistically significant (Table S6).

Re-expression of *TCF7* or *TCF7L1* in QKO mESCs similarly rescue differentiation deficits and biases *in vitro* and *in vivo*

As we observed a dramatic and similar change in the transcriptome of QKO mESCs upon re-expression of *TCF7* or *TCF7L1*, we were interested in determining if this correlated with a similar impact on the function of QKO mESCs. We used hanging-drop embryoid body (EB) assays, in which WT EBs reproducibly generate cell types of all 3 germ-layer lineages, which frequently include spontaneously contracting cardiomyocytes that can be detected visually through light microscopy. We conducted 8 independent EB assays with WT, QKO, QT7 and QT7L1 mESCs and found that QKO mESCs never gave rise to detectable contracting cardiomyocytes (Figure 5A). By contrast, WT, QT7 and QT7L1 mESCs produced a high percentage of beating EBs, within 7-14 days of differentiation *in vitro*. Spontaneous contractions were first observed in WT EBs, 7 days after the initiation of differentiation, whereas QT7L1 and QT7 EBs first displayed detectable contractions on days 8 and 9, respectively. At day 14, approximately 80% of QT7 and QT7L1 EBs were beating, on average, the highest percentage observed over the time course. We observed the maximum number of beating WT EBs on days 9-10, and they comprised approximately 40% of the EBs.

An evaluation of lineage-specific differentiation markers by using qRT-PCR revealed that transcripts of the mesoderm markers *T* and *Mesp1* were not detectable in QKO EBs over a 6-day time-course, whereas they were detected in QT7 and QT7L1 EBs (Figure 5B). Similar patterns of expression were observed for the endoderm markers *FoxA2* and *Sox17*, with barely detectable levels observed in QKO samples, but higher levels observed over the differentiation time-course for the other samples (Figure 5B). Of note, *FoxA2* expression was markedly higher in QT7L1 EBs (approx. 10-fold higher than WT levels), with a spike in expression occurring at day 4 of differentiation. The neurectoderm markers, *Nestin* and *Pax6*, were readily detected in EBs derived from all types of mESCs. The QKO and QT7 EBs displayed very high levels of *Pax6* at day 3 of differentiation, which was approx. 6-fold higher than that observed in WT EBs (Figure 5B).

We also assessed the levels of two Wnt-responsive genes, *Axin 2* and *Wnt3*, in the various EBs described above. WT EBs had a strong upregulation of *Axin2* and *Wnt3* expression by day 3 of EB differentiation, and TCF7L1 EBs also displayed an increase in the expression of these genes, which was less robust (Figure 5B). The QKO and QT7 EBs did not show appreciable increases in *Axin2* transcript levels, but QT7 EBs displayed a gradual increase in *Wnt3* transcript levels that were not apparent in QKO samples (Figure 5B).

To determine if our mRNA expression data were consistent with changes at the protein level, we used western blot assays to examine the markers β -III-tubulin (neurectoderm), Gata4 (endoderm) and myosin heavy chain (mesoderm). QKO EB samples contained very high levels of β -III tubulin protein, which were much higher than the levels in WT EBs at all time points and QT7L1 and QT7 also expressed detectable levels of β -III-tubulin by day 14 of differentiation (Figure 5C). Gata4 was readily detectable in Day 14 EBs generated by all types of mESCs, however in QKO EBs there appeared to be a delay in Gata4 protein expression (Figure 5C). By contrast, QKO EB samples had undetectable levels of myosin heavy chain protein over the 14 day

time-course, whereas in WT, QT7 and QT7L1 samples, myosin was detectable by days 10-14 of differentiation (Figure 5C).

With the striking cardiomyocyte phenotype, we further examined a focused set of mesoderm/muscle markers at days 9 and 14 of EB differentiation, timepoints where cardiac muscle markers would be expected to be observed in EBs containing cardiac muscle tissue. The most cardiac-specific of these markers, *Tnnt2* (cardiac troponin type 2), was absent in QKO EBs, whereas it was highly expressed in WT, QT7, and QT7L1 rescued EBs (Figure 5D). Taken together, the marker expression is consistent with a block to mesoderm differentiation in QKO EBs.

The similar abilities of TCF7 and TCF7L1 to rescue efficient trilineage differentiation of QKO mESCs *in vitro* could arise from both factors gaining the ability to transactivate target genes during early stages of differentiation. Thus, we examined the ability of QT7 and QT7L1 EBs to activate a TCF reporter introduced into cells by using a lentiviral approach. Successfully transduced cells expressed mCherry driven by a constitutive promoter and expressed GFP if they possessed transactivating TCF/LEFs. We chose to examine EBs at day 4 of differentiation, as we observed changes in marker gene and Wnt target gene expression at this time point in the QT7L1 EBs (Figure 5B). Cells isolated from untreated EBs and EBs that had been treated for 24 hours with CHIR were assessed by using flow cytometry. Only WT EBs contained a significant (4%) population of cells that expressed detectable levels of GFP under basal conditions, but both WT and QT7 EBs responded to CHIR treatment, as evidenced by the presence of GFP-positive cells (11.9% of WT cells and 6.45% of QT7 cells) (Figure 5E). Western blots of WT, QKO, QT7L1 and QT7 cells, treated in the exact same manner as the those presented in Figure 5E, indicate that at day 4 of differentiation, the levels of QT7L1A and QT7A, as detected by their common 3xFLAG

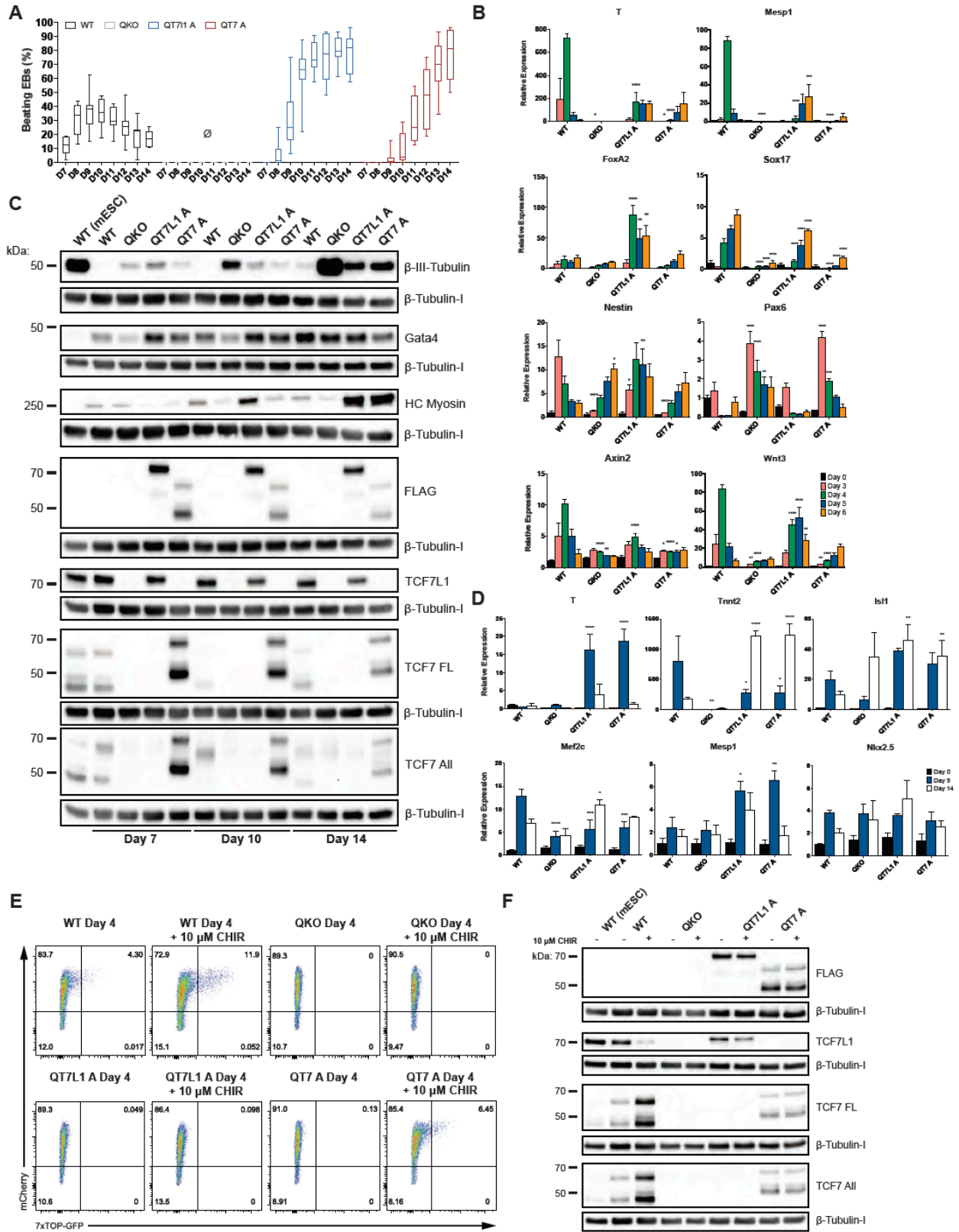


Figure 5. QKO mESCs re-expressing TCF7 or TCF7L1 are rescued in their ability to generate mesoderm in EB assays. (A) Box plots summarizing the percentage of spontaneously contracting EBs observed from days 7 to 14 for WT, QKO, QT7 and QT7L1 cell lines (8 independent experiments). Black dots indicate the mean. Grey boxes indicate the interquartile range. Whiskers above and below boxes show the locations of the maxima and minima, respectively. (B) qRT-PCR analysis of relative transcript levels of the indicated germ layer lineage markers expressed in EBs derived from WT, QKO, QT7 and QT7L1 mESCs from days 3-6 of differentiation. Values are normalized to the values obtained in WT mESCs at day 0. Bars = mean of 3 independent experiments \pm SEM. *, $P < 0.05$, **, $P < 0.01$, ***, $P < 0.001$, ****, $P < 0.0001$; two-way ANOVA's were performed comparing QKO, QT7 and QT7L1 to WT controls for each time-point separately. (C) Western blot analysis of WT, QKO, QT7 and QT7L1 EBs generated from days 7, 10 and 14 of differentiation. Protein lysates were probed with antibodies against β -III-tubulin, Gata4, Heavy Chain Cardiac Myosin, 3X-FLAG, TCF7, TCF7L1 and β -tubulin (loading control), as indicated. (D) qRT-PCR analysis of relative transcript levels of the indicated cardiac lineage markers expressed in EBs derived from WT, QKO, QT7 and QT7L1 mESCs from days 9 and 14 of differentiation. Values are normalized to the values obtained in WT mESCs at day 0. Bars = mean of 3 independent experiments \pm SEM. *, $P < 0.05$, **, $P < 0.01$, ***, $P < 0.001$, ****, $P < 0.0001$; two-way ANOVA's were performed comparing QKO, QT7 and QT7L1 to WT controls for each time-point separately. (E) Flow cytometric analyses of WT, QKO, QT7 and QT7L1 mESCs transduced with a GFP-based TCF-reporter on day 4 of EB differentiation, with or without stimulation with 10 μ M CHIR for 24 hours on day 3, as indicated. (F) Western blot analyses of WT, QKO, QT7 and QT7L1 mESCs on day 4 of EB differentiation, with or without stimulation with 10 μ M CHIR for 24 hours on day 3, as indicated.

tags, are very similar (Figure 5F). Thus, the lack of 7xTOP-GFP signal in CHIR-treated QT7L1 cells (Figure 5E) is not due to reduced protein expression of QT7L1 compared to QT7, at the assessed time point.

A standard assay of pluripotency for mESCs is the formation of teratomas in recipient mice. When 5 million WT, QKO, QT7 or QT7L1 mESCs were injected subcutaneously into the hind limbs of immunocompromised mice (NOD/SCID), teratomas formed in all cases, although the progression of teratoma development was more rapid for those derived from QKO mESCs or QKO-rescued mESCs (Figure S5A). H&E staining combined with an immunohistochemical assay for mesoderm (myosin heavy chain), revealed that while WT, QT7 and QT7L1 cells all produced teratomas containing all three germ-layer lineages, the QKO teratomas did not display striated muscle staining, contained scant endoderm, and were comprised predominantly of neural pseudorosettes (Figure 6A, 6B, S5B). There were no clear differences observed in the cell proliferation marker Ki67 between samples from WT, QKO, QT7L1 and QT7 teratomas (Figure 6C). Markers for all three germ layers, assessed by using qRT-PCR analysis of samples obtained from each of three independent teratomas derived from the four different mESC lines, were consistent with our histological assays (Figure 6D). Thus, QKO cells displayed a differentiation capacity in the teratoma environment, that was comparable to that observed in the *in vitro* EB milieu.

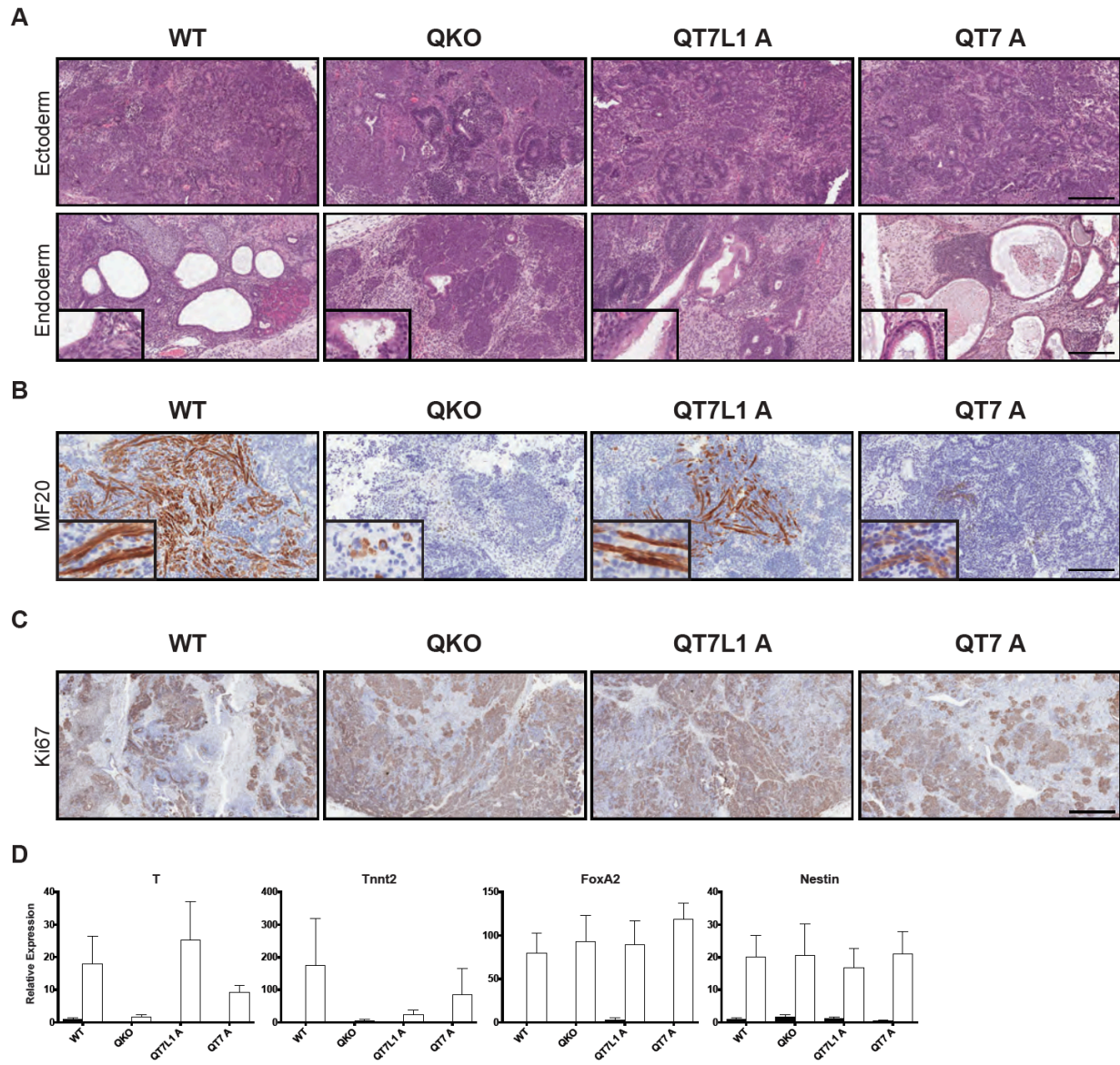


Figure 6. QKO mESCs re-expressing TCF7 or TCF7L1 are rescued in their ability to generate mesoderm in Teratomas. (A) H&E stained sections from teratomas derived from WT QKO, QT7, and QT7L1 mESCs display neural rosettes indicative of ectoderm and epithelial structures indicative of endoderm, in all four tissue types. Bar = 100 μ M. (B) Immunohistochemical staining of teratoma sections with the mesodermal marker, pan-myosin antibody MF20. Bar = 100 μ M. (C) Immunohistochemical staining of teratoma sections with the proliferative marker, Ki-67. Bar = 100 μ M. (D) qRT-PCR analysis of relative transcript levels of the indicated germ layer lineage markers expressed in teratomas derived from WT, QKO, QT7 and QT7L1 mESCs. Values are normalized to the values obtained in WT mESCs at day 0. Bars = mean of 3 independent experiments \pm SEM.

DISCUSSION

The findings of our study suggest that there is a higher degree of functional redundancy between TCF/LEF factors than might be expected from their activities, as determined by reporter assays. To our knowledge, our study is the first to examine mammalian cells lacking all full-length TCF/LEF factors (QKO) and the capacity of individual TCF/LEF factors to rescue functional deficits arising from the complete absence of these factors.

Genetic studies in mice have previously shown that the four TCF/LEF factors, when individually knocked out give rise to markedly different phenotypes (Roose and Clevers, 1999). Mice lacking TCF7 display defects in thymocyte differentiation (Verbeek, *et al.*, 1995). LEF1 knockout mice lack teeth, mammary glands, neural crest derived neurons, whiskers and hair, and display postnatal lethality, but they have no obvious lymphoid cell defects at birth (van Genderen, *et al.*, 1994). TCF7L2 knockout mice show an absence of epithelial stem cells in the small intestine (Korinek, *et al.*, 1998). TCF7L1 knockout mice display the most severe phenotype and are embryonic lethal, with expanded and frequently duplicated axial mesodermal structures (Merrill, *et al.*, 2004). Crosses between knockout mice, where possible, give rise to double-knockout mice with more severe phenotypes (Roose and Clevers, 1999). Although there are clearly differences between the TCF/LEF family members, their varied expression patterns throughout development and their co-regulation of each other has made it difficult to assess the degree to which the family members are functionally redundant at the biochemical level in living cells.

We used mouse embryonic stem cells in our study for several reasons: 1) they express all four TCF/LEF factors, albeit at different levels; 2) they are ostensibly normal cells; 3) they can be tested in well-defined assays of their function; 4) they are relevant cells for studying developmental processes in which Wnt/ β -catenin signaling plays a role.

The most striking phenotype of QKO mESCs was that they did not differentiate properly toward mesendodermal lineages in both *in vitro* and *in vivo* differentiation assays. The absence of spontaneously contracting cardiomyocytes in QKO EBs suggests a block to mesoderm differentiation, which was supported by analysis of mesoderm and cardiac markers. This phenotype is similar to mutants of upstream Wnt signaling molecules, *Porcn*, *Wls* and *Wnt3*, which fail to undergo gastrulation and do not produce endoderm or mesoderm (Biechele, *et al.*, 2011; Fu, *et al.*, 2009; Liu, *et al.*, 1999). Likewise, mESCs lacking β -catenin display defects in mesendodermal germ layer formation but in addition, display impaired neuronal differentiation (Lyashenko, *et al.*, 2011). Although the cell-adhesion properties of β -catenin have been suggested to be more important than its function as a transcription factor, in definitive endoderm differentiation (Lyashenko, *et al.*, 2011), endodermal differentiation deficiencies of our QKO mESCs suggest that there is still an important role for β -catenin's interactions with the TCF/LEFs in this process.

In our *in vitro* experiments with cultured mESCs and EBs, the QKO mESCs had a well-defined and reproducible phenotype that was characterized by: 1) dramatically altered global gene expression; 2) absence of *T*, *Mesp1*, and *Tnnt2* expression and highly attenuated expression of other mesendoderm markers during EB differentiation; 3) premature induction of *Pax6* expression and early, sustained, expression of β -III-tubulin protein in EB assays, 4) absence of a TCF-reporter signal in response to Wnt/ β -catenin pathway activators; 5) an inability to generate beating EBs; and 6) enhanced self-renewal in colony formation assays.

Re-introduction of either *TCF7* or *TCF7L1* into QKO mESCs by rescuing one copy of their CRISPR/Cas9-mutated alleles resulted in a reversal of all QKO traits except for the inability to activate TCF-reporters, which only re-expression of *TCF7* could remedy. We observed strong rescues despite lower than expected production of TCF7 and TCF7L1 proteins, which is likely due

to a loss of cross-regulation by the other TCF/LEFs. Our data indicate that TCF activity, as determined by reporter assays, is not required for mESCs to exit the pluripotent state and to differentiate into cells of all three germ layers *in vitro*.

There has been a strong focus on TCF7L1 in mESC research for the following reasons: 1) it is the most abundant of the four TCF/LEFs in these cells, 2) mESCs lacking TCF7L1 are severely compromised in their ability to differentiate efficiently *in vitro*, 3) its absence obviates a requirement for CHIR in 2i medium [reviewed in: (Merrill, 2012)].

The mechanism through which TCF7L1 regulates mESC pluripotency and differentiation has been suggested to involve a switch between repressive TCF7L1 and activating TCF7 (Yi, *et al.*, 2011). Our data reveal that this switch mechanism is not an absolute requirement for maintenance of a WT-like mESC state, as TCF7L1 or TCF7 are capable of rescuing QKO mESCs to a similar extent. Intriguingly, a recent report has found that disrupting interactions between the “activating” TCFs and β -catenin is capable of reconstituting naïve pluripotency in mESCs (Saj, *et al.*, 2017), with the suggestion that TCF7 activity is largely responsible for promoting the differentiation of mESCs in their exit from the pluripotent state.

Strikingly, we show that both re-introduced TCF7 or TCF7L1, although expressed from their endogenous promoters at different levels, similarly revert the transcriptome of the rescued mESCs to approximate that of WT mESCs. Intriguingly, at the protein level, in response to CHIR, TCF7 and TCF7L1 were regulated in an opposite manner, with TCF7 protein levels increasing, and TCF7L1 protein levels decreasing (Figure S2E). How these differentially regulated factors, with dramatically different transactivation capacities, act to similarly affect the properties of QKO mESCs remains to be elucidated. We propose that the DNA-binding function of TCF/LEFs, through their conserved HMG domains that bind and bend DNA through minor-groove

interactions, coupled with their ability to be de-repressed, may be sufficient for them to regulate key target genes involved in mesodermal differentiation.

The QKO mESC RNA-seq data analysis revealed that in the absence of TCF/LEFs, mESCs acquire a gene expression pattern that is enriched in a large number of cancers, cell cycle and metabolism genesets. This highlights that even in the absence of Wnt ligands, the TCF/LEFs play a critical role in cellular homeostasis. We observed that QKO mESCs not only had better self-renewal properties, as determined by colony formation assays, but they also gave rise to larger colonies. The increased colony size suggests that differentiating QKO mESCs may have an increased rate of proliferation compared to WT mESCs, which would be consistent with our observation that cell cycle genes are misregulated in QKO mESCs. Indeed, one of the most highly down-regulated genes in QKO mESCs was *CCNG2*, a negative regulator of the cell cycle that is frequently reduced in a variety of cancers, including Wnt-related cancers (Wang, *et al.*, 2016). Although no proliferative difference between QKO and WT cells was observed in self-renewal conditions with routine cell passaging, more differentiated cell types within long-term colonies may be more sensitive to alterations in normal cell cycle regulation.

Our cell cycle analyses of QKO, QT7L1 and QT7 in serum and defined media (Figure 4D, 4E) are consistent with a role for the TCF/LEFs in cell cycle regulation. As a very short G1/0 phase is a trait of naïve mESCs, and lengthening of this phase occurs upon differentiation (Coronado, *et al.*, 2013), our data suggests that in serum conditions, the QKO, QT7 and QT7L1 are retained in a more naïve state, whereas in 2i conditions, which would be expected to enhance naïve pluripotency, expression of TCF7L1 in QKO mESCs appears to push the cells towards a primed pluripotent state. Thus, imbalances in the expression of TCF/LEF factors, with resultant effects on cell cycle parameters may influence mESC pluripotency/differentiation.

When evaluating Wnt target genes, especially as related to tumorigenesis, it is common to focus on those genes that are upregulated upon Wnt treatment. Our QKO gene expression data strongly suggest that important cancer-related TCF-regulated genes may be down regulated upon modulation of TCF factors, and we believe our QKO dataset provides a valuable resource that will help identify these important, but somewhat neglected, genes. Taken together, the data presented in our study provide important new insights into the mechanisms through which Wnt/ β -catenin signaling can exert its effects, by highlighting an unexpected degree of functional redundancy between “activating” and “repressive” TCF/LEFs and revealing the importance of TCF/LEFs, even in the absence of Wnt stimulation, in maintaining cellular homeostasis.

EXPERIMENTAL PROCEDURES

Cell culture

Routine maintenance of mESCs in serum-containing and serum-free media, and preparation of Wnt3a-conditioned medium, has been previously described (Kelly, *et al.*, 2011b). Details are provided in the supplemental materials and methods.

Construction of CRISPR guide RNAs

Guide RNAs with the lowest off-targets were designed utilizing the online tool: Optimized CRISPR design (crispr.mit.edu). DNA oligonucleotides harboring the forward and reverse sequences of the 20bp guide RNA, not including the PAM sequence, were ordered through IDT (idtdna.com). The forward and reverse oligonucleotides were annealed to generate a double-stranded DNA fragment with 4bp overhangs compatible with ligation into BpiI-digested pX459 CRISPR-Cas9 plasmid (addgene.org/62988/).

Generation QKO mESC lines using CRISPR/Cas9 Methodology

Conventional CRISPR-Cas9 plasmids targeting exon 1 of each TCF/LEF factor were prepared as described above. 2 million mouse ESCs were transfected with 4 μ l of Lipofectamine LTX and 5 μ g of the CRISPR constructs and subsequently plated on a single 60mm dish in standard mESC medium. After 24 hours, fresh mESC medium containing 2.5 μ g/ml puromycin was added to perform a 24-hour pulse of selection. After an additional 24 hours in selection, cells were plated at clonal density in standard mESC medium without selection. 6-8 days later, 30 colonies were picked and expanded to 2, 24-well plates. One plate was used to make whole cell protein lysates and one was maintained in culture. Successful gene knockouts were verified through western blot analysis, and heterozygous or homozygous positive clones were subsequently expanded and frozen in liquid nitrogen. After indel validation by sequencing, one *LEF1* homozygous knockout mESC

line was targeted to ablate the *TCF7L1* gene, as described above. A western blot and sequence verified *LEF1/TCF7L1* homozygous double knockout mESC line was subsequently used to target *TCF7L2* and *TCF7* with their CRISPR constructs simultaneously. Three *LEF1/TCF7L1/TCF7L2/TCF7* homozygous quadruple knockout ES cell lines were validated and verified through western blot and sequencing. These three cell lines were used in subsequent experiments.

CyQuant Cell Proliferation Assay

10,000 cells were plated in standard mESC media, onto a single well of a 96-well plate, in triplicate. A single plate was used for 6, 12, 24, 48, and 72 hour time-points. At each time-point, medium was aspirated, and plates were frozen and stored at -80°C . At the 48 hour time-point, fresh mESC medium was added to the 72 hour plate. After the final time-point was collected and frozen, 200 μl of a 2.5x CyQuant GR dye/cell lysis buffer was added to each well and incubated at room temperature (RT) for 5 minutes. The fluorescence was subsequently measured using a FLUOstar Omega microplate reader (BMG Labtech). A reference standard curve was created using dilutions corresponding to a range of 0-300,000 cells.

Generation of 3xFLAG-*TCF7L1* or -*TCF7* rescued mESC lines with TALENs

3xFLAG-*TCF7L1* and -*TCF7* targeting constructs with approximately 1kb homology arms, cloned using PCR with genomic DNA, were designed to introduce a Floxed neomycin resistance cassette. TALENs targeting *TCF7L1* and *TCF7* were designed with the TALEN targeter tool 2.0, such that they could only cleave the endogenous loci (<https://tale-nt.cac.cornell.edu/node/add/talen>). TALENs were subsequently assembled using Golden Gate assembly and the TALE-toolbox (<http://www.addgene.org/tale-toolbox/>). 4×10^6 mESCs were transfected with 5 μg of each TALEN and 1 μg targeting vector and plated at clonal density. Cells

were supplemented with fresh media 24 hours post transfection, and neomycin-resistant clones placed into selective medium containing G418 (250 µg/mL) 48 hours post-transfection. Six to eight days later, 60 colonies were isolated and plated in duplicate, with one plate used to carry out PCR-based screens for successful homologous recombination. Positive clones were expanded and frozen down. The neomycin cassette was excised by transfecting 2×10^6 cells with 2.5 µg of pCX-Cre-Puro and plating at clonal density. Transfected cells were pulsed with 2µg/ml puromycin the day after transfection for 24 hours, after which they were grown in standard mESC media for 6-8 days. Individual clones were picked and duplicate-plated to screen for their sensitivity to G418. Two independent clones of both 3xFLAG-*TCF7L1* and *-TCF7* rescued QKO mESCs were used for subsequent analyses.

Sequencing of the TCF/LEF factor loci

Primers flanking CRISPR or TALEN target sites were used to PCR amplify the region of interest and gel extracted using the Qiagen MinElute Gel Extraction kit (Qiagen). This DNA was subsequently inserted into pJet1.2 (Thermo Scientific). DNA from 6 colonies was purified using Invitrogen PureLink DNA Mini kit (Life Technologies) and sent for Sanger-sequencing (Mobix Lab, McMaster).

Cell Lysate Preparation

Cell lysates were prepared as previously described (Kelly, *et al.*, 2011b).

Antibodies

A list of antibodies used is provided in supplementary experimental procedures.

Quantitative RT-PCR

Total RNA was isolated using the PureLink RNA Mini Kit (Life Technologies) and 1 µg was used to generate cDNA with qScript cDNA SuperMix (Quanta Biosciences). The cDNA was

diluted 1/5 to a total 100 μ l and 3 μ l of this was used for each 10 μ l PCR reaction with SsoAdvanced SYBR Green SuperMix (BioRad). Rpl13a was used as the reference gene. Bio-Rad's CFX96 instrument and software were used to determine relative gene expression levels using the delta-delta Ct method. Primer sequences were designed using IDT's online primer design software (idtdna.com) or were obtained from prior publications and are listed in Table 3. For experiments in which transcript levels were assessed following CHIR99021 treatment of WT ESCs, ESCs were plated into LIF- containing medium supplemented with CHIR99021 at 10 μ m for 48 hours before RNA isolation.

Teratoma Assays

Teratomas were performed in NOD/SCID mice, by The Centre for Phenogenomics. Briefly, 5 million mESCs suspended in matrigel were injected subcutaneously and unilaterally in one hind limb of each experimental mouse (3 mice per cell line).

Immunohistochemical analysis of teratomas

The McMaster Centre for Gene Therapeutics core histology lab performed all immunohistochemical procedures. Briefly, paraffin-embedded samples were sectioned, dewaxed and rehydrated via standard procedures. For Ki-67 and MF20, antigen retrieval was performed using heat-induced antigen retrieval in sodium citrate buffer (pH 6.0). For the detection of mouse and rabbit antibodies in mouse tissues, the Animal Research Kit (ARK, K3594, Dako Canada) and the Envision+ System-HRP labeled Polymer Anti-rabbit (K4003, Dako Canada) were used, respectively. The following primary antibody concentrations were used: Ki-67, 1:500; MF20, 1:100.

TCF/LEF reporter Assays

Luciferase-based reporter assays in mESCs were performed as described previously (Kelly, *et al.*, 2011b). For TCF/LEF reporter assays performed on embryoid bodies, mESCs were infected with a lentiviral reporter, 7TGC, a gift from Dr. R. Nusse (<https://www.addgene.org/24304/>), expressing constitutive cherry red fluorescence and TCF/LEF-responsive green fluorescence. WT, QKO cl.A, QT7L1 cl.A, QT7 cl.A were infected at an MOI of 5, which produced >90% mCherry-positive cells, as assessed by flow cytometry. These cell lines were then used to prepare hanging-drop EBs that were subsequently assessed by flow cytometry for GFP and mCherry. For experiments performed with 10 μ M CHIR99021, 15% FBS media supplemented with the inhibitor was added to half of the EBs on Day 3, the remaining half was supplemented with standard 15% FBS media, for 24hrs.

Alkaline Phosphatase Staining

Standard medium: Mouse ESCs lines were grown on feeders for at least one passage. Single cell suspensions were obtained by using Accutase (Stem Cell Technologies) and 600 cells were plated onto gelatin-coated 6-well plates in the indicated serum-containing media conditions, with daily medium replacement. After 5 days, cells were fixed in 4% paraformaldehyde for 2 minutes, washed in 0.2% TBS-T and incubated in AP staining reagent (Fast Red Violet Solution:Naphthol:ddH₂O in a 2:1:1 ratio; Millipore, SCR004) for 20 minutes at room temperature in the dark. A final wash with 0.2% TBS-T was performed before the cells were resuspended in 1x PBS.

Serum-free medium: 1000 cells were plated on poly-ornithine/laminin-coated 6-well plates and medium was replenished daily. After 6 days, cells were fixed with 65% acetone, 25% citrate and 8% formaldehyde, washed with ddH₂O and incubated in AP stain reagent (Sodium Nitrite Solution:FRV-Alkaline:Naphthol AS-BI:ddH₂O in a 1:1:1:45; Sigma, 86R-1KT) for 45 minutes at RT in the dark. A final wash with ddH₂O was performed before the cells were resuspended in

1x PBS. Cells were scanned using a Epson Perfection V750-M Pro and scored manually. Colony size was determined using a script in ImageJ (see supplemental methods).

RNA-sequencing

Total RNA was extracted using the PureLink RNA Mini Kit (Life Technologies). RNA from two independent cell lines was isolated, from independent experiments (e.g. QKO cl. A1 from the first experiment cl. B8 from a second experiment). In the case of WT mESCs samples from two independent experiments were prepared. Samples were diluted to a concentration of 100 ng/μl in 15 μl and sent for library preparation and sequencing at the McGill University and Genome Quebec Innovation Centre (MUGQIC). Libraries were generated using the TruSeq Stranded RNA kit (Illumina). Libraries were then subjected to 100bp paired-end sequencing on the Illumina HiSeq2000 instrument. 4 samples were multiplexed per lane for a total of 8 samples in two lanes (E14T N1, E14T N2; QKO cl.A N1, QKO cl.B N2; QT7L1 cl.A N1, QT7L1 cl.B N2; QT7 cl. A N1, QT7 cl. B N2).

RNA-Seq Analyses

The STAR aligner (Dobin, *et al.*, 2013) was used to generate BAM files of aligned RNA-Seq reads. The BAM files were uploaded to the open source GALAXY platform (usegalaxy.org) and htseq-count was used to count aligned reads that overlap features in the mouse GRCm38.84.gtf file. The complete dataset and analyses are available on the publicly available Galaxy instance (<https://usegalaxy.org/u/braddoble/h/deseq2-qko-lines>).

Files obtained from the HTseq module of Galaxy were used for principal component and hierarchical clustering analyses and visualizations (Anders, *et al.*, 2015). Genes showing zero counts in all 8 samples were removed, and the remaining values were normalized with the *TMM*

normalization method and then transformed with *voom* transformation (Law, *et al.*, 2014; Robinson and Oshlack, 2010).

Principal Component Analysis and Hierarchical Clustering were performed and visualized with *rgl* (<https://CRAN.R-project.org/package=rgl>) and *stats* (built-in R package; <https://stat.ethz.ch/R-manual/R-devel/library/stats/html/00Index.html>) packages respectively. Hierarchical Clustering was performed by using average linkage and Euclidean distance metrics. All analyses were performed in the R ver 3.3.0 environment (Team, 2016).

For gene set enrichment analysis (GSEA), differentially expressed genes were ranked by Log2 fold change and used with GSEAPreranked module v.4.2 (Subramanian, *et al.*, 2005; Mootha, *et al.*, 2003) in GenePattern environment (Reich, *et al.*, 2006) to examine Gene Set Enrichment in the groups of interest. For the query we used C2 collection of gene sets (MSigDB v5.2). Networks were created by using Enrichment Map plugin v. 2.0.1 (Merico, *et al.*, 2010) in Cytoscape ver. 3.2.1 (Shannon, *et al.*, 2003). For each comparison a separate enrichment map (network) was created, and then all 6 maps were combined into 1 global enrichment map to examine the differences and the similarities across these networks.

Author Contributions

B.W.D. designed the experiments, conducted experiments and wrote the paper. S.M. conducted experiments and wrote the paper. E.P., V.G., S.A., S.M. and J.C. conducted experiments. A.B. and A.D.-G. provided analyses and visualization of RNA-seq data. G.A.W. provided assistance with the interpretation of teratoma data.

Acknowledgments

Funding for this study and required infrastructure was provided by the Canadian Institutes of Health Research to BWD (MOP133610), the Canada Research Chairs Program (BWD), the

Ontario Ministry of Research and Innovation (BWD), the Canada Foundation for Innovation (BWD), OCRI Project: Ontario Ministry of Economic Development and Innovation (BWD), and the Ontario Ministry of Training, Colleges and Universities (SA).

References

- Anders, S., Pyl, P.T., and Huber, W. (2015). HTSeq--a Python framework to work with high-throughput sequencing data. *Bioinformatics* 31, 166-9.
- Arce, L., Yokoyama, N.N., and Waterman, M.L. (2006). Diversity of LEF/TCF action in development and disease. *Oncogene* 25, 7492-504.
- Atlasi, Y., Noori, R., Gaspar, C., Franken, P., Sacchetti, A., Rafati, H., Mahmoudi, T., Decraene, C., Calin, G.A., Merrill, B.J., *et al.* (2013). Wnt signaling regulates the lineage differentiation potential of mouse embryonic stem cells through Tcf3 down-regulation. *PLoS genetics* 9, e1003424.
- Baillie-Johnson, P., van den Brink, S.C., Balayo, T., Turner, D.A., and Martinez Arias, A. (2015). Generation of Aggregates of Mouse Embryonic Stem Cells that Show Symmetry Breaking, Polarization and Emergent Collective Behaviour In Vitro. *J Vis Exp*.
- Biechele, S., Cox, B.J., and Rossant, J. (2011). Porcupine homolog is required for canonical Wnt signaling and gastrulation in mouse embryos. *Dev Biol* 355, 275-85.
- Cadigan, K.M., and Waterman, M.L. (2012). TCF/LEFs and Wnt signaling in the nucleus. *Cold Spring Harb Perspect Biol* 4.
- Cole, M.F., Johnstone, S.E., Newman, J.J., Kagey, M.H., and Young, R.A. (2008). Tcf3 is an integral component of the core regulatory circuitry of embryonic stem cells. *Genes Dev* 22, 746-55.
- Coronado, D., Godet, M., Bourillot, P.Y., Tapponnier, Y., Bernat, A., Petit, M., Afanassieff, M., Markossian, S., Malashicheva, A., Iacone, R., *et al.* (2013). A short G1 phase is an intrinsic determinant of naive embryonic stem cell pluripotency. *Stem Cell Res* 10, 118-31.
- Dobin, A., Davis, C.A., Schlesinger, F., Drenkow, J., Zaleski, C., Jha, S., Batut, P., Chaisson, M., and Gingeras, T.R. (2013). STAR: ultrafast universal RNA-seq aligner. *Bioinformatics* 29, 15-21.
- Fu, J., Jiang, M., Mirando, A.J., Yu, H.M., and Hsu, W. (2009). Reciprocal regulation of Wnt and Gpr177/mouse Wntless is required for embryonic axis formation. *Proc Natl Acad Sci U S A* 106, 18598-603.
- Hoffman, J.A., Wu, C.-I., and Merrill, B.J. (2013). Tcf711 prepares epiblast cells in the gastrulating mouse embryo for lineage specification. *Development (Cambridge, England)*.
- Huang, C., and Qin, D. (2010). Role of Lef1 in sustaining self-renewal in mouse embryonic stem cells. *J Genet Genomics* 37, 441-9.
- Kelly, K.F., Ng, D.Y., Jayakumaran, G., Wood, G.A., Koide, H., and Doble, B.W. (2011a). beta-catenin enhances Oct-4 activity and reinforces pluripotency through a TCF-independent mechanism. *Cell Stem Cell* 8, 214-27.

- Kelly, K.F., Ng, D.Y., Jayakumaran, G., Wood, G.A., Koide, H., and Doble, B.W. (2011b). β -catenin enhances Oct-4 activity and reinforces pluripotency through a TCF-independent mechanism. *Cell Stem Cell* 8, 214-227.
- Korinek, V., Barker, N., Moerer, P., van Donselaar, E., Huls, G., Peters, P.J., and Clevers, H. (1998). Depletion of epithelial stem-cell compartments in the small intestine of mice lacking Tcf-4. *Nature genetics* 19, 379-83.
- Law, C.W., Chen, Y., Shi, W., and Smyth, G.K. (2014). voom: Precision weights unlock linear model analysis tools for RNA-seq read counts. *Genome Biol* 15, R29.
- Liu, P., Wakamiya, M., Shea, M.J., Albrecht, U., Behringer, R.R., and Bradley, A. (1999). Requirement for Wnt3 in vertebrate axis formation. *Nature genetics* 22, 361-5.
- Logan, C.Y., and Nusse, R. (2004). The Wnt signaling pathway in development and disease. *Annual review of cell and developmental biology* 20, 781-810.
- Lyashenko, N., Winter, M., Migliorini, D., Biechele, T., Moon, R.T., and Hartmann, C. (2011). Differential requirement for the dual functions of beta-catenin in embryonic stem cell self-renewal and germ layer formation. *Nature cell biology* 13, 753-61.
- MacDonald, B.T., Tamai, K., and He, X. (2009). Wnt/beta-catenin signaling: components, mechanisms, and diseases. *Developmental cell* 17, 9-26.
- Merico, D., Isserlin, R., Stueker, O., Emili, A., and Bader, G.D. (2010). Enrichment map: a network-based method for gene-set enrichment visualization and interpretation. *PLoS one* 5, e13984.
- Merrill, B.J. (2012). Wnt pathway regulation of embryonic stem cell self-renewal. *Cold Spring Harb Perspect Biol* 4, a007971.
- Merrill, B.J., Pasolli, H.A., Polak, L., Rendl, M., Garcia-Garcia, M.J., Anderson, K.V., and Fuchs, E. (2004). Tcf3: a transcriptional regulator of axis induction in the early embryo. *Development* 131, 263-74.
- Mootha, V.K., Lindgren, C.M., Eriksson, K.F., Subramanian, A., Sihag, S., Lehar, J., Puigserver, P., Carlsson, E., Ridderstrale, M., Laurila, E., *et al.* (2003). PGC-1 α -responsive genes involved in oxidative phosphorylation are coordinately downregulated in human diabetes. *Nature genetics* 34, 267-73.
- Morrison, G., Scognamiglio, R., Trumpp, A., and Smith, A. (2016). Convergence of cMyc and beta-catenin on Tcf711 enables endoderm specification. *EMBO J* 35, 356-68.
- Pereira, L., Yi, F., and Merrill, B.J. (2006). Repression of Nanog gene transcription by Tcf3 limits embryonic stem cell self-renewal. *Molecular and cellular biology* 26, 7479-91.
- Reich, M., Liefeld, T., Gould, J., Lerner, J., Tamayo, P., and Mesirov, J.P. (2006). GenePattern 2.0. *Nature genetics* 38, 500-1.

- Robinson, M.D., and Oshlack, A. (2010). A scaling normalization method for differential expression analysis of RNA-seq data. *Genome Biol* 11, R25.
- Roose, J., and Clevers, H. (1999). TCF transcription factors: molecular switches in carcinogenesis. *Biochim Biophys Acta* 1424, M23-37.
- Saito-Diaz, K., Chen, T.W., Wang, X., Thorne, C.A., Wallace, H.A., Page-McCaw, A., and Lee, E. (2013). The way Wnt works: components and mechanism. *Growth Factors* 31, 1-31.
- Saj, A., Chatterjee, S.S., Zhu, B., Cukuroglu, E., Gocha, T., Zhang, X., Goke, J., and DasGupta, R. (2017). Disrupting Interactions Between beta-Catenin and Activating TCFs Reconstitutes Ground State pluripotency In Mouse Embryonic Stem Cells. *Stem Cells*.
- Shannon, P., Markiel, A., Ozier, O., Baliga, N.S., Wang, J.T., Ramage, D., Amin, N., Schwikowski, B., and Ideker, T. (2003). Cytoscape: a software environment for integrated models of biomolecular interaction networks. *Genome Res* 13, 2498-504.
- Shy, B.R., Wu, C.-I., Khramtsova, G.F., Zhang, J.Y., Olopade, O.I., Goss, K.H., and Merrill, B.J. (2013). Regulation of Tcf711 DNA Binding and Protein Stability as Principal Mechanisms of Wnt/ β -Catenin Signaling. *CellReports*.
- Solberg, N., Machon, O., Machonova, O., and Krauss, S. (2012). Mouse Tcf3 represses canonical Wnt signaling by either competing for beta-catenin binding or through occupation of DNA-binding sites. *Mol Cell Biochem* 365, 53-63.
- Subramanian, A., Tamayo, P., Mootha, V.K., Mukherjee, S., Ebert, B.L., Gillette, M.A., Paulovich, A., Pomeroy, S.L., Golub, T.R., Lander, E.S., *et al.* (2005). Gene set enrichment analysis: a knowledge-based approach for interpreting genome-wide expression profiles. *Proc Natl Acad Sci U S A* 102, 15545-50.
- Team, R.D.C. (2016). R: A Language and Environment for Statistical Computing. In (Vienna, Austria: R Foundation for Statistical Computing).
- van Genderen, C., Okamura, R.M., Farinas, I., Quo, R.G., Parslow, T.G., Bruhn, L., and Grosschedl, R. (1994). Development of several organs that require inductive epithelial-mesenchymal interactions is impaired in LEF-1-deficient mice. *Genes Dev* 8, 2691-703.
- Verbeek, S., Izon, D., Hofhuis, F., Robanus-Maandag, E., Te Riele, H., Watering, M., Oosterwegel, M., Wilson, A., Robson Macdonald, H., and Clevers, H. (1995). An HMG-box-containing T-cell factor required for thymocyte differentiation. *Nature* 374, 70-74.
- Wallmen, B., Schrempp, M., and Hecht, A. (2012). Intrinsic properties of Tcf1 and Tcf4 splice variants determine cell-type-specific Wnt/beta-catenin target gene expression. *Nucleic acids research*.
- Wang, S., Zeng, Y., Zhou, J.M., Nie, S.L., Peng, Q., Gong, J., and Huo, J.R. (2016). MicroRNA-1246 promotes growth and metastasis of colorectal cancer cells involving CCNG2 reduction. *Mol Med Rep* 13, 273-80.

Wray, J., Kalkan, T., Gomez-Lopez, S., Eckardt, D., Cook, A., Kemler, R., and Smith, A. (2011). Inhibition of glycogen synthase kinase-3 alleviates Tcf3 repression of the pluripotency network and increases embryonic stem cell resistance to differentiation. *Nature cell biology* 13, 1-9.

Wu, C.-I., Hoffman, J.A., Shy, B.R., Ford, E.M., Fuchs, E., Nguyen, H., and Merrill, B.J. (2012). Function of Wnt/ β -catenin in counteracting Tcf3 repression through the Tcf3- β -catenin interaction.

Yi, F., Pereira, L., Hoffman, J.A., Shy, B.R., Yuen, C.M., Liu, D.R., and Merrill, B.J. (2011). Opposing effects of Tcf3 and Tcf1 control Wnt stimulation of embryonic stem cell self-renewal. *Nature cell biology* 13, 1-11.

Yu, J., and Virshup, D.M. (2014). Updating the Wnt pathways. *Biosci Rep* 34.

Supplemental Information

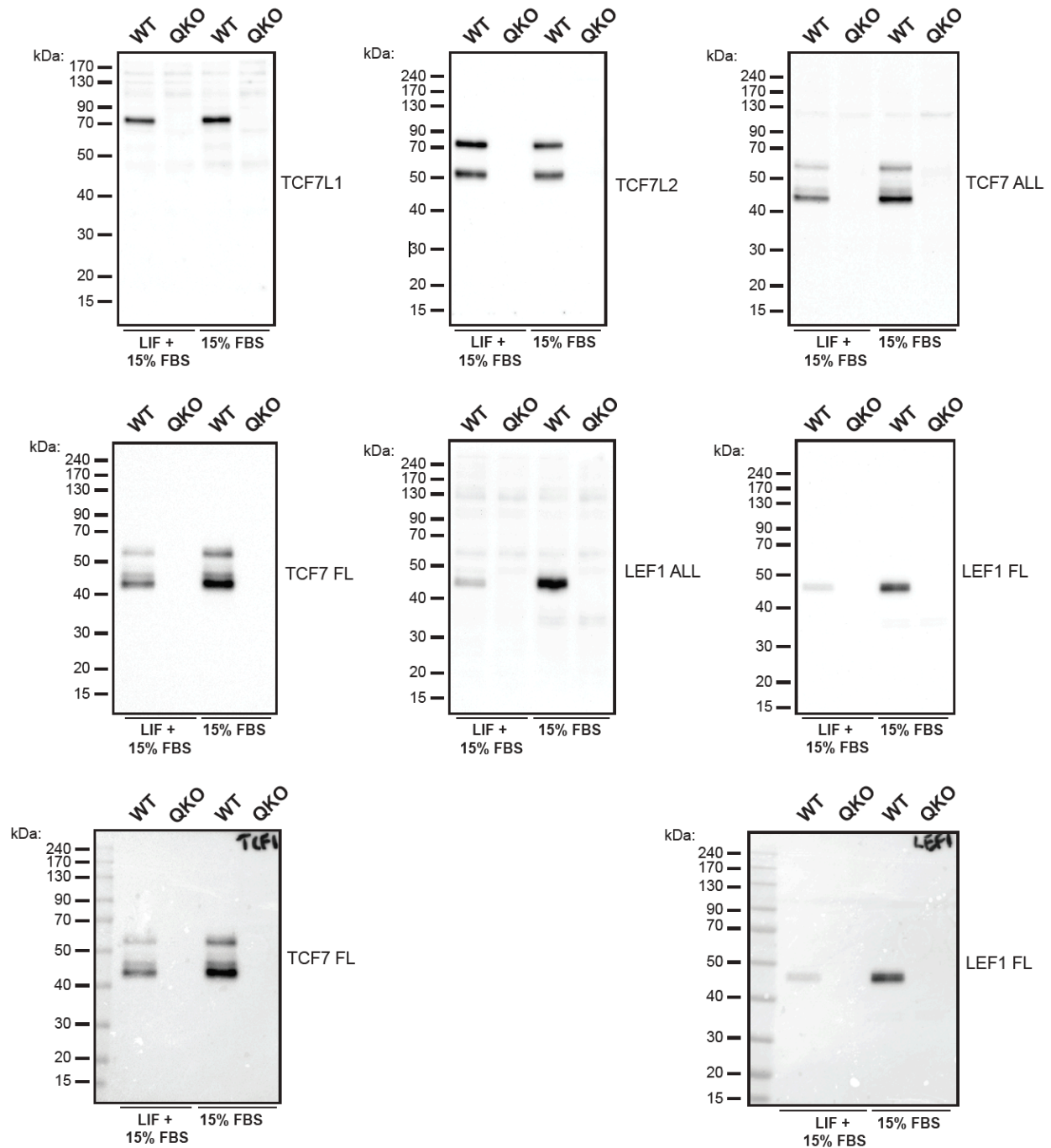


Figure S1, Related to Figure 1

Uncropped full western blots for all TCF/LEFs in WT and QKO lysates from cells maintained 48h in 15% FBS±LIF corresponding to Figure 1C.

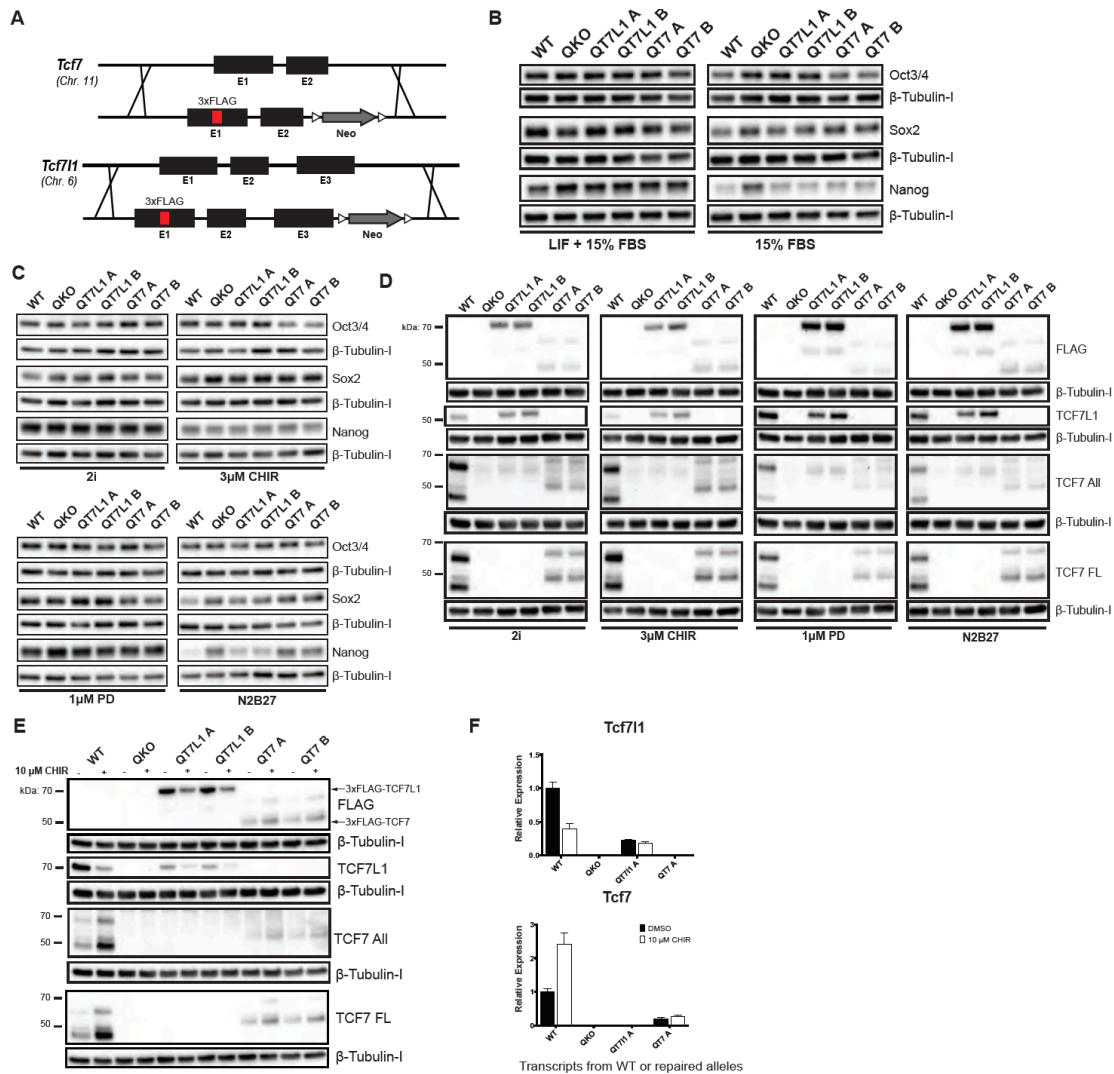


Figure S2, Related to Figure 3

(A) Schematic representation of the TALEN strategy used to simultaneously repair and introduce an N-terminal 3X-FLAG epitope-tag at endogenous TCF7 and TCF7L1 loci in QKO mESCs. (B) Western blot analyses for pluripotency markers Oct4, Sox2 and Nanog in lysates from WT, QKO, QT7 and QT7L1 mESCs maintained in 15% FBS ± LIF for 48 hours. (C) Western blot analyses for pluripotency markers Oct4, Sox2 and Nanog in lysates from WT, QKO, QT7 and QT7L1 mESCs maintained in 2i, 3μM CHIR, 1μM PD, and N2B27 alone for 48 hours. (D) Western blot analyses for TCF7, TCF7L1 and FLAG in lysates from WT, QKO, QT7 and QT7L1 mESCs maintained in 2i, 3μM CHIR, 1μM PD, and N2B27 alone for 48 hours. (E) Western blot analysis of WT, QKO, QT7 and QT7L1 cells treated with 10 μM CHIR or DMSO control for 48 hours. Protein lysates were probed with antibodies against TCF7, TCF7L1, 3X-FLAG and β-tubulin (loading control), as indicated. (F) qRT-PCR analyses of TCF7 and TCF7L1 relative transcript levels in WT and QKO cells treated with 10 μM CHIR or DMSO control for 48 hours. Bars = mean of 3 independent experiments ± SEM, normalized to vehicle-treated WT cells.

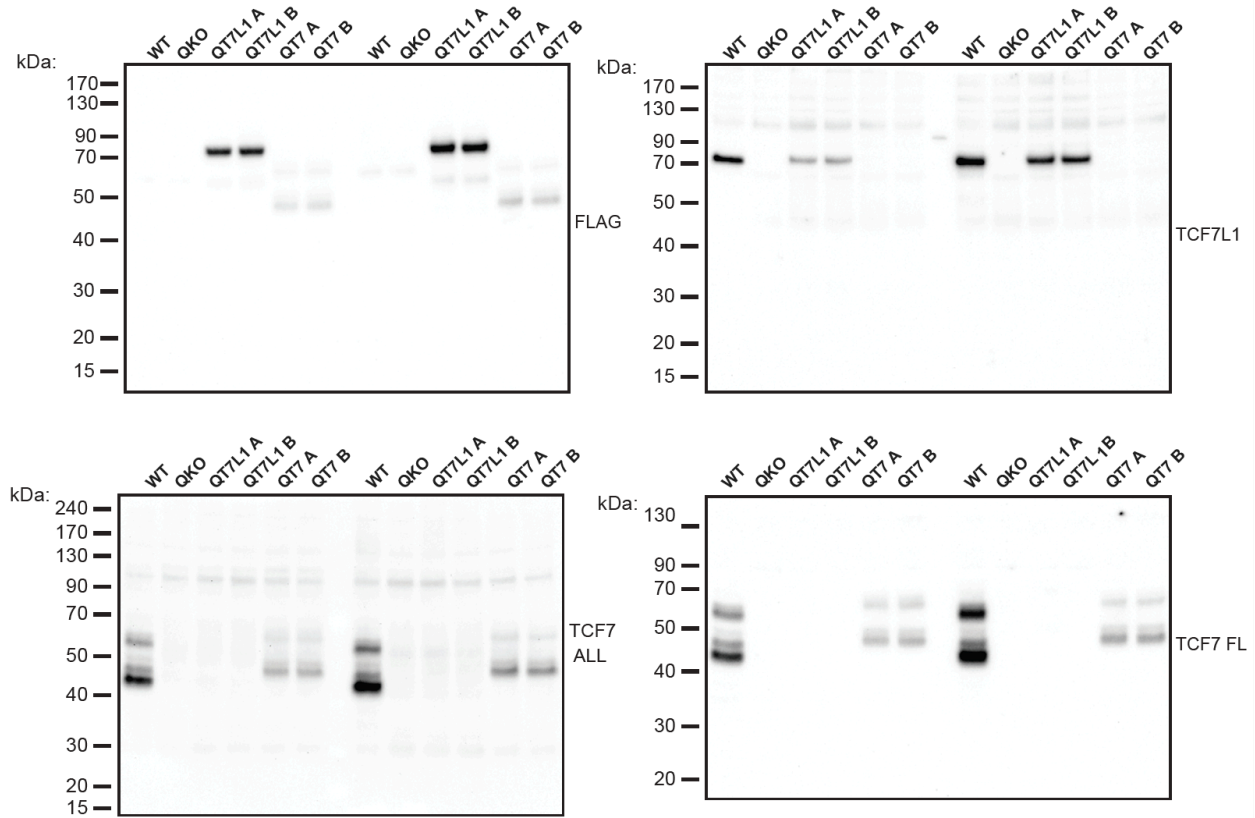


Figure S3, Related to Figure 3A

Uncropped full western blots for TCF7, TCF7L1 and FLAG in WT, QKO, QT7 and QT7L1 lysates from cells maintained 48h in 15% FBS±LIF corresponding to Figure 3A.

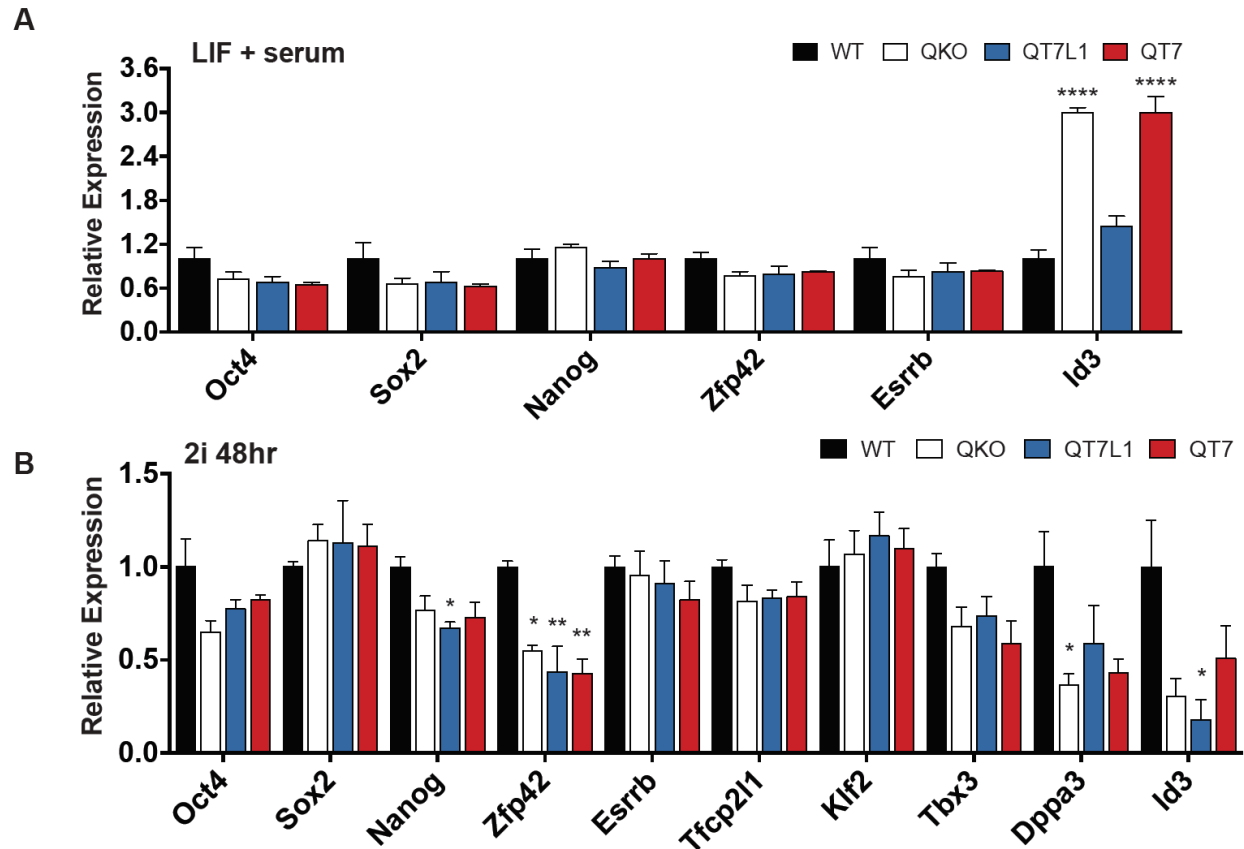


Figure S4, Related to Figure 3

(A) qRT-PCR analyses of the relative transcript levels for pluripotency markers in WT, QKO, QT7 and QT7L1 mESCs maintained in serum-containing or defined serum-free media for 48 hours, as indicated. Bars represent the mean of 3 independent experiments \pm SEM. *, $P < 0.05$, **, $P < 0.01$, ****, $P < 0.0001$; one-way ANOVA analyses were performed comparing QKO, QT7, QT7L1 to WT controls.

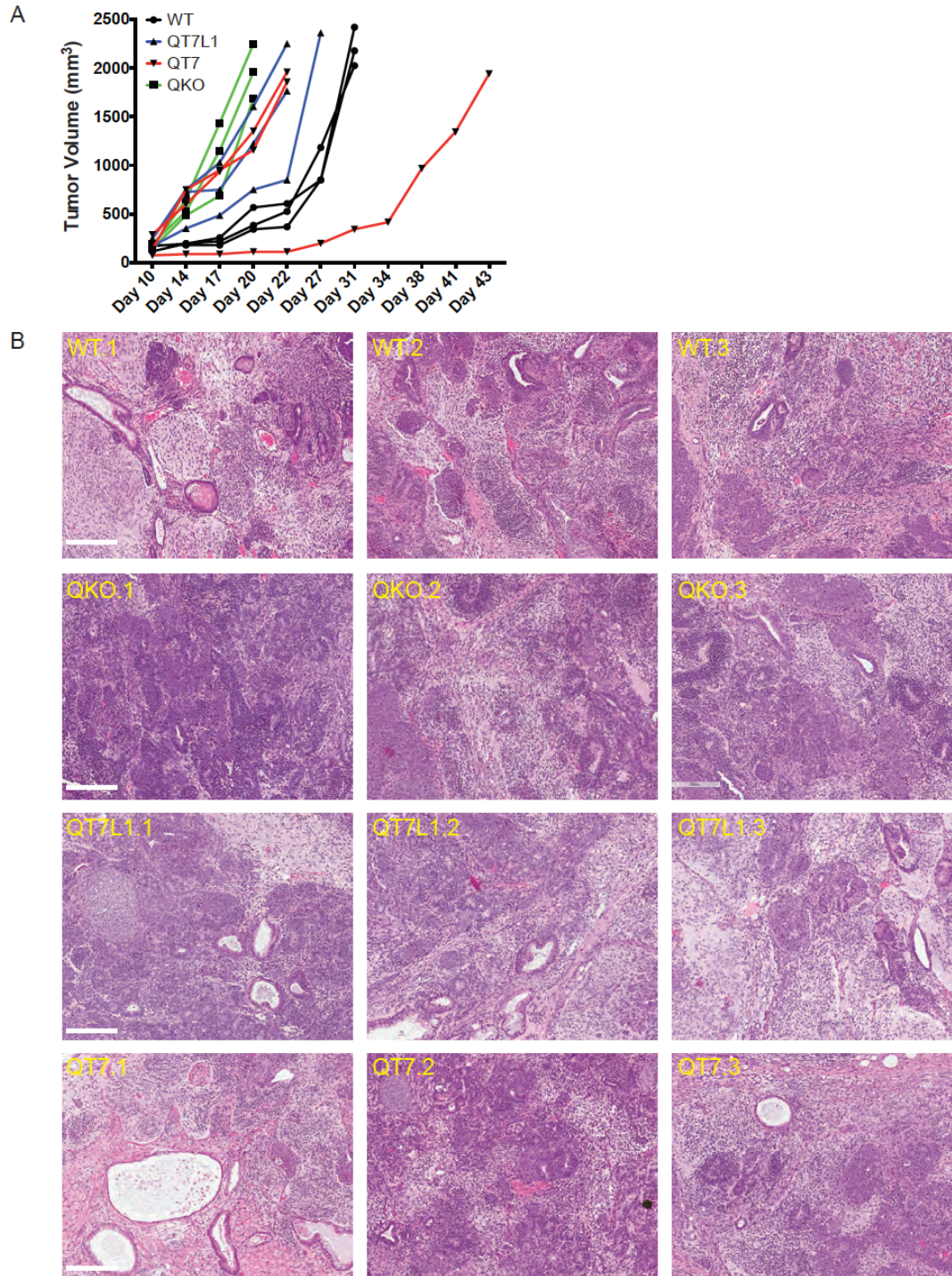


Figure S5, Related to Figure 6

(A) Relative tumor volume of teratomas generated for WT, QKO, QT7 and QT7L1 cell lines (3 independent experiments) were measured at the indicated time-points. (B) H&E stained sections from all 3 biological teratoma replicates derived from WT, QKO, QT7, and QT7L1 mESCs. Bar = 100µM.

Table S1. TALEN RVD and CRISPR sgRNA Sequences***TCF7L1* and *TCF7* TALEN RVD sequences**

	RVD Sequence (5' – 3')
<i>TCF7L1</i> Fwd	NG HD HD HD NH NH NI NH NI NG NG NH NH NG HD NI NH HD
<i>TCF7L1</i> Rev	HD HD NI NH NH HD HD HD NG NG NH HD HD HD NI NI HD NG NG NG HD NG
<i>TCF7</i> Fwd	HD HD NH HD NH HD HD HD HD NH HD NI HD HD HD NH NH HD NH HD
<i>TCF7</i> Rev	HD HD NI NH HD NG NH HD NH NH HD NI NG NH NH

TCF/LEF Guide RNAs (PAM sequences are highlighted in red)

	Sequence (PAM)
<i>TCF7</i>	5' - GGTCCCGGCGTCCGAGTACA -3'(TGG)
<i>TCF7L1</i>	5' - GGAGAATCAGAGCAGTAGCT -3'(CGG)
<i>TCF7L2</i>	5' - GAAGAACTCGGAAAACCTCCT -3'(CGG)
<i>LEF1</i>	5' - CGAGATCAGTCATCCCGAAG -3'(AGG)

Table S2. Quantitative RT-PCR Primers

Gene	Sequence
<i>Rpl13a</i>	Fwd: 5'-TCCCTCCACCCTATGACAAG-3' Rev: 5'-GTCACTGCCTGGTACTTCC-3'
<i>Axin2</i>	Fwd: 5'-AAAGAAACTGGCAAGTGTCCACGC-3' Rev: 5'-GGCAAATTCGTCACCTCGCCTTCTT-3'
<i>Cdx1</i>	Fwd: 5'-AGAGCGGCAGGTAAAGATCTGGTT-3' Rev: 5'-AGAAGGCCAGCATTAGTAGGGCAT-3'
<i>Brachyury</i>	Fwd: 5'-AGCTCTCCAACCTATGCGGACAAT-3' Rev: 5'-TGGTACCATTGCTCACAGACCAGA-3'
<i>Oct4</i>	Fwd: 5'-AGCTGCTGAAGCAGAAGAGGATCA-3' Rev: 5'-TCTCATTGTTGTCGGCTTCCTCCA-3'
<i>Nanog</i>	Fwd: 5'-AACCAAAGGATGAAGTGCAAGCGG-3' Rev: 5'-TCCAAGTTGGGTTGGTCCAAGTCT-3'
<i>Sox2</i>	Fwd: 5'-AAAGGAGAGAAGTTTGGAGCCCGA-3' Rev: 5'-GGGCGAAGTGCAATTGGGATGAAA-3'
<i>Esrrb</i>	Fwd: 5'-CATGAAATGCCTCAAAGTGGG-3' Rev: 5'-AAATCGGCAGGTTCAAGTAG-3'
<i>Dppa3</i>	Fwd: 5'-TTCAAAGCGCCTTTCCCAA-3' Rev: 5'-ACATCTGAATGGCTCACTG-3'
<i>Zfp42</i>	Fwd: 5'-GTCCTGCACACAGAAGAAA-3' Rev: 5'-GTCTTAGCTGCTTCCTTCTTGA-3'
<i>Tfcp2L1</i>	Fwd: 5'-TCTATCGACAGGGTCCCG-3' Rev: 5'-CAGAGTCCACACTTCAGGATG-3'
<i>Klf2</i>	Fwd: 5'-GGCAAGACCTACACCAAGAG-3' Rev: 5'-TGTGCTTTCGGTAGTGGC-3'
<i>Id3</i>	Fwd: 5'-CACTTACCCTGAACTCAACGC-3' Rev: 5'-CCCATTCTCGGAAAAGCCAG-3'
<i>Nestin</i>	Fwd: 5'-AAGTTCCCAGGCTTCTCTTG-3' Rev: 5'-GTCTCAAGGGTATTAGGCAAGG-3'
<i>Pax6</i>	Fwd: 5'-CCCTACCAACACGTACAG-3' Rev: 5'-TCATAACTCCGCCCATTCAC-3'
<i>FoxA2</i>	Fwd: 5'-AAGTATGCTGGGAGCCGTGAAGAT-3' Rev: 5'-CGCGGACATGCTCATGTATGTGTT-3'
<i>Sox17</i>	Fwd: 5'-CGATGAACGCCTTTATGGTG-3' Rev: 5'-TTCTCTGCCAAGGTCAACG-3'
<i>Mesp1</i>	Fwd: 5'-GTCTGCAGCGGGGTGTCGTG-3' Rev: 5'-CGGCGGGTCCAGGTTTCTA-3'

<i>Tnnt2</i>	Fwd: 5'-CAGAGGAGGCCAACGTAGAAG-3' Rev: 5'-CTCCATCGGGGATCTTGGGT-3'
<i>Mef2c</i>	Fwd: 5'-ATCCCGATGCAGACGATTCAG-3' Rev: 5'-AACAGCACACAATCTTTGCCT-3'
<i>Isl1</i>	Fwd: 5'-TCGATGCTACTTCACTGCC-3' Rev: 5'-ATGATGGTGGTTTACAGGC-3'
<i>Nkx2.5</i>	Fwd: 5'-CTGTGCTTGCCTTGTAGC-3' Rev: 5'-GACAAAGCCGAGACGGATGG-3'
<i>Wnt3</i>	Fwd: 5'- TGGAAGTGTACCACCATAGATGAC-3' Rev: 5'- ACACCAGCCGAGGCGATG-3'
<i>Tcf7</i>	Fwd: 5'- GCGTCCGAGTACATGGAGA-3' Rev: 5'- AAGTCTCTGCGAAGTGTGCTC-3'
<i>Tcf7l1</i>	Fwd: 5'-TGGTCAACGAATCGGAGAAT-3' Rev: 5'-TCACTTCGGCGAAATAGTCG -3'

Table S3. LIF + serum cell cycle chi-squared analysis (related to Figure 4)

Experiment 1 (LIF + Serum):

Summary:

	WT	QKO	QT7L1	QT7
G1/0				
S				
G2/M				

	significantly more than expected
	significantly less than expected
	n.s. or different trends in different replicates

Detailed Table (significant p-values are marked in Bold)




			WT	QKO	QT7L1	QT7
Replicate A	G1/0	Counts	1422	1262	1265	1258
		Adj. standardized residuals	9.45	-4.21	-0.84	-3.86
		p-values	3.39E-21	2.5352E-05	0.4022117	0.00011268
	S	Counts	8027	9830	9083	9746
		Adj. standardized residuals	-2.93	1.15	-0.08	1.69
		p-values	3.40E-03	0.25195147	0.9395911	0.09187408
	G2/M	Counts	988	1459	1307	1412
		Adj. standardized residuals	-5.60	2.71	0.94	1.64
		p-values	2.16E-08	0.00678696	0.3466662	0.10105407
Replicate B	G1/0	Counts	1180	914	1060	1090
		Adj. standardized residuals	10.25	-7.37	-2.09	-0.14
		p-values	1.14E-24	1.72E-13	3.64E-02	8.92E-01
	S	Counts	6954	8819	8657	8390
		Adj. standardized residuals	-4.41	5.41	0.52	-1.83
		p-values	1.06E-05	6.13E-08	6.00E-01	6.76E-02
	G2/M	Counts	964	1297	1339	1346
		Adj. standardized residuals	-3.94	-0.06	1.28	2.47
		p-values	8.23E-05	9.56E-01	1.99E-01	1.34E-02
Replicate C	G1/0	Counts	1357	950	729	827
		Adj. standardized residuals	13.24	-4.08	-6.32	-3.17
		p-values	5.16E-40	4.51E-05	2.63E-10	1.52E-03
	S	Counts	9016	9456	7931	8027
		Adj. standardized residuals	0.00	0.70	0.78	-1.51
		p-values	9.97E-01	4.85E-01	4.36E-01	1.31E-01
	G2/M	Counts	1074	1566	1374	1407
		Adj. standardized residuals	-11.41	2.65	4.47	4.61
		p-values	3.92E-30	8.12E-03	7.65E-06	4.10E-06

Table S4. LIF + 2i cell cycle chi-squared analysis (related to Figure 4)

Experiment 2 (LIF + 2i):

Summary:

	WT	QKO	QT7L1	QT7
G1/0				
S				
G2/M				

 significantly more than expected
 significantly less than expected
 n.s. or different trends in different replicates

Detailed Table (significant p-values are marked in Bold):

			WT	QKO	QT7L1	QT7
Replicate A	G1/0	Counts	2725	2398	3044	2349
		Adj. standardized residuals	-1.73	-5.79	19.58	-10.91
		p-values	8.32E-02	6.94E-09	2.35E-85	1.08E-27
	S	Counts	10640	10166	7971	10827
		Adj. standardized residuals	2.39	5.77	-15.64	6.59
		p-values	1.67E-02	8.09E-09	3.64E-55	4.41E-11
	G2/M	Counts	1284	1214	1025	1461
		Adj. standardized residuals	-1.38	-1.10	-2.30	4.61
		p-values	1.68E-01	2.70E-01	2.15E-02	4.00E-06
Replicate B	G1/0	Counts	3115	2512	3229	2630
		Adj. standardized residuals	1.68	-7.13	10.24	-4.82
		p-values	9.39E-02	1.01E-12	1.33E-24	1.45E-06
	S	Counts	11011	10553	9792	10010
		Adj. standardized residuals	1.00	9.64	-6.82	-3.83
		p-values	3.16E-01	5.57E-22	9.00E-12	1.26E-04
	G2/M	Counts	1166	1030	1080	1572
		Adj. standardized residuals	-4.04	-5.39	-3.66	13.16
		p-values	5.32E-05	7.12E-08	2.53E-04	1.46E-39
Replicate C	G1/0	Counts	2755	2539	3229	2714
		Adj. standardized residuals	-3.45	-9.67	13.16	0.34
		p-values	5.69E-04	4.00E-22	1.56E-39	7.37E-01
	S	Counts	10783	11085	9105	10248
		Adj. standardized residuals	3.12	5.90	-16.56	7.28
		p-values	1.82E-03	3.65E-09	1.31E-61	3.24E-13
	G2/M	Counts	1508	1658	1650	1055
		Adj. standardized residuals	-0.20	3.75	7.82	-11.46
		p-values	8.40E-01	1.77E-04	5.46E-15	2.05E-30

SUPPLEMENTAL EXPERIMENTAL PROCEDURES

Cell Culture

E14TG2a mESCs were obtained from ATCC (ATTC® CRL-182™) and were used to generate all derivative cell lines. Standard medium for mESC maintenance was: DMEM (Sigma D5671) supplemented with 15% FBS (Gibco), 1X GlutaMax (Gibco), 1X non-essential amino acids (HyClone), 1X Sodium Pyruvate (HyClone), 1X 2-mercaptoethanol (Sigma M7522) and 1000 U/mL mLIF (Miltenyi Biotec). Cells were maintained in a humidified incubator at 37°C, 5% CO₂, on plates containing a monolayer of feeder mouse embryonic fibroblasts or pre-coated with sterile 0.1% gelatin (Sigma G1890). Differentiation medium (EB medium) used for embryoid body assays was identical to ESC medium without LIF supplementation.

For serum-free based experiments in N2B27, ESCs were plated on to feeders for a single passage in standard LIF+serum media and cultured for an additional 2 passages on gelatin-coated plates. 1/3 of a 6 well was utilized to begin adapting the ESCs to N2B27 + LIF 2i. ESCs were passaged at least 5 passages in N2B27 + LIF 2i before being utilized for experiments. Thereafter, cells were routinely cultured in N2B27 + LIF 2i at a split ratio of 1/3-1/6 every 48hrs on 0.2% gelatin coated plates.

Hanging drop embryoid bodies were produced in 10 cm² petri dishes (800 ESCs/30µl drop in EB medium initially) for 3 days and were subsequently transferred to ultra-low attachment 96-well plates (Corning). EB medium was replenished every 2 days. In both embryoid body formation methods, cells were maintained on a monolayer of feeders in ESC maintenance medium for at least one passage.

L-cells stably expressing Wnt-3a and control wildtype L-cells were obtained from the ATCC, and conditioned medium was prepared according to the protocol provided with the cells. For experiments, conditioned medium was mixed with ESC maintenance medium at a ratio of 1:1.

CRISPR Plasmid Construction

DNA oligonucleotides harboring the forward and reverse sequences of the 20bp guide RNA, not including the PAM sequence, were ordered through IDT (idtdna.com). The forward and reverse oligonucleotides were annealed to generate a double-stranded DNA fragment with 4bp overhangs compatible with ligation into BpiI-digested pX459 CRISPR-Cas9 plasmid (addgene.org/62988/).

Generation of TCF/LEF Quadruple Knockout Cells:

2 million mouse ESCs were transfected with 4µl of Lipofectamine LTX and 5 µg of the CRISPR constructs and subsequently plated on a single 60mm dish in standard mESC medium. After 24 hours, fresh mESC medium containing 2.5µg/ml puromycin was added to perform a 24-hour pulse of selection. After an additional 24 hours in selection, cells were plated at clonal density in standard mESC medium without selection. 6-8 days later, 30 colonies were picked and expanded to 2, 24-well plates. One plate was used to make whole cell protein lysates and one was maintained in culture. Successful gene knockouts were verified through western blot analysis, and heterozygous or homozygous positive clones were subsequently expanded and frozen in liquid nitrogen. After indel validation by sequencing, one *LEF1* homozygous knockout mESC line was targeted to ablate the *TCF7L1* gene, as described above. A western blot and sequence verified *LEF1/TCF7L1* homozygous double knockout mESC line was subsequently used to target *TCF7L2* and *TCF7* with their CRISPR constructs simultaneously. Three *LEF1/TCF7L1/TCF7L2/TCF7* homozygous quadruple knockout ES cell lines were validated and verified through western blot and sequencing. These three cell lines were used in subsequent experiments.

Sequencing of TCF/LEF loci

Primers flanking CRISPR or TALEN target sites were used to PCR amplify the region of interest and gel extracted using the Qiagen MinElute Gel Extraction kit (Qiagen). This DNA was subsequently inserted into pJet1.2 (Thermo Scientific). DNA from 6 colonies was purified using Invitrogen PureLink DNA Mini kit (Life Technologies) and sent for Sanger-sequencing (Mobix Lab, McMaster).

Antibodies

The following primary antibodies were used for western blot and/or immunofluorescent staining: mouse anti-β-Tubulin-I (T7816, Sigma); rabbit anti-β-Actin (13E5, Cell Signaling Technologies); mouse anti-FLAG M2 (F1804, Sigma); rabbit anti-LEF1 FL (C12A5, Cell Signaling Technologies); rabbit anti-LEF1 All (C18A7, Cell Signaling Technologies); rabbit anti-TCF7 FL (C63D9, Cell Signaling Tech.); rabbit anti-TCF7 All (C46C7, Cell Signaling Tech.); rabbit anti-TCF7L1 (ab86175, Abcam); rabbit anti-TCF7L2 (C48H11, Cell Signaling

Tech.); rabbit anti- Nanog (A300-397A, Bethyl Laboratories); mouse anti-Oct3/4 (sc-5279, Santa Cruz); mouse anti-Sox2 (561469, BD Biosciences); mouse anti- β -III-Tubulin (MAB1195, R&D Systems); rabbit anti-GATA4 (sc-9053, Santa Cruz); mouse anti-heavy chain cardiac Myosin (ab50967, Abcam); mouse anti-heavy chain Myosin (MF20) (Developmental Studies Hybridoma Bank).

Fluorochrome-conjugated secondary antibodies were obtained from Invitrogen and used at 1/2000 (Molecular Probes): rabbit anti-goat Alexa Fluor 488. Horseradish peroxidase-conjugated secondary antibodies for western blotting were purchased from Bio-Rad (170-6516 and 170-6515; goat anti-mouse and goat anti-rabbit, respectively) or R&D Systems (HAF109; donkey anti-goat).

Cell lysate preparation

To generate whole cell extracts, 6-well plates of ESCs were rinsed twice with PBS at room temperature, and ice-cold $1 \times$ RIPA buffer was added directly to the dishes, on ice. The $1 \times$ RIPA buffer contained: 150 mM NaCl, 1% NP-40, 0.5% DOC, 0.1% SDS, 50 mM Tris pH 8.0, 1 mM EDTA as well as 1x Halt Protease and Phosphatase Inhibitor cocktail (Life Technologies). After 10 minutes, the cell suspension was harvested into microcentrifuge tubes and centrifuged at 14,000 rpm for 12 minutes at 4°C. The supernatant containing soluble proteins was removed and quantified using the Lowry method (DC Protein Assay; Bio-Rad). The samples were subsequently prepared in 1X LDS buffer (Invitrogen) with 5% TCEP Bond-Breaker solution (Thermo Scientific) and heated at 95°C for 5 minutes prior to immunoblot analyses using the indicated antibodies.

Alkaline phosphatase staining of colonies

Media with serum: mESCs were grown on feeders for at least one passage. Single-cell suspensions were obtained by using Accutase (Stem Cell Technologies), and 600 cells were plated onto gelatin-coated 6-well plates, with daily medium replacement. After 5 days, cells were fixed in 4% PFA for 2 minutes, washed in 0.2% TBS-T and incubated in AP staining reagent (Millipore, SCR004) for 20 min. (RT in the dark). A final wash with 0.2% TBS-T was performed before the addition of 1x PBS.

Serum-free media: 1000 cells were plated on poly-ornithine/laminin-coated 6-well plates and medium was replenished daily. After 6 days, cells were fixed with 65% acetone, 25% citrate and 8% formaldehyde, washed with ddH₂O and incubated in AP stain reagent (Sigma, 86R-1KT) for 45 min. (RT in the dark). A final wash with ddH₂O was followed by the addition of 1x PBS. Colonies were scanned using a flatbed scanner and were scored manually. Colony size was determined using a script in ImageJ.

Teratoma Assays

Mouse ESCs were maintained on feeder cells for a single passage before being pre-plated on gelatin-coated dishes to eliminate feeders and plated on gelatin-coated dishes for one passage. Cells were treated with Accutase (Stem Cell Technologies) to obtain single-cell suspensions and diluted in matrigel (diluted 1/3 in DMEM), such that each 100 μ l contains 5×10^6 cells. 100 μ l of these suspensions (5×10^6 cells) were unilaterally injected, subcutaneously into the hind limbs of NOD/SCID mice (JAX) using a 26-gauge needle. At endpoint, which is when the tumors reached a volume of approximately 2mm³, the animals were sacrificed and teratomas were harvested. Small samples were collected for RNA and protein isolation. The remainder of the tissue samples were fixed overnight at 4°C in neutral-buffered formalin and then paraffin embedded for subsequent sectioning and histological/immunohistological analyses.

TCF/LEF Reporter Assays with mESCs

Mouse ESCs were co-transfected with the constructs 8XTOPFlash (1.8 μ g), driving firefly luciferase production, and pRL-CMV (0.2 μ g), driving constitutive expression of renilla luciferase for normalization (Promega). For experiments performed with 10 μ M CHIR99021 or Wnt3a conditioned medium treatments, ESCs were resuspended directly into the appropriate media. Cells were washed twice with PBS 24 hours following transfection and lysed with 1x passive lysis buffer (Promega). The firefly and luciferase activities were measured using a 96-well-based luminometer as per the manufacturer's instructions (Promega Dual-Light System).

CyQuant Cell Proliferation Assay

10,000 cells were plated in standard mESC media, onto a single well of a 96-well plate, in triplicate. A single plate was used for 6, 12, 24, 48, and 72 hour time-points. At each time-point, medium was aspirated, and plates were frozen and stored at -80°C. At the 48 hour time-point, fresh mESC medium was added to the 72 hour plate. After the final time-point was collected and frozen, 200 μ l of a 2.5x CyQuant GR dye/cell lysis buffer was added to each well and incubated at room temperature (RT) for 5 minutes. The fluorescence was subsequently measured using a FLUOstar Omega microplate reader (BMG Labtech). A reference standard curve was created using dilutions corresponding to a range of 0-300,000 cells.

RNA-seq Analyses

HTseq files were used for principal component and hierarchical clustering analyses (PCA, HC) and visualizations (Anders, *et al.*, 2015). Genes showing zero counts in all 8 samples were removed, and remaining values were normalized with the TMM normalization method and then transformed with voom transformation (Law, *et al.*, 2014; Robinson and Oshlack, 2010).

PCA and HC were performed and visualized with *rgl* and *stats* (<https://CRAN.R-project.org/package=rgl> and <https://stat.ethz.ch/R-manual/R-devel/library/stats/html/00Index.html>) packages, respectively. Hierarchical Clustering was performed by using average linkage and Euclidean distance metrics. All analyses were performed in the R v3.3.0 environment (Team, 2016).

For gene set enrichment analysis (GSEA), differentially expressed genes were ranked by Log₂ fold-change and used with GSEAPreranked module v4.2 (Subramanian, *et al.*, 2005; Mootha, *et al.*, 2003) in GenePattern environment (Reich, *et al.*, 2006) to examine Gene Set Enrichment in the groups of interest. For the query, we used C2 collection of gene sets (MSigDB v5.2). Networks were created by using Enrichment Map plugin v2.0.1 (Merico, *et al.*, 2010) in Cytoscape v3.2.1 (Shannon, *et al.*, 2003). For each comparison, a separate enrichment map (network) was created, and then all 6 maps were combined into 1 global enrichment map to examine the differences and the similarities across these networks.

Cell Cycle Analysis with mESCs

Cell cycle analysis was performed using Invitrogen's Click-iT® EdU 488 Flow Cytometry Kit (C10425). Mouse ES cells were plated at a density of 40,000 (LIF+serum) or 80,000 (N2B27+2i) on a single well of a 24 well plate. Following 48 hours, cells were labelled with a 10uM EdU solution for 45 minutes in the incubator. Cells were then collected and washed with 1% BSA/PBS, and subsequently strained into a Flow Cytometry tube. Cells were then incubated at room temperature for 15 mins in Click-iT fixative. Following a 1% BSA/PBS wash, cells were permeabilized using the saponin based wash buffer for 30 minutes and room temperature. Following a 1% BSA/PBS wash, the Click-iT 488 reaction cocktail was added and incubated for 30 minutes at room temperature. Finally, cells were washed once with 1% BSA/PBS and incubated overnight at 4°C in DAPI solution (0.1M Tris pH7.4, 150mM NaCl, 1mM CaCl₂, 0.5mM MgCl₂, 0.2% BSA, 0.1% NP-40, 10µg/ml DAPI). The following morning 20,000 cells were assessed by flow cytometry.

Cell cycle statistical analysis

Pearson Chi-square analysis was followed by examination of the adjusted standardized residuals for each of the cells (Beasley TM and Schumacker RE (1995) Multiple regression approach to analyzing contingency tables: post hoc and planned comparison procedures. *The Journal of Experimental Education*, 64 (1): 79-93; Garcia-perez, Miguel A., and Vicente Nunez-Anton. "Cellwise residual analysis in two-way contingency tables." *Educational and psychological measurement* 63.5 (2003): 825-839). The significance of the residuals was established based on their p-values. P-values < 0.0042 (Bonferroni-corrected p-value) were considered to be significant. Only results shown to be significant in all 3 biological replicates were considered for further examination.

SUPPLEMENTAL REFERENCES:

Anders, S., Pyl, P.T., and Huber, W. (2015). HTSeq--a Python framework to work with high-throughput sequencing data. *Bioinformatics* 31, 166-9.

Law, C.W., Chen, Y., Shi, W., and Smyth, G.K. (2014). voom: Precision weights unlock linear model analysis tools for RNA-seq read counts. *Genome Biol* 15, R29.

Merico, D., Isserlin, R., Stueker, O., Emili, A., and Bader, G.D. (2010). Enrichment map: a network-based method for gene-set enrichment visualization and interpretation. *PloS one* 5, e13984.

Mootha, V.K., Lindgren, C.M., Eriksson, K.F., Subramanian, A., Sihag, S., Lehar, J., Puigserver, P., Carlsson, E., Ridderstrale, M., Laurila, E., *et al.* (2003). PGC-1alpha-responsive genes involved in oxidative phosphorylation are coordinately downregulated in human diabetes. *Nature genetics* 34, 267-73.

Reich, M., Liefeld, T., Gould, J., Lerner, J., Tamayo, P., and Mesirov, J.P. (2006). GenePattern 2.0. *Nature genetics* 38, 500-1.

Robinson, M.D., and Oshlack, A. (2010). A scaling normalization method for differential expression analysis of RNA-seq data. *Genome Biol* 11, R25.

Shannon, P., Markiel, A., Ozier, O., Baliga, N.S., Wang, J.T., Ramage, D., Amin, N., Schwikowski, B., and Ideker, T. (2003). Cytoscape: a software environment for integrated models of biomolecular interaction networks. *Genome Res* 13, 2498-504.

Subramanian, A., Tamayo, P., Mootha, V.K., Mukherjee, S., Ebert, B.L., Gillette, M.A., Paulovich, A., Pomeroy, S.L., Golub, T.R., Lander, E.S., *et al.* (2005). Gene set enrichment analysis: a knowledge-based approach for interpreting genome-wide expression profiles. *Proc Natl Acad Sci U S A* 102, 15545-50.

Team, R.D.C. (2016). R: A Language and Environment for Statistical Computing. In (Vienna, Austria: R Foundation for Statistical Computing).

CHAPTER 3

TCF7L1 AND TCF7 DIFFERENTIALLY REGULATE SPECIFIC MOUSE ES CELL GENES IN RESPONSE TO GSK-3 INHIBITION

Preamble

This chapter is available as an unpublished preprint article. It is presented in its preprint format.

“This research was originally posted on the bioRxiv. Steven Moreira, Caleb Seo, Enio Polena, Sujeivan Mahendram, Eloi Mercier, Alexandre Blais and Bradley W. Doble. Variable TCF7L1 and TCF7 binding at specific genomic loci upon GSK-3 inhibition in mouse ESCs. <https://doi.org/10.1101/473801>. © 2018 The Authors. Preprint posted by Cold Spring Harbor Laboratory.”

Together Dr. Bradley Doble and I, conceived the study, designed experiments and wrote the paper. Caleb Seo provided technical assistance with Co-IP assays. Enio Polena provided technical assistance with generating the 3xFLAG TCF7 cell lines. Sujeivan Mahendram generated the TCF7 TALENs and targeting construct. Dr. Yu Lu, Sansi Xing, and Ruilin Wu provided technical assistance with mass spectrometry. Eloi Mercier and Dr. Alexandre Blais provided technical assistance with ChIP-seq analysis and visualization. To date, TCF7 and TCF7L1 ChIP-seq experiments have been performed in mouse ES cells, albeit utilizing poor antibodies that are either not very specific or applicable for ChIP. Although there is great conservation of the TCF/LEF DNA binding domain, there is evidence to suggest that each TCF/LEF factor is able to bind an overlapping set of genes, but also a unique set of genes. These studies however are confounded by the fact that any differences in TCF/LEF factor binding to genes may have arisen due to differences in antibody specificities and affinities for the respective factor. To circumvent this issue, we have employed a system where both TCF7L1 and TCF7 have been endogenously tagged with a 3xFLAG epitope in separate mouse ES cell lines.

**TCF7L1 and TCF7 differentially regulate specific
mouse ES cell genes in response to GSK-3
inhibition**

Steven Moreira¹, Caleb Seo¹, Enio Polena¹, Sujeivan Mahendram¹, Eloi Mercier², Alexandre
Blais³ and Bradley W. Doble^{1*}

1. Department of Biochemistry and Biomedical Sciences, Stem Cell and Cancer Research Institute, Michael G. DeGroot School of Medicine, McMaster University, Hamilton, ON L8N 3Z5, Canada.

2. Canadian Centre for Computational Genomics, Montreal Node, McGill University and Genome Quebec Innovation Center, Montréal, QC H3A 0G1, Canada

3. Ottawa Institute of Systems Biology, Department of Biochemistry, Microbiology, and Immunology, and Department of Cellular and Molecular Medicine, Faculty of Medicine, University of Ottawa, Ottawa, ON K1H 8M5, Canada

*Correspondence:

dobleb@mcmaster.ca

Summary

The genome-wide chromatin occupancy of the TCF/LEF factors and its modulation by Wnt pathway activation remain poorly defined. Here, we describe mouse ES cell (mESC) lines expressing a single copy knock-in of the 3xFLAG epitope at the N-terminus of TCF7L1 and TCF7, the two most-highly expressed TCF/LEF factors in mESCs. TCF7L1 protein levels, detected by immunoblotting with a FLAG antibody, were much higher than TCF7 in mESCs maintained in standard serum- and LIF-supplemented medium, even in the presence of the GSK-3 inhibitor, CHIR99021 (CHIR). We used FLAG antibody-mediated ChIP-seq to determine TCF7 and TCF7L1 chromatin occupancy in mESCs cultured in standard medium with or without CHIR for 14 hours. TCF7 and TCF7L1 displayed very few overlapping ChIP peaks across the genome, with TCF7L1 binding significantly more genes than TCF7 in both culture conditions. Despite a reduction in total TCF7L1 protein after CHIR treatment, the TCF7L1 ChIP peak profile was not uniformly attenuated. Our data demonstrate that TCF7L1 chromatin occupancy upon short-term CHIR treatment is modulated in a target-specific manner. Our findings also suggest that Wnt target genes in mESCs are not regulated by TCF/LEF switching, and TCF7L1, although often called a constitutive repressor, may serve as a transcriptional activator of certain target genes in CHIR-treated mESCs.

Highlights

- TCF7L1 ChIP data do not suggest its direct regulation of *Nanog* expression in mESCs.
- TCF7L1 remains associated with β -catenin in the presence of CHIR99021.
- TCF7 and TCF7L1 display different chromatin occupancies in mESCs.
- TCF7L1 binding at specific genomic sites is variably altered by CHIR99021.

eTOC Blurp

Moreira *et al.* characterize the genomic binding profile of TCF7 and TCF7L1 in mouse ES cells cultured in standard conditions and treated with a Wnt agonist CHIR. By using 3xFLAG-tagged TCF7 and TCF7L1 single copy knock-in's, in a wildtype background, they reveal differential binding of TCF7 and TCF7L1 to the mouse genome.

INTRODUCTION

Wnt/ β -catenin signaling plays important roles in the regulation of self-renewal and differentiation of embryonic stem cells (ESCs) and many somatic stem cells, however, nuclear signaling mechanisms remain unclear (Clevers *et al.*, 2014; Nusse and Clevers, 2017). Wnt ligands stimulate the accumulation of cytosolic β -catenin, followed by its subsequent nuclear translocation. Nuclear β -catenin associates with T-cell factor/lymphoid enhancer factor (TCF/LEF) transcription factors bound to Wnt-responsive elements (WRE), thereby activating transcription of Wnt target genes (Hrckulak *et al.*, 2016). In the absence of Wnt pathway activation, glycogen synthase kinase-3 (GSK-3), as part of a multi-protein destruction complex, phosphorylates β -catenin, priming it for proteasomal degradation (Gammons and Bienz, 2018).

GSK-3 inhibition promotes self-renewal and pluripotency in mouse ESCs (mESCs) (Sato *et al.*, 2004). Ablation of GSK-3 α and GSK-3 β in mESCs leads to elevated levels of β -catenin and pluripotency-associated factors, OCT4 and NANOG, and highly attenuated differentiation (Doble *et al.*, 2007; Kelly *et al.*, 2011). Mouse ES cells can also be propagated in the presence of two inhibitors, CHIR99021 (CHIR), a GSK-3 inhibitor and activator of the Wnt/ β -catenin pathway, and PD0325901, a MEK (MAP kinase kinase) inhibitor, which together, promote the homogeneous expression of a circuit of pluripotency-associated transcription factors (Ying *et al.*, 2008).

TCF7L1 and TCF7 are the most abundantly expressed TCF/LEF factors in mESCs (Pereira *et al.*, 2006), although all four family members: TCF7, TCF7L2, TCF7L1, and LEF1, are detectable at the protein level (Kelly *et al.*, 2011; Wallmen *et al.*, 2012). In mESCs TCF7L1 was first implicated as a negative regulator of pluripotency, where it was linked to repression of *Nanog* expression (Pereira *et al.*, 2006). TCF7L1 has been thought to function as a constitutive repressor in the circuitry of transcription factors regulating self-renewal and pluripotency (Cole *et al.*, 2008;

Marson *et al.*, 2008; Yi *et al.*, 2008), although it has been suggested that Wnt stimulation may promote activation of pluripotency-associated genes by β -catenin binding to genes occupied by TCF7L1 (Cole *et al.*, 2008). Derepression of TCF7L1 has been demonstrated to be essential for the self-renewal enhancing effects of the GSK-3 inhibitor CHIR (Wray *et al.*, 2011a; Yi *et al.*, 2011), and *ESRRB* has been shown to be a critical downstream target of derepressed TCF7L1 (Martello *et al.*, 2012). Mechanistically, it has been suggested that this derepression involves removal of TCF7L1 from the chromatin mediated by its binding to β -catenin and subsequent degradation (Shy *et al.*, 2013). TCF7L1 downregulation in response to CHIR also occurs at the transcriptional level, facilitated by c-Myc repression (Moreira *et al.*, 2017; Morrison *et al.*, 2016). Liberation of TCF7L1 from Wnt-responsive elements (WREs) has been suggested to allow for a TCF switch, in which repressive TCF7L1 is exchanged with activating TCF7- β -catenin complexes (Yi *et al.*, 2011). However, such a TCF switch is not required for maintenance of self-renewing mESCs or their transition from primed to naïve pluripotency (Moreira *et al.*, 2017; Saj *et al.*, 2017).

It has been difficult to quantitatively compare chromatin occupancy of the various TCF/LEFs due to inherent differences in TCF/LEF antibody affinities and specificities. A quantitative comparison of the genomic distribution between ectopically expressed HA-tagged human TCF7 and TCF7L2 at select Wnt target genes: *Axin2*, *Cdx1*, *Cdx2*, *T*, and *Sp5*, demonstrated differential binding of the two factors (Wallmen *et al.*, 2012). Global genomic occupancy of TCF7 and TCF7L1 in mESCs has been obtained by using chromatin immunoprecipitation followed by next-generation sequencing (ChIP-seq), which revealed that both factors regulate context-dependent Wnt signaling responses by binding to distinct target genes (De Jaime-Soguero *et al.*, 2017).

To increase our understanding of individualized TCF/LEF functions, we developed mESC lines in which TCF7 and TCF7L1 were each 3xFLAG-tagged, allowing for quantitative

comparisons. We performed ChIP-seq to identify genomic regions occupied by TCF7 and/or TCF7L1 in medium containing serum and LIF, and the absence and presence of CHIR stimulation for fourteen hours. Our data reveal very few regions of overlap between the genomic loci bound by TCF7 and TCF7L1, with TCF7L1 bound at significantly more genomic locations in both culture conditions.

RESULTS

Generation of mESC lines with N-terminal 3xFLAG tags knocked into single copies of endogenous TCF7 and TCF7L1 loci

To circumvent the differing affinities and specificities of commercially available TCF7 and TCF7L1 antibodies, we introduced the 3xFLAG tag into one copy of the endogenous loci of either *TCF7* or *TCF7L1* in independent wildtype (WT) mESC cell lines, by using TALEN-facilitated homologous recombination. The expression of 3xFLAG-TCF7 and 3xFLAG-TCF7L1 in targeted mESC lines was confirmed and compared by western blot analysis after 48 hours of growth in standard medium containing serum and LIF as well as medium lacking LIF (Figures 1A and S1A). Total protein levels of TCF7 and TCF7L1 in the knock-in cell lines were comparable to those observed in WT mESCs (Figure 1A and S1A). The protein levels of both TCF7 and TCF7L1 were increased in LIF-free conditions that promote differentiation (Figure 1A and S1A). Doublet bands, absent in WT blots, were clearly observed in western blots probed with anti-TCF7 antibodies, helping to confirm that 3xFLAG-TCF7 knock-in lines were heterozygous (Figure 1A and S1A).

Due to the higher molecular weight of TCF7L1, 3xFLAG-TCF7L1 and WT TCF7L1 co-migrated as a tight doublet. Heterozygosity was verified by using Sanger sequencing. TCF7L1 was expressed at much higher levels than TCF7 in standard (16-fold difference) and LIF-free (5-fold difference) medium (Figures 1A, S1A, and Table S1). These data are different from what is observed in mESCs lacking all full-length TCF/LEFs that have been rescued by single-copy

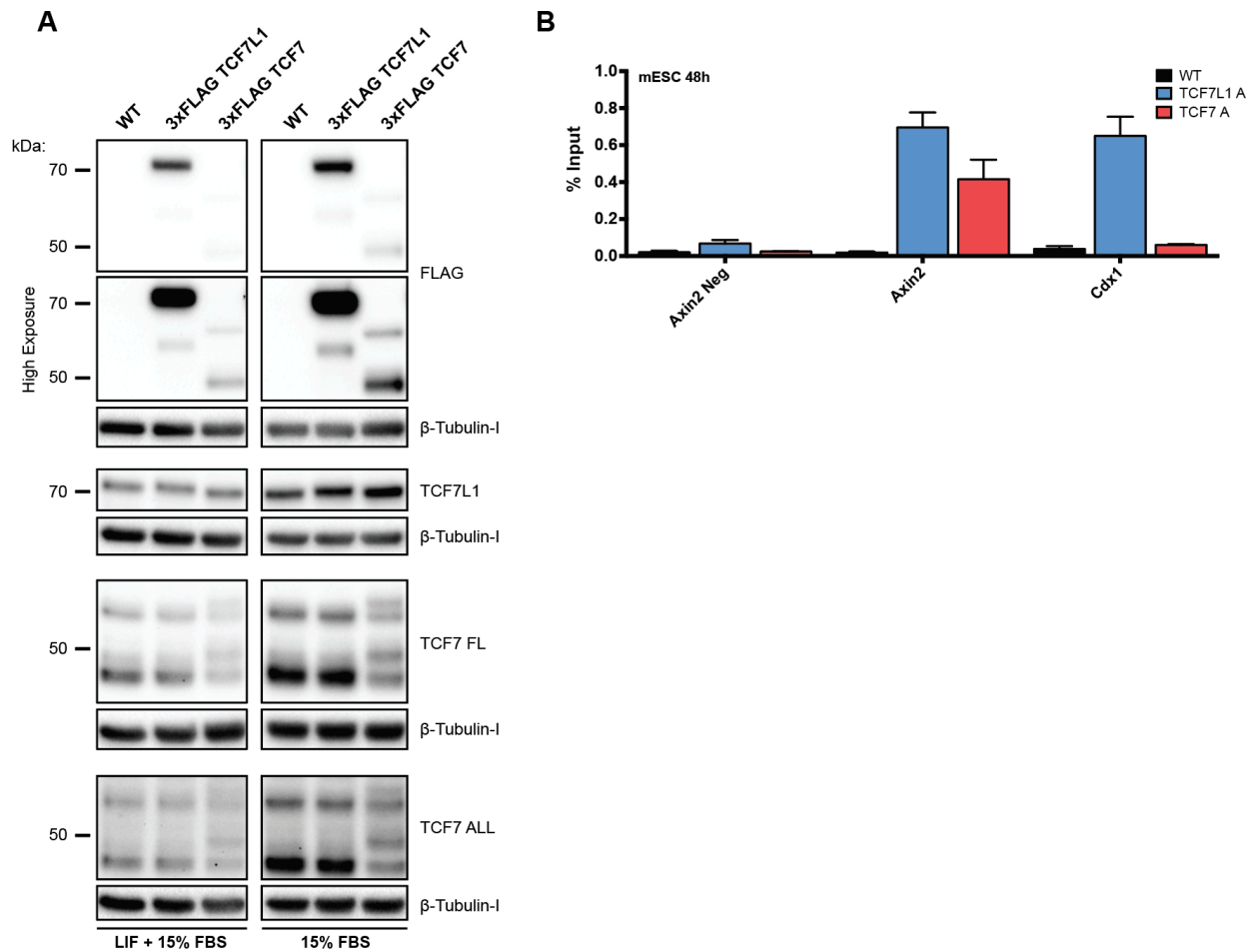


Figure 1. Characterization of 3xFLAG-TCF7 and 3xFLAG-TCF7L1 mESC lines. (A)

Western blot analyses of 3xFLAG-TCF7 and 3xFLAG-TCF7L1 protein expression in cells maintained 48h in medium with or without LIF supplementation. Lysates were probed with antibodies against TCF7L1, TCF7, FLAG and β -Tubulin, as indicated. (B) Quantitative ChIP results obtained by using a FLAG antibody with chromatin isolated from WT, 3xFLAG-TCF7L1 and TCF7 mESCs, cultured in standard medium containing 15%FBS and LIF, for 48h. Percent input was calculated for regions bound by TCF/LEFs in *Axin2* and *Cdx1* genes, as well as a negative control locus 11kb upstream of *Axin2*. Bars represent the mean of 3 independent experiments \pm SEM.

expression of 3xFLAG-tagged endogenous *TCF7* and *TCF7L1* loci, highlighting the importance of cross-regulation among the TCF/LEF factors (Moreira *et al.*, 2017).

To evaluate occupancy of the 3xFLAG-tagged TCF7 and TCF7L1 proteins at known Wnt target genes, *Axin2* and *Cdx1*, we used chromatin immunoprecipitation (ChIP) with a well-validated highly specific FLAG antibody, followed by quantitative RT-PCR with chromatin from mESCs cultured in standard medium for 48 hours (Figure 1B, S1B). TCF7L1 bound near the transcriptional start sites of *Axin2* and *Cdx1*, as previously reported (Figure 1B, S1B) (Shy *et al.*, 2013; Wallmen *et al.*, 2012). Levels of TCF7L1 enrichment were only 1.67 times higher than TCF7 at the transcriptional start site of *Axin2*, despite significantly lower TCF7 protein levels (Figure 1B, S1B). We did not detect TCF7 binding at the transcriptional start site of *Cdx1*, which has been reported previously (Wallmen *et al.*, 2012).

Neither 3xFLAG-TCF7 nor 3xFLAG-TCF7L1 protein levels inversely correlate with NANOG protein expression in mESCs

We examined the protein expression of both 3xFLAG-TCF7L1, 3xFLAG-TCF7, and NANOG in self-renewing and differentiating mESCs. We used intracellular flow cytometric analyses to assess FLAG and NANOG levels in cells grown continuously in LIF-supplemented medium for 48h or cells grown for 24h in LIF-containing medium, which was replaced with medium lacking LIF (Figure 2A). In standard LIF-supplemented medium, TCF7L1 was highly expressed, with approximately 35% of the population demonstrating detectable levels, whereas TCF7 was expressed in about 14% of the population (Figures 2A, S1A, 2B, and S2B). Neither TCF7L1 nor TCF7 levels negatively correlated with NANOG expression as evidenced by representative flow cytometric data (Figure 2A, S1A). The FLAG⁺ NANOG⁺ double-positive cells were fewer than FLAG⁻ NANOG⁺ single-positive cells at days 0-2 of differentiation, but by day three the numbers of both populations were similar. Importantly, the FLAG⁺ NANOG⁺

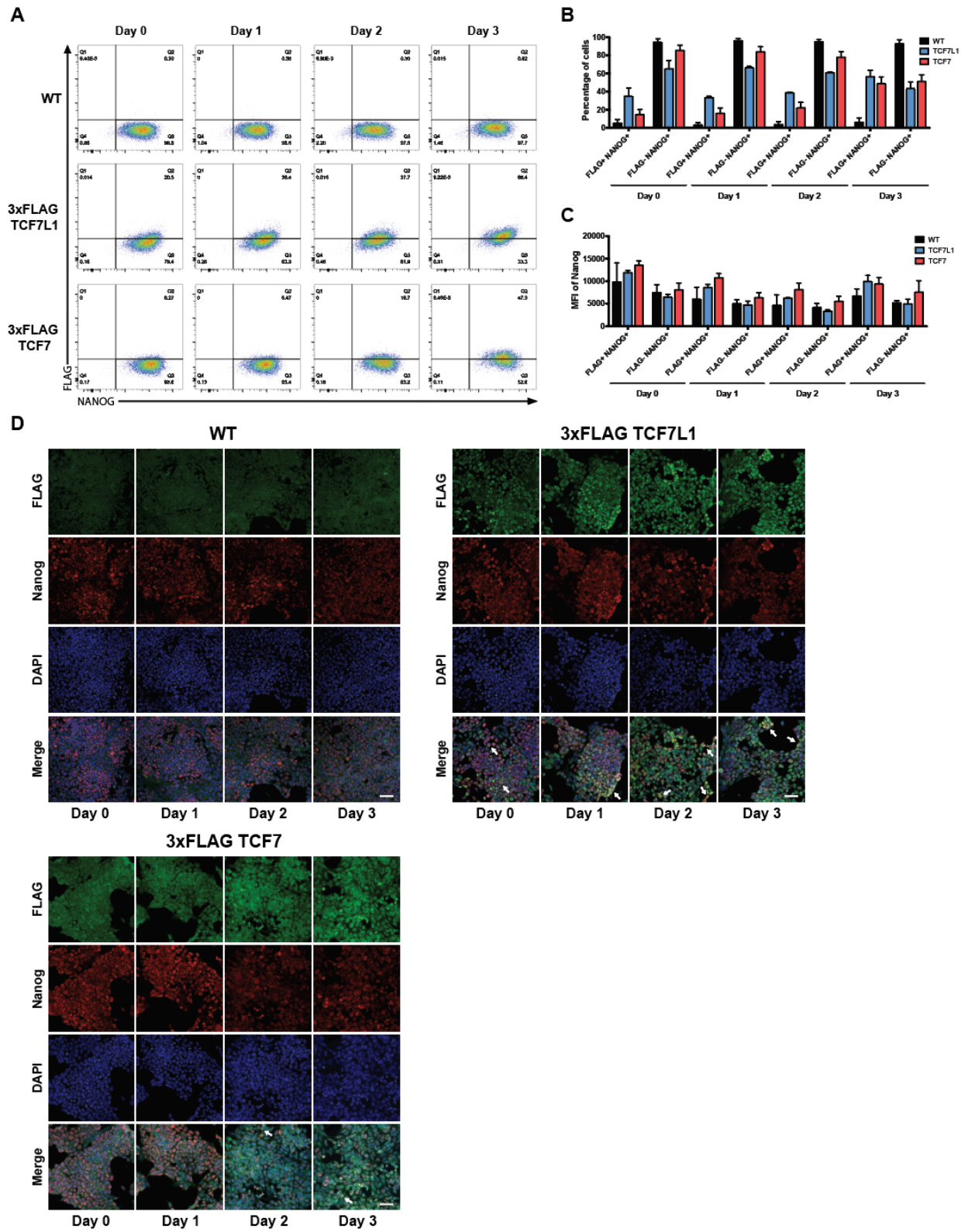


Figure 2. Neither TCF7L1 nor TCF7 expression inversely correlate with NANOG levels in self-renewing and differentiating mESCs. (A) Representative intracellular flow cytometric analysis of NANOG and FLAG levels in WT, 3xFLAG- TCF7L1 and 3xFLAG-TCF7 mESCs cultured in medium containing LIF (Day 0) and then differentiated in the absence of LIF (Day 1-3), as indicated. (B) Graph of the proportion of single-positive (FLAG- NANOG+) and double-positive (FLAG+ NANOG+) cells. Bars represent the mean of 3 independent experiments \pm SEM. (C) Graph of the median fluorescence intensity of NANOG in single-positive (FLAG- NANOG+) and double-positive (FLAG+ NANOG+) cells. Bars represent the mean of 3 independent experiments \pm SEM. (D) Immunofluorescence analysis of WT, 3xFLAG-TCF7L1 and 3xFLAG-TCF7 mESCs, cultured in medium containing LIF (Day 0) and then differentiated in the absence of LIF (Day 1-3), as indicated. Cells were stained for NANOG, FLAG and DAPI. Scale bar represents 50 μ m. White arrows indicate cells with high levels of FLAG and NANOG.

populations displayed a higher median fluorescence intensity of NANOG than the FLAG-NANOG⁺ populations for both the 3xFLAG-TCF7L1 and 3xFLAG-TCF7 mESCs at all differentiation time points (Figures 2B, 2C, S2C).

Immunofluorescence microscopy of mESCs treated in the same manner as those analyzed by flow cytometry supported our flow cytometric analyses (Figure 2D, S1D). TCF7L1 expression, assessed with a FLAG antibody, revealed a heterogeneous nuclear expression pattern, with fluorescence increasing throughout the duration of LIF removal and peaking at 72 hours (Figure 2D, S1D). Similarly, we observed heterogeneous nuclear and diffuse cytosolic expression of TCF7, which also increased throughout the course of LIF withdrawal, peaking again at 72 hours (Figure 2D, S1D). We also observed heterogeneous nuclear NANOG staining, which was highest at Day 0, before LIF was withdrawn from the culture medium (Figure 2D, S1D). Unexpectedly, many mESCs with elevated levels of NANOG and TCF7L1 persisted throughout the differentiation time course (Figure 2D, S1D). We also observed a small number of mESCs with elevated levels of NANOG and TCF7 at 48 and 72 hours after LIF withdrawal (Figure 2D, S1D).

Consequences of GSK-3 inhibition on TCF7L1 and TCF7 function in mESCs

Derepression of TCF7L1 has been described as being essential for reinforcing the pluripotent state in mESCs treated with CHIR (Wray *et al.*, 2011a; Wu *et al.*, 2012; Yi *et al.*, 2011). We sought to explore the mechanisms underlying this derepression with our unique system. To determine the timepoint at which maximal Wnt pathway activation occurred in response to CHIR, we used a lentiviral TCF/LEF reporter system in wildtype mESCs. The fluorescent protein, mCherry, driven by a constitutive promoter identifies transduced cells, whereas GFP expression is driven by tandem Wnt-responsive elements and is only expressed in the presence of transactivating β -catenin–TCF/LEF complexes. We used flow cytometry to determine mCherry and GFP levels in mESCs treated with 5 μ M CHIR, examining treated cells every 2 hours, for 18 hours. We

observed minimal GFP expression in transduced control mESCs treated with DMSO (1.12%), with nearly the entire population expressing the transduction marker, mCherry (91.5%) (Figure 3A).

Over the course of CHIR treatment, there was an approximately 6% increase in GFP-positive cells at every 2-hour timepoint, until 16 hours, where levels plateaued, with the GFP-positive population stabilizing at approximately 40% (Figure 3A). Based on these results, in subsequent experiments mESCs were treated with 5 μ M CHIR for 14 hours.

The effects of CHIR have been shown previously to dramatically reduce TCF7L1 levels while stimulating the expression of TCF7 (Moreira *et al.*, 2017; Morrison *et al.*, 2016; Shy *et al.*, 2013). We used Western blot analysis to evaluate 3xFLAG-TCF7L1 and 3xFLAG-TCF7 protein levels in cells treated with 5 μ M CHIR or DMSO (vehicle), for 14-hours (Figure 3B, S3A). Consistent with previous studies, protein levels of TCF7L1 were reduced (approx. 1.4-fold), whereas levels of TCF7 increased (approx. 2.5-fold) (Figure 3B, S3A, Table S2). TCF7L1 was expressed at higher levels than TCF7, in both DMSO (approx. 15-fold) and 5 μ M CHIR (approx. 3-fold) conditions (Figure 3B, S3A, Table S2). To examine the effects of CHIR treatment on a population of 3xFLAG-TCF7L1 and 3xFLAG-TCF7 mESCs, we also used immunofluorescence analyses (Figure 3C, S3B). Consistent with immunofluorescence performed in standard LIF-containing medium, mESCs stained for FLAG revealed heterogeneous expression of TCF7L1 and TCF7 in DMSO and CHIR conditions (Figure 3C, S3B). Although there was an overall reduction in total TCF7L1 protein levels in response to CHIR treatment (Figure 3B, S3A), we observed several cells that sustained elevated levels TCF7L1, as assessed by FLAG staining (Figure 3C, S3B). Similarly, although total TCF7 protein levels increased after CHIR treatment (Figure 3B, S3A), we observed some cells with slightly elevated levels of TCF7 in the presence of CHIR (Figure 3C, S3B).

To determine whether the levels of β -catenin correlated with elevated or reduced levels of

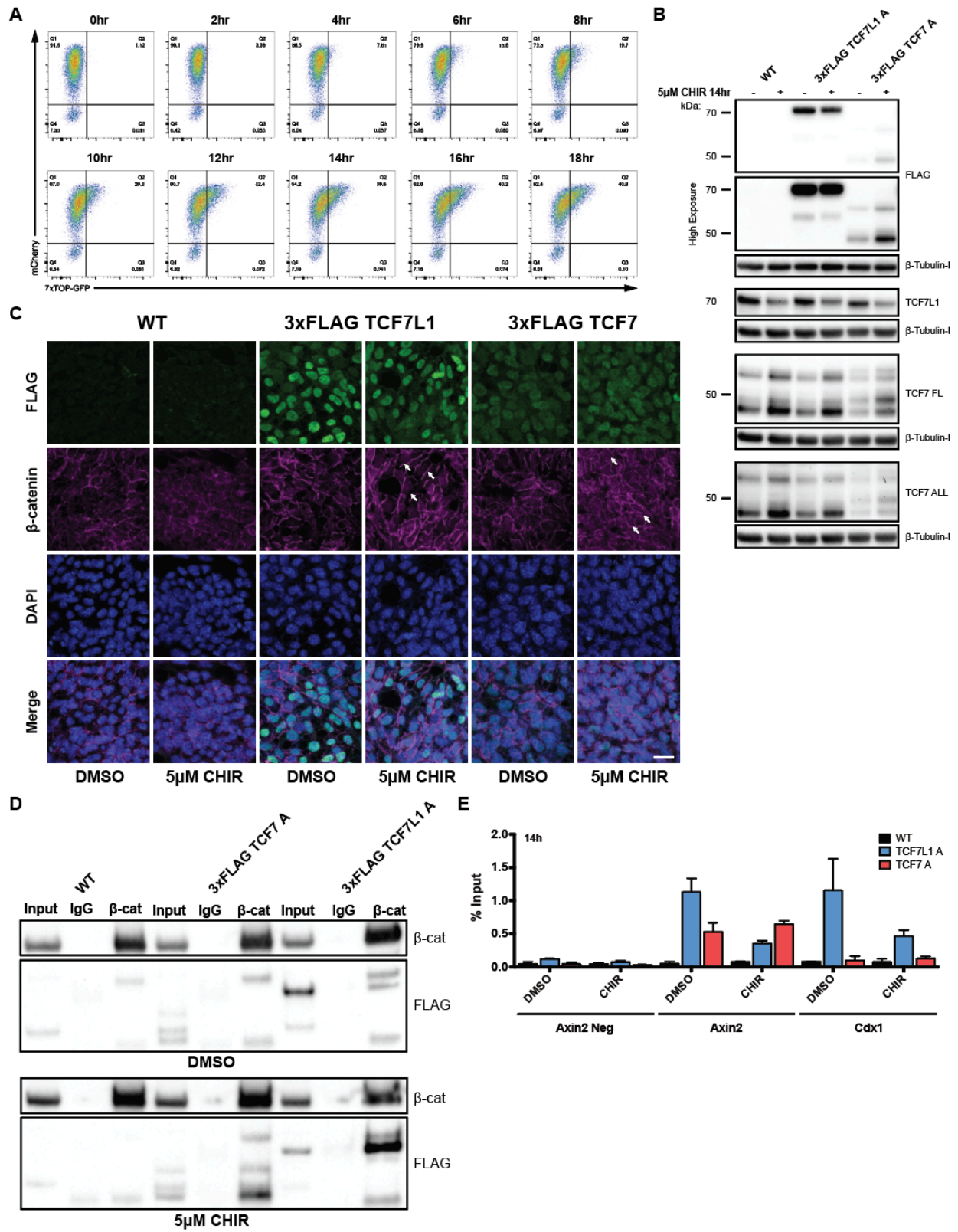


Figure 3. GSK-3 inhibition promotes association of β -catenin with 3xFLAG-TCF7 and 3xFLAG-TCF7L1. (A) Flow cytometric analysis of WT mESCs transduced with a GFP-based TCF-reporter cultured in standard LIF-supplemented medium and treated with 5 μ M CHIR every 2h for 18h, as indicated. (B) Western blot analysis of WT, 3xFLAG-TCF7L1 and 3xFLAG-TCF7 mESCs, cultured in standard LIF-supplemented medium and treated with 5 μ M CHIR or DMSO control for 14h. Lysates were probed with antibodies against TCF7L1, TCF7, FLAG and β -Tubulin, as indicated. (C) Immunofluorescence analysis of WT, 3xFLAG-TCF7L1 and 3xFLAG-TCF7 mESCs, cultured in standard LIF-supplemented medium and treated with 5 μ M CHIR or DMSO control for 14h. Cells were stained for β -catenin, FLAG and DAPI. Scale bar represents 20 μ m. White arrows indicate cells with elevated levels of FLAG and nuclear localization of β -catenin. (D) Co-immunoprecipitation analysis of WT, 3xFLAG-TCF7L1 and 3xFLAG-TCF7 mESCs, cultured in standard LIF-supplemented medium and treated with 5 μ M CHIR or DMSO control for 14h. Lysates were immunoprecipitated using β -catenin antibody and were probed with antibodies against β -catenin and FLAG, as indicated. (E) Quantitative ChIP using the FLAG antibody on WT, 3xFLAG-TCF7L1 and 3xFLAG-TCF7 mESCs, cultured in standard LIF-supplemented medium and treated with 5 μ M CHIR or DMSO control for 14h. Percent input was calculated for WREs in *Axin2* and *Cdx1*, as well as a negative control locus 11kb upstream of *Axin2*. Bars represent the mean of 3 independent experiments \pm SEM.

TCF7L1 and TCF7, respectively, we also performed immunofluorescence analysis of 'active' β -catenin (Figure 3C, S3B). We observed similar levels of nuclear active β -catenin in cells containing high and low levels of 3xFLAG-TCF7L1 or 3xFLAG-TCF7 (Figure 3C, S3B).

Intrigued by the apparent lack of a correlation between activated β -catenin and TCF7L1/TCF7 levels, we sought to determine which of the two factors associated with higher levels of β -catenin in the presence of CHIR. We analyzed the 3xFLAG-TCF/ β -catenin interactions, by immunoprecipitating β -catenin and subsequently probing for 3xFLAG-TCF7L1 and 3xFLAG-TCF7 using anti-FLAG antibody, in lysates from mESCs treated with 5 μ M CHIR (Figure 3D). β -catenin was associated with higher levels of TCF7L1 compared to TCF7, in the presence of CHIR (Figure 3D), in agreement with our data showing higher TCF7L1 protein levels compared to TCF7, even in the presence of CHIR (Figure 3B).

A reduction in TCF7L1 occupancy at *Axin2* and *Cdx1* has previously been observed in mESCs treated with CHIR (Shy *et al.*, 2013). We were therefore interested in comparing the effects of CHIR on the occupancy of both TCF7L1 and TCF7 at these two Wnt-associated genes. We performed ChIP using the FLAG antibody, followed by quantitative RT-PCR on 3xFLAG - TCF7L1 and 3xFLAG-TCF7 mESCs cultured in standard medium containing LIF treated with 5 μ M CHIR or DMSO for 14 hours (Figure 3E, S3C). Consistent with previous data, in the presence of CHIR we observed a reduction in TCF7L1 occupancy at a locus near the *Axin2* promoter, but only a slight reduction in occupancy at the *Cdx1* promoter (Figure 3E, S3C). Unexpectedly, in response to CHIR, despite an increase in TCF7 protein (Figure 3B, S3A), we did not observe a substantial increase in TCF7 occupancy at the promoter of *Axin2*, nor *Cdx1* (Figure 3E, S3C). However, there was more TCF7 compared to TCF7L1, at the promoter of *Axin2* in the presence of CHIR (Figure 3E, S3C).

Examining genome-wide TCF7L1 and TCF7 chromatin occupancy

Having observed differential binding of 3xFLAG-TCF7L1 and 3xFLAG-TCF7 to *Axin2* and *Cdx1* loci, we were interested in elucidating the global differences in chromatin distribution between these two TCF factors. We performed ChIP-seq analyses using the FLAG antibody, on wildtype, 3xFLAG-TCF7L1 and 3xFLAG-TCF7 mESCs cultured under standard LIF-supplemented conditions and after 14 hours of 5 μ M CHIR treatment. ChIP-seq reads were aligned to the mouse genome using BWA, where duplicates and low-quality reads were discarded. Subsequent peaks were identified using MACS, followed by *de novo* motif discovery and gene ontology analysis performed using HOMER (Benner *et al.*, 2017).

We identified 760 (in 658 genes) and 582 (in 527 genes) 3xFLAG-TCF7L1-bound regions (peaks) in standard medium and in response to CHIR treatment for 14 hours, respectively (Table S3). Among the 3xFLAG-TCF7L1-bound genes, there were 359 genes (43.46%) of overlap, in both control and CHIR conditions (Figure S4B). 299 (36.20%) and 168 (20.33%), 3xFLAG-TCF7L1-bound genes were unique to control and CHIR conditions, respectively (Figure S4B). We sought to validate the 658 genes bound by 3xFLAG-TCF7L1 with a previously published list of 1351 TCF7L1 bound genes, which was also obtained from mESCs maintained in standard media conditions with serum and LIF (Figure S4A). Surprisingly, only 177 genes were shared between the two TCF7L1 ChIP-seq datasets (Figure S4A).

A majority of 3xFLAG-TCF7L1 peaks, 37% in control conditions and 38% in CHIR, were bound within a gene's exon or intron (Figure 4A TOP). 9% of control and 8% of CHIR 3xFLAG-TCF7L1 peaks were bound to 'promoter' regions within 2kb of a transcriptional start site (TSS) (Figure 4A TOP). Additionally, we observed 31% of 3xFLAG-TCF7L1 peaks distributed at 'enhancer' regions, falling within 2kb to 100kb upstream of a TSS, in both control and CHIR conditions (Figure 4A TOP). Interestingly, the genomic distribution of 3xFLAG-TCF7L1 bound

regions remained nearly unaffected by CHIR treatment (Figure 4A TOP).

Our 3xFLAG-TCF7 ChIP-seq identified considerably less peaks, 17 (in 16 genes) and 84 (in 75 genes), in control and CHIR conditions, respectively (Table S3). Among these 3xFLAG-TCF7 bound genes, there were 12 genes (15.19%) with overlapping peaks, in control and CHIR conditions (Figure S4B). Four (5.06%) and 63 (79.75%), 3xFLAG-TCF7 bound genes were unique to control and CHIR conditions, respectively (Figure S4B). The significantly lower number of 3xFLAG-TCF7 bound regions can likely be attributed to lower 3xFLAG-TCF7 protein levels observed in the cells, which only slightly increases upon CHIR supplementation (Figure 3B). These 3xFLAG-TCF7 bound regions are biologically relevant in this context, and they display robust 3xFLAG-TCF7 peaks, despite its low protein levels.

We also assessed the genomic distribution of 3xFLAG-TCF7 peaks and found that the majority, 24% in control and 27% in CHIR conditions, were bound within a gene's exons or introns (Figure 4B TOP). A large portion were also bound to 'promoter' regions within 2kb of a TSS, 29% and 24%, in control and CHIR conditions, respectively (Figure 4B TOP). Furthermore, we observed that 12% and 25% of 3xFLAG-TCF7 peaks, in control and CHIR conditions, respectively, were distributed at 'enhancer' regions, falling within 2kb to 100kb upstream of a TSS (Figure 4B TOP). Interestingly, 29% and 20% of 3xFLAG-TCF7 peaks, in control and CHIR conditions, respectively, were located at regions that could not be categorized (Figure 4B TOP).

Due to our ability to utilize the FLAG antibody to perform ChIP-seq on both 3xFLAG-tagged TCF7L1 and 3xFLAG-TCF7, we were interested in comparing the genes bound by both factors. Intriguingly, we did not observe a large overlap in the genes bound by both TCF7L1 or TCF7 (Figure S4C). In control medium, 6 genes were common between both factors, which represents 37.5% and 0.92% of genes bound by 3xFLAG-TCF7 and 3xFLAG-TCF7L1, respectively (Figure S4C). We observed a similar trend in the presence of CHIR, with 33 genes

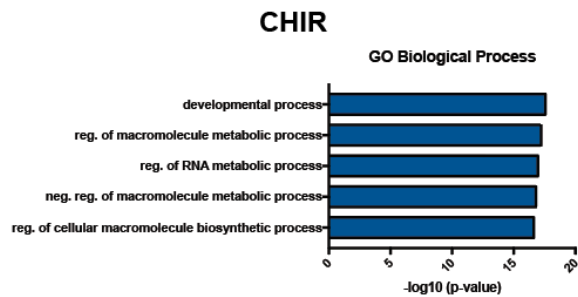
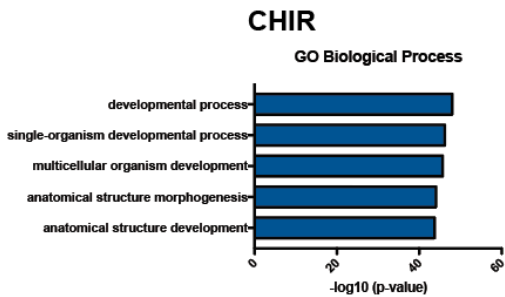
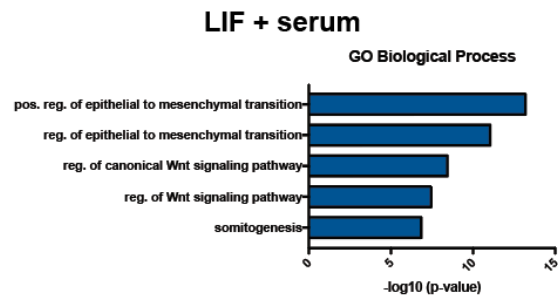
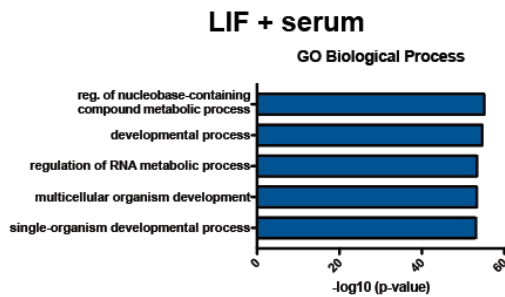
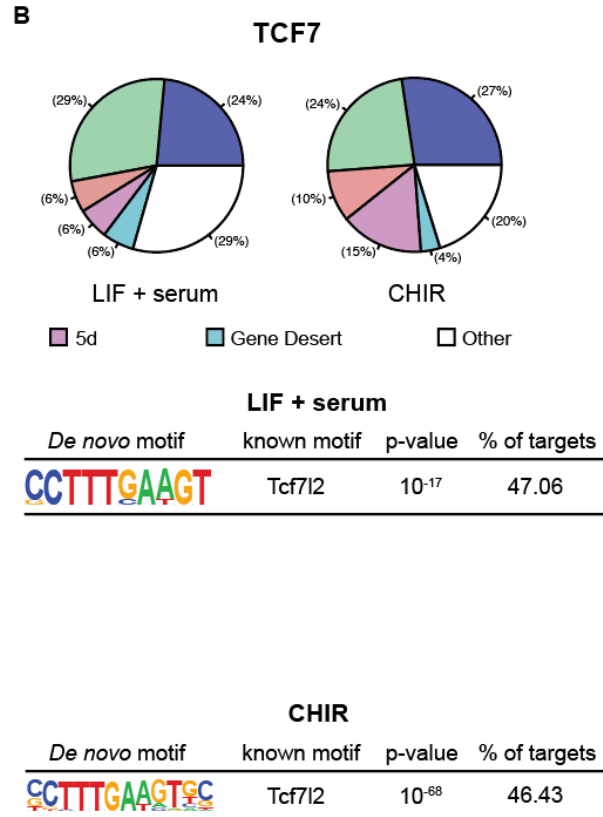
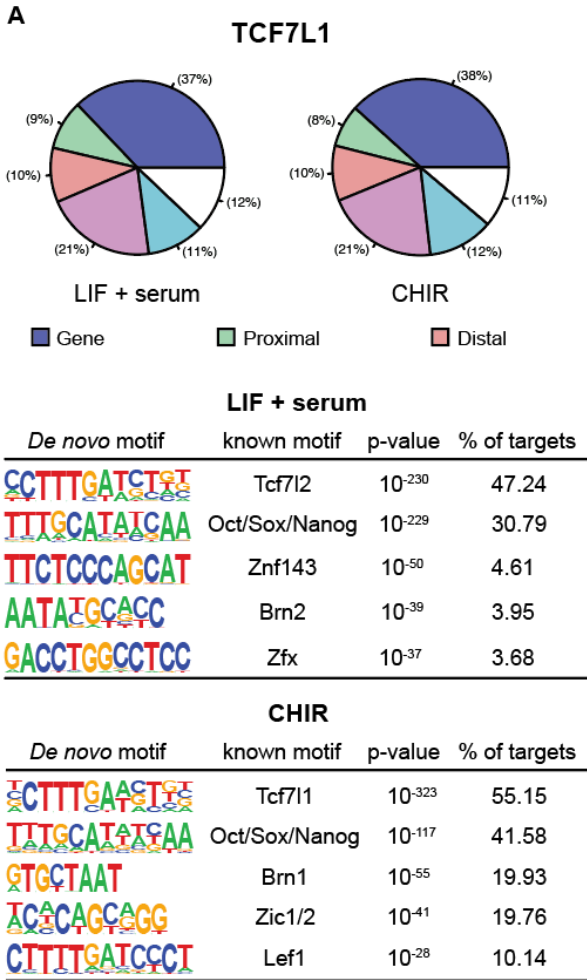


Figure 4. Characterization of genomic regions bound by 3xFLAG-TCF7L1 or 3xFLAG-

TCF7 in mESCs. (A) TOP: Genomic distribution of 3xFLAG-TCF7L1 ChIP-seq peaks for mESCs maintained in standard medium (LIF and serum) or medium supplemented with 5 μ M CHIR for 14h. Gene: exon or intron. Proximal: 2kb upstream of a transcriptional start site (TSS). Distal: between 10kb upstream and 2kb upstream of a TSS. 5d: between 100kb upstream and 10kb upstream of a TSS. Gene desert: 100kb upstream or downstream of a TSS. Other: anything not included above. MID: Enriched motifs from a *de novo* motif search of sequences contained in 3xFLAG-TCF7L1 peaks in control and CHIR conditions. BOT: Gene ontology analysis of 3xFLAG-TCF7L1 ChIP-seq peaks in control and CHIR conditions. Values are presented as negative log-base 10 of their p-values. (B) TOP: Genomic distribution of 3xFLAG-TCF7 ChIP-seq peaks in control and CHIR conditions. Gene: exon or intron. Proximal: 2kb upstream of a TSS. Distal: between 10kb upstream and 2kb upstream of a TSS. 5d: between 100kb upstream and 10kb upstream of a TSS. Gene desert: 100kb upstream or downstream of a TSS. Other: anything not included above. MID: Enriched motifs from a *de novo* motif search of sequences contained in 3xFLAG-TCF7 peaks in control and CHIR conditions. BOT: Gene ontology analysis of 3xFLAG-TCF7 ChIP-seq peaks in control and CHIR conditions. Values are presented as negative log-base 10 of their p-values.

bound by both factors, representing 44% and 6.68% of genes bound by TCF7 and TCF7L1, respectively (Figure S4C).

Importantly, the TCF/LEF consensus binding motif (Wnt responsive element; WRE) was the top *de novo* motif identified, representing 47.24% and 55.15% of 3xFLAG-TCF7L1 peaks, in control and CHIR conditions, respectively (Figure 4A MID). An additional TCF/LEF consensus binding motif was discovered in CHIR, representing 10.14% of 3xFLAG-TCF7L1 peaks (Figure 4A MID). As anticipated, the top *de novo* motif observed in 3xFLAG-TCF7 peaks was also the TCF/LEF consensus binding motif, representing 47.06% and 46.43% of TCF7 peaks, in control and CHIR conditions, respectively (Figure 4B MID).

In addition to the TCF/LEF consensus binding motif, 3xFLAG-TCF7 and 3xFLAG-TCF7L2 are capable of binding to adjacent ‘helper sites’ via a cysteine-clamp (C-clamp) domain (Atcha *et al.*, 2007; Hoverter *et al.*, 2012). To identify helper sites, we scanned 3xFLAG-TCF7 and 3xFLAG-TCF7L1 for the presence of WRE motif peaks using HOMER, followed by scanning for helper sites located 200bp upstream or downstream of the WRE. As anticipated, a considerable fraction of 3xFLAG-TCF7 peaks contained both a WRE and the helper site, specifically, 12 (70.59%) and 40 (47.62%) peaks, in control or CHIR conditions, respectively (Table S4). By contrast, 3xFLAG-TCF7L1 peaks were not enriched for helper sites, as only 66 (11.34%) and 72 (9.47%) peaks identified in mESC or CHIR conditions, respectively, contained both a WRE and helper site, consistent with the absence of a c-clamp in TCF7L1 (Table S4).

TCF7L1 is a part of an extended network of transcription factors regulating pluripotency. This was reflected in our ChIP-seq data, which revealed a *de novo* motif associated with POU5F1/SOX2/NANOG co-bound genomic regions (Figure 4A MID) (Chen *et al.*, 2008). This motif was the second most enriched *de novo* motif, which was present in 30.79% of 3xFLAG-TCF7L1 peaks in control conditions and surprisingly, represented 41.58% of TCF7L1 peaks in the

presence of CHIR (Figure 4A MID). *De novo* motifs associated with *Znf143*, *Brn2*, and *Zfx* were also discovered in control conditions, although these motifs were present in less than 5% of 3xFLAG-TCF7L1 peaks (Figure 4A MID). Intriguingly, in CHIR conditions, *de novo* motifs associated with *Brn1* and *Zic1/2*, were discovered in 19.93% and 19.76% of 3xFLAG-TCF7L1 associated peaks (Figure 4A MID).

Gene Ontology (GO) analysis was performed using HOMER to search for functional biological process GO categories enriched in 3xFLAG-TCF7L1 bound genes (Figure 4A BOT). Three out of the top five most enriched biological process GO terms for 3xFLAG-TCF7L1 bound genes in both control and CHIR conditions were associated with developmental processes (Figure 4A BOT). In control conditions, 3xFLAG-TCF7L1-bound genes were also associated with the biological process GO terms ‘regulation of nucleobase-containing compound metabolism’ and ‘regulation of RNA metabolism’ (Figure 4A BOT). Finally, in CHIR conditions, the biological process GO terms ‘anatomical structure morphogenesis’ and ‘anatomical structure development’ were also enriched in regions bound by 3xFLAG-TCF7L1 (Figure 4A BOT).

Gene ontology analysis of genes bound by 3xFLAG-TCF7 was also conducted (Figure 4B BOT). In control conditions, the two most enriched biological process GO terms for 3xFLAG-TCF7 peaks, were both associated with regulation of the epithelial to mesenchymal transition (Figure 4B BOT). Furthermore, two biological process GO terms associated with regulation of Wnt signaling and canonical Wnt signaling were identified, despite only identifying 16 genes bound by 3xFLAG-TCF7 in control conditions (Figure 4B BOT). In CHIR-treated mESCs, three out of the top five most enriched biological process GO terms for 3xFLAG-TCF7 bound genes, were associated with macromolecule metabolism or biosynthesis (Figure 4B BOT). The remaining two biological process GO terms ‘developmental process’ and ‘regulation of RNA metabolism’ were also observed in genes bound by 3xFLAG-TCF7L1 in control conditions (Figure 4B BOT).

3xFLAG-TCF7L1 and 3xFLAG-TCF7 display differential chromatin occupancy

To further explore the differential binding of 3xFLAG-TCF7L1 and 3xFLAG-TCF7 to their respective target genes and the effects of Wnt pathway activation using CHIR, we employed CSAW (Lun and Smyth, 2015). CSAW allows for quantitative evaluation of differential binding between experimental conditions and samples instead of qualitatively assessing absence or presence (Lun and Smyth, 2015). Additionally, CSAW allows for rigorous statistical analysis, controlling for false discovery rate across constant regions or windows across the genome and accounting for biological variation between samples (Lun and Smyth, 2015).

Differential binding analysis using was performed on 3xFLAG-TCF7L1 and 3xFLAG-TCF7 ChIP-seq datasets, comparing not only genes bound by a single factor in both conditions, but also comparing genes bound by both factors in a single condition (Table S5). We first analyzed 3xFLAG-TCF7L1 occupancy in control vs CHIR conditions (Figure 5A). Surprisingly, 307 peaks in genes including *Bmper*, *Bdh1*, *Ext1*, and *Dkk4*, were preferentially bound in CHIR, compared to 332 preferentially bound peaks identified in control conditions, found in genes such as *Myb*, *Ptch1*, *Fgfr2*, and *Trp53bp1* (Figure 5A). Differential binding analysis performed on 3xFLAG-TCF7, revealed 17 peaks preferentially bound in control conditions (Figure 5A). However, it should be noted that with the exception of *Camk2a*, none of these genes were identified as peaks with MACS (Figure 5A). Conversely, in CHIR-treated mESCs, 463 peaks were preferentially bound, including peaks found in the genes, *Tcf7l2*, *Gbx2*, *Bmper*, and *Mllt6* (Figure 5A).

To determine regions differentially bound by 3xFLAG-TCF7L1 and 3xFLAG-TCF7, we also compared the binding of the two factors in a single condition. In control conditions, 40 and 2036 regions were preferentially bound by 3xFLAG-TCF7 and 3xFLAG-TCF7L1, respectively (Figure 5B). Of the 40 regions preferentially bound by 3xFLAG-TCF7, a majority of those topmost enriched were associated with genes involved in Wnt signaling, namely *Zfp703*, *Tcf7*, *Nkd1*, *Lef1*,

Lg5, and *Ccnd1* (Figure 5B). Similarly, the most enriched genes preferentially bound by 3xFLAG-TCF7L1 were associated with both Wnt signaling and pluripotency, and included: *Mllt6*, *Ctnnd2*, *Id3*, *Cdx1*, *Klf2*, *Sp5* and *Tfcp2l1* (Figure 5B).

Conversely, in the presence of CHIR, 92 and 1761 regions were preferentially bound by 3xFLAG-TCF7 and 3xFLAG-TCF7L1, respectively (Figure 5B). Of the 92 regions preferentially bound by 3xFLAG-TCF7, the topmost abundant genes were once again associated with genes involved in Wnt signaling, such as *Zfp703*, *Tcf7*, *T*, *Nkd1*, *Lef1*, *Axin2*, and *Ccnd1* (Figure 5B). Similarly, a majority of the most enriched genes preferentially bound by 3xFLAG-TCF7L1 were associated with both Wnt signaling and pluripotency, and included: *Tfcp2l1*, *Bdh1*, *Ctnnd2*, *Sp5*, *Fzd7*, *Dkk4* and *Lifr* (Figure 5B).

To further explore 3xFLAG-TCF7L1 and 3xFLAG-TCF7 binding patterns, we examined the peak profiles at select Wnt and pluripotency-associated genes. In either condition, of the two factors, 3xFLAG-TCF7 was associated with the Wnt related genes, *Zfp703*, *Lef1*, *Msx2*, *Tcf7*, *Lef1*, and *Nkd1* (Figure 5C, S5A). All of these genes were bound by 3xFLAG-TCF7 in control conditions and demonstrated increased binding after addition of CHIR for 14 hours (Figure 5C, S5A). Moreover, in the presence of CHIR, 3xFLAG-TCF7 was detected at the Wnt target, *T* (Figure S5A). By contrast, 3xFLAG-TCF7L1 was exclusively located at only two Wnt-associated genes, *Lgr5* and *Dkk4* (Figure S5A). *Lgr5* was bound by 3xFLAG-TCF7L1 in both control and CHIR conditions, however a slight reduction in binding was observed in response to CHIR (Figure 5C, S5A). 3xFLAG-TCF7L1 was only detected at *Dkk4* in the presence of CHIR (Figure S5A). In control conditions, TCF7L1 was also solely detected at *Mllt6*, *Sp5*, *Cdx1*, and *Tcf7l1* (Figure 5C, S5A).

Minimal overlap in 3xFLAG-TCF7L1 and 3xFLAG-TCF7 occupancies at Wnt-associated genes was observed in control conditions, with the exception of *Axin2* and *Lef1*. At *Axin2*, both

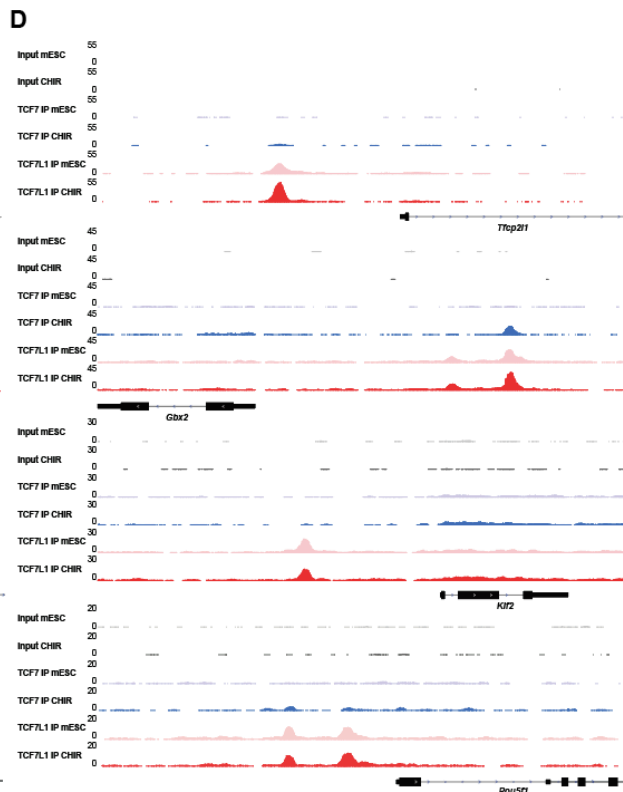
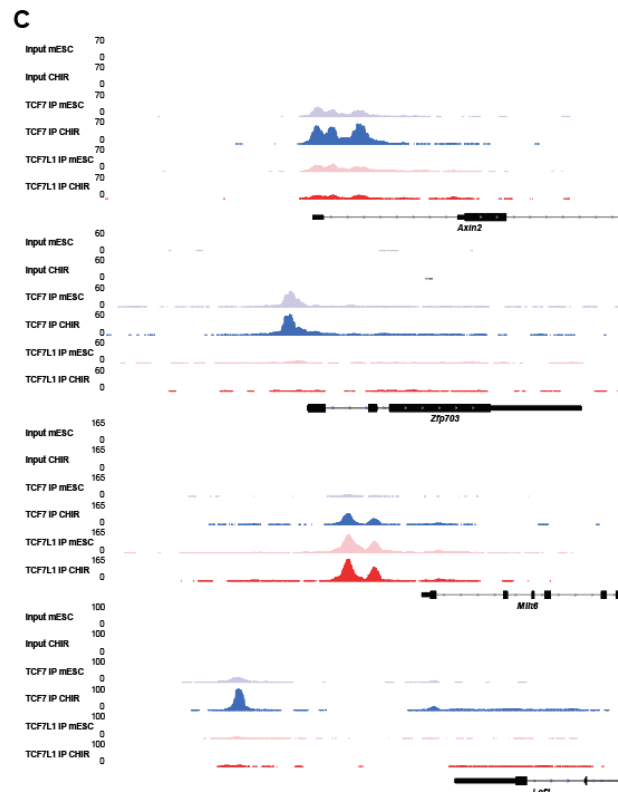
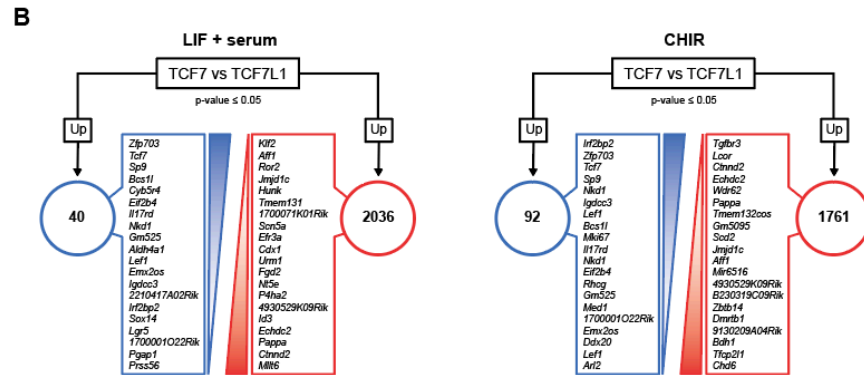
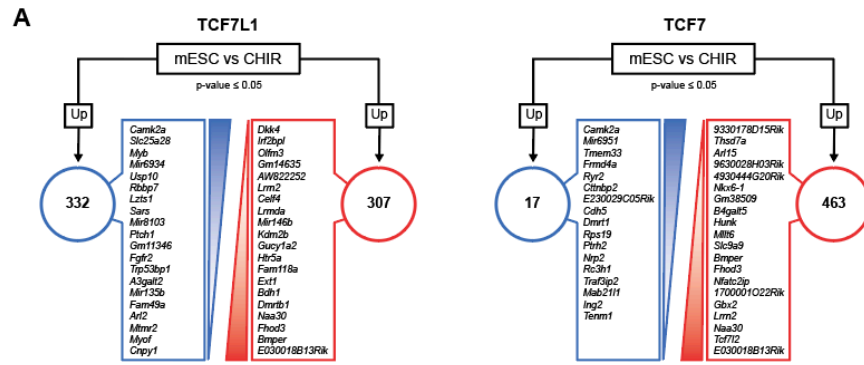


Figure 5. 3xFLAG-TCF7L1 and 3xFLAG-TCF7 exhibit differential occupancy at Wnt target and pluripotency-associated genes. (A) Target genes preferentially bound by 3xFLAG-TCF7L1 (LEFT) or 3xFLAG-TCF7 (RIGHT) in control and CHIR conditions. Differential binding was determined using CSAW with a cutoff of 0.05. (B) Target genes preferentially bound by 3xFLAG-TCF7 versus 3xFLAG-TCF7L1, in mESCs cultured control (LEFT) or CHIR conditions (RIGHT). Differential binding was determined by using CSAW with a cutoff of 0.05. (C) Genomic tracks showing 3xFLAG-TCF7 (blue) and 3xFLAG-TCF7L1 (red) peaks at selected Wnt-associated genes in mESCs cultured in control medium (light shade) or CHIR-containing medium (dark shade). Pooled control and CHIR input peaks are in grey and dark grey, respectively. Genomic positions reflect NCBI mouse genome build mm10. (D) Genomic tracks showing 3xFLAG-TCF7 (blue) and 3xFLAG-TCF7L1 (red) peaks at selected pluripotency-associated genes in mESCs cultured control (light shade) or CHIR conditions (dark shade). Genomic tracks showing pooled control and CHIR input peaks are in grey and dark grey, respectively. Genomic positions reflect NCBI mouse genome build mm10.

factors were equally bound within the same regions, located near the 5'UTR (Figure 5C).

Treating with CHIR led to a reduction in 3xFLAG-TCF7L1 binding, whereas 3xFLAG-TCF7 binding was increased, at *Axin2*, conflicting with our previous qChIP results (Figure 5C, 3E). However, mESCs utilized for ChIP-seq were cultured on feeders beforehand for 2 passages, whereas the mESCs used for quantitative ChIP had been maintained for multiple passages on gelatin-coated plates, which may have altered cellular properties such as chromatin accessibility. This likely also effected *Cdx1* occupancy as assessed by ChIP-seq, as we were able to detect 3xFLAG-TCF7 in the presence of CHIR (Figure S5A). Furthermore, at *Cdx1*, we observed an increase, not a decrease, in 3xFLAG-TCF7L1 binding in response to CHIR stimulation (Figure S5A). At *Lef1*, 3xFLAG-TCF7 was bound to a higher extent than 3xFLAG-TCF7L1 in both control and CHIR conditions (Figure 5C). In the presence of CHIR, 3xFLAG-TCF7L1 and 3xFLAG-TCF7 demonstrated some overlap with respect to Wnt related genes. In addition to *Axin2* and *Cdx1*, both factors were detected at *Mllt6*, *Sp5*, *Tcf7l2*, and *Tcf7l1* (Figure 5C, S5A), although 3xFLAG-TCF7L1 was more abundant at *Mllt6*, *Tcf7l2* and *Tcf7l1* in the CHIR condition (Figure 5C, S5A).

3xFLAG-TCF7L1 was predominantly associated with pluripotency-related genes, occupying regions within: *Tfcp2l1*, *Gbx2*, *Klf2*, *Pou5f1*, *Klf4*, *Sox2*, *Nanog*, *Esrrb*, *Nodal*, *Zfp42*, and *Dppa3*, in both control and CHIR conditions (Figure 5D, S5B). Unexpectedly, 3xFLAG-TCF7L1 occupancy was only slightly reduced in response to CHIR at *Klf2*, *Nanog* and one of the three peaks discovered at both *Klf4* or *Esrrb* (Figure 5D, S5B). Furthermore, 3xFLAG-TCF7L1 occupancy at *Tfcp2l1*, *Gbx2*, *Pou5f1*, *Sox2*, *Nodal*, *Zfp42*, and two of the 3 peaks identified at both *Klf4* or *Esrrb*, remained unchanged or actually increased upon CHIR treatment (Figure 5D, S5B). 3xFLAG-TCF7, in control medium, was only slightly enriched at *Sox2* and treatment with CHIR led to an increase in 3xFLAG-TCF7 binding (Figure S5B). At *Sox2*, both 3xFLAG-TCF7L1 and

3xFLAG-TCF7 were identified at similar levels (Figure S5B). In the presence of CHIR, we observed slight increases in 3xFLAG-TCF7 binding to *Gbx2*, *Pou5f1*, and *Nodal*, although 3xFLAG-TCF7L1 levels remained higher at all 3 gene loci (Figure 5D, S5B).

TCF7L1 acts as a transcriptional activator in response to CHIR-mediated GSK-3 inhibition

Id3 was one of the most significantly upregulated genes in cells lacking all full-length TCF/LEF factors (Moreira *et al.*, 2017). As we observed that 3xFLAG-TCF7L1 remained bound to pluripotency-associated genes in the presence of CHIR, we analyzed the 3xFLAG-TCF7L1 binding profile at the *Id3* locus. In control conditions, we observed a significant 3xFLAG-TCF7L1 peak located 1.5kb downstream of the *Id3* gene (Figure 6A). CHIR treatment for 14 hours did not cause apparent 3xFLAG-TCF7L1 dissociation from the chromatin. Instead, the 3xFLAG-TCF7L1 peak at *Id3* was detected to an equal or slightly greater extent (Figure 6A). Additionally, only a negligible amount of 3xFLAG-TCF7 was bound to the *Id3*-associated peak in the presence of CHIR (Figure 6A). This suggested to us that CHIR could potentially convert TCF7L1 from a transcriptional repressor into a transcriptional activator. To further explore this possibility, we examined the effects of CHIR on *Id3* transcript levels in wildtype mESCs, mESCs lacking all 4 full-length TCF/LEFs (QKOs), as well as QKOs rescued with a single copy of 3xFLAG-TCF7L1 (QT7L1) or -TCF7 (QT7) (Figure 6B). We supplemented standard medium with 10 μ M CHIR or DMSO vehicle control for 48 hours. In wildtype mESCs, addition of CHIR caused a 3-fold upregulation of *Id3* transcript levels compared to DMSO control, revealing that *Id3* is responsive to activation by GSK-3 inhibition (Figure 6B). QKO mESCs demonstrated elevated levels of *Id3* in DMSO controls, linking control of its expression to the TCF/LEFs (Figure 6B). Re-expression of a single copy of 3xFLAG-TCF7 did not significantly affect *Id3* expression in QKO mESCs, likely a result of a lack of its binding to the *Id3* locus (Figure 6B). By contrast, rescue with a single copy of 3xFLAG-TCF7L1, restored basal levels of *Id3*, suggesting that in the absence of CHIR,

TCF7L1 mediates the repression of *Id3* (Figure 6B). In response to CHIR, QT7L1 cells, in which only 3xFLAG-TCF7L1 is present, demonstrated an upregulation of *Id3* (Figure 6B). Coupled with our observation that TCF7L1 remains bound to the *Id3* locus in cells treated with CHIR, this suggests that CHIR converts TCF7L1 from a repressor of *Id3*, into an activator.

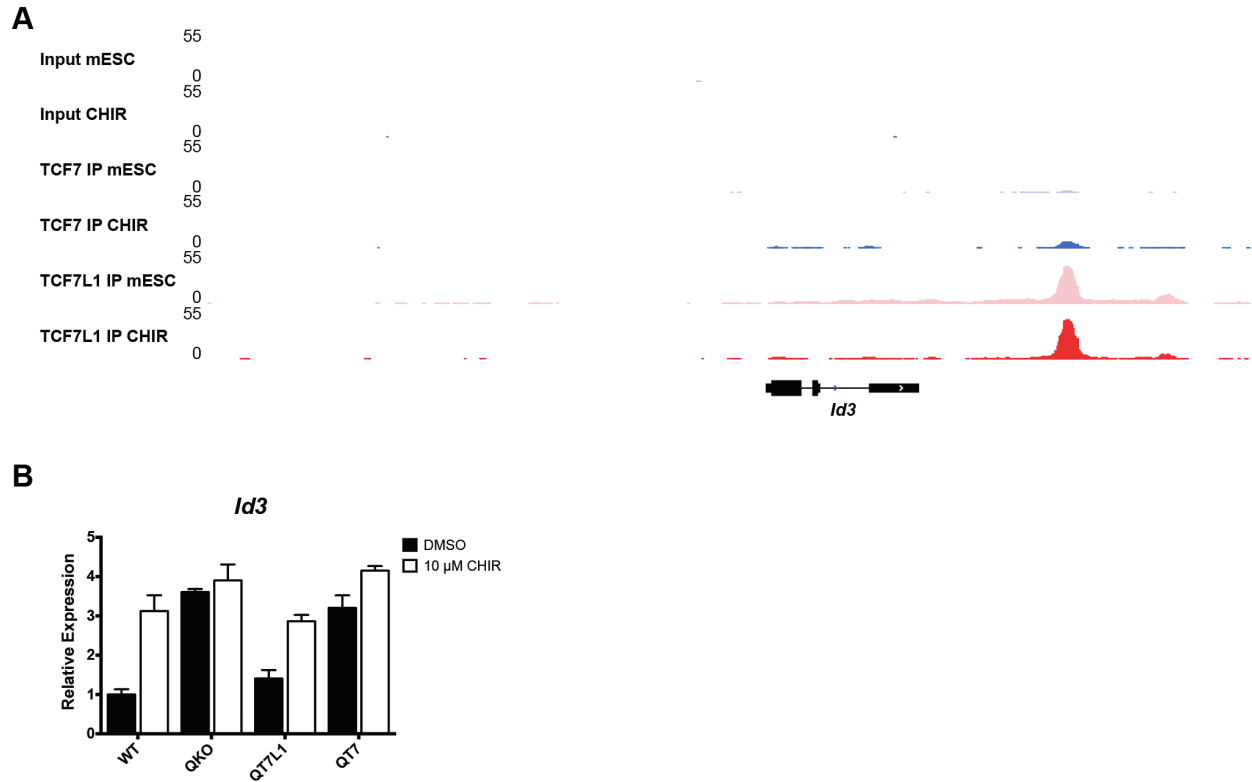


Figure 6. *Id3* activation is mediated by conversion of TCF7L1 into a transcriptional activator in the presence of CHIR. (A) Genomic tracks showing 3xFLAG-TCF7 (blue) and 3xFLAG-TCF7L1 (red) peaks at *Id3* in mESCs cultured in standard medium containing LIF and serum (light shade) or treated with 5 μ M CHIR for 14hr (dark shade). Pooled control and CHIR input peaks are in grey and dark grey, respectively. Genomic positions reflect NCBI mouse genome build mm10. (B) qRT-PCR analyses of relative *Id3* transcript levels in WT, QKO, QT7 and QT7L1 cells treated with 10 μ M CHIR or DMSO control for 48 hours. Bars = mean of 3 independent experiments \pm SEM, normalized to vehicle-treated WT cells.

DISCUSSION

Our findings suggest that in pluripotent mouse embryonic stem cells (mESCs) there is minimal overlap between TCF7L1 and TCF7 chromatin occupancy, in both the on and off states of the Wnt/ β -catenin signaling pathway. Employing cell lines with endogenously epitope-tagged TCF7 and TCF7L1 and a well-characterized FLAG antibody in our study offers multiple advantages. The FLAG M2 monoclonal antibody has been extensively used in over 1500 peer-reviewed publications and has been used previously for ChIP-seq studies, including a recent study proposing its applicability for large scale ChIP-seq analyses of endogenously tagged transcription factors. By using single well-characterized monoclonal antibody to detect endogenously tagged TCF7 and TCF7L1, we are able to conduct quantitative comparisons between these factors.

Few studies have examined the genome-wide binding profiles of two TCF/LEF factors simultaneously. Strikingly, we observed minimal overlap between genes bound by TCF7 or TCF7L1 in both standard maintenance conditions and in the presence of the GSK-3 inhibitor, CHIR. This differential binding occurs even though the *de novo* consensus DNA binding motif generated for both factors is a conventional TCF/LEF-binding WRE. In a similar study to ours, Wallmen *et al.* described differential binding of ectopically expressed human TCF7 and TCF7L2 to select Wnt target genes in mESCs including: *Axin2*, *Cdx1*, *T* and *Sp5* (Wallmen *et al.*, 2012). Another recent ChIP-seq study in mESCs, using commercially available antibodies to TCF7L1 and TCF7, also revealed minimal overlap between both factors but identified disparate TCF7 and TCF7L1 DNA binding motifs (De Jaime-Soguero *et al.*, 2017).

Wnt-mediated reinforcement of self-renewal and pluripotency has been suggested to involve a switch between repressive TCF7L1 and activating TCF7 through a β -catenin-dependent mechanism (Yi *et al.*, 2011). Our data suggest that in response to CHIR, not only do β -catenin/3xFLAG-TCF7L1 interactions increase, but 3xFLAG-TCF7L1 is also found bound to a

greater number of genes than 3xFLAG-TCF7. While we did observe some overlap between TCF7L1 and TCF7 occupancies, there were few regions in which CHIR led to a reduction in TCF7L1 binding with a concomitant increase in TCF7, with the exception of *Axin2* and *T*. Taken together, our data reveal that a TCF7L1-TCF7 switch is not a global requirement for TCF/LEF target gene regulation, but may facilitate Wnt regulation of *Axin2* and *T*. Our 3xFLAG-TCF7 ChIP-seq data revealed a relatively small number of genes bound in control and CHIR conditions. This is likely a reflection of significantly lower 3xFLAG-TCF7 protein levels compared to TCF7L1 in these conditions. However, having identified the TCF/LEF consensus binding sequence as our most enriched *de novo* motif for 3xFLAG-TCF7, we are confident that our 3xFLAG-TCF7 data are biologically relevant.

Despite being expressed at low levels, 3xFLAG-TCF7 was more abundant than 3xFLAG-TCF7L1 at some specific Wnt-associated genes, namely: *Zfp703*, *Tcf7*, *Lef1* and *Nkd1*. Presumably, 3xFLAG-TCF7 outcompetes 3xFLAG-TCF7L1 for binding, even though 3xFLAG-TCF7L1 protein is more abundant. Indeed, so called ‘E-tail’ isoforms of TCF7 and TCF7L2, contain a cysteine-clamp that binds to a secondary DNA motif referred to as a ‘helper site’, which is essential for TCF7/TCF7L2-mediated repression and Wnt responsiveness (Archbold *et al.*, 2014; Atcha *et al.*, 2007; Zhang *et al.*, 2014). We observed multiple helper sites associated with these particular Wnt target genes. However, there were 3xFLAG-TCF7 and 3xFLAG-TCF7L1 co-occupied Wnt target genes, such as *Axin2*, *Lef1* and *1700001O22Rik* in control and CHIR conditions and *Apod*, *Zfp3611*, *mir8110*, *Zfp423*, *mir7020*, and *Sp5*, in CHIR treated cells only. Some genes containing both WREs and helper sites were found bound to only 3xFLAG-TCF7 or 3xFLAG-TCF7L1 exclusively. This suggests that there are contexts in which TCF7 is unable to outcompete TCF7L1 for binding. In support of this notion, in mouse hair follicle stem cells, TCF7L1 and the E-tail containing TCF7L2, demonstrated a significant amount of overlap in co-

bound genes (Lien *et al.*, 2014). Mechanistically, this could be attributed to suboptimal helper site configurations at specific Wnt target (Archbold *et al.*, 2014).

The genomic binding profile of TCF7L1 was the first of the TCF/LEFs to be characterized in mouse ES cells, demonstrating a large overlap in binding with master transcriptional regulators of pluripotency, namely POU5F1, SOX2, and NANOG (Cole *et al.*, 2008; Marson *et al.*, 2008). In our study, in both control and CHIR culture conditions, the second most enriched motif identified was a POU5F1/SOX2/NANOG motif, associated with peaks co-bound by all 3 factors. Interestingly, this motif represented a significant proportion of 3xFLAG-TCF7L1 peaks in our control pluripotency maintenance conditions, which increased in the presence of CHIR. Still, we observed minimal overlap between our 3xFLAG-TCF7L1-bound genes in control conditions, and those identified in similar conditions by Marson *et al.* (Marson *et al.*, 2008). This discrepancy between our study and that of Marson *et al.* could be due to differences in the parental mESCs used in the two studies, differences between the antibodies used for ChIP and/or differences in the chromatin fragmentation methods that were used (sonication vs. enzymatic).

It has been suggested that Wnt signaling regulates TCF7L1 expression through β -catenin mediated removal of TCF7L1 from the chromatin, and subsequent proteasomal degradation (Shy *et al.*, 2013). Unexpectedly, despite lower 3xFLAG-TCF7L1 levels, we observed only a slight decrease in total 3xFLAG-TCF7L1-bound genes in the presence of CHIR compared control conditions. We also identified nearly an equal number of genes preferentially bound by TCF7L1, with a 43% overlap, between conditions. Our data indicate that 3xFLAG-TCF7L1 is far more abundant than 3xFLAG-TCF7 in CHIR-treated mESCs, and that more 3xFLAG-TCF7L1 than 3xFLAG-TCF7 is associated with β -catenin in this condition. This suggests that TCF7L1 is the primary mediator of Wnt target gene regulation in mESCs and TCF7L1 dissociation from the

chromatin is not necessarily required. However, at specific loci such as *Axin2* this mechanism of TCF7L1 derepression is likely employed.

In the absence of a Wnt signal, TCF7L1 is thought to mediate the repression of pluripotency associated genes, including *Nanog* (Cole *et al.*, 2008; Marson *et al.*, 2008; Pereira *et al.*, 2006; Yi *et al.*, 2008). Neither 3xFLAG-TCF7L1TCF7L1 nor 3xFLAG-TCF7L1TCF7, negatively correlated with expression of NANOG in self-renewing or differentiating mESC populations, as assessed by flow cytometry and immunofluorescence. Our ChIP-seq data detected only low levels of 3xFLAG-TCF7L1 bound to an upstream enhancer of *Nanog* in control culture conditions. This suggests that TCF/LEFs may mediate indirect effects on *Nanog* expression in a context-dependent manner.

Stimulation of mouse ES cells with a Wnt signal promotes self-renewal and pluripotency, primarily through the derepression of TCF7L1 (Wray *et al.*, 2011; Yi *et al.*, 2011). This is thought to be promoted by degradation of TCF7L1 upon β -catenin binding (Shy *et al.*, 2013). Unexpectedly, we observed equal or greater TCF7L1 occupancy, in CHIR-treated mESCs, at many Wnt and pluripotency-related genes. Previously, we identified *Id3* as one of the most upregulated genes in cells lacking all full-length TCF/LEF factors (Moreira *et al.*, 2017). In our current study, we provide data supporting the conversion of TCF7L1 from a repressor into an activator of *Id3* expression in response to GSK-3 inhibition with CHIR. In support of this, in *Xenopus* embryos and mouse keratinocytes, TCF7L1 has been shown to activate a TCF reporter and *Klf4*, respectively (Cao *et al.*, 2018; Merrill *et al.*, 2001).

The TCF/LEF factors, TCF7 and LEF1 as well as TCF7L2 and TCF7L1, have been classified as ‘activators’ and ‘repressors’, respectively. Our TCF7L1 ChIP-seq data suggest that TCF7L1 is the most abundant TCF factor associated with mESC chromatin, mediating the majority of Wnt/ β -catenin transcriptional responses. Future experiments are needed to evaluate the roles of

the other two TCF/LEF factors, LEF1 and TCF7L2, in mediating β -catenin-dependent transcription in later stages of mESC differentiation, when the level of expression of these factors becomes high enough to be relevant. Also, the roles of the numerous splice variants of the TCF/LEFs need to be incorporated in future studies employing epitope-tagged cell lines, where quantitative comparisons between the various isoforms can be systematically evaluated.

Collectively, the data presented in our study provide new insights into the mechanisms through which TCF7L1 and TCF7 regulate transcription, highlighted by an unexpected lack of overlap between TCF7L1 and TCF7 binding sites at the whole-genome level and revealing diverse effects of CHIR on the occupancy of both factors.

EXPERIMENTAL PROCEDURES

Unless otherwise stated, chemicals were obtained from Sigma-Aldrich.

Cell culture

Routine maintenance of mESCs in serum-containing media, has been previously described (Moreira, *et al.*, 2017).

Chromatin Immunoprecipitation assays

ChIP was performed according to the manufacturers protocol (Cell Signaling Technology, 9005S). Briefly, DNA-protein complexes were prepared from 4×10^6 mouse ES cells cultured in standard LIF + serum or treated with vehicle (DMSO) or $5 \mu\text{M}$ CHIR for 14 hr. For ChIP-seq experiments DNA-protein complexes were prepared from 50×10^6 mouse ES cells cultured in standard LIF + serum or treated with $5 \mu\text{M}$ CHIR for 14 hr. Chemical crosslinking of DNA-protein complexes was performed using 1% paraformaldehyde for 11 min at room temperature. Crosslinking was quenched by addition of 125mM glycine for 5 min at room temperature. Cells were washed twice with ice-cold PBS and scraped into PBS with 1x protease inhibitor cocktail (PIC). Cells were centrifuged, and the pellet was resuspended in buffer A + DTT + PIC followed by a 10 min incubation on ice. After subsequent centrifugation the pellet (nuclei) was resuspended in buffer B + DTT + micrococcal nuclease and incubated for 20 min at 37°C with frequent mixing. Chromatin was digested to a length of 150-900 base pairs. 2% inputs were removed and stored overnight at -80°C . Chromatin was immunoprecipitated with anti-FLAG[®] M2 antibody (Sigma-Aldrich, F1804) overnight at 4°C with rotation. DNA-protein-antibody complexes were captured with a 2hr incubation at 4°C using ChIP-grade protein G magnetic beads, followed by 3x low salt and 1x high salt, washes. DNA-protein complexes were resuspended in elution buffer and incubated for 30 min at 65°C . Eluted chromatin was reverse crosslinked by addition of 0.2M NaCl

and proteinase K, followed by incubation at 65°C overnight. DNA was subsequently column purified using reagents supplied and used for quantitative RT-PCR or next generation sequencing. Primer sequences used for ChIP-qRT-PCR: *Axin2 Neg* (TGATGTCCTTCACACCCTCA, GATGCCCCACCTTAAACTCCA), *Axin2* (GATAAGGTCCTGGCAACTCAGTAA, CCACCTTTTACAGCAAAGCTCTC), *Cdx1* (AAGGAGACAAATTGCCGCCCT, CCCGTTTGAAGTCAGCCTTGC).

Author Contributions

B.W.D. and S.M. designed the experiments, conducted experiments and wrote the paper. C.S, E.P. and S.M. conducted experiments. E.M provided ChIP-seq analyses and visualization. A.B. provided guidance with ChIP-seq.

Acknowledgments

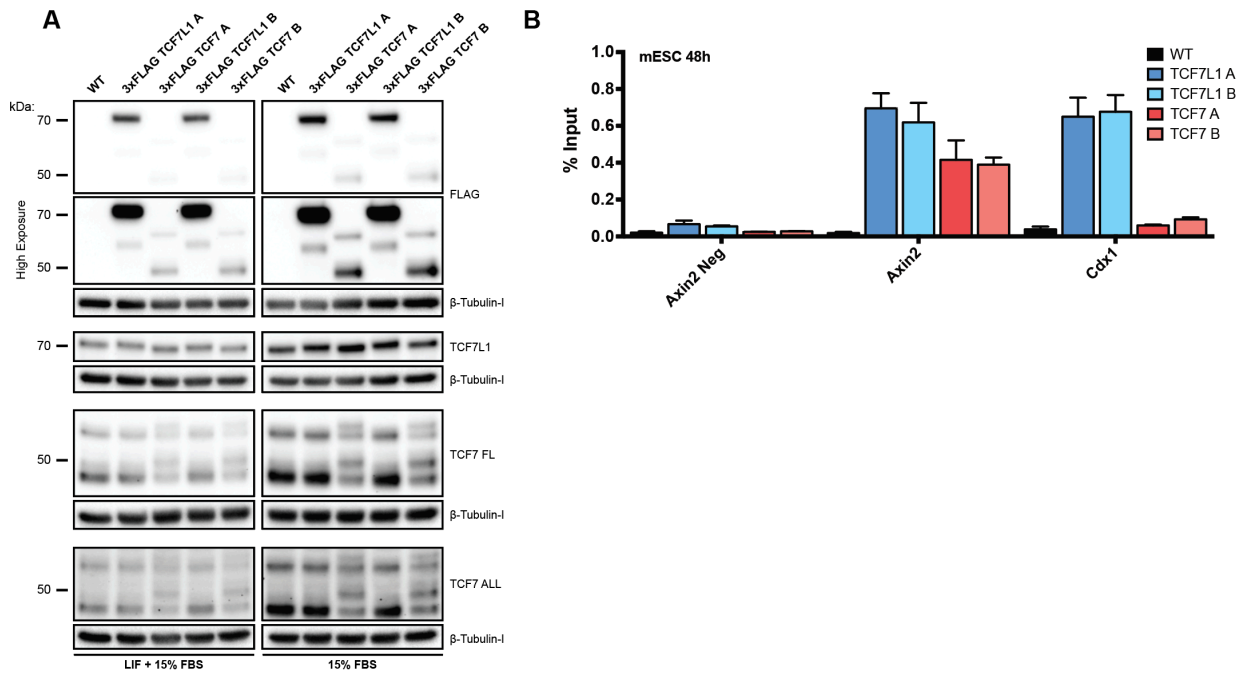
Funding for this study and required infrastructure was provided by the Canadian Institutes of Health Research to BWD (MOP133610), the Canada Research Chairs Program (BWD), the Ontario Ministry of Research and Innovation (BWD), the Canada Foundation for Innovation (BWD), and the OCRiT Project: Ontario Ministry of Economic Development and Innovation (BWD).

References

- Archbold, H.C., Broussard, C., Chang, M. V, and Cadigan, K.M. (2014). Bipartite Recognition of DNA by TCF/Pangolin Is Remarkably Flexible and Contributes to Transcriptional Responsiveness and Tissue Specificity of Wingless Signaling. *PLoS Genet.* *10*.
- Atcha, F.A., Syed, A., Wu, B., Hoverter, N.P., Yokoyama, N.N., Ting, J.-H.T., Munguia, J.E., Mangalam, H.J., Lawrence Marsh, J., Waterman, M.L., *et al.* (2007). A unique DNA binding domain converts T-cell factors into strong Wnt effectors. *Mol. Cell. Biol.* *27*, 8352–8363.
- Benner, C., Heinz, S., and Glass, C.K. (2017). HOMER - Software for motif discovery and next generation sequencing analysis.
- Cao, Q., Shen, Y., Zheng, W., Liu, H., and Liu, C. (2018). Tcf711 promotes transcription of Kruppel-like factor 4 during *Xenopus* embryogenesis. *32*, 215–221.
- Clevers, H., Loh, K.M., and Nusse, R. (2014). Stem cell signaling. An integral program for tissue renewal and regeneration: Wnt signaling and stem cell control. *Science* *346*, 1248012.
- Cole, M.F., Johnstone, S.E., Newman, J.J., Kagey, M.H., and Young, R.A. (2008). Tcf3 is an integral component of the core regulatory circuitry of embryonic stem cells. *Genes & Dev.* *22*, 746–755.
- Doble, B.W., Patel, S., Wood, G.A., Kockeritz, L.K., and Woodgett, J.R. (2007). Article Functional Redundancy of GSK-3a and GSK-3b in Wnt / b-Catenin Signaling Shown by Using an Allelic Series of Embryonic Stem Cell Lines. *Dev. Cell* *12*, 957–971.
- Gammons, M., and Bienz, M. (2018). Multiprotein complexes governing Wnt signal transduction. *Curr. Opin. Cell Biol.* *51*, 42–49.
- Hoverter, N.P., Ting, J.-H.H., Sundaresh, S., Baldi, P., and Waterman, M.L. (2012). A WNT/p21 circuit directed by the C-clamp, a sequence-specific DNA binding domain in TCFs. *Mol. Cell. Biol.* *32*, 3648–3662.
- Hrckulak, D., Kolar, M., Strnad, H., and Korinek, V. (2016). TCF/LEF transcription factors: An update from the internet resources. *Cancers (Basel)*. *8*.
- De Jaime-Soguero, A., Aulicino, F., Ertaylan, G., Griego, A., Cerrato, A., Tallam, A., del Sol, A., Cosma, M.P., and Lluís, F. (2017). Wnt/Tcf1 pathway restricts embryonic stem cell cycle through activation of the Ink4/Arf locus. *PLoS Genet.* *13*.
- Kelly, K.F., Ng, D.Y., Jayakumaran, G., Wood, G. A., Koide, H., and Doble, B.W. (2011). catenin enhances Oct-4 activity and reinforces pluripotency through a TCF-independent mechanism. *Cell Stem Cell* *8*, 214–227.
- Lien, W.-H., Polak, L., Lin, M., Lay, K., Zheng, D., and Fuchs, E. (2014). In vivo transcriptional governance of hair follicle stem cells by canonical Wnt regulators. *Nat. Cell Biol.* *16*, 179–190.
- Marson, A., Levine, S.S., Cole, M.F., Frampton, G.M., Brambrink, T., Johnstone, S., Guenther, M.G., Johnston, W.K., Wernig, M., Newman, J., *et al.* (2008). Connecting microRNA Genes to the Core Transcriptional Regulatory Circuitry of Embryonic Stem Cells. *Cell* *134*, 521–533.
- Martello, G., Sugimoto, T., Diamanti, E., Joshi, A., Hannah, R., Ohtsuka, S., Göttgens, B., Niwa, H., and Smith, A. (2012). Esrrb is a pivotal target of the gsk3/tcf3 axis regulating embryonic stem cell self-renewal. *Cell Stem Cell* *11*, 491–504.

- Merrill, B.J., Gat, U., DasGupta, R., and Fuchs, E. (2001). Tcf3 and Lef1 regulate lineage differentiation of multipotent stem cells in skin. *Genes & Dev.* *15*, 1688–1705.
- Moreira, S., Polena, E., Gordon, V., Abdulla, S., Mahendram, S., Cao, J., Blais, A., Wood, G.A., Dvorkin-Gheva, A., and Doble, B.W. (2017). A Single TCF Transcription Factor, Regardless of Its Activation Capacity, Is Sufficient for Effective Trilineage Differentiation of ESCs. *Cell Rep.* *20*, 2424–2438.
- Morrison, G., Scognamiglio, R., Trumpp, A., and Smith, A. (2016). Convergence of cMyc and -catenin on Tcf711 enables endoderm specification. *EMBO J.* *35*, 356–368.
- Nusse, R., and Clevers, H. (2017). Wnt/ β -Catenin Signaling, Disease, and Emerging Therapeutic Modalities. *Cell* *169*, 985–999.
- Pereira, L., Yi, F., and Merrill, B.J. (2006). Repression of Nanog gene transcription by Tcf3 limits embryonic stem cell self-renewal. *Mol. Cell. Biol.* *26*, 7479–7491.
- Saj, A., Chatterjee, S.S., Zhu, B., Cukuroglu, E., Gocha, T., Zhang, X., Göke, J., and Dasgupta, R. (2017). Disrupting Interactions Between β -Catenin and Activating TCFs Reconstitutes Ground State Pluripotency in Mouse Embryonic Stem Cells. *Stem Cells*.
- Sato, N., Meijer, L., Skaltsounis, L., Greengard, P., and Brivanlou, A.H. (2004). Maintenance of pluripotency in human and mouse embryonic stem cells through activation of Wnt signaling by a pharmacological GSK-3-specific inhibitor. *Nat Med* *10*, 55–63.
- Shy, B.R., Wu, C.-I.I., Khramtsova, G.F., Zhang, J.Y., Olopade, O.I., Goss, K.H., and Merrill, B.J. (2013). Regulation of Tcf711 DNA Binding and Protein Stability as Principal Mechanisms of Wnt/ β -Catenin Signaling. *Cell Rep.* *4*, 1–9.
- Wallmen, B., Schrempp, M., and Hecht, A. (2012). Intrinsic properties of Tcf1 and Tcf4 splice variants determine cell-type-specific Wnt/ β -catenin target gene expression. *Nucleic Acids Res.* *40*, 9455–9469.
- Wray, J., Kalkan, T., Gomez-Lopez, S., Eckardt, D., Cook, A., Kemler, R., and Smith, A. (2011a). Inhibition of glycogen synthase kinase-3 alleviates Tcf3 repression of the pluripotency network and increases embryonic stem cell resistance to differentiation. *Nat Cell Biol* *13*, 838–845.
- Wu, C.-I., Hoffman, J. a, Shy, B.R., Ford, E.M., Fuchs, E., Nguyen, H., and Merrill, B.J. (2012). Function of Wnt/ β -catenin in counteracting Tcf3 repression through the Tcf3- β -catenin interaction. *Development* *139*, 2118–2129.
- Yi, F., Pereira, L., and Merrill, B.J. (2008). Tcf3 Functions as a Steady-State Limiter of Transcriptional Programs of Mouse Embryonic Stem Cell Self-Renewal. *Stem Cells* *26*, 1951–1960.
- Yi, F., Pereira, L., Hoffman, J.A., Shy, B.R., Yuen, C.M., Liu, D.R., and Merrill, B.J. (2011). Opposing effects of Tcf3 and Tcf1 control Wnt stimulation of embryonic stem cell self-renewal. *Nat Cell Biol* *13*, 762–770.
- Ying, Q.-L.L., Wray, J., Nichols, J., Battle-Morera, L., Doble, B., Woodgett, J., Cohen, P., and Smith, A. (2008). The ground state of embryonic stem cell self-renewal. *Nature* *453*, 519–523.
- Zhang, C.U., Blauwkamp, T.A., Burby, P.E., and Cadigan, K.M. (2014). Wnt-Mediated Repression via Bipartite DNA Recognition by TCF in the *Drosophila* Hematopoietic System. *PLoS Genet.* *10*.

Supplemental Information

**Figure S1, Related to Figure 1**

(A) Western blot analysis of WT, and both 3xFLAG- TCF7L1 and 3xFLAG-TCF7 clones (A and B), cultured in 15% FBS \pm LIF for 48h. Lysates were probed with antibodies against TCF7L1, TCF7, FLAG and β -Tubulin (loading control), as indicated. (B) Quantitative ChIP using the FLAG antibody on chromatin isolated from WT, and both 3xFLAG- TCF7L1 and TCF7 clones, cultured in 15%FBS + LIF for 48h. Percent input was calculated for regions bound by TCF/LEFs in *Axin2* and *Cdx1*, as well as a negative control locus 11kb upstream of *Axin2*. Bars represent the mean of 3 independent experiments \pm SEM.

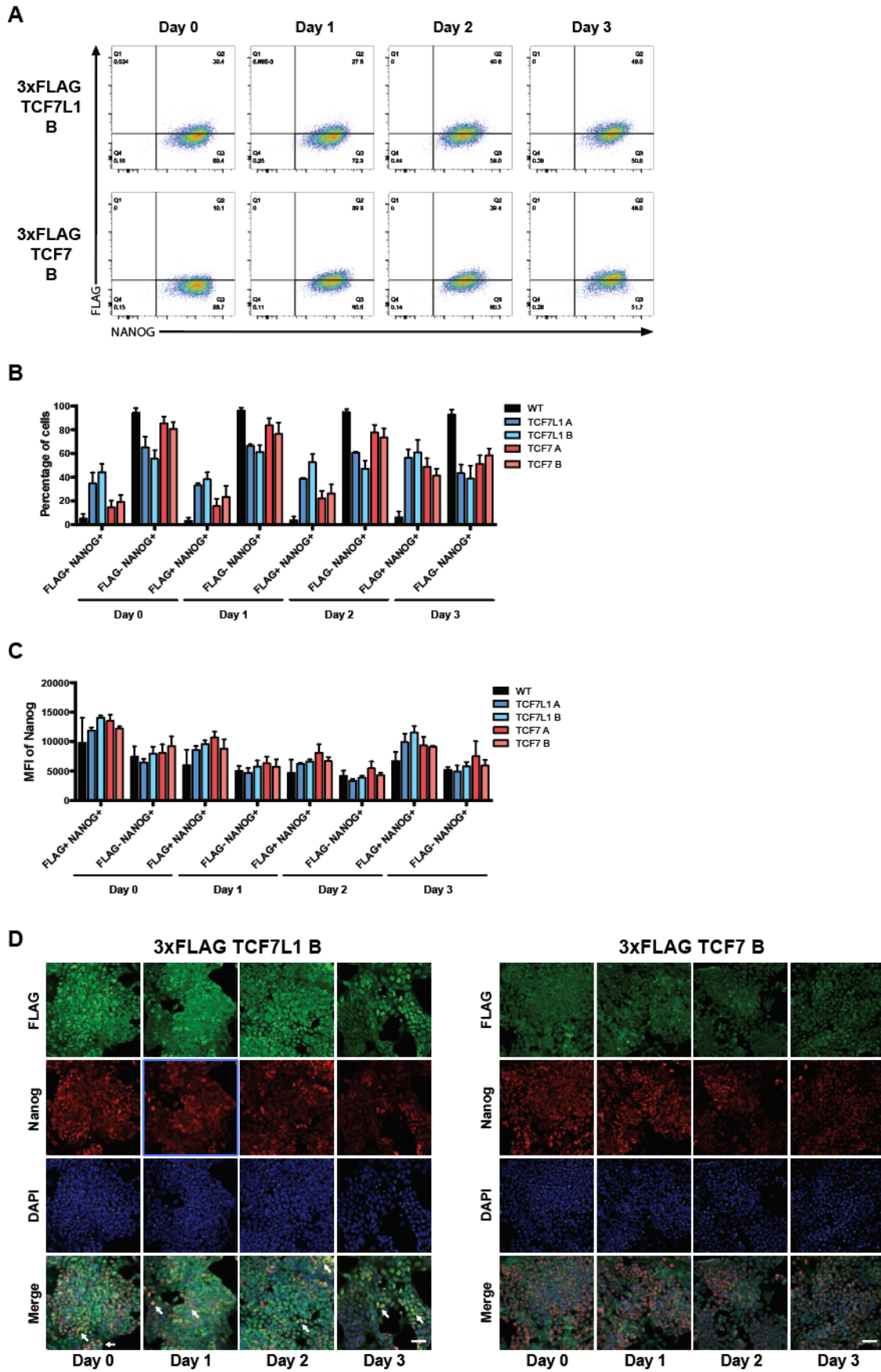


Figure S2, Related to Figure 2

(A) Representative flow cytometry profiles of intracellular flow analysis of NANOG, and FLAG levels in 3xFLAG-TCF7L1 and 3xFLAG-TCF7 mESCs (clones not presented in paper) cultured in 15% FBS + LIF (Day 0) and 15% FBS (Day 1-3), as indicated. (B) Graph of the proportion of single-positive FLAG-NANOG⁺ and double-positive FLAG+NANOG⁺ cells in WT, 3xFLAG-TCF7L1 and 3xFLAG-TCF7 mESCs. Bars represent the mean of 3 independent experiments \pm SEM. (C) Graph of the median fluorescence intensity of NANOG in single-positive FLAG-NANOG⁺ and double-positive FLAG+NANOG⁺ cells in WT, 3xFLAG-TCF7L1 and 3xFLAG-TCF7 clones. Bars represent the mean of 3 independent experiments \pm SEM. (D) Immunofluorescence analysis of 3xFLAG-TCF7L1 and 3xFLAG-TCF7 mESCs (clones not presented in paper), cultured in 15%FBS + LIF (Day 0) and 15%FBS (Day 1-3), as indicated. Cells were stained for NANOG, FLAG and DAPI. Scale bar represents 50 μ m. White arrows indicate cells with elevated levels of FLAG and NANOG.

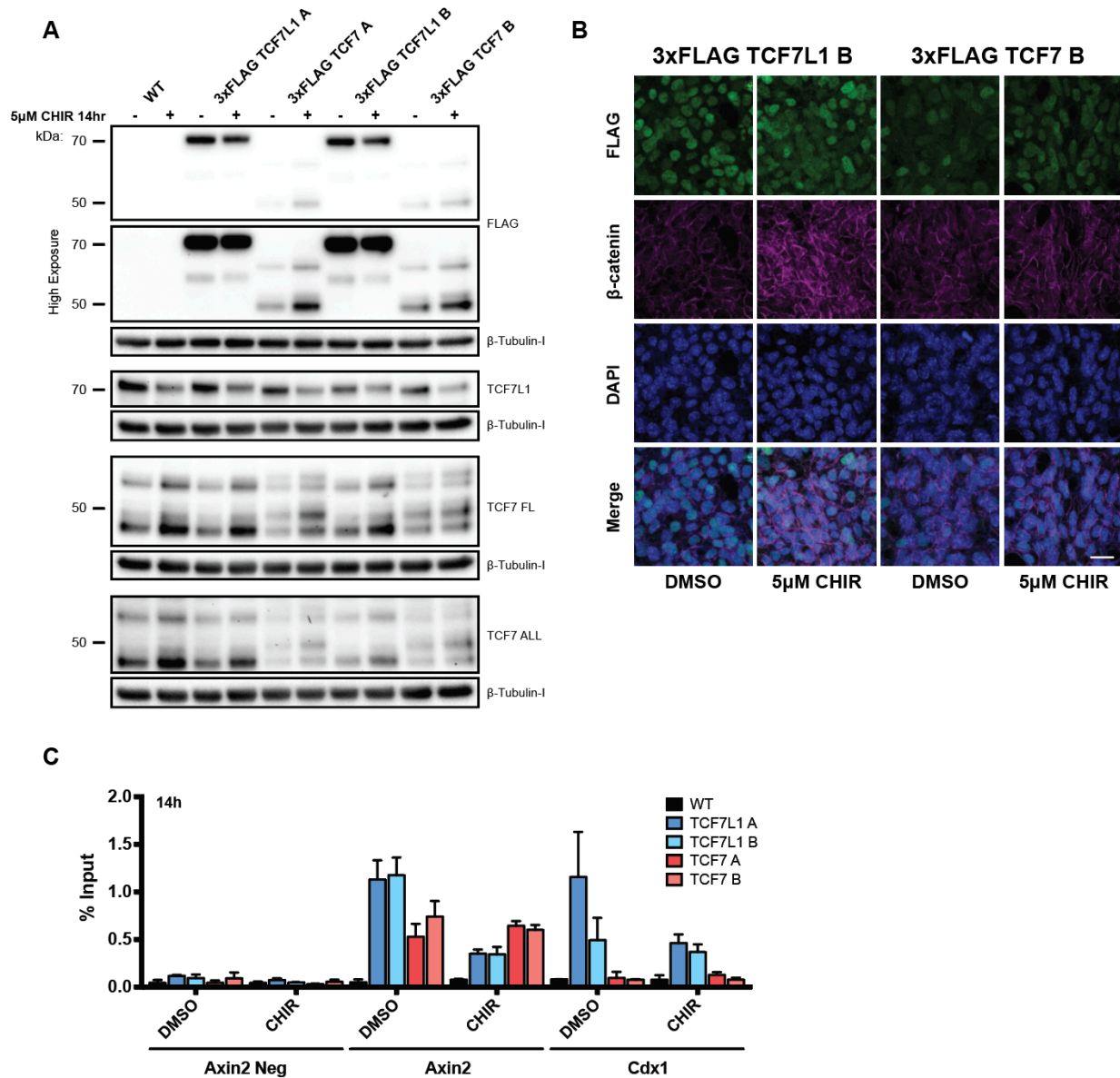


Figure S3, Related to Figure 3

(A) Western blot analysis of WT, 3xFLAG- TCF7L1 (clones A and B) and TCF7 (clones A and B) mESCs, cultured in 15% FBS + LIF treated with 5 μ M CHIR or DMSO control for 14 hours. Lysates were probed with antibodies against TCF7L1, TCF7, FLAG and β -Tubulin (loading control), as indicated. (B) Immunofluorescence analysis of WT, 3xFLAG- TCF7L1 and 3xFLAG-TCF7 mESCs (clones not presented in paper), cultured in 15%FBS + LIF treated with 5 μ M CHIR or DMSO control for 14 hours, as indicated. Cells were stained for β -catenin, FLAG and DAPI. Scale bar represents 20 μ m. (C) Quantitative ChIP using the FLAG antibody on WT, and all clones of 3xFLAG- TCF7L1 and 3xFLAG-TCF7 mESCs, cultured in 15%FBS + LIF treated with 5 μ M CHIR or DMSO control for 14 hours. Percent input was calculated for regions bound by TCF/LEFs in *Axin2* and *Cdx1*, as well as a negative control locus 11kb upstream of *Axin2*. Bars represent the mean of 3 independent experiments \pm SEM.

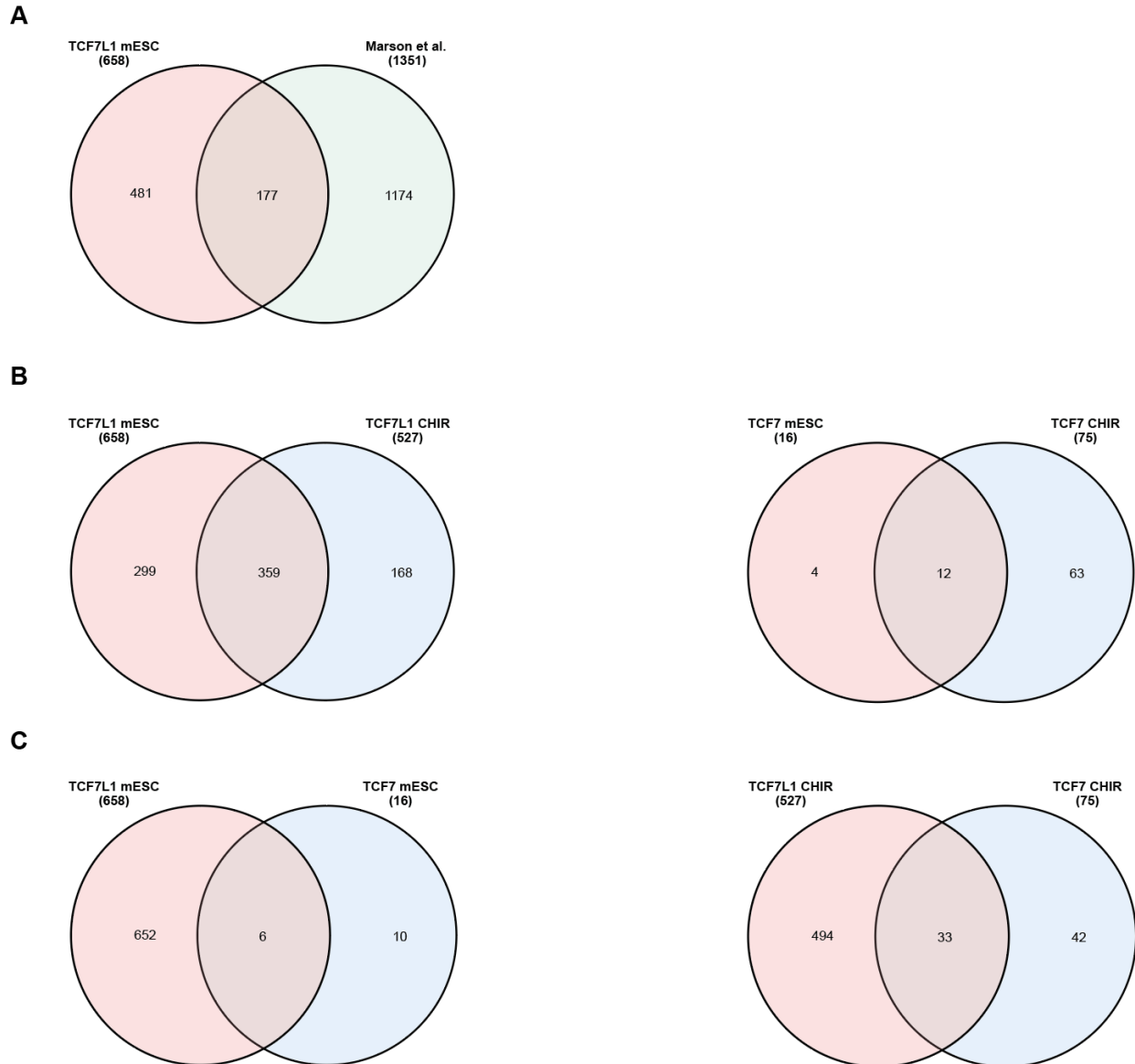
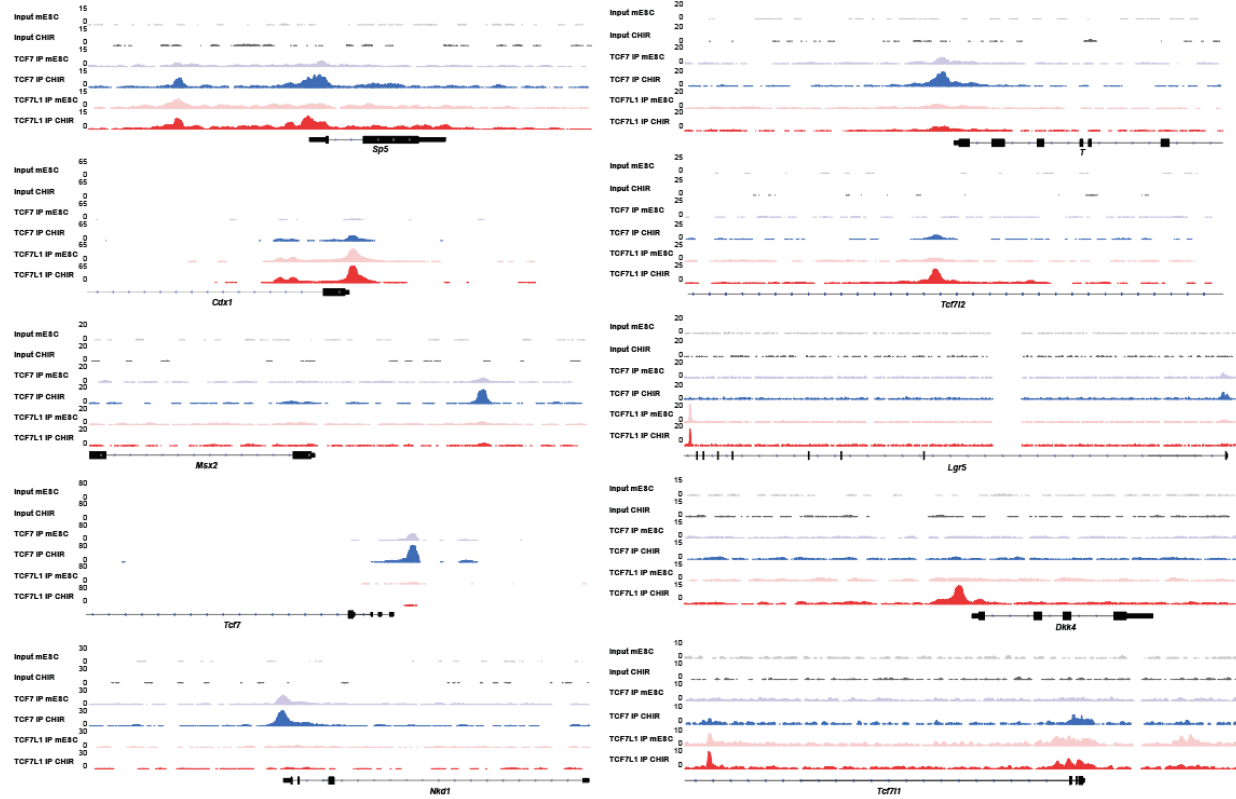


Figure S4, Related to Figure 4

(A) Venn diagram showing the overlap between 3xFLAG-TCF7L1-bound genes in mESCs maintained in standard LIF + Serum (mESC) or 14h 5 μ M CHIR (CHIR) media and TCF7L-bound genes from Table S2 of the supplemental data found in Marson *et al.* (B) Venn diagram showing the overlap between 3xFLAG-TCF7L1 (LEFT) or 3xFLAG-TCF7 (RIGHT) bound genes in mESCs maintained in standard LIF + Serum (mESC) or 14h 5 μ M CHIR (CHIR) media. (C) Venn diagram showing the overlap between 3xFLAG-TCF7L1- and 3xFLAG-TCF7-bound genes in mESCs maintained in LIF + Serum (mESC) or 14h 5 μ M CHIR (CHIR) media.

A



B

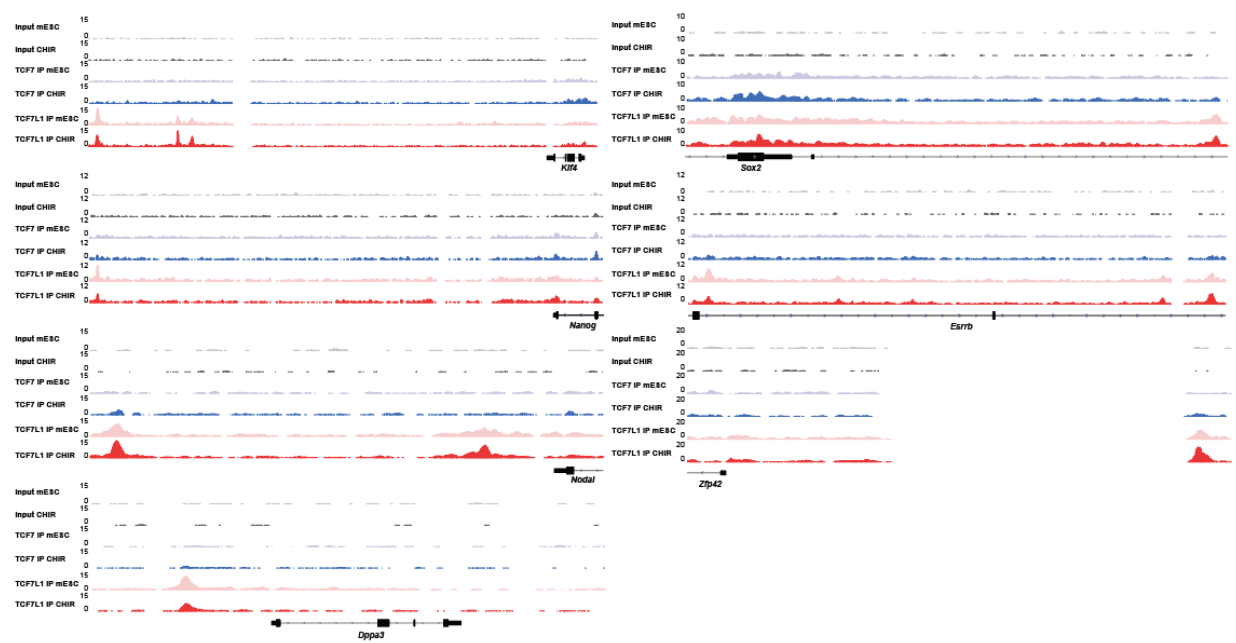


Figure S1 5, Related to Figure 5

(A) Genomic tracks showing 3xFLAG-TCF7 (blue) and 3xFLAG-TCF7L1 (red) peaks at additional Wnt associated genes in mESCs cultured in standard LIF + serum (light shade) or treated with 5 μ M CHIR for 14 hours (dark shade). Pooled LIF + serum and 14hr 5 μ M CHIR input peaks are in grey and dark grey, respectively. Genomic positions reflect NCBI mouse genome build mm10.

SUPPLEMENTAL EXPERIMENTAL PROCEDURES

Immunofluorescence

For immunofluorescence staining, cells were washed twice with PBS between all steps. Cells on ibidi® 8-well slides were fixed with cold 4% paraformaldehyde/PBS for 10 minutes at room temperature. Cells were subsequently permeabilized with 0.1% Triton X-100 for 5 minutes at room temperature. Samples were blocked with 10% goat serum/PBS for 1hr followed by incubation overnight at 4°C in primary antibody diluted in 3% goat serum/PBS. The next day, samples were incubated in secondary (Alexa Fluor) antibodies diluted 1:1500 in antibody dilution buffer for 1 hour at room temperature. Cells were mounted with 1-2 drops/well of Pro-Long Gold antifade (containing DAPI) solution (Life Technologies, P36935). Cells were subsequently imaged using a Zeiss LSM 700 laser-scanning confocal fluorescence microscope.

Intracellular Flow Cytometry

Cells were plated on 12-well plates. Cells were detached and dispersed into a single-cell suspension with Accutase (Innovative Cell Technologies). After washing once with PBS, cells were resuspended in PEF buffer (2% FBS and 2 mM EDTA in PBS). Cells were subsequently strained through a 35 µm flow tube and fixed with BD Cytotfix™ fixation buffer (554655, BD Biosciences). Cells were washed with 1x BD Perm/Wash™ buffer (554723, BD Biosciences) and pelleted. Cells were then incubated in anti-Nanog and FLAG antibodies diluted (1/800) in 1x BD Perm/Wash™ buffer overnight at 4°C. Cells were then washed with 1x BD Perm/Wash™ buffer and pelleted. Pellets were resuspended in secondary antibodies, goat anti-mouse Alexa Fluor 488 and goat anti-rabbit Alexa Fluor 647, diluted (1/4000) in 1x BD Perm/Wash™ buffer, and incubated for 1h at 4°C. A final wash was performed with 1x BD Perm/Wash™ buffer and cells were pelleted. Cells were subsequently resuspended in PEF buffer and analyzed by flow cytometry.

Cell lysate preparation

Cell lysates were prepared as previously described (Moreira *et al.*, 2017).

Western Blot Analysis

Western blots were performed as previously described (Moreira, *et al.*, 2017).

Co-Immunoprecipitation Assays

Approximately 5-10 x 10⁶ cells of the indicated mESC lines were cultured on 100 mm gelatin-coated dishes in standard mESC medium, prior to initiation of the assay. The cells were rinsed twice with PBS and lysed for 10 minutes on ice with Buffer LB (14321B, ThermoFisher Scientific), which contained 100 mM NaCl, 0.5% Triton™ X-100, 2 mM MgCl₂, 1 mM DTT, 1x Halt Protease and Phosphatase Inhibitor cocktail (78440, ThermoFisher Scientific). The cells were subsequently harvested, and the lysates were clarified at 18 000 x g for 10 minutes. The supernatant was transferred to a new pre-chilled tube and the lysates were quantified by the Lowry method (DC Protein Assay; 5000112, Bio-Rad). Equivalent amounts of protein extract were used per IP within each co-immunoprecipitation experiment (typically ~500µg of protein per IP). The following antibody was used for the assay, mouse anti-β-catenin (610153, BD Transduction). 7.5 µg per IP was pre-conjugated to 1.5mg of Protein-G Dynabeads™ M-270 Epoxy for 24 hours at 37°C according to the manufacturer's instructions (14321B, ThermoFisher Scientific). Extracts from the indicated mESC lines were added to the antibody-bead complex, and the mixture was incubated for 1 hours at 4°C, rotating. The immunoprecipitates were subsequently rinsed 3 times using the lysis buffer (including inhibitors) followed by a final wash with LWB buffer (14321B, ThermoFisher Scientific). Samples were eluted from the beads with EB buffer (14321B, ThermoFisher Scientific) via a 5-minute incubation at 25°C. Prior to western blot analysis, 3x NuPage™ LDS buffer (NP0007, ThermoFisher Scientific) with 5% TCEP Bond Breaker solution (77720, ThermoFisher Scientific) was added to the eluate without boiling.

Quantitative RT-PCR

Total RNA was isolated using the PureLink RNA Mini Kit (Life Technologies) and 1 µg was used to generate cDNA with qScript cDNA SuperMix (Quanta Biosciences). The cDNA was diluted 1/5 to a final volume of 100 µL and 3 µL of this was used for each 10 µL PCR reaction with SsoAdvanced SYBR Green SuperMix (BioRad). *Rpl13a* was used as the reference gene. Bio-Rad's CFX96 instrument and software were used to determine relative gene expression

levels using the delta-delta Ct method. Primer sequences were designed using IDT's online primer design software (idtdna.com) or were obtained from prior publications. For experiments in which transcript levels were assessed following CHIR99021 treatment of WT ESCs, ESCs were plated into LIF- containing medium supplemented with CHIR99021 at 10 μ M for 48 hours before RNA isolation. Primer sequences used for qRT-PCR: *Id3* (CACTTACCCTGAACCTCAACGC, CCCATTCTCGGAAAAGCCAG).

Antibodies

The following primary antibodies were used for western blot, co-immunoprecipitation, and/or immunofluorescent staining: mouse anti- β -Tubulin-I (T7816, Sigma); mouse anti-FLAG M2 (F1804, Sigma); rabbit anti-TCF7L1 (ab86175, Abcam); rabbit anti-TCF7 FL (C63D9, Cell Signaling Tech.); rabbit anti-TCF7 All (C46C7, Cell Signaling Tech.); rabbit anti-Nanog (A300-397A, Bethyl Laboratories); mouse anti- β -catenin (610153, BD Transduction); rabbit anti-Non-phospho- β -catenin (D13A1, Cell Signaling Tech.); and rabbit anti- β -catenin Amino-terminal antigen (9581S, Cell Signaling Tech.).

Fluorochrome-conjugated secondary antibodies were obtained from ThermoFisher Scientific and used at 1/1500 (Molecular Probes): goat anti-mouse Alexa Fluor 488; and goat anti-rabbit Alexa Fluor 647.

Generation of 3xFLAG- *TCF7L1* and *TCF7* knock-in mESC lines using TALENs.

TCF7L1 and *TCF7* targeting constructs and TALENs were designed and assembled as previously described (Moreira, *et al.*, 2017). Cell lines were generated as previously described (Moreira, *et al.*, 2017). Two independent clones of both 3xFLAG-TCF7L1 and 3xFLAG-TCF7 knock-in mESCs were used for subsequent analyses. Heterozygosity was confirmed using western blotting, Sanger sequencing and genomic DNA genotyping.

ChIP-seq library preparation and next generation sequencing

Library preparation and sequencing was performed by McMaster University's Farncombe Metagenomics Facility. ChIP DNA was initially quantitated using the QuantiFluor dsDNA System reagents (Promega, E2670) and the Promega QuantiFluor ST fluorometer. ChIP-seq libraries were prepared using NEBNext[®] Ultra[™] II DNA library preparation kit for Illumina[®] according to manufacturer's instructions (New England Biolabs, E7645). Input libraries from WT, 3xFLAG-TCF7L1 clones A and B, and 3xFLAG-TCF7 clones A and B, cultured in standard mESC medium containing LIF and serum (L+S) or the same medium supplemented with 5 μ M CHIR for 14h, were pooled to create a L+S and CHIR inputs, respectively. Fragment size distribution for all libraries was assessed using a Bioanalyzer and concentrations were assessed using qPCR on BioRad's iCycler IQ5 using the KAPA-SYBR Fast qPCR Master Mix (BioRad, KM4105). Sequencing was configured for single-end 51 bp reads and 8 bp dual indices on an Illumina HiSeq 1500 instrument, with Rapid v2 chemistry and on-board cluster generation. Input libraries from L+S and CHIR, were pooled with libraries generated from anti-FLAG ChIPs conducted on chromatin isolated from WT, 3xFLAG-TCF7L1 clones A and B, and 3xFLAG-TCF7 clones A and B, cultured in L+S or CHIR and were sequenced across 4 lanes, resulting in approximately 50 million reads per sample.

ChIP-seq trimming, alignment, and tracks

Reads were trimmed from the 3' end to have a phred score of at least 30. Illumina Universal adapters were removed from the reads. Resulting reads shorter than 50 bp and orphaned reads were discarded. Trimming and clipping were performed using Trimmomatic v0.35 (Bolger *et al.*, 2014). Trimmed reads were then aligned to the mouse reference genome GRCh38 using BWA v0.7.12 (Li *et al.*, 2009). Multi-mappers and duplicate reads were excluded from subsequent analyses. Tracks were generated using bedtools v2.27.0 (Quinlan and Hall, 2010). Bedgraphs were generated from bam files and normalized by a scale factor, which is inversely proportional to the number of reads (genomeCoverageBed -bg -split -scale -scalefactor).

ChIP-seq peak calling, annotation, motif discovery, and gene ontology

Narrow peaks were called by MACS v2.1.0 (Zhang *et al.*, 2008) in single end mod (format = BAM), no shifting model (-nomodel) and defaults parameters (mfold = [5,50], q-value cut-off = 0.05). Input-CHIR-Pool and Input-mESC-Pool were used as control for CHIR and mESC samples respectively. Peak annotation, known and *de novo* motif discovery, and gene ontology analysis were performed by HOMER v4.7 (Heinz *et al.*, 2010). Peak tracks were visualized using the Integrative Genomics Viewer (IGV) v2.4 (Robinson *et al.*, 2011).

Differential Binding Analysis

Differential binding analysis was performed with the R packages *csaw* v1.10 (Lun and Smyth, 2015) and *edgeR* 3.18.1 (Robinson *et al.*, 2009) with R 3.4.1. Briefly, the *windowCounts* function was used to count the number of reads in a sliding window in every BAM file with the following parameters: minimum quality of 30, fragment length of 150, single-end reads and a window size of 50. After calculating for normalization factors and filtering with negative control (using wildtype samples) to remove uninterested windows, the remaining regions were tested for differential binding using the *edgeR* workflow. Benjamini-Hochberg multiple test correction method was used to compute the False Discovery Rate within each pairwise comparison.

TCF/LEF helper site identification

To identify a potential interaction between TCF/LEF motifs and the helper site, we first identified the presence of the WRE motifs within MACS identified at TCF7 or TCF7L1 peaks, using HOMER. Helper sites were subsequently identified 200 bp up- or downstream of each WRE, using HOMER. To this end, Position Weight Matrices (PWM) were manually created for the core binding site of TCF/LEF motifs (5'-CTTTGWWS-3' (W=A/T S=G/C) and the helper site 5'-RCCGCC-3' (R=A/G) (Hoverter *et al.*, 2014). HOMER v4.7 (Heinz *et al.*, 2010) was used to scan the previously identified peaks for these motifs with a score of 5 or more. Peaks containing both motifs were selected for further analyses.

Supplementary References

- Bolger, A.M., Lohse, M., and Usadel, B. (2014). Trimmomatic: A flexible trimmer for Illumina sequence data. *Bioinformatics* 30, 2114–2120.
- Heinz, S., Benner, C., Spann, N., Bertolino, E., Lin, Y.C., Laslo, P., Cheng, J.X., Murre, C., Singh, H., and Glass, C.K. (2010). Simple Combinations of Lineage-Determining Transcription Factors Prime cis-Regulatory Elements Required for Macrophage and B Cell Identities. *Mol. Cell* 38, 576–589.
- Hoverter, N.P., Zeller, M.D., McQuade, M.M., Garibaldi, A., Busch, A., Selwan, E.M., Hertel, K.J., Baldi, P., and Waterman, M.L. (2014). The TCF C-clamp DNA binding domain expands the Wnt transcriptome via alternative target recognition. *Nucleic Acids Res.* 42, 13615–13632.
- Li, H., Handsaker, B., Wysoker, A., Fennell, T., Ruan, J., Homer, N., Marth, G., Abecasis, G., and Durbin, R. (2009). The Sequence Alignment/Map format and SAMtools. *Bioinformatics* 25, 2078–2079.
- Lun, A.T.L., and Smyth, G.K. (2015). *csaw*: A Bioconductor package for differential binding analysis of ChIP-seq data using sliding windows. *Nucleic Acids Res.* 44.
- Moreira, S., Polena, E., Gordon, V., Abdulla, S., Mahendram, S., Cao, J., Blais, A., Wood, G.A., Dvorkin-Gheva, A., and Doble, B.W. (2017). A Single TCF Transcription Factor, Regardless of Its Activation Capacity, Is Sufficient for Effective Trilineage Differentiation of ESCs. *Cell Rep.* 20, 2424–2438.
- Quinlan, A.R., and Hall, I.M. (2010). BEDTools: A flexible suite of utilities for comparing genomic features. *Bioinformatics* 26, 841–842.
- Robinson, J.T., Thorvaldsdóttir, H., Winckler, W., Guttman, M., Lander, E.S., Getz, G., and Mesirov, J.P. (2011). Integrative genomics viewer. *Nat. Biotechnol.* 29, 24–26.
- Robinson, M.D., McCarthy, D.J., and Smyth, G.K. (2009). *edgeR*: A Bioconductor package for differential expression analysis of digital gene expression data. *Bioinformatics* 26, 139–140.
- Zhang, Y., Liu, T., Meyer, C.A., Eeckhoute, J., Johnson, D.S., Bernstein, B.E., Nussbaum, C., Myers, R.M., Brown, M., Li, W., *et al.* (2008). Model-based analysis of ChIP-Seq (MACS). *Genome Biol.* 9.

CHAPTER 4

ENDOGENOUS BioID ELUCIDATES TCF7L1 INTERACTOME MODULATION UPON GSK-3 INHIBITION IN MOUSE ESCS

Preamble

This chapter is available as an unpublished preprint article. It is presented in its preprint format.

“This research was originally posted on the bioRxiv. Steven Moreira, Caleb Seo, Victor Gordon, Sansi Xing, Ruilin Wu, Enio Polena, Vincent Fung, Deborah Ng, Cassandra Wong, Brett Larsen, Brian Raught, Anne-Claude Gingras, Yu Lu and Bradley W. Doble. Endogenous BioID elucidates TCF7L1 interactome modulation upon GSK-3 inhibition in mouse ESCs. <https://doi.org/10.1101/431023>. © 2018 The Authors. Preprint posted by Cold Spring Harbor Laboratory.”

Together Dr. Bradley Doble and I, conceived the study, designed experiments and wrote the paper. Enio Polena, Vincent Fung and I, generated the BirA* TCF7L1 cell lines. Caleb Seo and Victor Gordon provided technical assistance with PLA and Co-IP assays. Dr. Yu Lu, Sansi Xing, and Ruilin Wu provided technical assistance with mass spectrometry. Dr. Brian Raught and Deborah Ng provided technical assistance with BioID. Dr. Anne-Claude, Dr. Brett Larsen, and Cassandra Wong provided technical assistance with ProHits analysis. The central question behind this chapter was prompted by the fact that TCF7L1 and TCF7 behaving opposingly on the TCF/LEF reporter, even in the presence of β -catenin. One explanation is that TCF7L1 and TCF7 bind to unique co-factors in both the absence and presence of β -catenin, owing to the unique functions of these proteins. To test this BioID was employed, unfortunately technical issues prevented the acquisition of reliable TCF7 data. Thus, this chapter focuses instead on comparing an overexpression (potentially required for TCF7) versus endogenous TCF7L1 BioID system.

**Endogenous BioID elucidates TCF7L1 interactome
modulation upon GSK-3 inhibition in mouse ESCs**

Steven Moreira¹, Caleb Seo¹, Victor Gordon¹, Sansi Xing¹, Ruilin Wu¹, Enio Polena¹, Vincent Fung¹, Deborah Ng^{2,3}, Cassandra J Wong^{4,5}, Brett Larsen^{4,5}, Brian Raught^{2,3}, Anne-Claude Gingras^{4,5}, Yu Lu and Bradley W. Doble^{1*}

1. Department of Biochemistry and Biomedical Sciences, Stem Cell and Cancer Research Institute, Michael G. DeGroot School of Medicine, McMaster University, Hamilton, ON L8N 3Z5, Canada.

2. Princess Margaret Cancer Centre, University Health Network, 101 College Street, Toronto, ON M5G 1L7, Canada.

3. Department of Medical Biophysics, University of Toronto, Toronto, ON M5G 1L7, Canada.

4. Lunenfeld-Tanenbaum Research Institute, Mount Sinai Hospital, 600 University Avenue, Toronto, ON M5G 1X5, Canada.

5. Department of Molecular Genetics, University of Toronto, Toronto, ON M5S 1A8, Canada.

*Correspondence: dobleb@mcmaster.ca

Summary

Modulation of Wnt target gene expression via the TCF/LEFs remains poorly understood. We employ proximity-based biotin labeling (BioID) to examine GSK-3 inhibitor effects on the TCF7L1 interactome in mouse ESCs. We generated ESC lines with biotin ligase BirA* fused to TCF7L1 by knocking it into the endogenous *TCF7L1* locus or by inserting a dox-inducible BirA*-TCF7L1 transgene into the *Rosa26* locus. Induction yielded BirA*-TCF7L1 levels 3-fold higher than in the endogenous system, but substantial overlap in biotinylated proteins with high peptide counts were detected by each method. Known TCF7L1 interactors TLE3/4 and β -catenin, and numerous proteins not previously associated with TCF7L1, were identified in both systems. Despite reduced BirA*-TCF7L1 levels, the number of hits identified with both BioID approaches increased after GSK-3 inhibition. We elucidate the network of TCF7L1 proximal proteins regulated by GSK-3 inhibition, validate the utility of endogenous BioID, and provide mechanistic insights into TCF7L1 target gene regulation.

Highlights

- BirA*-TCF7L1 at single-copy physiological levels generates robust BioID data
- CHIR99021 reduces TCF7L1 levels but increases detectable TCF7L1-proximal proteins.
- The TCF7L1 interactome of largely epigenetic/transcription factors fluctuates with GSK-3 inhibition
- JMJD1C, SALL4 and BRG1/SMARCA4 are validated as TCF7L-interacting proteins

eTOC Blurb

Moreira *et al.* compare and contrast inducible BirA*-TCF7L1 overexpression versus BirA*-TCF7L1 knock-in approaches for BioID analyses in mouse ESCs. Single-copy expression of BirA*-TCF7L1, which is less likely to disrupt its function and cellular homeostasis, is sufficient to assemble a TCF7L1 interactome that provides insights into mechanisms regulating TCF7L1 function.

INTRODUCTION

The Wnt/ β -catenin signaling pathway regulates tissue homeostasis and mammalian development. Inappropriate activation leads to a variety of cancers, most prominently colorectal cancer (Clevers and Nusse, 2012; Nusse and Clevers, 2017). Wnt ligands and cognate cell surface receptors initiate a cascade of intracellular signaling events, which ultimately lead to activation of Wnt target genes via β -catenin interactions with the T-Cell Factor/Lymphoid Enhancer Factor (TCF/LEF) family of transcription factors (Cadigan and Waterman, 2012).

In mouse embryonic stem cells (mESCs) all four TCF/LEF family members, TCF7, TCF7L1, TCF7L2, and LEF1 are expressed at detectable protein levels (Moreira *et al.*, 2017; Wallmen *et al.*, 2012), although TCF7L1 is the most abundant and best characterized TCF/LEF in this cell type (Pereira *et al.*, 2006). TCF7L1 is part of an extended network of transcription factors regulating pluripotency (Cole *et al.*, 2008; Marson *et al.*, 2008). Derepression of TCF7L1 is necessary for the enhancement of self-renewal in mESCs in response to Wnt activation (Wray *et al.*, 2011; Yi *et al.*, 2011). Stimulation with the GSK-3 inhibitor CHIR99021 (CHIR) or Wnt3a results in the reduction of TCF7L1 transcript levels as well as β -catenin-dependent proteasomal degradation of TCF7L1 (Shy *et al.*, 2013).

Despite being extensively studied, the precise mechanisms through which TCF7L1 regulates mESC pluripotency remain poorly characterized. Additionally, few TCF/LEF protein-protein interactions have been described in the literature. In the absence of β -catenin, TCF7L1 is thought to act as a constitutive transcriptional repressor in association with co-repressors, including members of the Transducin-Like Enhancer of Split (TLE) family (Groucho in *Drosophila*) and C-terminal binding protein (CtBP) (Atlasi *et al.*, 2013; Brannon *et al.*, 1999; Eshelman *et al.*, 2017; Lien *et al.*, 2014; Pereira *et al.*, 2006; Tam *et al.*, 2008; Wu *et al.*, 2012; Yi *et al.*, 2011). In the presence of a Wnt signal the TCF/LEFs interact with β -catenin, which recruits co-activators such

as P300, CBP, SMARCA4 and BCL9 (Barker *et al.*, 2001a; Hecht, 2000; Kramps *et al.*, 2002; Takemaru and Moon, 2000; Thompson *et al.*, 2002).

Many protein-protein interactions have been identified by using affinity purification coupled with mass spectrometry, however, due to the insolubility of chromatin-associated proteins, this technique is restricted to strong interactions and is prone to false positives. Proximity-dependent biotinylation, BioID, is a novel technique for identifying protein-protein interactions in cells (Roux *et al.*, 2012). This technique employs a promiscuous biotin ligase mutant BirA*, which is coupled to a “bait” protein allowing for the labelling of vicinal proteins within a radius of 10nm (Kim *et al.*, 2014; Roux *et al.*, 2012). The BioID method allows for vigorous cell lysis, as biotinylated proteins are affinity purified via high-affinity interactions with immobilized streptavidin. The technique also permits detection of transient and/or weak interactions.

Here, we use BioID to identify novel TCF7L1-interacting proteins in differentiating mouse embryonic stem cells, both in the absence or presence of the Wnt mimetic small molecule CHIR. BioID conventionally employs stable cell lines with constitutively or inducibly overexpressed baits. To minimize potential overexpression artefacts, we used homologous recombination to introduce BirA* at the N-terminus of endogenously expressed TCF7L1 and compared our BioID results from this approach with a doxycycline-inducible BirA*-TCF7L1 overexpression system. Our data reveal 146 putative TCF7L1 proximal proteins, offering new insights into mechanisms of TCF7L1 function and the influence of Wnt signaling on the TCF7L1 interactome.

RESULTS

Inducible and endogenous BirA*-TCF7L1 BioID systems

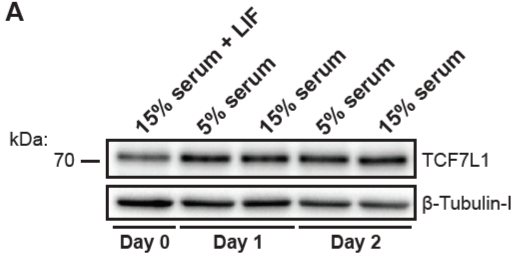
To ensure a high degree of confidence in our TCF7L1 BioID screen, we first identified the condition that provided us with maximal levels of TCF7L1 protein in wild-type (WT) E14TG2a mouse ESCs. The expression of TCF7L1 was assessed in WT cells cultured in standard medium

containing 15% serum plus LIF, medium lacking LIF, and medium with 5% serum and lacking LIF (Figure 1A). The levels of TCF7L1 increased similarly with LIF withdrawal in both serum conditions (Figure 1A), thus we used 5% serum in subsequent experiments to minimize serum effects.

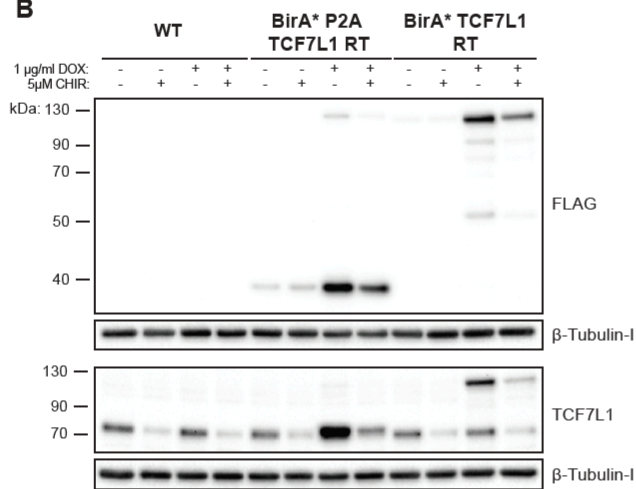
To generate mESCs with inducible BirA*-TCF7L1, we subcloned a doxycycline (dox) inducible expression system into a targeting vector directing homologous recombination within the safe harbour *ROSA26* locus. We employed a TALEN-facilitated knock-in approach to introduce a single copy of dox-inducible 3xFLAG-BirA*-P2A- or 3xFLAG-BirA*-tagged TCF7L1 into the *ROSA26* locus. We will refer to the TCF7L1 inducible lines as BirA*-P2A-TCF7L1 RT, a control cell line incorporating a P2A self-cleaving peptide between the BirA* and TCF7L1 coding sequences, or BirA*-TCF7L1 RT (the RT suffix denotes **R**osa **T**etOne).

Expression of inducible proteins in RT clones was confirmed by western blotting (Figure 1B, 1D, S1A). Addition of 1µg/mL doxycycline induced expression of both the BirA*-P2A-TCF7L1 RT control and the BirA*-TCF7L1 RT fusion protein (Figure 1B, S1A). Treatment with CHIR reduced TCF7L1 protein levels significantly (Figure 1B). Total TCF7L1 levels were elevated in BirA*-TCF7L1 RT lines after doxycycline addition, whereas dox had no effect on TCF7L1 levels in wild-type mESCs. Unexpectedly, after dox treatment BirA*-P2A-TCF7L1 RT lines also demonstrated more detectable TCF7L1 at 70 kDa. BirA*-P2A-TCF7L1 RT controls also displayed a detectable uncleaved BirA*-P2A-TCF7L1 fusion product of approximately 130 kDa (upper panel, Figure 1B). The levels of BirA* (~40 kDa) in the BirA*-P2A-TCF7L1 RT line and BirA*-TCF7L1 fusion protein (~130 kDa) in the BirA*-TCF7L1 RT line were reduced in response to CHIR, suggesting post-transcriptional regulation of TCF7L1 (Figure 1B).

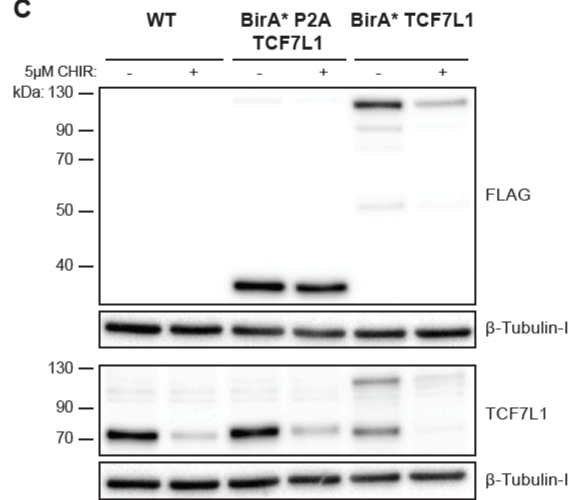
A



B



C



D

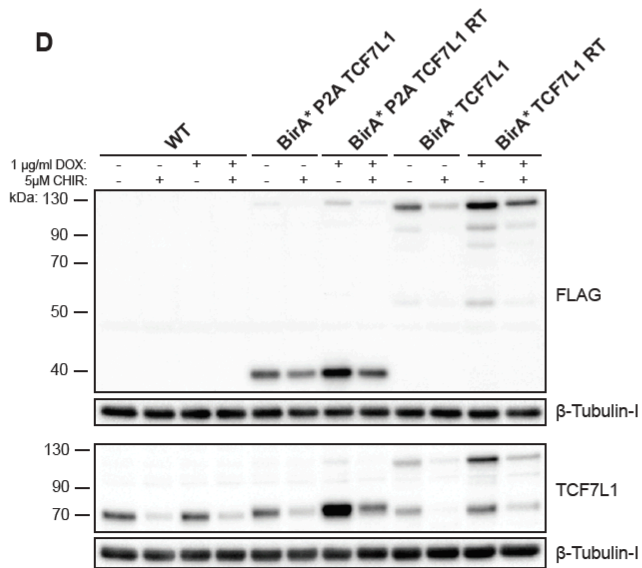


Figure 1. BirA*-P2A-TCF7L1 and BirA*-TCF7L1 expression in inducible and endogenous BioID systems. (A) Western blot analyses of WT mESCs maintained for up to 48h in 5% or 15% serum, as indicated. Lysates were probed with antibodies against TCF7L1 and β -Tubulin-I, as indicated. (B) Western blots obtained with lysates from BirA*-P2A-TCF7L1 RT, BirA*-TCF7L1 RT and WT cells maintained in 5% serum for 24h and subsequently treated with 5 μ M CHIR and/or 1 μ g/mL DOX for 24h. Lysates were probed with antibodies against FLAG, TCF7L1, and β -Tubulin-I, as indicated. (C) Western blots assessing lysates from BirA*-P2A-TCF7L1, BirA*-TCF7L1 and WT cells maintained in 5% serum for 24hr and then treated with 5 μ M CHIR, for 24h. Lysates were probed with antibodies against FLAG, TCF7L1, and β -Tubulin-I, as indicated. (D) Western blots obtained with lysates from WT, BirA*-P2A-TCF7L1, BirA*-P2A-TCF7L1 RT, BirA*-TCF7L1, and BirA*-TCF7L1 RT cells maintained in 5% serum for 24hr and then treated with 5 μ M CHIR and/or 1 μ g/mL DOX, for 24h. Lysates were probed with antibodies against FLAG, TCF7L1, and β -Tubulin-I, as indicated.

To generate the endogenous TCF7L1 BioID system, we used TALEN-facilitated homologous recombination to introduce a single copy of 3xFLAG-BirA*-P2A- and 3xFLAG-BirA*-tagged TCF7L1 at the endogenous *TCF7L1* locus. We will refer to the TCF7L1 endogenous lines as BirA*-P2A-TCF7L1 or BirA*-TCF7L1.

Expression of BirA*-P2A-TCF7L1 or BirA*-TCF7L1 in targeted clones was confirmed by western blotting (Figure 1C, S1B). We did not observe appreciable changes in total TCF7L1 protein levels in either BirA*-P2A or BirA*-TCF7L1 mESC lines. A reduction in TCF7L1 was observed in the presence of CHIR (Figure 1C). Again, we observed a minimal amount of uncleaved BirA*-P2A-TCF7L1 in BirA*-P2A controls. As observed in the dox-inducible system, BirA* levels in control cell lines were reduced in the presence of CHIR in the endogenous system.

Expression levels of BirA* fusion proteins in the two BioID systems were compared by western blotting (Figure 1D). The inducible system demonstrated a significant increase in both BirA*-P2A-TCF7L1 and BirA*-TCF7L1 protein levels compared to the endogenous system (Figure 1D).

Inducible and endogenous TCF7L1 BioID systems demonstrate biotinylation of proteins *in vivo*

We observed heterogeneous expression and nuclear localization of BirA* in BirA*-P2A-TCF7L1 RT and BirA*-TCF7L1 RT mESC lines when anti-FLAG immunofluorescent staining was visualized (Figure 2A). However, BirA*-P2A-TCF7L1 RT cells, in addition to nuclear fluorescence, displayed diffuse cytosolic signal. Although treatment with CHIR caused a reduction in total TCF7L1 protein (Figure 1B), there were many individual cells that retained elevated levels of TCF7L1 (Figure 2A).

We used fluorescently conjugated streptavidin to detect levels of biotinylation in WT, BirA*-P2A-TCF7L RT and BirA*-TCF7L1 RT mESC lines induced with doxycycline in the

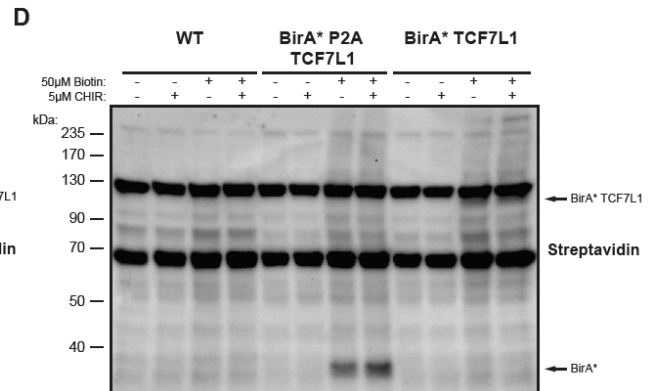
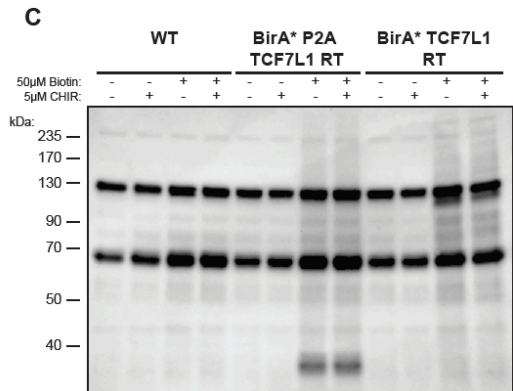
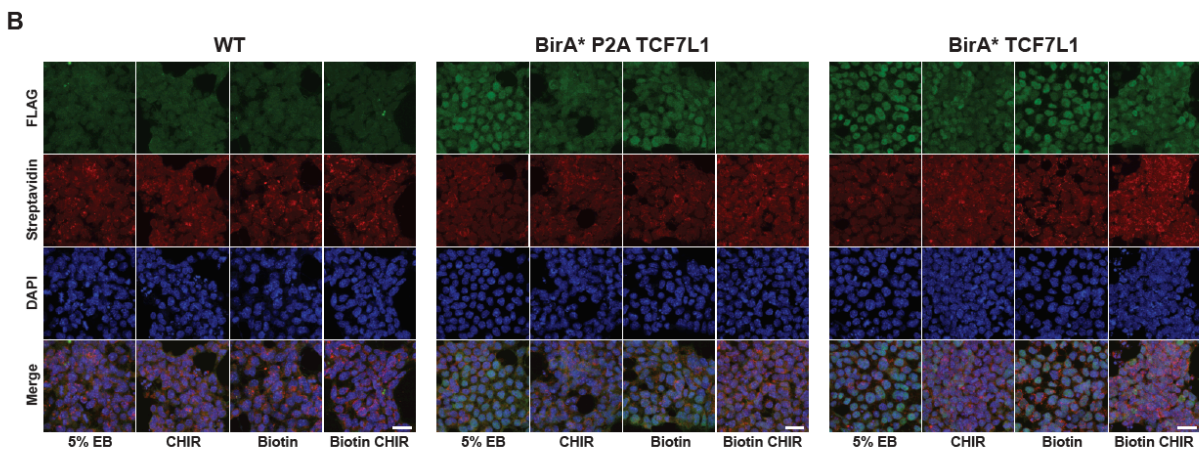
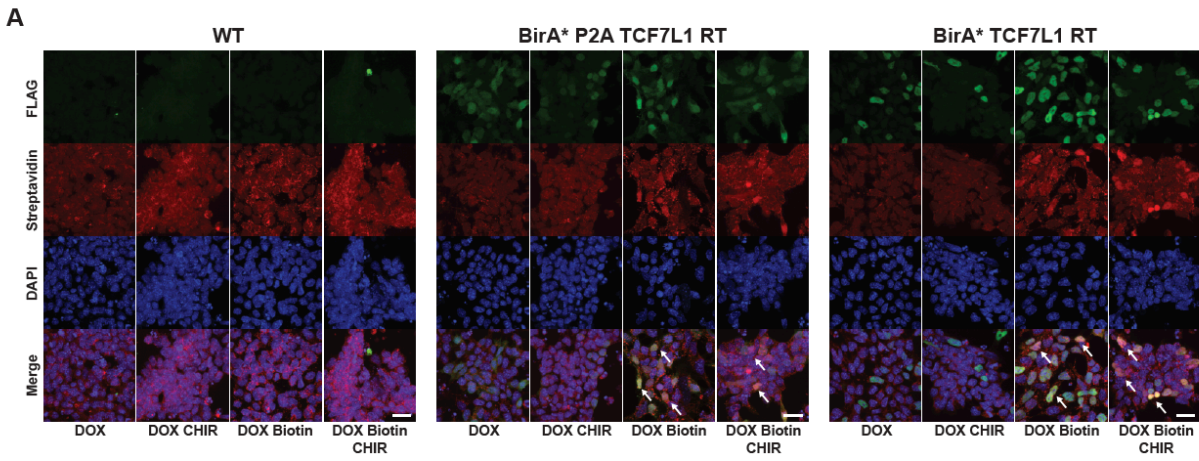


Figure 2. Inducible and endogenous TCF7L1 BioID systems demonstrate biotinylation of proteins in vivo. (A) Immunofluorescence images of BirA*-P2A-TCF7L1 RT, BirA*-TCF7L1 RT and WT mESCs maintained in 5% serum for 24h followed by supplementation with combinations of 5µM CHIR, 1µg/mL doxycycline, and 50µM biotin, for 24h. Staining was performed with anti-FLAG (green), fluorophore-conjugated streptavidin (red) and DAPI. Scale bar, 20µm. White arrowheads mark cells with elevated levels of FLAG-tagged BirA* or FLAG-tagged BirA*-TCF7L1 as well as high levels of detectable biotinylation. (B) Immunofluorescence images of BirA*-P2A-TCF7L1, BirA*-TCF7L1 and WT cells maintained in 5% serum for 24h, and then treated with 5µM CHIR and/or 50µM biotin, for 24h. Staining was performed with anti-FLAG (green), fluorophore-conjugated streptavidin (red) and DAPI. Scale bar, 20µm. (C) Western blot analysis of biotinylated proteins in lysates of BirA*-P2A-TCF7L1 RT, BirA*-TCF7L1 RT or WT cells maintained in 5% serum for 24h and then treated with 5µM CHIR and/or 50µM biotin, in the presence of 1µg/mL doxycycline, for 24h. Lysates were probed with streptavidin-HRP. Arrows point to 3xFLAG-BirA* fusion proteins. (D) Western blot analysis of biotinylated proteins in a single clone of BirA*-P2A-TCF7L1, BirA*-TCF7L1 and WT cells maintained in 5% serum for 24h, followed by supplementation with 5µM CHIR or 50µM biotin, for 24h. Lysates were probed with streptavidin-HRP. Arrows point to 3xFLAG-BirA* fusion proteins.

absence or presence of biotin and/or CHIR (Figure 2A). Streptavidin staining revealed a considerable amount of background biotinylation in wildtype mESCs, even in the absence of biotin. Despite appreciable levels of background biotinylation, we observed elevated biotinylation in BirA*-P2A-TCF7L1 RT and BirA*-TCF7L1 RT mESCs with the highest levels of detectable BirA* (Fig 2A).

We used the same immunofluorescence approach to examine the biotinylation activity in endogenous BirA* P2A-TCF7L1 and BirA*-TCF7L1 mESC lines (Figure 2B). BirA* expression as assessed by FLAG immunofluorescence, was lower and more homogeneous in the endogenous system when compared to the inducible system. As in the inducible system, BirA* P2A-TCF7L1 and BirA*-TCF7L1 localized to the nucleus, with the P2A controls also demonstrating diffuse cytosolic staining. Treating with CHIR led to an overall reduction in TCF7L1, however, again we observed individual cells where TCF7L1 levels remained elevated. In contrast to the inducible BioID system, we did not observe any visible increase in biotinylation in BirA*-P2A or BirA*-TCF7L1 cell lines, as assessed by streptavidin staining.

To detect biotinylation activity with higher sensitivity, we used chemiluminescent visualization of streptavidin-HRP. In the inducible BioID system we observed biotinylation of unidentified proteins as well as auto-biotinylation of BirA*-P2A-TCF7L1 RT and BirA*-TCF7L1 RT fusions in the absence and presence of CHIR (Figure 2C). Despite an undetectable increase in biotinylation as assessed by immunofluorescence, we observed auto-biotinylation of BirA*-P2A-TCF7L1 and BirA*-TCF7L1, as well as biotinylation of unidentified proteins, in the endogenous BioID system (Figure 2D).

BioID-based assembly of the TCF7L1 interactome

As we observed biotinylation of unidentified proteins in the inducible and endogenous BioID systems, we were confident in our ability to identify these proteins in a large-scale BioID

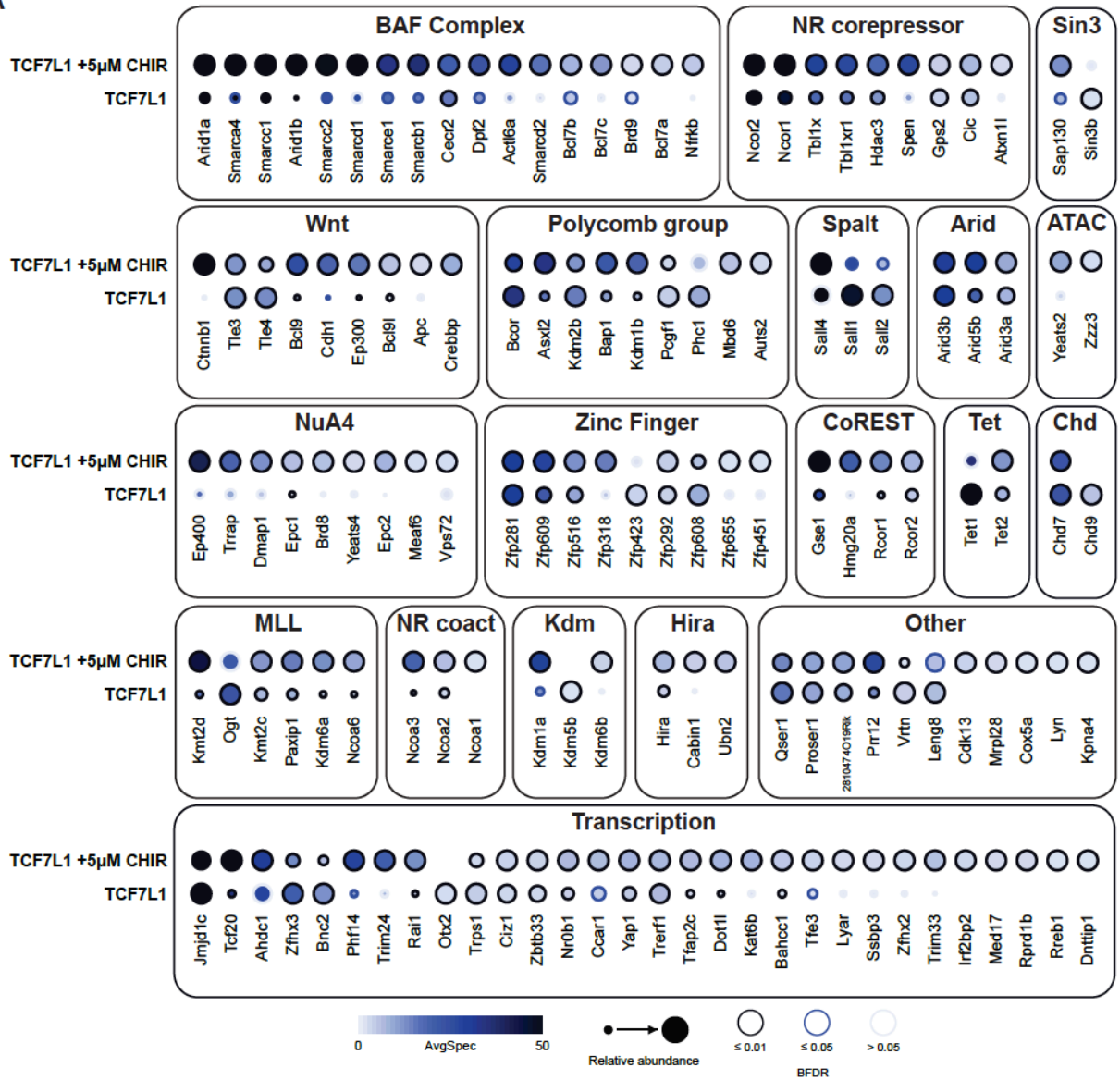
pull-down followed by mass-spectrometry. Cells were cultured in 5% serum for an initial 24 hours, followed by supplementation with biotin, with or without CHIR for 24 hours. For the inducible system, cells were also treated with dox at the time of biotin addition. BioID was performed on 3 biologically independent clones for each expression system including the BirA*-P2A-TCF7L1 controls. We isolated biotinylated proteins via streptavidin-biotin affinity purification, and subsequently analyzed them by using LC-MS/MS mass spectrometry. Data were searched using the ProHits suite, and SAINTexpress was used to calculate the probability of each potential proximal-protein relative to control samples.

Both BioID screens identified Wnt pathway components. Known TCF7L1-associated co-repressor proteins TLE3 and TLE4 were among the biotinylated proteins detected, in the absence and presence of CHIR (Figure 3A, 3B). In the endogenous BioID screen both proteins were of lower confidence in the absence of CHIR and more abundant, with a higher confidence, in its presence (Figure 3A, 3B). By contrast, in the inducible BioID screen, we observed an enrichment of both TLE3 and TLE4 in the absence of CHIR and lower levels in its presence (Figure 3A, 3B). Despite their acknowledged role in TCF/LEF-mediated control of transcription, TLE3 and TLE4 were not highly abundant in either BioID screen.

The most abundant Wnt signaling component detected in the screens was β -catenin, identified in the presence of CHIR in both systems (Figure 3A, 3B). The inducible BioID screen also detected additional Wnt-associated proteins, including BCL9, CDH1, P300, and BCL9L, which were more abundant in the presence of CHIR but also detected in its absence (Figure 3B). APC and CBP were enriched exclusively in the presence of CHIR (Figure 3B).

In both BioID approaches, CHIR treatment resulted in identification of a higher number of TCF7L1 proximal proteins with elevated peptide counts (Figure 3A, 3B). This is despite lowered TCF7L1 ‘bait’ protein levels (and detected peptides) in the presence of CHIR.

A



B

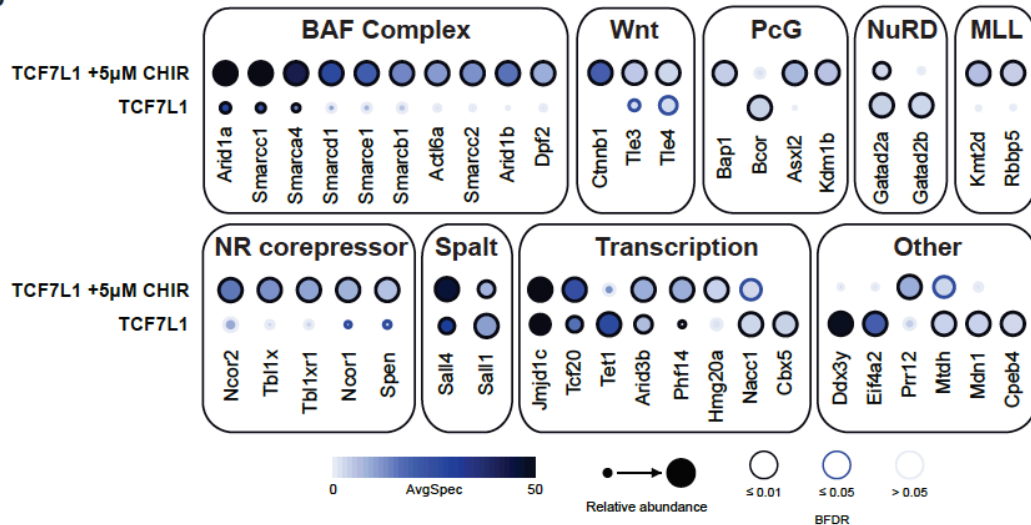


Figure 3. Proteins biotinylated by BirA*-TCF7L1 in inducible and endogenous BioID systems in the presence and absence of CHIR. (A) Dot plot of TCF7L1-proximal proteins identified by using the inducible BioID system in mESCs cultured in 5% serum for 24h and then treated with 50 μ M biotin, 1 μ g/mL DOX and 5 μ M CHIR for 24h. (B) Dot plot of TCF7L1-proximal proteins identified by using the endogenous BioID system in cultured in 5% serum for 24h and then treated with 50 μ M biotin and 5 μ M CHIR for 24h. In both systems, all biotinylated proteins identified demonstrated a BFDR \leq 0.05 and a SAINT score $>$ 0.8 in at least one of the 2 conditions. Spectral counts were capped at 50.

In addition to Wnt-associated proteins, we identified many complexes involved in the regulation of transcription, including the BAF chromatin remodeling complex, which was the most abundant complex identified in both BioID screens (Figure 3A, 3B). BAF components ARID1A, SMARCA4, and SMARCC1, were detected in both BioID screens, with and without CHIR treatment but were enriched in the CHIR condition (Figure 3A, 3B).

Another multi-subunit complex we observed in both BioID screens was the nuclear receptor corepressor complex (Figure 3A, 3B). NCOR1, NCOR2, TBL1X, TBL1XR1, and SPEN were enriched in the presence of CHIR (Figure 3A, 3B). In the absence of CHIR, NCOR1 was detected in both BioID screens albeit at much lower levels (Figure 3A, 3B). We also identified members and putative members of the polycomb group proteins, such as BRCA associated protein-1 (BAP1), BCL-6 Corepressor (BCOR), ASXL Transcriptional Regulator 2 (ASXL2) and Lysine demethylase 1B (KDM1B); as well as components of the mixed lineage leukemia (MLL) complex in both BioID screens (Figure 3A, 3B).

Along with complexes involved in transcriptional regulation we also identified numerous transcriptional regulators, including JMJD1C, an H3K9me2 demethylase, which was the most abundant hit observed in both screens +/- CHIR (Figure 3A, 3B). Four other abundant transcriptional regulators identified in both BioID screens were, two Spalt transcription factors SALL4 and SALL1; TCF20, a transcriptional coactivator; and ARID3B, a context-dependent transcriptional activator or repressor (Figure 3A, 3B).

Inducible and endogenous BioID screens detect similar, but distinct, TCF7L1 interactomes

Although our main objective was identifying TCF7L1 proximal and potentially interacting proteins, we also wanted to compare single-copy endogenous BioID with commonly used inducible overexpression of single-copy BioID transgenes. Both approaches were able to identify similar proximal proteins when considering the most abundant statistically significant top hits. Of

the 43 proteins identified in the endogenous screen with and without CHIR, only 10 were unique to the endogenous BioID screen, indicating a large overlap in hits detected by the two systems.

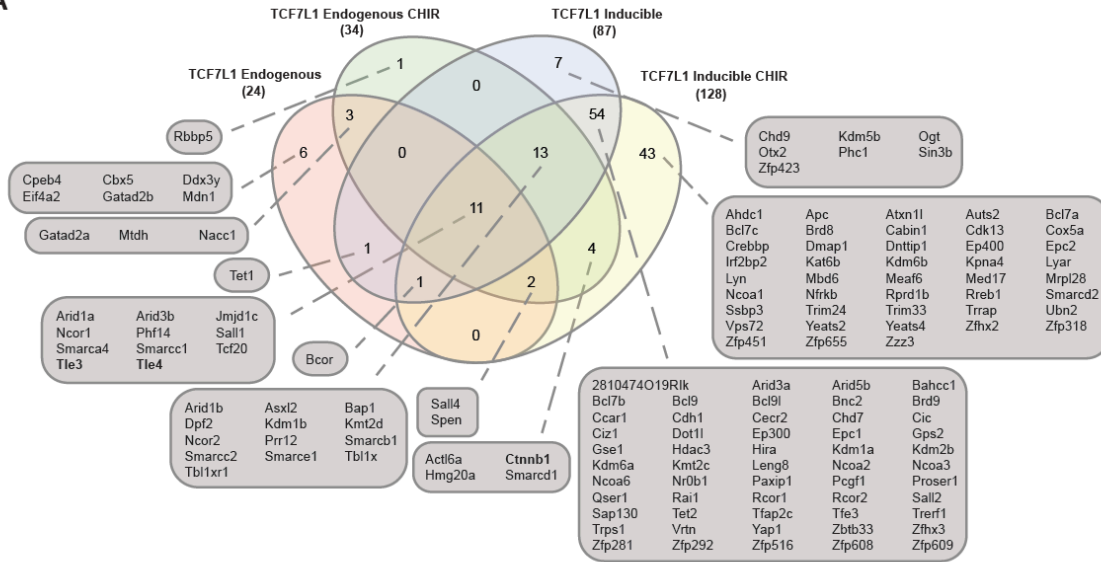
The inducible BioID screen was able to identify more low-abundance hits (Figure 3A, 4A). Specifically, in the absence of CHIR, the inducible screen identified 7 unique proteins, of which only OGT, an O-GlcNAc transferase, was of moderate abundance (Figure 4A, 4B). Similarly, in the presence of CHIR, the inducible screen identified 43 unique proteins, which included AHDC1, EP400, SMARCD2, TRIM24, and TRRAP (Figure 4A, 4B).

In contrast to the inducible BioID screen, the endogenous BioID screen produced a more tractable list of candidate TCF7L1 proximal proteins (Figure 4A, 4B). In the absence of CHIR, the endogenous screen identified 6 unique proteins, all of low abundance: CPEB4, CBX5, DDX3Y, EIF4A2, GATAD2B, and MDN1. In the presence of CHIR, the endogenous screen identified 1 unique protein, RBBP5 (Figure 4A, 4B).

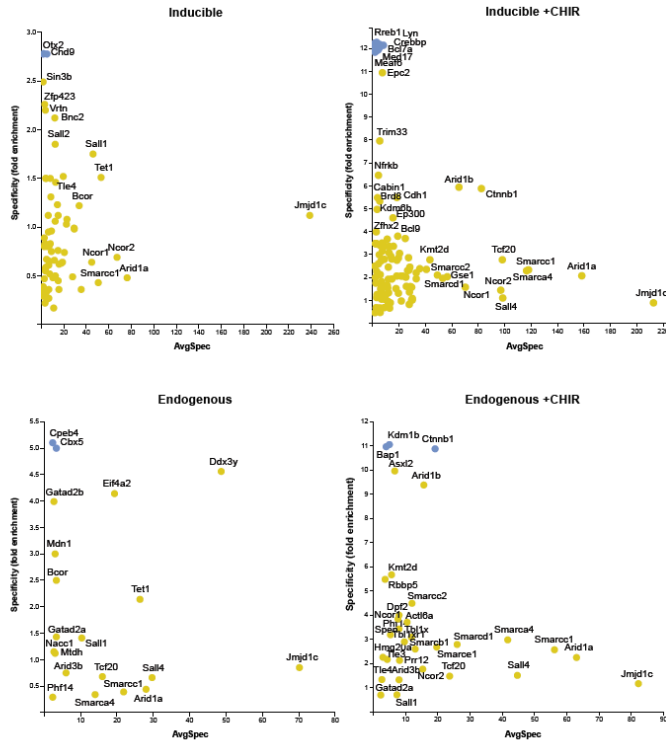
Although we observed unique proteins in both screens, with or without CHIR, the majority were of low abundance. Focusing on abundant proteins in the absence of CHIR, the only protein observed in both screens was TET1, a methylcytosine dioxygenase involved in DNA demethylation (Figure 4A, 4B). Conversely, with CHIR treatment we detected β -catenin; two components of the BAF complex, ACTL6A and SMARCD1; and a CoREST subunit, HMG20A; in both screens (Figure 4A, 4B).

Eleven proteins were observed in all conditions in both BioID screens: 3 subunits of the BAF complex ARID1A, SMARCA4, and SMARCC1; TLE3 and TLE4; and ARID3B, JMJD1C, NCOR1, PHF14, SALL1, and TCF20 (Figure 4A, 4B). With the exception of the TLEs, the levels of most of these proteins were unchanged or enriched in the presence of CHIR (Figure 3A, 3B). SALL1 was observed at lower levels in both screens in the presence of CHIR (Figure 3A, 3B).

A



B



C

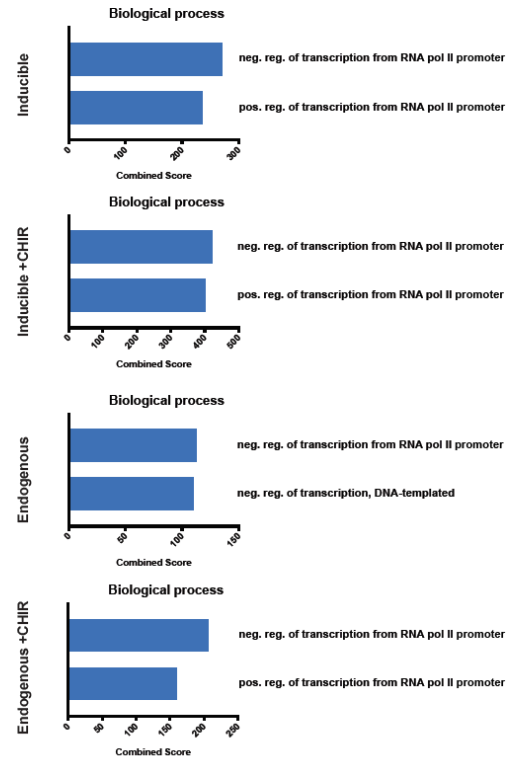


Figure 4. Inducible and endogenous BioID screens detect similar, but distinct, TCF7L1 interactomes. (A) Venn diagram showing overlapping biotinylated proteins identified in the endogenous and inducible BioID systems in the absence or presence of 5 μ M CHIR, as indicated. Previously known TCF7L1-interacting proteins are highlighted in bold. (B) Prey specificity graphs of TCF7L1-proximal proteins identified by using either the endogenous or inducible BioID systems in the absence or presence of 5 μ M CHIR, as indicated. Fold enrichment is calculated based on the spectral counts of each prey vs TCF7L1 in each condition, relative to the entire dataset for both conditions. A BDFR cutoff of 0.01 was used. Blue circles indicate preys with infinite specificity (C) Gene ontology of the TCF7L1 proximal proteins identified by using endogenous and inducible BioID systems in absence or presence of 5 μ M CHIR, as indicated.

Thirteen proteins were identified in all screens except the endogenous screen in the absence of CHIR: 5 BAF subunits (ARID1B, DPF2, SMARCB1, SMARCC2, and SMARCE1); 3 polycomb group proteins (ASXL2, BAP1 and KDM1B); 3 components of the nuclear receptor corepressor complex (NCOR2, TBL1X, and TBL1XR1); and KMT2D and PRR12 (Figure 4A, 4B). All of these proteins were detected by the inducible BioID screen without CHIR, albeit at much lower levels.

In total, we identified 146 potential TCF7L1 interacting proteins in the absence and presence of Wnt/ β -catenin pathway stimulation via CHIR. Gene ontology (GO) analysis revealed terms associated with negative regulation of transcription in both screens, with and without CHIR (Figure 4C). In the absence of CHIR, the inducible BioID screen contained terms associated with both positive and negative regulation of transcription, in contrast to the endogenous BioID screen, which only contained repressive factors (Figure 4C). GO terms in both BioID screens performed in the presence of CHIR were associated with positive and negative regulation of transcription (Figure 4C).

Validation of JMJD1C, SALL4, and SMARCA4 interactions with TCF7L1 in mESCs

The putative TCF7L1 interactors JMJD1C, SALL4, and SMARCA4 were abundantly identified in the endogenous and inducible BioID screens in the absence or presence of CHIR stimulation. We employed the proximity ligation assay (PLA) to gain additional evidence for the existence of interactions between these proteins and TCF7L1. With this technique, interacting proteins appear as fluorescent foci based on the close proximity of specific antibodies against each of the putative interacting proteins.

To facilitate our characterization of putative TCF7L1-interacting proteins, we generated 3xFLAG-TCF7L1 knock-in mESC lines in which the 3xFLAG epitope was added to the N-terminus of one allele of endogenous *TCF7L1*. FLAG- or JMJD1C- specific antibodies, when used

individually in PLA assays using 3xFLAG-TCF7L1 knock-in mESCs, resulted in background levels of fluorescence (Figure 5A). However, when these cells were probed with both FLAG and JMJD1C antibodies, a significant increase in predominantly nuclear punctae was observed (Figure 5A). Similarly, when 3xFLAG-TCF7L1 knock-in mESCs were probed with FLAG- or SMARCA4- specific antibodies individually, background levels of fluorescence with few punctae were detected, whereas numerous strong nuclear punctae were observed when both FLAG and SMARCA4 antibodies were used together (Figure 5B). We obtained similar PLA results when assaying for interactions between SALL4 and FLAG-tagged TCF7L1, although the number of punctae was fewer and some cells did not display any punctae (Figure 5C). The observation of fewer punctae is consistent with the BioID data (Figure 3), which suggest less interaction between TCF7L1 and SALL4 in the absence of CHIR, the condition in which the PLA experiments were conducted. Nonetheless, in co-immunoprecipitation experiments, we obtained convincing western blot data suggesting that SALL4 (isoform SALL4A, but not SALL4B) and FLAG-tagged TCF7L1 interact (Figure 5D). By contrast, we were unable to obtain co-immunoprecipitates between 3xFLAG-TCF7L1 and JMJD1C or SMARCA4.

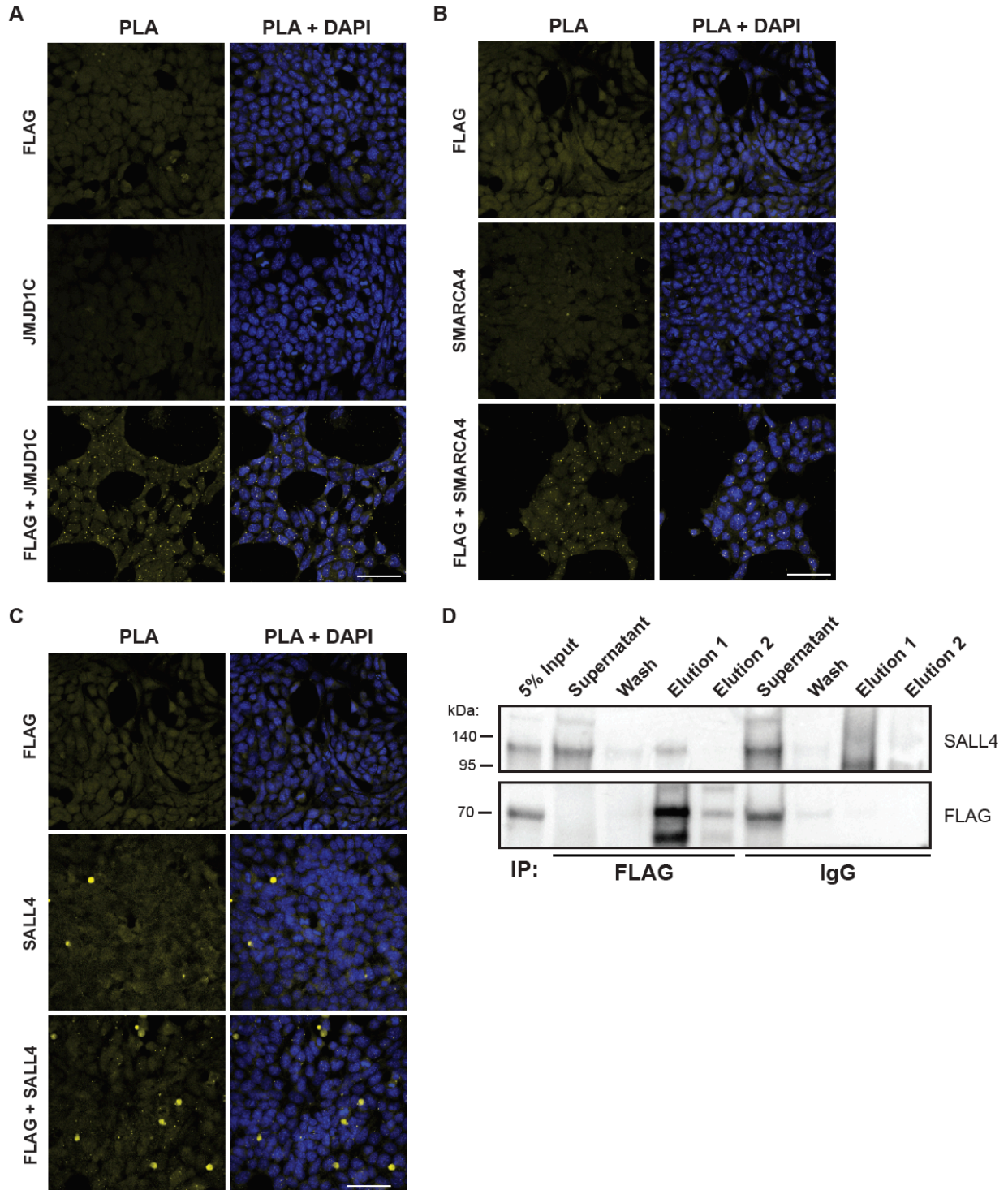


Figure 5. Validation of JMJD1C, SALL4, and SMARCA4 interactions with TCF7L1 in mESCs. (A) PLA results obtained by using 3xFLAG-TCF7L1 knock-in mESCs cultured in standard medium (serum and LIF) and anti-FLAG and anti-JMJD1C primary antibodies or single antibody controls. Nuclei were visualized with DAPI. Scale bar, 50µm. (B) PLA results obtained by using 3xFLAG-TCF7L1 knock-in mESCs cultured in standard medium (serum and LIF) and anti-FLAG and anti-SMARCA4 primary antibodies or single antibody controls. Nuclei were visualized with DAPI. Scale bar, 50µm. (C) PLA results obtained by using 3xFLAG-TCF7L1 knock-in mESCs cultured in standard medium (serum and LIF) and anti-FLAG and anti-SALL4 primary antibodies or single antibody controls. Nuclei were visualized with DAPI. Scale bar, 50µm. (D) Western blot data for coimmunoprecipitations conducted with anti-FLAG pull-downs and subsequent FLAG and SALL4 immunoblotting using lysates from mESCs with a 3xFLAG epitope knocked into the endogenous TCF7L1 locus.

DISCUSSION

Our data suggest that TCF7L1 interacts with numerous transcriptional regulators and chromatin remodeling complexes both in the presence and absence of CHIR-mediated Wnt pathway activation in mESCs. We used mESCs for our study for the following reasons: 1) mESCs express high levels of TCF7L1, 2) Wnt signals regulate TCF7L1 function and stability in mESCs through poorly understood mechanisms, and 3) Identification of putative TCF7L1 interactors by using conventional transgenic as well as endogenous single-copy BioID approaches provides biological insights into mechanisms of TCF7L1 function and highlights the consequences of even small variations in expression of BioID baits.

There was significant overlap in the biotinylated proteins identified by using both BioID methods, but the modest 2- to 3-fold increase in BirA*-TCF7L1 in the inducible system yielded approximately one hundred putative TCF7L1 proximal proteins that were undetected with the endogenous system.

TCF7L1 is potent in its ability to promote mESC differentiation, and its levels are strictly controlled (Pereira *et al.*, 2006; Shy *et al.*, 2013; Yi *et al.*, 2008, 2011). It is not surprising that even low-level overexpression yielded different BioID data from the endogenous system and that the expression of more “bait” identified more hits. As the endogenous BioID screen contains physiological levels of TCF7L1, we suggest that its hits are more likely to be biologically relevant. A smaller list of candidate TCF7L1 proximal proteins facilitates subsequent validation and helps build a meaningful interactome with less noise contributed by false-positive hits that are likely in an overexpression system.

Our introduction of BirA* at the N-terminus of endogenous TCF7L1 provides another distinct advantage in that all splice-variant isoforms of TCF7L1 present in mESCs will serve as

BioID baits, whereas conventional inducible overexpression systems are restricted to a single isoform.

β -catenin binding to the TCF/LEF factors was once thought to result in the displacement of TLEs, followed by recruitment of co-activators and Wnt target gene activation (Daniels and Weis, 2005; Hecht, 2000; Takemaru and Moon, 2000). This model has been challenged as it was demonstrated that β -catenin and TLE1 bind to independent regions and do not compete for binding to TCF7L1 (Chodaparambil *et al.*, 2014). Furthermore, through BioID and co-immunoprecipitation experiments it has been demonstrated that the co-activator BCL9-related β -catenin-binding protein, B9L, is able to form a complex with TCF7L2 together with TLE3 and TLE4, in both the presence and absence of Wnt stimulation in HEK293 cells (van Tienen *et al.*, 2017).

Our BioID screens suggest that TCF7L1 associates with TLE3 and TLE4 with and without CHIR, consistent with current working models. Notably, TLE3 and TLE4 were not highly abundant TCF7L1 vicinal proteins in either screen. Intriguingly, the changes observed in TLE3 and TLE4 binding in the absence or presence of CHIR were different between the two BioID systems. Unexpectedly, in the endogenous BioID screen both TLE3 and TLE4 were enriched in the presence of CHIR, despite a downregulation of TCF7L1 protein levels. This is consistent with a B9L BioID screen that identified an increase in TLE3 and TLE4 after stimulation with Wnt-conditioned media (van Tienen *et al.*, 2017). By contrast, in the inducible system, TLE3 and TLE4 were reduced with CHIR treatment. This discrepancy could be due to a change in the stoichiometry of Wnt enhanceosome complex components arising from supra-physiological TCF7L1 levels in the inducible cells.

A putative TCF7L1-associated protein that was highly abundant in both screens, specifically in the absence of CHIR, was TET1. TCF7L1 has also been shown to promote the

transition from naïve to primed pluripotency (Hoffman *et al.*, 2013). TET1 is of particular interest, as together with ZFP281, identified in the inducible BioID screen, it promotes the transition from the naïve to primed pluripotent states (Fidalgo *et al.*, 2016). Future studies will be needed to determine potential interplay between TET1 and TCF7L1 in the regulation of naïve to primed pluripotency.

The three proteins we chose for validation purposes include the H3K9 demethylase JMJD1C, the chromatin remodeling factor BRG1/SMARCA4, and the transcription factor SALL4. Recently, it has been reported that JMJD1C is required for the maintenance of embryonic stem cell self-renewal and is downregulated during differentiation from the pluripotent state (Xiao *et al.*, 2017). SALL4 is also essential for maintenance of self-renewing pluripotent stem cells and is lost upon ESC differentiation (Rao *et al.*, 2010; Yang *et al.*, 2008; Zhang *et al.*, 2006). Intriguingly, *SALL4* has been reported to be directly activated by TCF/LEF binding to the *SALL4* promoter (Böhm *et al.*, 2006). Our successful co-immunoprecipitation of SALL4 and TCF7L1 suggests that they are not only proximal to each other, they interact with each other, either directly or indirectly, in a complex. Our PLA data also suggest that the same may be true for JMJD1C and TCF7L1.

The most abundant complex identified in both BioID screens was the BAF complex. Components of the BAF (SWI/SNF) chromatin remodeling complex have been shown to exert differential effects on Wnt target genes. OSA a *Drosophila* ortholog of ARID1A, was found to be necessary for repression of Wingless (*Drosophila* ortholog of Wnt) target genes (Collins and Treisman, 2000). SMARCA4 has been shown to interact with β -catenin, promoting Wnt target gene activation in a TCF-dependent manner (Barker *et al.*, 2001b). Furthermore, recent work demonstrated that SMARCA4 was required for activation of Wnt target genes and deletion of SMARCA4 prevented Wnt-driven tumorigenesis in the small intestine of mice (Holik *et al.*, 2014). SMARCC1 and multiple BAF subunits, identified as negative regulators of *NANOG* in an RNAi

screen, were shown to promote heterochromatin and chromatin compaction at the *NANOG* locus (Schaniel *et al.*, 2009). Similarly, TCF7L1 has also been shown to bind to the *NANOG* locus, repressing its expression (Cole *et al.*, 2008; Marson *et al.*, 2008; Pereira *et al.*, 2006). Taken together, our BioID screen suggests that in the absence of a Wnt signal, TCF7L1 recruits BAF complex members at target genes to promote chromatin compaction and subsequent transcriptional repression.

In our BioID screens we observed an enrichment in TCF7L1 association with BAF components during CHIR stimulation, despite post-transcriptional downregulation of TCF7L1 (Moreira *et al.*, 2017; Shy *et al.*, 2013). This could be explained by recruitment of additional BAF complex subunits mediated by the TCF7L1- β -catenin interaction. In particular SMARCD1 was only observed in presence of CHIR in both TCF7L1 BioID screens. It is part of an ESC-specific BAF complex, which facilitates the activation of pluripotency associated genes (Ho *et al.*, 2009).

TCF7L1 repression of Wnt target genes can be alleviated through β -catenin-dependent TCF7L1 degradation and subsequent derepression of target genes (Morrison *et al.*, 2016; Shy *et al.*, 2013). However, the precise mechanism through which β -catenin promotes proteasomal degradation of TCF7L1 remains elusive. A complex identified in our BioID screen that offers potential insights into this mechanism is the nuclear receptor co-repressor complex (NCoR). Both TBL1X and TBL1XR1 have been shown to mediate transcriptional activation by recruiting the ubiquitin-conjugating/19S proteasome complex, which enables a switch from corepressor to coactivator usage (Ogawa *et al.*, 2004; Perissi *et al.*, 2004, 2008). TBL1X has also been linked to proteasomal degradation of β -catenin in response to genotoxic stress-mediated p53 activation, forming a SCF-like E3 complex consisting of SIAH1, SIP, SKP1, APC and TBL1X (Matsuzawa and Reed, 2001). Conversely, TBL1X and TBL1XR1 also interact with β -catenin in response to

Wnt signals, binding to target gene promoters to mediate transcriptional activation (Li and Wang, 2008).

Whether TBL1X and TBL1XR1 regulate TCF7L1 protein levels and subsequent Wnt target gene transcription remains to be elucidated. We propose that β -catenin binding to TCF7L1 could mediate the recruitment of TBL1X-TBL1XR1, leading to subsequent proteasomal degradation of TCF7L1 and/or its associated corepressors. Subsequently, target genes could either be derepressed or activated via recruitment of co-activators. In support of this, TBL1X-TBL1XR1 were only associated with TCF7L1 in the presence of CHIR in the endogenous BioID screen. Although TBL1X-TBL1XR1 associated with TCF7L1 without CHIR in the inducible screen, this could be a compensatory mechanism to reduce abnormally elevated levels of TCF7L1 protein.

When determining the effects of the TCF/LEFs on Wnt target genes, the emphasis has been on transcriptional regulation conferred by the corepressor TLEs and co-activators recruited by β -catenin, in the absence and presence of a Wnt signal, respectively. Our TCF7L1 BioID data strongly suggest that TCF7L1 associates more abundantly with numerous other transcriptional regulators and complexes. Furthermore, our BioID screens provide insight into TCF7L1 associated complexes capable of mediating post-transcriptional regulation of TCF7L1 levels, as well as β -catenin-mediated Derepression and/or activation of target genes. Future work interrogating the precise mechanisms of TCF7L1 regulation by TET1 and the BAF and NCoR complexes will be instrumental in determining how Wnt- β -catenin signaling mediates derepression/activation of TCF7L1, to regulate stem cell self-renewal and pluripotency.

EXPERIMENTAL PROCEDURES

Unless otherwise stated, chemicals were obtained from Sigma-Aldrich.

Proximity Ligation Assay

We used the Duolink® In Situ Red Starter kit (Sigma), with cells grown on ibidi μ -slide 8 well chamber slides (ibiTreat surface), according to manufacturer's instructions. Pro-Long Gold antifade (containing DAPI) solution (Life Technologies) was used to preserve processed cells (1-2 drops/well). Cells were imaged using a Zeiss LSM 700 laser-scanning confocal fluorescence microscope.

BioID

Cells were cultured for a total of 48h on five or ten 15 cm plates (for inducible or endogenous BirA* lines, respectively) in 5% FBS medium and were treated with 50 μ M Biotin during the final 24h. Cell pellets were lysed in 1 mL/plate ice-cold RIPA lysis buffer (50 mM Tris-HCl pH 7.5, 150 mM NaCl, 1% NP-40, 1 mM EDTA, 1 mM EGTA, 0.1% SDS, protease inhibitor cocktail (P8340) 1:500, and 0.5% Sodium deoxycholate, supplemented with 250U of benzonase) for 1h at 4°C. The lysates were sonicated at 4°C using three 30s bursts, with 1' pauses, at 30% amplitude. The lysates were then centrifuged at 4°C for 30' at 20k x g. Streptavidin sepharose beads (17-5113-01, GE) were washed 3x with 1 mL RIPA buffer and pelleted at 2000 x g for 2'. Biotinylated proteins were captured from cleared lysates by incubating 3h at 4°C, with 10 μ L of packed beads per 15 cm plate. The beads were pelleted at 2000 x g for 2' and transferred to 1.5 mL tubes in 1 mL RIPA buffer. 6 washes were performed with 1 mL 50 mM ammonium bicarbonate. Beads were then resuspended in 200 μ L ammonium bicarbonate and 1 μ g of trypsin (PRV5111, Promega) was added. The samples were incubated at 37°C overnight, followed by an additional 2-4h incubation with an additional 0.5 μ g trypsin. The beads were pelleted, and the

supernatant was transferred to a new tube. The beads were then rinsed twice with 150 μL ammonium bicarbonate and the wash fractions were pooled together with the supernatant. The samples were lyophilized in a speed-vac, resuspended in 8 μL formic acid, and 1/4 was used per mass spectrometric analysis.

Mass Spectrometry

All BioID samples and controls were analyzed by mass spectrometry with at least three biological replicates. Liquid chromatography was conducted using a home-made trap-column (5 cm x 200 μm inner diameter) and a home-made analytical column (50 cm x 50 μm inner diameter; Monitor 5 μm 100A C18 resin). A 2h reversed-phase gradient was run at 70 nL/min on a Thermo Fisher Ultimate 3000 RSLC Nano UPLC system coupled to a Thermo QExactive HF quadrupole-Orbitrap mass spectrometer. A parent ion scan was performed using a resolving power of 120 000, and up to the 10 most intense peaks were selected for MS/MS (minimum ion count of 1000 for activation) using higher energy collision induced dissociation (HCD) fragmentation. Dynamic exclusion was activated such that MS/MS of the same m/z (within a range of 10 ppm; exclusion list size = 500) detected twice within 5s were excluded from analysis for 30s.

Mass Spectrometric Data Analysis

Mass spectrometric data from the Thermo QExactive HF quadrupole-Orbitrap were stored, searched and analyzed using the ProHits laboratory information management system (Liu *et al.*, 2010). Raw files were searched using Mascot and Comet, against the MouseV53cRapRevTagA database, which includes common contaminants (Eng *et al.*, 2013; Perkins *et al.*, 1999). The database parameters were set to search for tryptic cleavages, allowing up to 1 missed cleavage site per peptide, with a parent MS tolerance of 12 ppm for precursors with charges of 2+ to 4+ and a fragment ion tolerance of ± 0.15 amu. Variable modifications were selected for deamidated

asparagine/glutamine and oxidized methionine. The results from each search were statistically validated through the Trans-Proteomic Pipeline, using iProphet (Deutsch *et al.*, 2010; Shteynberg *et al.*, 2011). SAINTexpress was used to calculate the probability of each potential proximal–protein from background contaminants using default parameters (Choi *et al.*, 2010). Controls were compressed to 2 samples. 2 unique peptides and a minimum iProphet probability of 0.95 were required for protein identification. SAINTexpress data were analyzed and visualized using ProHits-Viz (Knight *et al.*, 2017).

Author Contributions

BWD and SM designed the experiments, conducted experiments and wrote the paper. CS, VG, EP, VF and DN conducted experiments. A-CG., BL, BR, and CJW provided BioID bioinformatic analyses. YL, SX and RW performed mass spectrometric data acquisition.

Acknowledgments

Funding for this study and required infrastructure was provided by the Canadian Institutes of Health Research to BWD (MOP133610), the Canada Research Chairs Program (BWD), the Ontario Ministry of Research and Innovation (BWD), the Canada Foundation for Innovation (BWD), and the OCRiT Project: Ontario Ministry of Economic Development and Innovation (BWD). Bioinformatics analysis was performed at the Network Biology Collaborative Centre at the Lunenfeld-Tanenbaum Research Institute, a facility supported by Canada Foundation for Innovation funding, by the Ontarian Government and by Genome Canada and Ontario Genomics (OGI-097, OGI-139).

References

- Atlasi, Y., Noori, R., Gaspar, C., Franken, P., Sacchetti, A., Rafati, H., Mahmoudi, T., Decraene, C., Calin, G.A., Merrill, B.J., *et al.* (2013). Wnt Signaling Regulates the Lineage Differentiation Potential of Mouse Embryonic Stem Cells through Tcf3 Down-Regulation. *PLoS Genet.* *9*, e1003424.
- Barker, N., Hurlstone, a, Musisi, H., Miles, a, Bienz, M., and Clevers, H. (2001a). The chromatin remodelling factor Brg-1 interacts with beta-catenin to promote target gene activation. *EMBO J.* *20*, 4935–4943.
- Barker, N., Hurlstone, A., Musisi, H., Miles, A., Bienz, M., and Clevers, H. (2001b). The chromatin remodelling factor Brg-1 interacts with beta-catenin to promote target gene activation. *EMBO J.* *20*, 4935–4943.
- Böhm, J., Sustmann, C., Wilhelm, C., and Kohlhase, J. (2006). SALL4 is directly activated by TCF/LEF in the canonical Wnt signaling pathway. *Biochem. Biophys. Res. Commun.* *348*, 898–907.
- Brannon, M., Brown, J.D., Bates, R., Kimelman, D., and Moon, R.T. (1999). XCTBP is a XTcf-3 co-repressor with roles throughout Xenopus development. *Development* *126*, 3159–3170.
- Cadigan, K.M., and Waterman, M.L. (2012). TCF/LEFs and Wnt Signaling in the Nucleus. *Cold Spring Harb Perspect Biol* *4*, a007906–a007906.
- Chodaparambil, J. V, Pate, K.T., Hepler, M.R.D., Tsai, B.P., Muthurajan, U.M., Luger, K., Waterman, M.L., and Weis, W.I. (2014). Molecular functions of the TLE tetramerization domain in Wnt target gene repression. *EMBO J.* *33*, 719–731.
- Choi, H., Larsen, B., Lin, Z.-Y., Breikreutz, A., Mellacheruvu, D., Fermin, D., Qin, Z.S., Tyers, M., Gingras, A.-C., and Nesvizhskii, A.I. (2010). SAINT: probabilistic scoring of affinity purification–mass spectrometry data. *Nat. Methods* *8*, 70–73.
- Clevers, H., and Nusse, R. (2012). Wnt/ β -Catenin Signaling and Disease. *Cell* *149*, 1192–1205.
- Cole, M.F., Johnstone, S.E., Newman, J.J., Kagey, M.H., and Young, R.A. (2008). Tcf3 is an integral component of the core regulatory circuitry of embryonic stem cells. *Genes & Dev.* *22*, 746–755.
- Collins, R.T., and Treisman, J.E. (2000). Osa-containing Brahma chromatin remodeling complexes are required for the repression of wingless target genes. *Genes Dev.* *14*, 3140–3152.
- Daniels, D.L., and Weis, W.I. (2005). Beta-catenin directly displaces Groucho/TLE repressors from Tcf/Lef in Wnt-mediated transcription activation. *Nat. Publ. Gr.* *12*, 364–371.
- Deutsch, E.W., Mendoza, L., Shteynberg, D., Farrah, T., Lam, H., Tasman, N., Sun, Z., Nilsson, E., Pratt, B., Prazen, B., *et al.* (2010). A guided tour of the Trans-Proteomic Pipeline. *Proteomics* *10*, 1150–1159.

- Eng, J.K., Jahan, T.A., and Hoopmann, M.R. (2013). Comet: An open-source MS/MS sequence database search tool. *Proteomics* *13*, 22–24.
- Eshelman, M.A., Shah, M., Raup-Konsavage, W.M., Rennoll, S.A., and Yochum, G.S. (2017). TCF7L1 recruits CtBP and HDAC1 to repress DICKKOPF4 gene expression in human colorectal cancer cells. *Biochem. Biophys. Res. Commun.* *487*, 716–722.
- Fidalgo, M., Huang, X., Guallar, D., Sanchez-Priego, C., Valdes, V.J., Saunders, A., Ding, J., Wu, W.S., Clavel, C., and Wang, J. (2016). Zfp281 Coordinates Opposing Functions of Tet1 and Tet2 in Pluripotent States. *Cell Stem Cell* *19*, 355–369.
- Hecht, a (2000). The p300/CBP acetyltransferases function as transcriptional coactivators of beta-catenin in vertebrates. *EMBO J.* *19*, 1839–1850.
- Ho, L., Ronan, J.L., Wu, J., Staahl, B.T., Chen, L., Kuo, A., Lessard, J., Nesvizhskii, A.I., Ranish, J., and Crabtree, G.R. (2009). An embryonic stem cell chromatin remodeling complex, esBAF, is essential for embryonic stem cell self-renewal and pluripotency. *Proc. Natl. Acad. Sci.* *106*, 5181–5186.
- Hoffman, J. a, Wu, C.-I., and Merrill, B.J. (2013). Tcf7l1 prepares epiblast cells in the gastrulating mouse embryo for lineage specification. *Development* *140*, 1665–1675.
- Holik, A.Z., Young, M., Krzystyniak, J., Williams, G.T., Metzger, D., Shorning, B.Y., and Clarke, A.R. (2014). Brg1 Loss Attenuates Aberrant Wnt-Signalling and Prevents Wnt-Dependent Tumourigenesis in the Murine Small Intestine. *PLoS Genet.* *10*.
- Kim, D.I., KC, B., Zhu, W., Motamedchaboki, K., Doye, V., and Roux, K.J. (2014). Probing nuclear pore complex architecture with proximity-dependent biotinylation. *Proc. Natl. Acad. Sci.* *111*, E2453–E2461.
- Knight, J.D.R., Choi, H., Gupta, G.D., Pelletier, L., Raught, B., Nesvizhskii, A.I., and Gingras, A.C. (2017). ProHits-viz: A suite of web tools for visualizing interaction proteomics data. *Nat. Methods* *14*, 645–646.
- Kramps, T., Peter, O., Brunner, E., Nellen, D., Froesch, B., Chatterjee, S., Murone, M., Züllig, S., and Basler, K. (2002). Wnt/Wingless signaling requires BCL9/legless-mediated recruitment of pygopus to the nuclear β -catenin-TCF complex. *Cell* *109*, 47–60.
- Li, J., and Wang, C.Y. (2008). TBL1-TBLR1 and β -catenin recruit each other to Wnt target-gene promoter for transcription activation and oncogenesis. *Nat. Cell Biol.* *10*, 160–169.
- Lien, W.-H., Polak, L., Lin, M., Lay, K., Zheng, D., and Fuchs, E. (2014). In vivo transcriptional governance of hair follicle stem cells by canonical Wnt regulators. *Nat. Cell Biol.* *16*, 179–190.
- Liu, G., Zhang, J., Larsen, B., Stark, C., Breitkreutz, A., Lin, Z.-Y., Breitkreutz, B.-J., Ding, Y., Colwill, K., Pasculescu, A., *et al.* (2010). ProHits: integrated software for mass spectrometry-based interaction proteomics. *Nat. Biotechnol.* *28*, 1015–1017.
- Marson, A., Levine, S.S., Cole, M.F., Frampton, G.M., Brambrink, T., Johnstone, S., Guenther, M.G., Johnston, W.K., Wernig, M., Newman, J., *et al.* (2008). Connecting microRNA Genes to

the Core Transcriptional Regulatory Circuitry of Embryonic Stem Cells. *Cell* 134, 521–533.

Matsuzawa, S. ichi, and Reed, J.C. (2001). Siah-1, SIP, and Ebi collaborate in a novel pathway for β -catenin degradation linked to p53 responses. *Mol. Cell* 7, 915–926.

Moreira, S., Polena, E., Gordon, V., Abdulla, S., Mahendram, S., Cao, J., Blais, A., Wood, G.A.G.A., Dvorkin-Gheva, A., and Doble, B.W.B.W.B.W. (2017). A Single TCF Transcription Factor, Regardless of Its Activation Capacity, Is Sufficient for Effective Trilineage Differentiation of ESCs. *Cell Rep.* 20, 2424–2438.

Morrison, G., Scognamiglio, R., Trumpp, A., and Smith, A. (2016). Convergence of cMyc and -catenin on Tcf7l1 enables endoderm specification. *EMBO J.* 35, 356–368.

Nusse, R., and Clevers, H. (2017). Wnt/ β -Catenin Signaling, Disease, and Emerging Therapeutic Modalities. *Cell* 169, 985–999.

Ogawa, S., Lozach, J., Jepsen, K., Sawka-Verhelle, D., Perissi, V., Sasik, R., Rose, D.W., Johnson, R.S., Rosenfeld, M.G., and Glass, C.K. (2004). A nuclear receptor corepressor transcriptional checkpoint controlling activator protein 1-dependent gene networks required for macrophage activation. *Proc. Natl. Acad. Sci.* 101, 14461–14466.

Pereira, L., Yi, F., and Merrill, B.J. (2006). Repression of Nanog gene transcription by Tcf3 limits embryonic stem cell self-renewal. *Mol. Cell. Biol.* 26, 7479–7491.

Perissi, V., Aggarwal, A., Glass, C.K., Rose, D.W., and Rosenfeld, M.G. (2004). A Corepressor/Coactivator Exchange Complex Required for Transcriptional Activation by Nuclear Receptors and Other Regulated Transcription Factors. *Cell* 116, 511–526.

Perissi, V., Scafoglio, C., Zhang, J., Ohgi, K.A., Rose, D.W., Glass, C.K., and Rosenfeld, M.G. (2008). TBL1 and TBLR1 Phosphorylation on Regulated Gene Promoters Overcomes Dual CtBP and NCoR/SMRT Transcriptional Repression Checkpoints. *Mol. Cell* 29, 755–766.

Perkins, D.N., Pappin, D.J.C., Creasy, D.M., and Cottrell, J.S. (1999). Probability-based protein identification by searching sequence databases using mass spectrometry data. In *Electrophoresis*, pp. 3551–3567.

Rao, S., Zhen, S., Roumiantsev, S., McDonald, L.T., Yuan, G.-C.C., Orkin, S.H., Shao, Z., Roumiantsev, S., McDonald, L.T., Yuan, G.-C.C., *et al.* (2010). Differential Roles of Sall4 Isoforms in Embryonic Stem Cell Pluripotency. *Mol. Cell. Biol.* 30, 5364–5380.

Roux, K.J., Kim, D.I., Raida, M., and Burke, B. (2012). A promiscuous biotin ligase fusion protein identifies proximal and interacting proteins in mammalian cells. *J. Cell Biol.* 196, 801–810.

Schaniel, C., Ang, Y.-S., Ratnakumar, K., Cormier, C., James, T., Bernstein, E., Lemischka, I.R., and Paddison, P.J. (2009). Smarcc1/Baf155 Couples Self-Renewal Gene Repression with Changes in Chromatin Structure in Mouse Embryonic Stem Cells. *Stem Cells* 27, N/A-N/A.

Shteynberg, D., Deutsch, E.W., Lam, H., Eng, J.K., Sun, Z., Tasman, N., Mendoza, L., Moritz, R.L., Aebersold, R., and Nesvizhskii, A.I. (2011). iProphet: Multi-level Integrative Analysis of Shotgun Proteomic Data Improves Peptide and Protein Identification Rates and Error Estimates.

Mol. Cell. Proteomics *10*, M111.007690.

Shy, B.R., Wu, C.-I.I., Khramtsova, G.F., Zhang, J.Y., Olopade, O.I., Goss, K.H., and Merrill, B.J. (2013). Regulation of Tcf7l1 DNA Binding and Protein Stability as Principal Mechanisms of Wnt/ β -Catenin Signaling. *CellReports* *4*, 1–9.

Takemaru, K.I., and Moon, R.T. (2000). The transcriptional coactivator CBP interacts with β -catenin to activate gene expression. *J. Cell Biol.* *149*, 249–254.

Tam, W.-L., Lim, C.Y., Han, J., Zhang, J., Ang, Y.-S., Ng, H.-H., Yang, H., and Lim, B. (2008). Tcf3 Regulates Embryonic Stem Cell Pluripotency and Self-Renewal by the Transcriptional Control of Multiple Lineage Pathways. *Stem Cells* *26*, 2019–2031.

Thompson, B., Townsley, F., Rosin-Arbesfeld, R., Musisi, H., and Bienz, M. (2002). A new nuclear component of the Wnt signalling pathway. *Nat. Cell Biol.* *4*, 367–373.

van Tienen, L.M., Mieszczanek, J., Fiedler, M., Rutherford, T.J., and Bienz, M. (2017). Constitutive scaffolding of multiple Wnt enhanceosome components by legless/BCL9. *Elife* *6*, 1–23.

Wallmen, B., Schrempp, M., and Hecht, A. (2012). Intrinsic properties of Tcf1 and Tcf4 splice variants determine cell-type-specific Wnt/ β -catenin target gene expression. *Nucleic Acids Res.* *40*, 9455–9469.

Wray, J., Kalkan, T., Gomez-Lopez, S., Eckardt, D., Cook, A., Kemler, R., and Smith, A. (2011). Inhibition of glycogen synthase kinase-3 alleviates Tcf3 repression of the pluripotency network and increases embryonic stem cell resistance to differentiation. *Nat Cell Biol* *13*, 838–845.

Wu, C.-I., Hoffman, J. a, Shy, B.R., Ford, E.M., Fuchs, E., Nguyen, H., and Merrill, B.J. (2012). Function of Wnt/ β -catenin in counteracting Tcf3 repression through the Tcf3- β -catenin interaction. *Development* *139*, 2118–2129.

Xiao, F., Liao, B., Hu, J., Li, S., Zhao, H., Sun, M., Gu, J., and Jin, Y. (2017). JMJD1C Ensures Mouse Embryonic Stem Cell Self-Renewal and Somatic Cell Reprogramming through Controlling MicroRNA Expression. *Stem Cell Reports* *9*, 927–942.

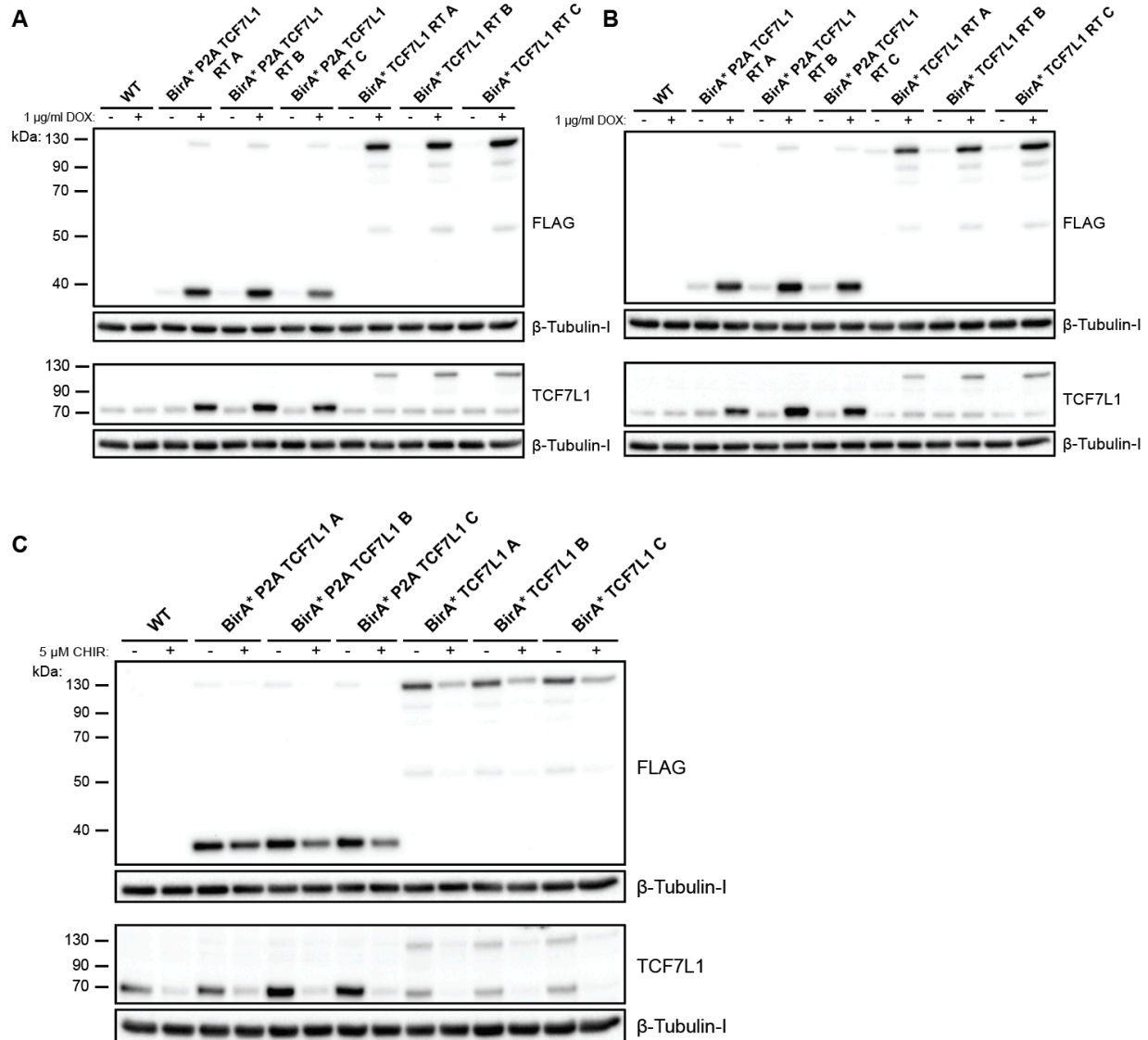
Yang, J., Chai, L., Fowles, T.C., Alipio, Z., Xu, D., Fink, L.M., Ward, D.C., and Ma, Y. (2008). Genome-wide analysis reveals Sall4 to be a major regulator of pluripotency in murine-embryonic stem cells. *Proc. Natl. Acad. Sci. U. S. A.* *105*, 19756–19761.

Yi, F., Pereira, L., and Merrill, B.J. (2008). Tcf3 Functions as a Steady-State Limiter of Transcriptional Programs of Mouse Embryonic Stem Cell Self-Renewal. *Stem Cells* *26*, 1951–1960.

Yi, F., Pereira, L., Hoffman, J.A., Shy, B.R., Yuen, C.M., Liu, D.R., and Merrill, B.J. (2011). Opposing effects of Tcf3 and Tcf1 control Wnt stimulation of embryonic stem cell self-renewal. *Nat Cell Biol* *13*, 762–770.

Zhang, J.Q., Tam, W.L., Tong, G.Q., Wu, Q., Chan, H.Y., Soh, B.S., Lou, Y.F., Yang, J.C., Ma, Y.P., Chai, L., *et al.* (2006). Sall4 modulates embryonic stem cell pluripotency and early embryonic development by the transcriptional regulation of Pou5f1. *Nat. Cell Biol.* 8, 1114-U125.

Supplemental Information

**Figure S1, Related to Figure 1**

(A) Western blot analysis of WT, BirA*-P2A-TCF7L1 RT and BirA*-TCF7L1 RT independent clones maintained in 5% serum for 24hr, which was supplemented with or without 1µg/ml DOX for an additional 24h. Lysates were probed with antibodies against FLAG, TCF7L1, and β-Tubulin-I, as indicated. (B) Western blot analysis of WT, BirA*-P2A-TCF7L1 RT and BirA*-TCF7L1 RT independent clones maintained in 5% serum for, which was supplemented with 5µM CHIR ± 1µg/ml DOX for an additional 24h. Lysates were probed with antibodies against FLAG, TCF7L1, and β-Tubulin-I, as indicated. (C) Western blot analysis of WT, BirA*-P2A-TCF7L1 and BirA*-TCF7L1 independent clones maintained in 5% serum for 24h, which was supplemented with ± 5µM CHIR for an additional 24h. Lysates were probed with antibodies against FLAG, TCF7L1, and β-Tubulin-I, as indicated.

SUPPLEMENTAL EXPERIMENTAL PROCEDURES

Cell culture

Routine maintenance of mESCs in serum-containing medium has been previously described (Moreira *et al.*, 2017).

Immunofluorescence

For immunofluorescence staining, cells were washed 2x with PBS in between all steps. Cells on ibidi 8-well slides were fixed with cold 4% paraformaldehyde for 10 minutes at room temperature. Cells were subsequently permeabilized with 0.1% Triton X-100 for 5 minutes at room temperature. Samples were blocked with 10% goat serum/PBS for 1hr followed by incubation overnight at 4°C in primary antibody diluted in 3% goat serum/PBS. Samples were incubated in secondary (Alexa Fluor) antibodies diluted 1:1500 in antibody dilution buffer for 1 hour at room temperature. Cells were mounted with 1-2 drops of Pro-Long Gold antifade (containing DAPI) solution per well (Life Technologies, P36935). Cells were subsequently imaged by using a Zeiss LSM 700 laser-scanning confocal fluorescence microscope.

Western Blot Analysis

Western blotting procedures have been previously described (Moreira, *et al.*, 2017). Streptavidin-HRP blots were completed as follows: membranes were blocked for 30' in BSA blocking buffer (1.5% BSA, 0.15% Triton X-100 in PBS). Membranes were incubated overnight at 4°C in Pierce™ High Sensitivity streptavidin-HRP (21134, ThermoFisher Scientific), diluted 1:40,000 in BSA blocking buffer. Three 5' PBS washes were performed, followed by additional blocking for 5' in blocking buffer (10% goat serum, 1% Triton X-100 in PBS). Membranes were washed 3x in PBS for 5' and visualized with a Bio-Rad chemidoc system.

Co-Immunoprecipitation Assays

Between 5-10 million mESCs were cultured on 100mm gelatin-coated dishes in standard mESC medium prior to initiation of the assay. Cells were rinsed twice with PBS, and lysed with Buffer LB (14321B, ThermoFisher Scientific): 100 mM NaCl, 0.5% Triton™ X-100, 2 mM MgCl₂, 1 mM DTT, 1x Halt Protease and Phosphatase Inhibitor cocktail (78440, ThermoFisher Scientific) for 10 minutes on ice. Lysates were clarified at 15000 x g for 10'. The supernatant was transferred to a new pre-chilled tube and protein content was determined with the DC Protein Assay (Bio-Rad). Equivalent amounts of protein extract were used per IP within each co-immunoprecipitation experiment (approx. 500µg of protein per IP). Rabbit anti-SALL4 (ab29112, Abcam) was pre-conjugated (7.5 µg per IP) to 1.5mg of Protein-G Dynabeads™ M-270 Epoxy for 24 hours at 37°C according to the manufacturer's instructions (14321B, ThermoFisher Scientific). Cell lysates were added to the antibody-bead complex, and the mixture was incubated for 1 hour at 4°C in a 1.5 mL tube on a tube rotator. Immunoprecipitates were subsequently rinsed 3x using lysis buffer (including inhibitors) followed by a final wash with LWB buffer (14321B, ThermoFisher Scientific). Samples were eluted from the beads with EB buffer (14321B, ThermoFisher Scientific) via a 5-minute incubation at 25°C. Prior to western blot analysis, 3x NuPage™ LDS buffer (NP0007, ThermoFisher Scientific) with 5% TCEP Bond Breaker solution (77720, ThermoFisher Scientific) was added to the eluate without boiling.

Antibodies

The following primary antibodies were used for western blot and/or immunofluorescent staining: mouse anti-β-Tubulin-I (T7816, Sigma); mouse anti-FLAG M2 (F1804, Sigma); rabbit anti-TCF7L1 (ab86175, Abcam); rabbit anti-JMJD1C (SAB3500094, Sigma); rabbit anti-SMARCA4 (49360S, Cell Signaling Technology). Alexa Fluor-568 conjugated streptavidin (S11226, ThermoFisher Scientific). Fluorochrome-conjugated secondary antibodies were obtained from ThermoFisher Scientific and used at 1/1500 (Molecular Probes): goat anti-mouse Alexa Fluor 488.

Generation of 3xFLAG BirA* and BirA* P2A -TCF7L1 inducible mRosa26 knock-in mESC lines by using TALENs

The *mRosa26* targeting vector was purchased from Sigma (CTIM-1KT) and a neo-resistance cassette was introduced by using PCR and conventional cloning. A bidirectional, all-in-one doxycycline inducible construct, pTetOne, was purchased from TaKaRa (634301). The *Rosa26* TetOne (RT) targeting vector was assembled by subcloning the all-in-one doxycycline inducible portion of pTetOne into the *mRosa26* targeting vector using NEBuilder (E5520S). The TCF7L1 full length ORF was isolated from mESCs by using RT-PCR of isolated genomic DNA that was cloned into pDONR221 (12536017, ThermoFisher Scientific). TCF7L1 was subsequently subcloned into RT by using PCR and verified by Sanger sequencing. The *TCF7L1* RT targeting construct in combination with *mRosa26* TALENs ELD and

KKR (AddGene: <https://www.addgene.org/60025/> and <https://www.addgene.org/60026/>) were used to generate cell lines as previously described (Moreira, *et al.* 2017) except that the NEO selection cassette was not removed using Cre recombinase. One round of subcloning was performed to ensure clonality of the mESC lines generated.

Generation of 3xFLAG BirA* and BirA* P2A -TCF7L1 knock-in mESC lines by using TALENs

pCDNA5-FRT-TO-3xFLAG-BirA* was a kind gift from Dr. Brian Raught. BirA* and P2A were subcloned into the *TCF7L1* targeting vector by using PCR and gBlocks® (IDT), respectively. The *TCF7L1* targeting construct and TALENs were designed and assembled as previously described (Moreira, *et al.*, 2017). Cell lines were generated as previously described (Moreira, *et al.*, 2017). Three independent clones of 3xFLAG BirA* and 3xFLAG BirA* P2A - *TCF7L1* knock-in mESCs were used for subsequent analyses.

Supplementary References

Moreira, S., Polena, E., Gordon, V., Abdulla, S., Mahendram, S., Cao, J., Blais, A., Wood, G.A., Dvorkin-Gheva, A., and Doble, B.W. (2017). A Single TCF Transcription Factor, Regardless of Its Activation Capacity, Is Sufficient for Effective Trilineage Differentiation of ESCs. *Cell Rep.* **20**, 2424–2438.

CHAPTER 5 DISCUSSION

5.0 TCF/LEFs: setting the stage for complex Wnt target gene regulation

One of the reasons why it is challenging to study the TCF/LEF factors is that they all share similar functional domains; the HMG domain which confers DNA binding; a β -catenin binding domain; and a TLE binding domain (Cadigan and Waterman, 2012). Another reason, discussed throughout this thesis, is that TCF/LEF factor expression and regulation is broadly overlapping, with more than a single factor being expressed in a given cell type. This allows for complex functional compensation, illustrated in the phenotypes observed in TCF/LEF double-mutant mice that display more aggressive phenotypes than single-mutant animals (Galceran *et al.*, 1999; Gregorieff *et al.*, 2004). However, single TCF/LEF mutant mice do display unique defects, likely owing to exclusive or predominant expression of an individual TCF/LEF factor in particular cell-types or contexts (van Genderon *et al.*, 1994; Korinek *et al.*, 1998b; Merrill *et al.*, 2004; Verbeek *et al.*, 1995).

In support of these concepts, TCF7 and LEF1 have both unique and redundant functions in T-cell lineage commitment. Both factors are required for thymocyte maturation and establishment of certain T-cell identities, in part through intrinsic HDAC activity (Okamura *et al.*, 1998; Xing *et al.*, 2016). However, TCF7 plays a unique role in the commitment of hematopoietic progenitors into the T-cell lineage (Weber *et al.*, 2011). Furthermore, there is interplay between TCF7 and LEF1, in which TCF7 behaves as a tumor suppressor in thymocyte maturation to restrict the expression of LEF1, preventing transformation (Yu *et al.*, 2012).

The TCF/LEFs have traditionally been ascribed particular functions, with TCF7 and LEF1 classified as activators, TCF7L1 designated a constitutive repressor, and TCF7L2 categorized as either an activator or repressor depending on the isoform (Kim *et al.*, 2000; Liu *et al.*, 2005; Merrill

et al., 2004; Reya *et al.*, 2000; Tsedensodnom *et al.*, 2011). However, it has become clear that these designations are overly simplistic, as all factors appear to have context-specific activities that can be either activating or repressive. Due to this complexity, it is important to study the TCF/LEF family in an unbiased and equivalent fashion in a given context.

Recent advances in gene editing, such as CRISPR-Cas9 and TALEN technologies, together with methods employing next generation sequencing, have allowed us to systematically manipulate multiple proteins in a given cell type and assess the functional consequences. In the studies presented in this thesis we have used these technologies to create robust models aimed at elucidating the functional redundancy among the different TCF/LEF factors. We have applied unbiased, global approaches to assess the molecular functions of the two most abundant TCF/LEF factors in mESCs, TCF7L1 and TCF7. Our data suggest that TCF/LEFs are broadly redundant and provide novel insights into TCF/LEF function through identification of new TCF/LEF target genes and interacting proteins in mESCs with Wnt signaling switched on or off. Overall, the body of work in this thesis has made important advances towards clarifying mechanisms of TCF/LEF target gene regulation and the effects of Wnt signaling on these mechanisms.

5.1 Unravelling redundant functions of the architectural TCF/LEF factors

Despite containing highly conserved DNA- and β -catenin-binding domains, genetic deletion of individual TCF/LEF family members has revealed different phenotypes (van Genderon *et al.*, 1994; Korinek *et al.*, 1998b; Merrill *et al.*, 2004; Verbeek *et al.*, 1995). Adding to this complexity, viable crosses between single TCF/LEF knockouts, result in double-mutant mice with more aggressive phenotypes, suggesting a context-dependent redundancy in TCF/LEF function (Galceran *et al.*, 1999; Gregorieff *et al.*, 2004). Although all TCF/LEF family members share similar functional protein domains, the degree to which these factors are functionally redundant at

the molecular level has been difficult to assess due to their diverse expression patterns throughout development and their ability to cross-regulate one another's expression.

These studies formed the basis for the conceptualization of Chapter 2, as we sought to answer how much functional redundancy exists between the TCF/LEF family members. We focused on TCF7 and TCF7L1 as they are the most abundantly expressed family members in mESCs and have been suggested to function opposingly, with TCF7 linked to activation of Wnt target genes and TCF7L1 believed to constitutively repress transcription (Kennedy *et al.*, 2016; Kim *et al.*, 2000; Liu *et al.*, 2005; Merrill *et al.*, 2004; Pereira *et al.*, 2006; Wu *et al.*, 2012; Yi *et al.*, 2011). To this end, we devised a model system that would allow for the assessment of individual TCF/LEF factor function in the absence of confounding compensation from the other factors (Chapter 2). By using CRISPR-Cas9 technology to genetically ablate all full-length TCF/LEF factors, we were able to re-introduce a single 3xFLAG-tagged TCF factor at its endogenous locus by using TALEN technology.

This system was able to provide insights into the most fundamental question regarding the degree of functional overlap between the TCF/LEFs. Specifically, these experiments revealed a surprising degree of functional compensation between two supposedly opposing TCF/LEFs, TCF7 and TCF7L1. Either factor could restore the transcriptome to a state highly resembling that of wild-type mESCs and could rescue the mesendodermal differentiation defects observed in QKO mESCs, despite their differing TCF reporter transactivation capabilities (Chapter 2). The precise mechanisms mediating the ability of these two TCF/LEFs to similarly rescue the properties of QKO mESCs, despite differential TCF reporter activities, remain to be fully elucidated. However, we propose that the DNA-binding function of the TCF/LEFs mediated by the HMG domain, that binds and sharply chinks DNA, coupled with the ability of both factors to reversibly bind β -

catenin, may be sufficient for regulation of Wnt target genes (Giese *et al.*, 1992; Love *et al.*, 1995; Molenaar *et al.*, 1996).

In eukaryotes, DNA is compacted into chromatin comprising basic subunits called nucleosomes that consist of DNA wrapped around histone octamers. Epigenetic modification of histone proteins and shuffling of nucleosomes greatly impact transcription of genes. Higher order chromatin compaction, required to package an entire genome into a tiny nucleus, requires sequences separated by very long distances, ranging from kilobases to megabases, being brought in close proximity to one another, forming chromatin subdomains that share a 3D space, called a topologically associated domain (TAD) (Gonzalez-Sandoval and Gasser, 2016). TAD borders are conserved across species and between cell types, with changes occurring mostly within individual TADs (Rao *et al.*, 2014; Vietri Rudan *et al.*, 2015).

In ES cells, lineage-specific developmental gene activation or silencing is facilitated by organizing multiple genes into individual TADs, which become demarcated from one another by CCCTC-binding factor (CTCF) and Cohesin complexes (Hu and Tee, 2017; Zuin *et al.*, 2014). This synchronous regulation of multiple genes is driven by intra-TAD chromatin structures, such as chromatin loops, known to mediate enhancer-promoter interactions, which also involve CTCF and Cohesin (Gómez-Díaz and Corces, 2014; Zuin *et al.*, 2014). Furthermore, TADs become reorganized during ES cell lineage specification to allow for appropriate establishment of transcriptional programs in response to signaling cues (Dixon *et al.*, 2015).

Although the TCF/LEF family members are context-dependent transcription factors that respond to external stimuli to drive cell-type specific gene circuitries, this is achieved in a milieu of dynamic chromatin structure. To date, β -catenin/TCF-dependent regulation of Wnt target genes has focused on the effects of recruited corepressors or coactivators on histone modifications and nucleosome remodeling in the on and off states of Wnt/ β -catenin signaling. The studies discussed

below underscore the crucial, yet understudied, roles that the TCF/LEF factors play in regulating the genome-wide topological organization of the chromatin, which has equally important implications for gene regulation.

TCF/LEFs were first linked to regulation of chromatin architecture through the identification of a TCF-coordinated chromatin loop at the Wnt target gene, *Myc* (Pomerantz *et al.*, 2009). A CRC risk variant at an enhancer region, rs6983267, demonstrated increased *Myc* expression and preferential binding of TCF7L2, which mediated chromatin interactions with the *Myc* gene and promoter located 330kb away (Pomerantz *et al.*, 2009). Similarly, a β -catenin/TCF-dependent chromatin loop was discovered at *Myc*, mediating the interaction between two WREs located at either end of the gene (Yochum *et al.*, 2010).

In human ES cells, genes associated with mesendodermal differentiation were discovered to be enriched for β -catenin/LEF1 complexes in response to Wnt3a (Estarás *et al.*, 2014). Intriguingly, the Cohesin loading subunit NIPBL localized to β -catenin/LEF1 bound enhancers and associated with β -catenin protein (Estarás *et al.*, 2014). Furthermore, NIPBL/ β -catenin/LEF1 enriched enhancers were shown to form chromatin loops with promoters of the Wnt target genes *EOMES* and *MIXL1* (Estarás *et al.*, 2014).

In colorectal cancer, dysregulation of the Wnt pathway also has important impacts on chromatin organization. Giakountis *et al.* demonstrated that the lincRNA, WiNTRLINC1, a direct Wnt target gene, increased the expression of *ASCL2*, an important regulator of stemness and neoplasia in intestinal crypts (Giakountis *et al.*, 2016; Schuijers *et al.*, 2015). WiNTRLINC1, in association with β -catenin/TCF7L2 complexes, mediated the formation of a topological loop between its own promoter, and regulatory regions of *ASCL2* (Giakountis *et al.*, 2016).

Despite TCF/LEFs being thought of as repressors in the absence of a Wnt signal, we observed that most genes were significantly downregulated in the absence of all the full length TCF/LEFs in QKO mESCs (Chapter 2). Furthermore, TCF7 and TCF7L1 were able to rescue the phenotypes observed in the QKO mESCs, while differentially transactivating the TCF reporter. One explanation for these findings is that dominant negative TCF/LEFs, which do not bind β -catenin and are expressed through alternate promoters, are expressed in the QKO mESCs, mediating the transcriptional repression of target genes. However, this does not explain how re-introduction of TCF7 or TCF7L1, which are also thought to behave as repressors in the absence of β -catenin, are able to similarly restore the transcriptome of QKO mESCs to a wild type-like state.

A possible explanation is that TCF/LEF-Cohesin complexes may coordinate the organization and insulation of individual TADs, which become disorganized in the QKO mESCs. Inappropriate TAD configurations in the QKO mESCs could cause a downregulation of TCF/LEF target genes, as this could lead to dysregulated modification of histones or destabilization of enhancer-promoter interactions. The association of β -catenin/TCF-LEF with Cohesin complexes could mediate the establishment of enhancer-promoter chromatin loops, poising genes for subsequent activation in response to extracellular signals. This could explain how both TCF7 and TCF7L1 are able to restore mesendodermal differentiation, which requires active Wnt signaling outputs.

In support of these notions, redistribution of architectural chromatin-associated proteins in response to environmental cues, leads to the reorganization of TADs (Li *et al.*, 2015). Furthermore, zebrafish mutants lacking a Cohesin subunit display downregulation of Wnt target genes and neurodevelopmental defects, which were rescued upon Wnt pathway activation (Pistocchi *et al.*, 2013). In summary, we believe that the architectural role of the TCF/LEFs has been

underappreciated. Global conformation capture experiments would further our understanding of Wnt signal modulation of chromatin structure and could unveil new mechanisms that TCF/LEFs may employ to regulate target genes.

5.2 Emphasizing mechanisms of TCF/LEF target gene selection and specificity

Given that TCF7 and TCF7L1 were both able to restore transcriptional changes observed in TCF/LEF QKO mESCs (Chapter 2), we became interested in determining the precise mechanisms that mediate the functional redundancy we observed. We used ChIP-seq analyses to determine the genomic occupancy of TCF7 and TCF7L1 and the effects of CHIR on their residency. A complete understanding of TCF7 and TCF7L1 genome-wide occupancy, together with the effects of CHIR on their binding, would allow us to characterize the amount of overlap between the two factors and to identify potential TCF7-TCF7L1 switching at specific target genes.

Recently, TCF7 and TCF7L1 ChIP-seq was performed in mESCs in the absence of Wnt stimulation (De Jaime-Soguero *et al.*, 2017). Minimal overlap and disparate binding of the two factors to a palindromic binding site (5'-CTCGCGAGA-3') and the WRE (5'-CTTTGATAT-3') were reported. However, this study used a commercial TCF7 antibody that is not recommended for any applications involving cell fixation, which possibly influenced the results. To circumvent differences in commercial TCF7 and TCF7L1 antibody specificities and affinities, we employed TALEN technology to separately knock-in the 3xFLAG epitope tag at a single allele of either the endogenous *Tcf7* or *Tcf7l1* genes, to generate isogenic cell lines in wildtype mESCs (Chapter 3). These cell lines allowed us to use a single, well-characterized, monoclonal FLAG antibody, known to exhibit high affinity and specificity towards the 3xFLAG-tag, to quantitatively characterize TCF7 and TCF7L1 protein levels and localization and to obtain ChIP-seq data that is truly comparable between the two proteins.

We observed that 3xFLAG-TCF7L1 was more abundant than 3xFLAG-TCF7 in self-renewing and differentiating mESCs and mESCs treated with CHIR (Chapter 3). In mESCs stimulated with CHIR, 3xFLAG-TCF7L1 was also more abundantly associated with β -catenin, likely as a result of its higher levels. Furthermore, our ChIP-seq experiments revealed minimal overlap in genomic distributions of 3xFLAG-TCF7 and 3xFLAG-TCF7L1, with 3xFLAG-TCF7L1 being the more prevalent factor regardless of the state of Wnt signaling. Coupled with the redundancy observed between TCF7 and TCF7L1 in Chapter 1, our data suggest that, in mESCs, TCF7L1 mediates a majority of Wnt target gene activation, in complex with β -catenin.

In support of this, we observed weak transactivation of a TCF reporter in QKO mESCs rescued with a single copy of TCF7L1 (Chapter 2). Although 3xFLAG-TCF7L1 occupancy was slightly reduced in the presence of CHIR, this is likely due to the reduction in overall 3xFLAG-TCF7L1 levels observed upon CHIR treatment in our western blot experiments. The lack of a dramatic difference in 3xFLAG-TCF7L1 genomic occupancy after CHIR treatment in our ChIP-seq data suggests that removal of TCF7L1 from the chromatin is not a global mechanism responsible for β -catenin-mediated derepression of target genes (Shy *et al.*, 2013). Intriguingly, TCF7 was bound to all four factors, and TCF7L1 was bound to *Lef1*, *Tcf7l2*, and itself, confirming that TCF/LEF factors can auto- and cross-regulate each other's expression in mESCs and in response to Wnt activation.

We observed that 3xFLAG-TCF7 and 3xFLAG-TCF7L1 were differentially enriched at specific genes in the presence and absence of CHIR, despite being differentially expressed. 3xFLAG-TCF7L1 was significantly more abundantly detected on the chromatin than 3xFLAG-TCF7 (Chapter 3). Generally, 3xFLAG-TCF7 was more abundant at select Wnt-associated genes, whereas 3xFLAG-TCF7L1 was the predominant factor at pluripotency-related genes.

The precise mechanisms that regulate TCF/LEF target gene selection and specificity, allowing specific TCF/LEF factors to regulate Wnt target genes in a context-dependent fashion, are poorly understood. Recent models have suggested that competitive binding by transcription factors is primarily regulated by binding strength and transcription factor abundance (Porter *et al.*, 2017). However, we believe that a combination of binding competition facilitated by additional DNA binding specificity and TCF/LEF abundance, as well as transcription factor cooperativity and accessory bridging factors, mediate the differential binding of TCF7 and TCF7L1 to the genome in mESCs (Atcha *et al.*, 2007).

3xFLAG-TCF7 was specifically enriched at known Wnt targets, such as *Axin2*, *Zfp703*, *Lef1*, *Tcf7*, *Nkd1*, and *Msx2* (Filali *et al.*, 2002; Kumar *et al.*, 2016; Lustig *et al.*, 2002; Roose *et al.*, 1999; Willert *et al.*, 2002; Yan *et al.*, 2001). The mechanism that enables 3xFLAG-TCF7 to outcompete with 3xFLAG-TCF7L1, which was much more abundant, for binding to Wnt target genes remains unknown and is a key question to be addressed in future experiments. One potential explanation relies on alternative splicing that occurs at the C-terminus of TCF7 and TCF7L2, generating “E-tail”-containing TCF/LEF isoforms (Atcha *et al.*, 2003). These E-tail isoforms contain an additional DNA-binding domain called the cysteine-clamp or “C-clamp”, capable of sequence-specific binding to GC-rich “helper sites” flexibly located upstream or downstream of WREs in either orientation (Atcha *et al.*, 2007; Hoverter *et al.*, 2012, 2014).

The C-clamp is thought to behave as an anchor, bringing TCF/LEFs closer to imperfect WREs, essential for robust activation of target genes, such as *Lef1*, *Sp5*, and *Cdx1* (Atcha *et al.*, 2007; Hoverter *et al.*, 2012, 2014; Weise *et al.*, 2010). In support of the C-clamp mediating the recruitment of TCF/LEF factors to weak WREs, specifically TCF7, we were able to locate multiple WRE-helper site pairs at *Axin2*, *Zfp703*, *Lef1*, *Tcf7* and *Nkd1*. At these particular genes, helper

sites may aid in recruiting an E-tail-containing TCF7 isoform to imperfect WREs, whereas TCF7L1, which lacks the C-clamp, is incapable of binding as strongly.

Conflictingly, to an equal or lesser degree, 3xFLAG-TCF7L1 binding was observed at *Axin2*, *Sp5*, and *Lef1*, and was enriched at additional helper site-containing genes such as *Nodal*, *Myc*, and *Ccnd1*. A possible explanation for 3xFLAG-TCF7L1 being able to outcompete 3xFLAG-TCF7 for binding at these particular genes is that within the population of cells submitted to ChIP-seq, specific cells do not express TCF7, allowing the more abundant TCF7L1 to bind these helper site-containing genes. Another potential explanation is that helper sites contain multiple CpG dinucleotides, which can be methylated, thereby blocking interactions with the C-clamp. In support of this, electrophoretic mobility shift assays, carried out using an E-tail-containing TCF7 variant, revealed that this isoform of TCF7 could bind an oligonucleotide probe with two WREs and two helper sites, but methylation of the CpG dinucleotides in the helper sites strongly reduced binding (Hoverter *et al.*, 2014). Moreover, the C-clamp is capable of inhibiting HMG DNA binding at genes where a WRE is not coupled to a helper site (Ravindranath and Cadigan, 2014). Therefore, methylated CpG dinucleotides at particular helper sites would specifically prevent the E-tail isoform of TCF7 from binding to Wnt target genes.

Fine-tuning of transcription is essential for proper mammalian development and tissue homeostasis. Proper spatial-temporal expression of genes is regulated by coordinated, cooperative binding of multiple context-specific transcription factors to promoters and enhancers, in response to signaling cues (Palstra and Grosveld, 2012). This coordination of transcription factor complexes depends on the abundance of these transcription factors, their affinities for DNA and their ability to interact with adjacently bound transcription factors (Panne *et al.*, 2007). TCF/LEFs also demonstrate context-specific binding and cooperation with other transcription factors allowing for crosstalk between Wnt and other signaling pathways.

In support of this, in MCF7 and HepG2 cells, TCF7L2 was associated with different sets of target genes, and binding to these two subsets depended on cell-type specific interactions with GATA3 and HNF4 α (Frietze *et al.*, 2012). Furthermore, TCF7L2 associates with specific transcription factors at different stages of oligodendrocyte differentiation (Zhao *et al.*, 2016). At the onset of differentiation, TCF7L2 binds ZBTB33 (Kaiso Transcription Factor), inhibiting Wnt signaling, whereas TCF7L2 promotes oligodendrocyte maturation through interactions with SOX10 (Zhao *et al.*, 2016). Similarly, in myoblasts, LEF1 requires SMAD3 in order to bind and regulate target genes (Aloysius *et al.*, 2018). Interestingly, our *de novo* motif analysis revealed that a substantial proportion (~20%) of 3xFLAG-TCF7L1-binding sites were significantly overrepresented with the binding-motif of BRN1 and ZIC1/2 (Chapter 3). Furthermore, numerous transcription factors were identified as putative TCF7L1-interacting proteins (Chapter 4). Context-specific association of TCF7L1 with different transcription factors could explain the recent disparate findings in which TCF7L1 in mESCs, was shown to repress genes involved in the maintenance of pluripotency, promoting the transition to an epiblast-like state (Hoffman *et al.*, 2013), whereas in hESCs TCF7L1 promoted maintenance of the pluripotent state, by repressing genes associated with primitive streak formation (Sierra *et al.*, 2018).

TCF7L1 is believed to regulate mESC self-renewal and differentiation by acting as a constitutive repressor, with β -catenin mediating a switch between repressive TCF7L1 and activating TCF7 (Yi *et al.*, 2008, 2011). However, multiple findings within the studies presented in this thesis suggest that this switch mechanism is not an absolute requirement for Wnt target gene activation and maintenance of the pluripotent state. Instead, our data suggest that TCF7L1, in association with β -catenin, may function as an activator of Wnt target genes, as 1) Both TCF7 and TCF7L1 were able to rescue QKO mESCs to a similar extent (Chapter 2); 2) TCF7L1 QKO rescues were able to weakly activate the TCF reporter (Chapter 2); 3) TCF7L1 is the most abundant

TCF/LEF in the presence of CHIR and binds more β -catenin (Chapter 3); 4) TCF7L1 was more prevalent on the chromatin, with and without CHIR, compared to TCF7, suggesting it predominantly mediates the Wnt response in mESCs (Chapter 3); 5) TCF7L1 remained associated with the core pluripotent transcriptional network on the chromatin in the presence of CHIR (Chapter 3); and 6) TCF7L1-interacting proteins were enriched in the presence of CHIR, despite a reduction in TCF7L1 levels (Chapter 4).

In agreement with our findings, TCF7L1 has been shown to activate a TCF/LEF reporter, as well as target genes, in a context-dependent manner (Cao *et al.*, 2018; Cole *et al.*, 2008; Ku *et al.*, 2017; Merrill *et al.*, 2001; Park *et al.*, 2015; Slyper *et al.*, 2012; Wang *et al.*, 2017). Specifically, SMAD2/3 and TCF7L1- β -catenin were shown to promote mesendodermal specification in hESCs by co-occupying enhancers at crucial genes and upregulating them, downstream of Wnt and Nodal signaling (Wang *et al.*, 2017). These TCF7L1- β -catenin activator complexes would explain the disparate findings of Waterman's group, showing that Wnt signaling promoted PS formation, whereas TCF7L1 promoted pluripotency by repressing PS genes, which conflicts with its reported role as a suppressor of pluripotency in mESCs (Sierra *et al.*, 2018). Presumably, TCF7L1 promotes pluripotency in primed hESCs by repressing PS genes in the absence of a Wnt signal, whereas upon Wnt stimulation and subsequent β -catenin binding, TCF7L1 behaves as an activator of PS and mesendodermal genes.

Taken together, identification of TCF7L1 and TCF7 genomic distributions (by using our 3xFLAG-tag strategy) have revealed potentially unexpected roles for TCF7L1. Strikingly, TCF7L1 remained the most abundant factor in the presence of CHIR and was associated with more β -catenin. This allowed TCF7L1 to remain widely bound to the chromatin, suggesting that TCF7L1 mediates the effects of CHIR. Indeed, we did observe a higher proportion of 3xFLAG-

TCF7L1-bound sites containing the OCT4/SOX2/NANOG co-motif with CHIR. Furthermore, we observed equal or greater 3xFLAG-TCF7L1 binding at many pluripotency genes in the presence of CHIR including *Id3*, which was activated in QKO mESCs rescued with TCF7L1 and treated with CHIR. Future experiments examining the effects of CHIR on histone marks surrounding TCF7L1 at these pluripotency-associated genes in QKO mESCs rescued with TCF7L1, will reinforce our hypothesis that TCF7L1 functions to activate these genes. The minimal overlap in TCF7L1 and TCF7 chromatin occupancy appears to conflict with the functional redundancy we observed in QKO rescues (Chapter 2). A potential explanation is that, in the QKO mESCs, sites normally occupied by the more abundant TCF7L1, become liberated, allowing re-introduced TCF7 to bind these sites in the absence of competing TCF7L1. Future experiments will need to be performed to better elucidate the complex interplay between the TCF/LEFs in the regulation of target genes. Specifically, determining the consequences of auxiliary DNA binding domains on TCF/LEF competition for binding to target genes will be critical in defining how Wnt signals are coordinated by the TCF/LEFs. Moreover, whether other context-specific transcription factors associate with a specific TCF/LEF to cooperatively regulate distinct subsets of target genes remains to be elucidated.

5.3 TCF/LEFs flicking the switch on Wnt/ β -catenin signaling

Wnt/ β -catenin signaling has been extensively studied over the past 30 years, yet, other than the TLEs, the transcriptional co-factors that mediate TCF/LEF regulation of Wnt target genes have been poorly characterized. Armed with the fact that TCF7 and TCF7L1 demonstrate redundant functions, despite previously being believed to function opposingly (Chapter 2) and exhibit minimal overlap in chromatin residency (Chapter 3), we next aimed to identify and compare potential TCF7 and TCF7L1 interacting proteins (Chapter 4). Our hope was to gain insights into TCF/LEF mechanisms of transcriptional regulation, which could potentially explain our findings

in Chapters 2 and 3. To address this final question, we utilized a novel technique for identifying protein-protein interactions that is based on proximity-dependent biotinylation, BioID (Roux *et al.*, 2012). In mESCs, TCF7 and TCF7L1 were endogenously tagged with BirA*, a promiscuous biotin ligase, and BioID was undertaken at timepoints of differentiation when the tagged proteins were most abundant.

Unfortunately, due to low TCF7 expression levels (consistent with our ChIP study), we obtained unsatisfactory TCF7 BioID data (Appendix I). However, with endogenously BirA*-tagged TCF7L1, we obtained a list of novel putative TCF7L1-interacting proteins. To evaluate whether limited overexpression of BirA*-tagged TCF/LEFs would provide meaningful data consistent with that obtained by using a knock-in approach, we undertook a comparison between BioID analysis obtained by using an inducibly driven BirA*-tagged TCF7L1 integrated at the *ROSA26* locus and our endogenous TCF7L1 BioID. The two BioID systems demonstrated a significant amount of overlap, but as somewhat expected, a 3-fold increase in TCF7L1 levels in the inducible system yielded 100 additional putative TCF7L1 interacting proteins that were undetected with the endogenous BioID system. Importantly, the most abundant putative TCF7L1 interacting proteins were detected in both BioID system. This suggests that although the endogenous BioID system contains physiological levels of TCF7L1, and presumably produces physiologically relevant data, an overexpression BioID system can still yield a biologically significant interactome and may be applicable for cases such as TCF7 in mESCs, where endogenous protein levels are very low.

Through our BioID experiments, we identified numerous highly abundant putative TCF7L1-binding and/or proximal partners, which were predominantly epigenetic/transcription factors. Importantly, despite CHIR-induced reduction of TCF7L1 levels, an increase in putative TCF7L1-interacting proteins was observed. Furthermore, upon Wnt pathway modulation with

CHIR, a majority of TCF7L1 proximal proteins were still detected. Specifically, TLE3 and TLE4 remained associated with TCF7L1 with and without CHIR, consistent with current working models suggesting that the TLEs are not displaced, but instead undergo a conformational change upon target gene activation (Chodaparambil *et al.*, 2014; van Tienen *et al.*, 2017). Collectively, our BioID data suggest that β -catenin may not displace TCF7L1-interactions but may instead promote these interactions through recruitment of additional components, as many TCF7L1 proximal proteins were more abundant after stimulation with CHIR.

TCF7L1 has been thought to constitutively repress Wnt target genes, and β -catenin-dependent removal of TCF7L1 from the chromatin, with subsequent TCF7L1 degradation, has been proposed as a mechanism of derepression (Kennedy *et al.*, 2016; Kim *et al.*, 2000; Liu *et al.*, 2005; Merrill *et al.*, 2004; Pereira *et al.*, 2006; Shy *et al.*, 2013; Wu *et al.*, 2012; Yi *et al.*, 2011). In the absence of β -catenin, our BioID screens identified numerous subunits of complexes that could function in TCF7L1-mediated repression of target genes, such as the nuclear receptor corepressor complex (NcoR), polycomb group proteins (PcG), and the nucleosome remodeling deacetylase (NuRD) complex (Chapter 4).

Notably, the NuRD complex was specifically enriched in the endogenous BioID screen, in the absence of CHIR. ZFP281 a TCF7L1 proximal protein identified in the inducible BioID screen, mediates the repression of *Nanog* by recruiting the NuRD complex (Fidalgo *et al.*, 2012). Furthermore, the downregulation of Wnt target genes has been shown to involve the NuRD complex in mESCs (Kim *et al.*, 2012). It is possible that TCF7L1 utilizes the NuRD complex to mediate Wnt target gene repression in the absence of β -catenin. This complex was not detected in the inducible BioID screen, in which a long isoform of TCF7L1 was overexpressed. This suggests that NuRD complex components could potentially interact specifically with short isoforms of

TCF7L1. Recently, it has been demonstrated that a short isoform of TCF7L1 promotes exit from the pluripotent state in mESCs (Cirera-Salinas *et al.*, 2017).

There were a few putative TCF7L1-interacting proteins specifically enriched in the absence of CHIR in both BioID systems, a BCL-6 corepressor (BcoR), SALL1, and TET1. Both BcoR and SALL1 mediate transcriptional repression of target genes by recruiting HDACs and the NuRD complex (Choi *et al.*, 2013; Huynh *et al.*, 2000; Kiefer *et al.*, 2002). SALL1 has a dual function in ES cells, positively regulating transcription of genes related to self-renewal in association with NANOG, simultaneously repressing expression of ectodermal and mesodermal differentiation markers (Karantzali *et al.*, 2011). SALL1 together with NANOG, are thought to play a role in regulating chromatin architecture in mESCs, reducing the number of dense chromatin fibers (Novo *et al.*, 2016). Unlike BcoR, SALL1 has been linked to regulation of Wnt/ β -catenin signaling, synergistically working with β -catenin to activate a TCF/LEF reporter (Sato *et al.*, 2004a). Whether BcoR and SALL1 bind to TCF7L1, mediating transcriptional repression of Wnt target genes, remains to be elucidated.

SALL1, in particular, is intriguing, as it provides a connection between epigenetic regulation and remodeling of chromatin conformation (Chapter 2), potentially allowing TCF7L1 to regulate genes at both levels. Importantly, SALL1 was not the only protein identified in our BioID screens that has been implicated in the regulation of chromatin topology. The mediator component, MED17, identified in the inducible BioID screen, binds to Cohesin complexes, predicting chromatin loops at enhancers and promoters of active genes in ES cells (Kagey *et al.*, 2010). Similarly, ZBTB33, also known as Kaiso, has been shown to associate with CTCF, which functions at TAD borders and mediates formation of topological loops (Defossez *et al.*, 2005). Future experiments are needed to determine whether TCF7L1 works in association with, not only

the factors discussed above, but also other proximal proteins identified in our BioID screens, to regulate chromatin architecture.

TET1 was highly abundant in both BioID screens, specifically in the absence of CHIR. TET1 is of particular interest, as together with ZFP281 that was identified in the inducible BioID screen, it promotes the transition from the naïve to primed pluripotent states (Fidalgo *et al.*, 2016). TCF7L1 has also been shown to promote the transition from naïve to primed pluripotency (Hoffman *et al.*, 2013). Similar to TCF7L1, TET1, despite being involved in DNA methylation erasure, also suppresses genes in mESC and mouse epiblast-like cells by recruiting polycomb repressive complex 2, to promoters (Khoueiry *et al.*, 2017; Wu *et al.*, 2011). Future studies will be needed to determine whether TET1 and TCF7L1 function together to repress target genes and regulate the transition from naïve to primed pluripotency.

As previously discussed, Chapter 3 revealed that more TCF7L1 was associated with chromatin than TCF7, both with and without CHIR. This suggests that in mESCs, TCF7L1, as the most abundant TCF factor, mediates the majority of target gene activation in response to Wnt signals. However, the precise mechanism through which β -catenin mediates the derepression of TCF7L1 and subsequent conversion to a potential transcriptional activator, remains elusive. Our BioID data provides some insights into these potential mechanisms, as our inducible system identified known β -catenin transcriptional coactivators such as the histone acetyl transferases CBP and p300, as well as BCL9, BCL9L, and the lysine methyltransferase KMT2D (MLL4), all of which were enriched with CHIR (Chapter 4) (Hecht *et al.*, 2000; Kramps *et al.*, 2002; Sierra *et al.*, 2006; Takemaru and Moon, 2000).

Additionally, we validated a TCF7L1 interaction with SMARCA4, a component of the BAF nucleosome remodeling complex (Chapter 4). SMARCA4 has recently been implicated in

the regulation of higher order chromatin structure and telomere structure, as SMARCA4 binding was enriched at TAD boundaries, which were weakened upon SMARCA4 knockdown (Barutcu *et al.*, 2016). The BAF complex was the most abundant complex identified in both BioID screens. Components of the BAF complex have been shown to exert differential effects on Wnt target genes. SMARCC1 and multiple BAF subunits, identified as negative regulators of *Nanog* in an RNAi screen, were shown to promote chromatin compaction at the *Nanog* locus (Schaniel *et al.*, 2009). This suggests that in the absence of β -catenin, TCF7L1 could be utilizing the BAF complex to shuffle nucleosomes to promote chromatin compaction and higher order chromatin reorganization facilitating target gene repression.

Conversely, SMARCA4 has been shown to interact with β -catenin, promoting Wnt target gene activation in a TCF-dependent manner (Barker *et al.*, 2001). In our BioID screens we observed an enrichment in TCF7L1 association with BAF components during CHIR stimulation (Chapter 4). This could be explained by recruitment of additional BAF complex subunits that requires the recruitment of β -catenin to TCF7L1. In particular, SMARCD1 was only observed in presence of CHIR in both TCF7L1 BioID screens. SMARCD1 is part of an ESC-specific BAF complex, which facilitates the activation of pluripotency associated genes (Ho *et al.*, 2009). TCF7L1- β -catenin complexes could promote chromatin relaxation and rearrangement of TADs by recruiting these specific BAF subunits, subsequently activating target genes.

In addition to SMARCA4, we validated two abundantly detected putative TCF7L1-interacting proteins, identified in the presence and absence of CHIR; JMJD1C and SALL4 (Chapter 4). JMJD1C is a H3K9 demethylase that plays a role in the activation of self-renewal genes and the suppression of differentiation promoting ERK/MAPK signals in mESCs (Xiao *et al.*, 2017). JMJD1C was the most abundant TCF7L1 proximal protein detected in all conditions,

however, it has not been linked to Wnt signaling. How JMJD1C functions to regulate Wnt target genes in association with TCF7L1 remains to be determined.

By contrast, SALL4 is a direct Wnt target gene and both SALL4 isoforms have been shown to associate with β -catenin, enhancing TCF reporter activity (Böhm *et al.*, 2006; Ma *et al.*, 2006). In mESCs SALL4 is thought to be an integral component of the core transcriptional circuitries regulating pluripotency, and it activates the expression of *Pou5f1* (Lim *et al.*, 2008; Zhang *et al.*, 2006). SALL4 was enriched in the presence of CHIR, which further supports the idea that TCF7L1- β -catenin complexes mediate the activation of Wnt target genes. Whether there is interplay between SALL1 and SALL4 upon Wnt modulation is also an interesting question, as SALL1 was enriched in the absence of CHIR, whereas SALL4 was enriched in the presence of CHIR. Both factors, coupled with TCF7L1, may play roles in establishing the appropriate chromatin architecture in response to Wnt signaling (Chapter 2).

Whether TCF7L1 behaves as an activator or constitutive repressor in the presence of β -catenin remains unclear, but evidence supporting TCF7L1 proteasomal degradation upon Wnt pathway activation is unequivocal (Chapter 2-3). NcoR is a complex identified in our BioID screen that offers potential insights into mechanisms of TCF7L1 degradation and derepression. Both TBL1X and TBL1XR1 have been shown to regulate transcriptional activation by recruiting the ubiquitin-conjugating/19S proteasome complex, allowing for a switch from corepressors to coactivators (Ogawa *et al.*, 2004; Perissi *et al.*, 2004, 2008). TBL1X and TBL1XR1 also interact with β -catenin and TCF7L2 in response to Wnt, binding Wnt target gene promoters and promoting transcriptional activation (Li and Wang, 2008). Whether TBL1X-TBL1XR1 regulates TCF7L1 protein levels or mediates a switch from corepressors to coactivators, allowing for subsequent Wnt target gene transcriptional activation, remains to be elucidated.

We propose that β -catenin could mediate the recruitment of TBL1X-TBL1XR1, leading to subsequent proteasomal degradation of TCF7L1 and/or its associated corepressors, thereby allowing for the recruitment of coactivators, activating/derepressing Wnt target genes. Another possibility is that NcoR complexes mediate the activation of Wnt target genes, as they have been shown to activate genes in specific contexts (Laschak *et al.*, 2011). In support of these notions, TBL1X-TBL1XR1 association with TCF7L1 was enriched in the presence of CHIR. A TBL1X-TBL1XR1 mediated reduction in TCF7L1 could also regulate the competitive binding dynamic between the TCF/LEF factors, as the other factors, which are less abundant, could now compete with TCF7L1 for binding to Wnt target genes (Chapter 3).

Identifying the TCF7L1 interactome and the effects of Wnt signaling modulation has provided insights into potential mechanisms of TCF/LEF target gene regulation. Previously, an emphasis has been placed on transcriptional regulation conferred by the TLE corepressors and coactivators recruited by β -catenin. Notably, the TLEs were not abundantly detected in either of our BioID screens. Furthermore, our BioID screens suggests that TCF7L1 associates more abundantly with various other epigenetic regulators, such as TET1, SALL1 and BCOR in the absence of CHIR. Moreover, treatment with CHIR increased putative TCF7L1-interactions with numerous complexes and epigenetic regulators implicated in transcriptional activation, such as the BAF and NcoR complexes and reduced TCF7L1 association with corepressors. Coupled with our observation that TCF7L1 remains associated with the chromatin in the presence of CHIR (Chapter 3), this is suggestive of TCF7L1 functioning as a transcriptional activator in the presence of β -catenin. All of this occurs despite CHIR-triggered reduction of TCF7L1 levels, potentially through the NcoR complex.

NcoR is particularly intriguing, as this complex could serve multiple functions including activating transcription, regulating TCF7L1 levels, and/or mediating transcriptional cofactor

switching. Future work probing the precise mechanisms of TCF7L1 regulation through gain and loss of function studies of these various transcriptional modulators will be critical in determining how TCF/LEFs translate Wnt signals into the appropriate regulation of downstream transcriptional outputs. Additionally, such experiments could confirm our hypothesis that β -catenin-mediated derepression of TCF7L1 involves the context-dependent conversion of TCF7L1 into a transcriptional activator in mESCs. Moreover, elucidating the TCF7 interactome and the influence of CHIR on this network will aid in determining the mechanisms that govern unique versus redundant transcriptional regulation by the TCF/LEF factors (Chapter 2-3).

5.4 Moving forward with mechanisms of TCF/LEF function

Interrogating the functional equivalence between TCF7 and TCF7L1 demonstrated the ability of both factors to restore mESC pluripotent properties (Chapter 2), despite minimal overlap in their genomic distributions (Chapter 3). Together with the identification of novel TCF7L1 proximal proteins using the BioID technique (Chapter 4), we have uncovered novel insights into the mechanisms that govern TCF/LEF regulation of Wnt target genes (Figure 1). In addition to the specific topics discussed above, the comparison between TCF7 and TCF7L1 has raised a number of additional questions regarding the transcriptional regulation of Wnt target genes, by the TCF/LEFs.

An intriguing function of the TCF/LEFs is their ability to induce sharp bends in the DNA, promoting long-range enhancer-promoter interactions, through chromatin loops (Estarás *et al.*, 2014; Pomerantz *et al.*, 2009). Recent technological advances have allowed for the monitoring of these long-range chromatin interactions by using chromatin conformation capture (3C) techniques, such as genome-wide chromatin conformation capture (Hi-C) (Schmitt *et al.*, 2016). The QKO mESCs offer an opportunity to examine the extent of TCF/LEF mediated chromatin organization, due to the ablation of all TCF/LEF factors. Liberation of Wnt target genes from TCF/LEF binding

in the QKO mESCs, would subsequently cause genome-wide changes in the chromosomal structure and TAD organization, which could be visualized by Hi-C. Furthermore, it would be interesting to examine the effects of re-introducing TCF7 or TCF7L1 on the chromatin conformation. Demonstrating the ability of both TCF7 and TCF7L1 to similarly restore the global chromatin conformation could explain how these two factors comparably elicit their effects on the QKO mESCs, despite possessing different TCF reporter activities.

Liberation of TCF/LEFs from chromatin in QKO mESCs could also allow for the binding of a re-introduced TCF/LEF factor to WREs that would otherwise be associated with a different TCF/LEF factor. Although there was minimal overlap between TCF7 and TCF7L1 binding to target genes in a wildtype background (Chapter 3), ChIP-seq analysis in the QKO mESCs rescued with TCF7, could reveal an expansion of TCF7 occupancy to additional target genes typically occupied by TCF7L1, in wildtype mESCs. This would explain the ability of both TCF7 and TCF7L1 to similarly restore the transcriptome of the QKO mESCs, despite an apparent lack of overlap in their genomic distribution as assessed by ChIP-seq in wildtype mESCs (Chapter 3). Additionally, performing ChIP-seq using the 3xFLAG-tag TCF7 and TCF7L1 knock-ins in wildtype mESCs during the course of differentiation could be informative, as the expression levels of both factors is upregulated upon removal of LIF. These experiments could potentially demonstrate an increase in the overlap between TCF7 and TCF7L1 genomic distribution, providing an explanation for their ability to redundantly restore mesendodermal differentiation in the QKO mESCs.

In addition to mediating target gene repression in the absence of a Wnt signal, the TCF/LEFs associate with β -catenin upon Wnt stimulation, activating target genes. However, due to functional redundancies and co-expression, the contribution of an individual TCF/LEF factor to Wnt/ β -catenin-dependent transcriptional control, remains to be fully elucidated. Global

transcriptional profiling could be performed on WT mESCs, QKO mESCs and QKO mESCs rescued with TCF7 and TCF7L1, treated with Wnt3a ligand and/or CHIR. This would test whether a single TCF/LEF was capable of restoring the transcriptome in response to a Wnt signal. A comparable rescue by both TCF7 and TCF7L1, of Wnt/ β -catenin-dependent transcription, would be further evidence to suggest that TCF7L1 can function as a transcriptional activator. Additionally, β -catenin has been shown to interact with numerous DNA-binding transcription factors, although it is unclear whether the TCF/LEFs are required for these interactions (Essers *et al.*, 2005; Kelly *et al.*, 2011). Identification of the global transcriptional changes in the QKO mESCs compared to WT mESCs, would aid in deciphering non-TCF/LEF, β -catenin-mediated transcriptional regulation.

Although we identified novel TCF7L1 proximal proteins and examined the consequences CHIR on these interactions, the initial goal was to perform BioID on both TCF7 (Appendix I) and TCF7L1 (Chapter 4). Unfortunately, the lower endogenous expression levels of TCF7 compared to TCF7L1, was an issue. To circumvent this, BioID was performed on mESCs differentiated for 3 days in medium lacking LIF, which led to an increase in endogenous TCF7 protein levels. However, due to technical issues with the mass-spectrometer and potentially, the streptavidin-pulldown, the TCF7 BioID failed to produce data of any significance (Appendix I). Repeating BioID analysis on TCF7 may require further optimization of conditions to further increase endogenous BirA*-TCF7 protein levels or moving to an inducible BirA*-TCF7 expression system that we validated for TCF7L1. Successful identification of TCF7 proximal proteins via BioID, will allow for a comparison between TCF7L1 vicinal proteins (Chapter 4). Comparing unique, versus common, TCF7 and TCF7L1 proximal proteins will undoubtedly aid in elucidating mechanisms common among both TCF factors as well as those that govern individual functions. These TCF7-

and TCF7L1 proximal proteins may provide insights into the ability of these factors to compensate for each other's functions (Chapter 2).

Numerous transcription factors crucial for mammalian development and stem cell differentiation display heterogeneous expression (Torres-Padilla and Chambers, 2014). Heterogeneous expression could have implications on cell fate commitment, as forced expression of lineage-related transcription factors, leads to biases observed in differentiating ES cells (McDonald *et al.*, 2014). Immunofluorescence analysis of the TCF/LEF factors revealed that they display heterogeneous expression in *in vitro* cultured ES cells (Chapter 2) as well as in the mouse epiblast (Hoffman *et al.*, 2013). Aimed at further assessing this heterogeneous expression, endogenous fluorescent protein fusions of TCF7 and TCF7L1 were generated (Appendix II). This enables tracking of TCF7 and TCF7L1 in individual cells within a population throughout the course of mESC differentiation. Additionally, mESCs can be sorted for low-, medium- and high-expressing TCF7 and TCF7L1 populations can be differentiated to examine biases imparted by either factor on cellular fate determination.

All four TCF/LEF family members, *Tcf7*, *Tcf7l1*, *Tcf7l2*, and *Lef1* are expressed at the protein level in mESCs (Pereira *et al.*, 2006; Wallmen *et al.*, 2012). Although, this thesis has focused on TCF7 and TCF7L1, future experiments on TCF7L2 and LEF1 are required to complete our understanding of unique versus redundant TCF/LEF functions. This would entail rescuing the QKO mESCs with a single copy of 3xFLAG-tagged TCF7L2 and LEF1 at their endogenous loci. Based on the functional redundancy highlighted in Chapter 2, we anticipate that TCF7L2 and LEF1 will similarly restore the differentiation defects and transcriptional changes observed in the QKO mESCs. Furthermore, the genomic residency of TCF7L2 and LEF1 and the effect of Wnt/ β -catenin pathway modulation, could be assessed by using 3xFLAG-tagged knock-ins, in a wildtype background. This would provide us with a complete list of genes directly bound by all 4 TCF/LEF

factors in mESCs and the effects of Wnt/ β -catenin signaling on the residency of the TCF/LEFs throughout the genome. Finally, to glean further insights into mechanisms of TCF/LEF gene regulation, TCF7L2 and LEF1 proximal-proteins could be identified by using BioID, providing us with a complete list of all TCF/LEF proximal-proteins in the context of differentiating mESCs.

Taken together, answering these questions would provide us with a more complete understanding of the functions and mechanisms of action of all four TCF/LEF family members in mESC biology.

5.5 Concluding remarks

The TCF/LEFs factors are the major downstream effectors of Wnt/ β -catenin signaling. TCF/LEFs are multifunctional and interact with numerous transcription factors and epigenetic modulators in a context-specific manner to facilitate Wnt target gene recognition and regulation. Within the context of TCF/LEF regulation of Wnt target genes, the goals of this thesis were to create a model that would allow us to systemically characterize the functional redundancy among the different TCF/LEF family members. Additionally, we aimed to identify and compare TCF/LEF target genes and interactomes utilizing unbiased global approaches. The studies within this thesis highlight the previously underappreciated ability of different TCF/LEF factors to compensate for one another, utilizing novel epigenetic/transcription factors and chromatin remodelers, despite an apparent minimal overlap in their genomic distributions in pluripotent mESCs (Chapter 2-4). Importantly, this thesis questions the categorization of certain TCF/LEF factors as “activators” or “repressors” (Chapter 2) and suggests that TCF7L1 may play a crucial role as an activator in response to Wnt signals in pluripotent and differentiating mESCs (Chapter 2-4). Additionally, this work suggests that for a complete understanding of Wnt/ β -catenin signaling, the effects of all four TCF/LEF factors on the regulation of Wnt target genes should be carefully considered. The work in this thesis highlights how the regulation and function of the TCF/LEF factors is complex and

can be difficult to interpret. Moreover, this thesis suggests that improved reporters of TCF/LEF activity are required, as current reporters can be misleading. It is my belief that the continued use of unbiased global approaches such as CRISPR, CHIP-seq, RNA-seq and BioID, will evolve our understanding of mechanisms of TCF/LEF Wnt target gene regulation by identifying common and unique target genes and interacting proteins, which will aid in the discovery of cancer and disease therapies where Wnt signaling is dysregulated.

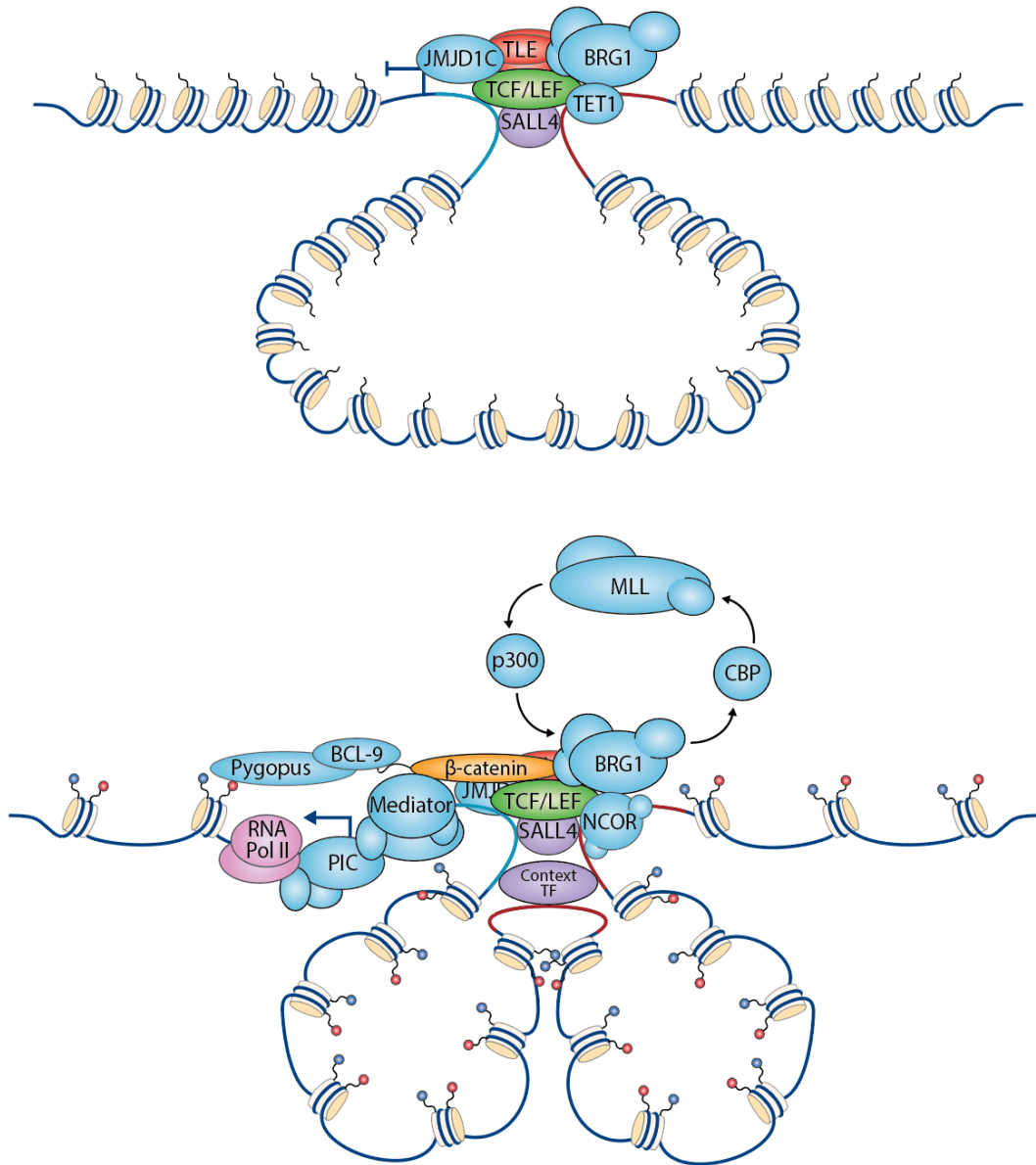


Figure 1. Model of TCF/LEF functions and mechanisms of Wnt target gene regulation.

The ability of TCF/LEFs to bind and bend the DNA at Wnt-responsive elements (WREs), promoting the formation of promoter and enhancer chromatin loops, is crucial in establishing the appropriate higher order chromatin structure and regulation of Wnt target genes. TCF7 and TCF7L1 bind distinct sets of Wnt target genes. In the absence of β -catenin, TCF7L1 interacts with the BAF complex, TET1, SALL4, and JMJD1C in addition to the TLEs, causing widespread histone deacetylation through HDAC recruitment, DNA and histone demethylation, and nucleosomal shuffling, thereby promoting chromatin compaction at promoters and enhancers that represses Wnt target genes. Binding of β -catenin potentially mediates the recruitment of the NCoR complex, allowing for degradation of TCF7L1 and its co-repressors and promoting the subsequent recruitment of transcriptional co-activators. This leads to widespread nucleosomal shuffling and eviction as well as epigenetic acetylation and methylation of histones, promoting an open chromatin structure that permits context-dependent transcription factor binding at additional enhancer elements, forming super enhancers that promote activation of Wnt target genes.

BIBLIOGRAPHY

- Aloysius, A., DasGupta, R., and Dhawan, J. (2018). The transcription factor Lef1 switches partners from β -catenin to Smad3 during muscle stem cell quiescence. *Sci. Signal.* *11*, eaan3000.
- Ang, S.-L., and Behringer, R.R. (2002). 3 – Anterior-Posterior Patterning of the Mouse Body Axis at Gastrulation. In *Mouse Development*, (Elsevier), pp. 37–53.
- Arce, L., Pate, K.T., and Waterman, M.L. (2009). Groucho binds two conserved regions of LEF-1 for HDAC-dependent repression. *BMC Cancer* *9*, 159.
- Atcha, F.A., Munguia, J.E., Li, T.W.H., Hovanes, K., and Waterman, M.L. (2003). A new beta-catenin-dependent activation domain in T cell factor. *J. Biol. Chem.* *278*, 16169–16175.
- Atcha, F.A., Syed, A., Wu, B., Hoverter, N.P., Yokoyama, N.N., Ting, J.-H.T., Munguia, J.E., Mangalam, H.J., Marsh, J.L., and Waterman, M.L. (2007). A unique DNA binding domain converts T-cell factors into strong Wnt effectors. *Mol. Cell. Biol.* *27*, 8352–8363.
- Atlasi, Y., Noori, R., Gaspar, C., Franken, P., Sacchetti, A., Rafati, H., Mahmoudi, T., Decraene, C., Calin, G.A., Merrill, B.J., *et al.* (2013). Wnt Signaling Regulates the Lineage Differentiation Potential of Mouse Embryonic Stem Cells through Tcf3 Down-Regulation. *PLoS Genet.* *9*.
- Avilion, A.A., Nicolis, S.K., Pevny, L.H., Perez, L., Vivian, N., and Lovell-Badge, R. (2003). Multipotent cell lineages in early mouse development on SOX2 function. *Genes Dev.* *17*, 126–140.
- Bakre, M.M., Hoi, A., Mong, J.C.Y., Koh, Y.Y., Wong, K.Y., and Stanton, L.W. (2007). Generation of multipotential mesendodermal progenitors from mouse embryonic stem cells via sustained Wnt pathway activation. *J. Biol. Chem.* *282*, 31703–31712.
- Barker, N., Huls, G., Korinek, V., and Clevers, H. (1999). Restricted high level expression of Tcf-4 protein in intestinal and mammary gland epithelium. *Am. J. Pathol.* *154*, 29–35.
- Barker, N., Hurlstone, a, Musisi, H., Miles, a, Bienz, M., and Clevers, H. (2001). The chromatin remodelling factor Brg-1 interacts with beta-catenin to promote target gene activation. *EMBO J.* *20*, 4935–4943.
- Barutcu, A.R., Lajoie, B.R., Fritz, A.J., McCord, R.P., Nickerson, J.A., Van Wijnen, A.J., Lian, J.B., Stein, J.L., Dekker, J., Stein, G.S., *et al.* (2016). SMARCA4 regulates gene expression and higherorder chromatin structure in proliferating mammary epithelial cells. *Genome Res.* *26*, 1188–

1201.

Beddington, R.S.P., and Robertson, E.J. (1999). Axis development and early asymmetry in mammals. *Cell* *96*, 195–209.

Van Beest, M., Dooijes, D., Van De Wetering, M., Kjaerulff, S., Bonvin, A., Nielsen, O., and Clevers, H. (2000). Sequence-specific high mobility group box factors recognize 10-12-base pair minor groove motifs. *J. Biol. Chem.* *275*, 27266–27273.

Behrens, J., von Kries, J.P., Kühl, M., Bruhn, L., Wedlich, D., Grosschedl, R., and Birchmeier, W. (1996). Functional interaction of beta-catenin with the transcription factor LEF-1. *Nature* *382*, 638–642.

ten Berge, D., Koole, W., Fuerer, C., Fish, M., Eroglu, E., and Nusse, R. (2008). Wnt Signaling Mediates Self-Organization and Axis Formation in Embryoid Bodies. *Cell Stem Cell* *3*, 508–518.

ten Berge, D., Kurek, D., Blauwkamp, T., Koole, W., Maas, A., Eroglu, E., Siu, R.K., and Nusse, R. (2011). Embryonic stem cells require Wnt proteins to prevent differentiation to epiblast stem cells. *Nat. Cell Biol.* *13*, 1070–1075.

Biechele, S., Cockburn, K., Lanner, F., Cox, B.J., and Rossant, J. (2013). Porcn-dependent Wnt signaling is not required prior to mouse gastrulation. *Development* *140*, 2961–2971.

Blauwkamp, T. a., Nigam, S., Ardehali, R., Weissman, I.L., and Nusse, R. (2012). Endogenous Wnt signalling in human embryonic stem cells generates an equilibrium of distinct lineage-specified progenitors. *Nat. Commun.* *3*, 1070.

Böhm, J., Sustmann, C., Wilhelm, C., and Kohlhase, J. (2006). SALL4 is directly activated by TCF/LEF in the canonical Wnt signaling pathway. *Biochem. Biophys. Res. Commun.* *348*, 898–907.

Boroviak, T., Loos, R., Bertone, P., Smith, A., and Nichols, J. (2014). Developmental Cell The ability of inner cell mass cells to self-renew as embryonic stem cells is acquired upon epiblast specification. *Nat. Cell Biol.* *16*, 516–528.

Boyer, L.A., Tong, I.L., Cole, M.F., Johnstone, S.E., Levine, S.S., Zucker, J.P., Guenther, M.G., Kumar, R.M., Murray, H.L., Jenner, R.G., *et al.* (2005). Core transcriptional regulatory circuitry in human embryonic stem cells. *Cell* *122*, 947–956.

Brantjes, H., Roose, J., Wetering, M. Van De, and Clevers, H. (2001). All Tcf HMG box

transcription factors interact with Groucho-related co-repressors. *Nucleic Acids Res.* *29*, 1410.

Brons, I.G.M., Smithers, L.E., Trotter, M.W.B., Rugg-Gunn, P., Sun, B., Chuva De Sousa Lopes, S.M., Howlett, S.K., Clarkson, A., Ahrlund-Richter, L., Pedersen, R.A., *et al.* (2007). Derivation of pluripotent epiblast stem cells from mammalian embryos. *Nature* *448*, 191–195.

Buecker, C., Srinivasan, R., Wu, Z., Calo, E., Acampora, D., Faial, T., Simeone, A., Tan, M., Swigut, T., and Wysocka, J. (2014). Reorganization of enhancer patterns in transition from naive to primed pluripotency. *Cell Stem Cell* *14*, 838–853.

Cadigan, K.M., and Waterman, M.L. (2012). TCF/LEFs and Wnt signaling in the nucleus. *Cold Spring Harb. Perspect. Biol.* *4*.

Cao, Q., Shen, Y., Zheng, W., Liu, H., and Liu, C. (2018). Tcf711 promotes transcription of Kruppel-like factor 4 during *Xenopus* embryogenesis. *32*, 215–221.

Carrera, I., Janody, F., Leeds, N., Duveau, F., and Treisman, J.E. (2008). Pygopus activates Wingless target gene transcription through the mediator complex subunits Med12 and Med13. *Proc. Natl. Acad. Sci. U. S. A.* *105*, 6644–6649.

Chambers, I., Colby, D., Robertson, M., Nichols, J., Lee, S., Tweedie, S., and Smith, A. (2003). Functional expression cloning of Nanog, a pluripotency sustaining factor in embryonic stem cells. *Cell* *113*, 643–655.

Chambers, I., Silva, J., Colby, D., Nichols, J., Nijmeijer, B., Robertson, M., Vrana, J., Jones, K., Grotewold, L., and Smith, A. (2007). Nanog safeguards pluripotency and mediates germline development. *Nature* *450*, 1230–1234.

Chatterjee, S.S., Saj, A., Gocha, T., Murphy, M., Gonsalves, F.C., Zhang, X., Hayward, P., Oksuz, B.A., Shen, S.S., Madar, A., *et al.* (2015). Inhibition of β -catenin-TCF1 interaction delays differentiation of mouse embryonic stem cells. *J. Cell Biol.* *211*, 39–51.

Chen, X., Xu, H., Yuan, P., Fang, F., Huss, M., Vega, V.B., Wong, E., Orlov, Y.L., Zhang, W., Jiang, J., *et al.* (2008). Integration of External Signaling Pathways with the Core Transcriptional Network in Embryonic Stem Cells. *Cell* *133*, 1106–1117.

Chew, J.-L., Loh, Y.-H., Zhang, W., Chen, X., Tam, W.-L., Yeap, L.-S., Li, P., Ang, Y.-S., Lim, B., Robson, P., *et al.* (2005). Reciprocal transcriptional regulation of Pou5f1 and Sox2 via the Oct4/Sox2 complex in embryonic stem cells. *Mol. Cell. Biol.* *25*, 6031–6046.

- Chia, N.-Y., Chan, Y.-S., Feng, B., Lu, X., Orlov, Y.L., Moreau, D., Kumar, P., Yang, L., Jiang, J., Lau, M.-S., *et al.* (2010). A genome-wide RNAi screen reveals determinants of human embryonic stem cell identity. *Nature* *468*, 316–320.
- Chodaparambil, J. V., Pate, K.T., Hepler, M.R.D., Tsai, B.P., Muthurajan, U.M., Luger, K., Waterman, M.L., and Weis, W.I. (2014). Molecular functions of the TLE tetramerization domain in Wnt target gene repression. *EMBO J.* *33*, 719–731.
- Chodelkova, O., Masek, J., Korinek, V., Kozmik, Z., and Machon, O. (2018). Tcf7L2 is essential for neurogenesis in the developing mouse neocortex. *Neural Dev.* *13*, 1–10.
- Choi, W. Il, Jeon, B.N., Yoon, J.H., Koh, D.I., Kim, M.H., Yu, M.Y., Lee, K.M., Kim, Y., Kim, K., Hur, S.S., *et al.* (2013). The proto-oncoprotein FBI-1 interacts with MBD3 to recruit the Mi-2/NuRD-HDAC complex and BCoR and to silence p21WAF/CDKN1A by DNA methylation. *Nucleic Acids Res.* *41*, 6403–6420.
- Cirera-Salinas, D., Yu, J., Bodak, M., Ngondo, R.P., Herbert, K.M., and Ciaudo, C. (2017). Noncanonical function of DGCR8 controls mESC exit from pluripotency. *J. Cell Biol.* *216*, 355–366.
- Clevers, H., Loh, K.M., and Nusse, R. (2014). Stem cell signaling. An integral program for tissue renewal and regeneration: Wnt signaling and stem cell control. *Science* *346*, 1248012.
- Cole, M.F., Johnstone, S.E., Newman, J.J., Kagey, M.H., and Young, R.A. (2008). Tcf3 is an integral component of the core regulatory circuitry of embryonic stem cells. *Genes Dev.* *22*, 746–755.
- Currier, N., Chea, K., Hlavacova, M., Sussman, D.J., Seldin, D.C., and Dominguez, I. (2010). Dynamic expression of a LEF-EGFP WNT reporter in mouse development and cancer. *Genesis* *48*, 183–194.
- Danielian, P.S., and McMahon, A.P. (1996). Engrailed-1 as a target of the Wnt-1 signalling pathway in vertebrate midbrain development. *Nature* *383*, 332–334.
- Daniels, D.L., and Weis, W.I. (2005). Beta-catenin directly displaces Groucho/TLE repressors from Tcf/Lef in Wnt-mediated transcription activation. *Nat. Struct. Mol. Biol.* *12*, 364–371.
- DasGupta, R., and Fuchs, E. (1999). Multiple roles for activated LEF/TCF transcription complexes during hair follicle development and differentiation. *Development* *126*, 4557–4568.

- Davidson, K.C., Adams, A.M., Goodson, J.M., McDonald, C.E., Potter, J.C., Berndt, J.D., Biechele, T.L., Taylor, R.J., and Moon, R.T. (2012). Wnt/beta-catenin signaling promotes differentiation, not self-renewal, of human embryonic stem cells and is repressed by Oct4. *Proc Natl Acad Sci U S A* *109*, 4485–4490.
- Defossez, P.-A., Kelly, K.F., Filion, G.J.P., Pérez-Torrado, R., Magdinier, F., Menoni, H., Nordgaard, C.L., Daniel, J.M., and Gilson, E. (2005). The human enhancer blocker CTC-binding factor interacts with the transcription factor Kaiso. *J. Biol. Chem.* *280*, 43017–43023.
- Dixon, J.R., Jung, I., Selvaraj, S., Shen, Y., Antosiewicz-Bourget, J.E., Lee, A.Y., Ye, Z., Kim, A., Rajagopal, N., Xie, W., *et al.* (2015). Chromatin architecture reorganization during stem cell differentiation. *Nature* *518*, 331–336.
- Doble, B.W., Patel, S., Wood, G.A., Kockeritz, L.K., and Woodgett, J.R. (2007). Functional redundancy of GSK-3alpha and GSK-3beta in Wnt/beta-catenin signaling shown by using an allelic series of embryonic stem cell lines. *Dev. Cell* *12*, 957–971.
- Dravid, G., Ye, Z., Hammond, H., Chen, G., Pyle, A., Donovan, P., Yu, X., and Cheng, L. (2005). Defining the Role of Wnt/{beta}-Catenin Signaling in the Survival, Proliferation, and Self-Renewal of Human Embryonic Stem Cells. *Stem Cells* *23*, 1489–1501.
- Duval, A., Rolland, S., Tubacher, E., Bui, H., Thomas, G., and Hamelin, R. (2000). The human T-cell transcription factor-4 gene: Structure, extensive characterization of alternative splicings, and mutational analysis in colorectal cancer cell lines. *Cancer Res.* *60*, 3872–3879.
- Essers, M.A.G., Burgering, B.M.T., and Korswagen, H.C. (2005). in *Oxidative Stress Signaling Functional Interaction Between b -Catenin and FOXO in Oxidative Stress Signaling.* *1181*, 1181–1185.
- Estarás, C., Benner, C., and Jones, K.A. (2014). SMADs and YAP Compete to Control Elongation of β -Catenin: LEF-1-Recruited RNAPII during hESC Differentiation. *Mol. Cell* *58*, 780–793.
- Evans, M.J., and Kaufman, M.H. (1981). Establishment in culture of pluripotential cells from mouse embryos. *Nature* *292*, 154–156.
- Factor, D.C., Corradin, O., Zentner, G.E., Saiakhova, A., Song, L., Chenoweth, J.G., McKay, R.D., Crawford, G.E., Scacheri, P.C., and Tesar, P.J. (2014). Epigenomic comparison reveals activation of “seed” enhancers during transition from naive to primed pluripotency. *Cell Stem Cell* *14*, 854–863.

- Faunes, F., Hayward, P., Descalzo, S.M., Chatterjee, S.S., Balayo, T., Trott, J., Christoforou, A., Ferrer-Vaquer, A., Hadjantonakis, A.K., Dasgupta, R., *et al.* (2013). A membrane-associated beta-catenin/Oct4 complex correlates with ground-state pluripotency in mouse embryonic stem cells. *Development* *140*, 1171–1183.
- Festuccia, N., Osorno, R., Halbritter, F., Karwacki-Neisius, V., Navarro, P., Colby, D., Wong, F., Yates, A., Tomlinson, S.R., and Chambers, I. (2012). Esrrb is a direct Nanog target gene that can substitute for Nanog function in pluripotent cells. *Cell Stem Cell* *11*, 477–490.
- Fidalgo, M., Faiola, F., Pereira, C., Ding, J., Saunders, A., Gingold, J., Schaniel, C., Lemischka, I.R., Silva, J.C.R., and Wang, J. (2012). Zfp281 mediates Nanog autorepression through recruitment of the NuRD complex and inhibits somatic cell reprogramming. *Proc. Natl. Acad. Sci. U. S. A.* *109*, 16202–16207.
- Fidalgo, M., Huang, X., Guallar, D., Sanchez-Priego, C., Valdes, V.J., Saunders, A., Ding, J., Wu, W.S., Clavel, C., and Wang, J. (2016). Zfp281 Coordinates Opposing Functions of Tet1 and Tet2 in Pluripotent States. *Cell Stem Cell* *19*, 355–369.
- Fiedler, M., Sánchez-Barrena, M.J., Nekrasov, M., Mieszczanek, J., Rybin, V., Müller, J., Evans, P., and Bienz, M. (2008). Decoding of Methylated Histone H3 Tail by the Pygo-BCL9 Wnt Signaling Complex. *Mol. Cell* *30*, 507–518.
- Filali, M., Cheng, N., Abbott, D., Leontiev, V., and Engelhardt, J.F. (2002). Wnt-3A/ β -catenin signaling induces transcription from the LEF-1 promoter. *J. Biol. Chem.* *277*, 33398–33410.
- Flack, J.E., Mieszczanek, J., Novcic, N., and Bienz, M. (2017). Wnt-Dependent Inactivation of the Groucho/TLE Co-repressor by the HECT E3 Ubiquitin Ligase Hyd/UBR5. *Mol. Cell* 1–13.
- Fossat, N., Jones, V., Khoo, P.-L., Bogani, D., Hardy, A., Steiner, K., Mukhopadhyay, M., Westphal, H., Nolan, P.M., Arkell, R., *et al.* (2011). Stringent requirement of a proper level of canonical WNT signalling activity for head formation in mouse embryo. *Development* *138*, 667–676.
- Frietze, S., Wang, R., Yao, L., Tak, Y.G., Ye, Z., Gaddis, M., Witt, H., Farnham, P.J., and Jin, V.X. (2012). Cell type-specific binding patterns reveal that TCF7L2 can be tethered to the genome by association with GATA3. *Genome Biol.* *13*, R52.
- Funa, N.S., Schachter, K.A., Lerdrup, M., Ekberg, J., Hess, K., Dietrich, N., Honoré, C., Hansen, K., and Semb, H. (2015). β -Catenin Regulates Primitive Streak Induction through Collaborative

Interactions with SMAD2/SMAD3 and OCT4. *Cell Stem Cell* *16*, 639–652.

Gadue, P., Huber, T.L., Paddison, P.J., and Keller, G.M. (2006). Wnt and TGF-beta signaling are required for the induction of an in vitro model of primitive streak formation using embryonic stem cells. *Proc. Natl. Acad. Sci. U. S. A.* *103*, 16806–16811.

Gafni, O., Weinberger, L., Mansour, A.A., Manor, Y.S., Chomsky, E., Ben-Yosef, D., Kalma, Y., Viukov, S., Maza, I., Zviran, A., *et al.* (2013). Derivation of novel human ground state naive pluripotent stem cells. *Nature* *504*, 282–286.

Galceran, J., Fariñas, I., Depew, M.J., Clevers, H., and Grosschedl, R. (1999). Wnt3a^{-/-}-like phenotype and limb deficiency in Lef1^(-/-)Tcf1^(-/-) mice. *Genes Dev.* *13*, 709–717.

Galceran, J., Miyashita-Lin, E.M., Devaney, E., Rubenstein, J.L., and Grosschedl, R. (2000). Hippocampus development and generation of dentate gyrus granule cells is regulated by LEF1. *Development* *127*, 469–482.

Galceran, J., Hsu, S.C., and Grosschedl, R. (2001). Rescue of a Wnt mutation by an activated form of LEF-1: regulation of maintenance but not initiation of Brachyury expression. *Proc. Natl. Acad. Sci. U. S. A.* *98*, 8668–8673.

Galonska, C., Ziller, M.J., Karnik, R., and Meissner, A. (2015). Ground State Conditions Induce Rapid Reorganization of Core Pluripotency Factor Binding before Global Epigenetic Reprogramming. *Cell Stem Cell* *17*, 462–470.

van Genderon, C., Okamura, R.M., Farinas, I., Quo, R.-G., Parslow, T.G., Bruhn, L., and Grosschedl, R. (1994). Development of several organs that require inductive epithelial-mesenchymal interactions is impaired in LEF-1 deficient mice. *Genes Dev.* *8*, 2691–2703.

Giakountis, A., Moulos, P., Zarkou, V., Oikonomou, C., Harokopos, V., Hatzigeorgiou, A.G., Reczko, M., and Hatzis, P. (2016). A Positive Regulatory Loop between a Wnt-Regulated Non-coding RNA and ASCL2 Controls Intestinal Stem Cell Fate. *Cell Rep.* *15*, 2588–2596.

Giese, K., Cox, J., and Grosschedl, R. (1992). The HMG domain of lymphoid enhancer factor 1 bends DNA and facilitates assembly of functional nucleoprotein structures. *Cell* *69*, 185–195.

Gómez-Díaz, E., and Corces, V.G. (2014). Architectural proteins: Regulators of 3D genome organization in cell fate. *Trends Cell Biol.* *24*, 703–711.

Gómez-Orte, E., Sáenz-Narciso, B., Moreno, S., and Cabello, J. (2013). Multiple functions of the

noncanonical Wnt pathway. *Trends Genet.* 29, 545–553.

Gonzalez-Sandoval, A., and Gasser, S.M. (2016). On TADs and LADs: Spatial Control Over Gene Expression. *Trends Genet.* 32, 485–495.

Grainger, S., and Willert, K. (2018). Mechanisms of Wnt signaling and control. *Wiley Interdiscip. Rev. Syst. Biol. Med.* 10, 1–22.

Greber, B., Wu, G., Bernemann, C., Joo, J.Y., Han, D.W., Ko, K., Tapia, N., Sabour, D., Sternecker, J., Tesar, P., *et al.* (2010). Conserved and Divergent Roles of FGF Signaling in Mouse Epiblast Stem Cells and Human Embryonic Stem Cells. *Cell Stem Cell* 6, 215–226.

Gregorieff, A., Grosschedl, R., and Clevers, H. (2004). Hindgut defects and transformation of the gastro-intestinal tract in *Tcf4(-)/Tcf1(-)* embryos. *EMBO J.* 23, 1825–1833.

Gregorieff, A., Pinto, D., Begthel, H., Destrée, O., Kielman, M., and Clevers, H. (2005). Expression pattern of Wnt signaling components in the adult intestine. *Gastroenterology* 129, 626–638.

Guo, G., Yang, J., Nichols, J., Hall, J.S., Eyres, I., Mansfield, W., and Smith, A. (2009). *Klf4* reverts developmentally programmed restriction of ground state pluripotency. *Development* 136, 1063–1069.

Guo, G., Von Meyenn, F., Santos, F., Chen, Y., Reik, W., Bertone, P., Smith, A., and Nichols, J. (2016). Naive Pluripotent Stem Cells Derived Directly from Isolated Cells of the Human Inner Cell Mass. *Stem Cell Reports* 6, 437–446.

Habib, S.J., Chen, B.C., Tsai, F.C., Anastassiadis, K., Meyer, T., Betzig, E., and Nusse, R. (2013). A localized Wnt signal orients asymmetric stem cell division in vitro. *Science* (80-.). 339, 1445–1448.

Haegel, H., Larue, L., Ohsugi, M., Fedorov, L., Herrenknecht, K., and Kemler, R. (1995). Lack of beta-catenin affects mouse development at gastrulation. *Development* 121, 3529–3537.

Hanna, J., Cheng, A.W., Saha, K., Kim, J., Lengner, C.J., Soldner, F., Cassady, J.P., Muffat, J., Carey, B.W., and Jaenisch, R. (2010). Human embryonic stem cells with biological and epigenetic characteristics similar to those of mouse ESCs. *Proc. Natl. Acad. Sci. U. S. A.* 107, 9222–9227.

Hao, J., Li, T.-G., Qi, X., Zhao, D.-F., and Zhao, G.-Q. (2006). WNT/beta-catenin pathway up-regulates *Stat3* and converges on LIF to prevent differentiation of mouse embryonic stem cells.

Dev. Biol. 290, 81–91.

Hatzis, P., van der Flier, L.G., van Driel, M.A., Guryev, V., Nielsen, F., Denissov, S., Nijman, I.J., Koster, J., Santo, E.E., Welboren, W., *et al.* (2008). Genome-wide pattern of TCF7L2/TCF4 chromatin occupancy in colorectal cancer cells. *Mol. Cell. Biol.* 28, 2732–2744.

Hayashi, K., Lopes, S.M.C. de S., Tang, F., and Surani, M.A. (2008). Dynamic Equilibrium and Heterogeneity of Mouse Pluripotent Stem Cells with Distinct Functional and Epigenetic States. *Cell Stem Cell* 3, 391–401.

Hecht, a, Vleminckx, K., Stemmler, M.P., van Roy, F., and Kemler, R. (2000). The p300/CBP acetyltransferases function as transcriptional coactivators of beta-catenin in vertebrates. *EMBO J.* 19, 1839–1850.

Hnisz, D., Schuijers, J., Lin, C.Y., Weintraub, A.S., Abraham, B.J., Lee, T.I., Bradner, J.E., and Young, R.A. (2015). Convergence of Developmental and Oncogenic Signaling Pathways at Transcriptional Super-Enhancers. *Mol. Cell* 58, 362–370.

Ho, L., Ronan, J.L., Wu, J., Staahl, B.T., Chen, L., Kuo, A., Lessard, J., Nesvizhskii, A.I., Ranish, J., and Crabtree, G.R. (2009). An embryonic stem cell chromatin remodeling complex, esBAF, is essential for embryonic stem cell self-renewal and pluripotency. *Proc Natl Acad Sci U S A* 106, 5181–5186.

Hoffman, J. a, Wu, C.-I., and Merrill, B.J. (2013). Tcf7l1 prepares epiblast cells in the gastrulating mouse embryo for lineage specification. *Development* 140, 1665–1675.

Hough, S.R., Thornton, M., Mason, E., Mar, J.C., Wells, C.A., and Pera, M.F. (2014). Single-cell gene expression profiles define self-renewing, pluripotent, and lineage primed states of human pluripotent stem cells. *Stem Cell Reports* 2, 881–895.

Hovanes, K., Li, T.W., and Waterman, M.L. (2000). The human LEF-1 gene contains a promoter preferentially active in lymphocytes and encodes multiple isoforms derived from alternative splicing. *Nucleic Acids Res.* 28, 1994–2003.

Hovanes, K., Li, T.W., Munguia, J.E., Truong, T., Milovanovic, T., Lawrence Marsh, J., Holcombe, R.F., and Waterman, M.L. (2001). Beta-catenin-sensitive isoforms of lymphoid enhancer factor-1 are selectively expressed in colon cancer. *Nat. Genet.* 28, 53–57.

Hoverter, N.P., Ting, J.-H.H., Sundaresh, S., Baldi, P., and Waterman, M.L. (2012). A

{WNT/p21} circuit directed by the C-clamp, a sequence-specific {DNA} binding domain in {TCFs}. *Mol. Cell. Biol.* *32*, 3648–3662.

Hoverter, N.P., Zeller, M.D., McQuade, M.M., Garibaldi, A., Busch, A., Selwan, E.M., Hertel, K.J., Baldi, P., and Waterman, M.L. (2014). The TCF C-clamp DNA binding domain expands the Wnt transcriptome via alternative target recognition. *Nucleic Acids Res.* *42*, 13615–13632.

Hsu, S.C., Galceran, J., and Grosschedl, R. (1998). Modulation of Transcriptional Regulation by LEF-1 in Response to Wnt-1 Signaling and Association with β -Catenin. *Mol. Cell. Biol.* *18*, 4807–4818.

Hu, Z., and Tee, W.-W. (2017). Enhancers and chromatin structures: regulatory hubs in gene expression and diseases. *Biosci. Rep.* *37*, BSR20160183.

Huang, C., and Qin, D. (2010). Role of Lef1 in sustaining self-renewal in mouse embryonic stem cells. *J. Genet. Genomics* *37*, 441–449.

Huang, Y., Osorno, R., Tsakiridis, A., and Wilson, V. (2012). In Vivo Differentiation Potential of Epiblast Stem Cells Revealed by Chimeric Embryo Formation. *Cell Rep.* *2*, 1571–1578.

Huber, O., Korn, R., McLaughlin, J., Ohsugi, M., Herrmann, B.G., and Kemler, R. (1996). Nuclear localization of beta-catenin by interaction with transcription factor LEF-1. *Mech. Dev.* *59*, 3–10.

Huelsken, J., Vogel, R., Brinkmann, V., Erdmann, B., Birchmeier, C., and Birchmeier, W. (2000). Requirement for beta-catenin in anterior-posterior axis formation in mice. *J. Cell Biol.* *148*, 567–578.

Huynh, K.D., Fischle, W., Verdin, E., and Bardwell, V.J. (2000). BCoR, a novel corepressor involved in BCL-6 repression. *Genes Dev.* *14*, 1810–1823.

De Jaime-Soguero, A., Aulicino, F., Ertaylan, G., Griego, A., Cerrato, A., Tallam, A., del Sol, A., Cosma, M.P., and Lluis, F. (2017). Wnt/Tcf1 pathway restricts embryonic stem cell cycle through activation of the Ink4/Arf locus. *PLoS Genet.* *13*.

Kagey, M.H., Newman, J.J., Bilodeau, S., Zhan, Y., Orlando, D.A., van Berkum, N.L., Ebmeier, C.C., Goossens, J., Rahl, P.B., Levine, S.S., *et al.* (2010). Mediator and cohesin connect gene expression and chromatin architecture. *Nature* *467*, 430–435.

Karantzali, E., Lekakis, V., Ioannou, M., Hadjimichael, C., Papamatheakis, J., and Kretsovali, A. (2011). Sall1 regulates embryonic stem cell differentiation in association with Nanog. *J. Biol.*

Chem. 286, 1037–1045.

Kelly, O.G. (2004). The Wnt co-receptors Lrp5 and Lrp6 are essential for gastrulation in mice. *Development* 131, 2803–2815.

Kelly, K.F., Ng, D.Y., Jayakumaran, G., Wood, G.A., Koide, H., and Doble, B.W. (2011). β -catenin enhances Oct-4 activity and reinforces pluripotency through a TCF-independent mechanism. *Cell Stem Cell* 8, 214–227.

Kennedy, M.W., Chalamalasetty, R.B., Thomas, S., Garriock, R.J., Jailwala, P., and Yamaguchi, T.P. (2016). Sp5 and Sp8 recruit β -catenin and Tcf1-Lef1 to select enhancers to activate Wnt target gene transcription. *Proc. Natl. Acad. Sci.* 113, 201519994.

Khoueiry, R., Sohni, A., Thienpont, B., Luo, X., Velde, J. Vande, Bartocchetti, M., Boeckx, B., Zwijsen, A., Rao, A., Lambrechts, D., *et al.* (2017). Lineage-specific functions of TET1 in the postimplantation mouse embryo. *Nat. Genet.* 49, 1061–1072.

Kiefer, S.M.L., McDill, B.W., Yang, J., and Rauchman, M. (2002). Murine Sall1 represses transcription by recruiting a histone deacetylase complex. *J. Biol. Chem.* 277, 14869–14876.

Kielman, M.F., Rindapää, M., Gaspar, C., van Poppel, N., Breukel, C., van Leeuwen, S., Taketo, M.M., Roberts, S., Smits, R., and Fodde, R. (2002). Apc modulates embryonic stem-cell differentiation by controlling the dosage of beta-catenin signaling. *Nat. Genet.* 32, 594–605.

Kim, C.H., Oda, T., Itoh, M., Jiang, D., Artinger, K.B., Chandrasekharappa, S.C., Driever, W., and Chitnis, A.B. (2000). Repressor activity of Headless/Tcf3 is essential for vertebrate head formation. *Nature* 407, 913–916.

Kim, J., Chu, J., Shen, X., Wang, J., and Orkin, S.H. (2008). An extended transcriptional network for pluripotency of embryonic stem cells. *Cell* 132, 1049–1061.

Kim, J.J., Khalid, O., Vo, S., Sun, H.H., Wong, D.T.W., and Kim, Y. (2012). A novel regulatory factor recruits the nucleosome remodeling complex to wingless integrated (Wnt) signaling gene promoters in mouse embryonic stem cells. *J. Biol. Chem.* 287, 41103–41117.

Kim, K., Cho, J., Hilzinger, T.S., Nunns, H., Liu, A., Ryba, B.E., and Goentoro, L. (2017). Two-Element Transcriptional Regulation in the Canonical Wnt Pathway. *Curr. Biol.* 27, 2357–2364.e5.

Kim, S., Xu, X., Hecht, A., and Boyer, T.G. (2006). Mediator is a transducer of Wnt/ β -catenin signaling. *J. Biol. Chem.* 281, 14066–14075.

Kitagawa, M., Hatakeyama, S., Shirane, M., Matsumoto, M., Ishida, N., Hattori, K., Nakamichi, I., Kikuchi, A., Nakayama, K., and Nakayama, K. (1999). An F-box protein, FWD1, mediates ubiquitin-dependent proteolysis of beta-catenin. *Embo J* *18*, 2401–2410.

Kojima, Y., Kaufman-Francis, K., Studdert, J.B., Steiner, K.A., Power, M.D., Loebel, D.A.F., Jones, V., Hor, A., De Alencastro, G., Logan, G.J., *et al.* (2014). The transcriptional and functional properties of mouse epiblast stem cells resemble the anterior primitive streak. *Cell Stem Cell* *14*, 107–120.

Korinek, V., Barker, N., Willert, K., Molenaar, M., Roose, J., Wagenaar, G., Markman, M., Lamers, W., Destree, O., and Clevers, H. (1998a). Two members of the Tcf family implicated in Wnt/beta-catenin signaling during embryogenesis in the mouse. *Mol. Cell. Biol.* *18*, 1248–1256.

Korinek, V., Barker, N., Moerer, P., van Donselaar, E., Huls, G., Peters, P.J., and Clevers, H. (1998b). Depletion of epithelial stem-cell compartments in the small intestine of mice lacking Tcf-4. *Nat. Genet.* *19*, 379–383.

Kramps, T., Peter, O., Brunner, E., Nellen, D., Froesch, B., Chatterjee, S., Murone, M., Züllig, S., and Basler, K. (2002). Wnt/Wingless signaling requires BCL9/legless-mediated recruitment of pygopus to the nuclear β -catenin-TCF complex. *Cell* *109*, 47–60.

Kratochwil, K., Galceran, J., Tontsch, S., Roth, W., and Grosschedl, R. (2002). FGF4, a direct target of LEF1 and Wnt signaling, can rescue the arrest of tooth organogenesis in Lef1^{-/-} mice. *Genes Dev.* *16*, 3173–3185.

Ku, A.T., Shaver, T.M., Rao, A.S., Howard, J.M., Rodriguez, C.N., Miao, Q., Garcia, G., Le, D., Yang, D., Borowiak, M., *et al.* (2017). TCF711 promotes skin tumorigenesis independently of β -catenin through induction of LCN2. *Elife* *6*, 1–32.

Kumar, A., Chalamalasetty, R.B., Kennedy, M.W., Thomas, S., Inala, S.N., Garriock, R.J., and Yamaguchi, T.P. (2016). β -Catenin / Tcf1 Complex. *36*, 1793–1802.

Kumar, R.M., Cahan, P., Shalek, A.K., Satija, R., Keyser, A.D., Li, H., Zhang, J., Pardee, K., Gennert, D., Trombetta, J.J., *et al.* (2014). Deconstructing transcriptional heterogeneity in pluripotent stem cells. *Nature* *516*, 56–61.

Kunath, T., Saba-El-Leil, M.K., Almousaillekh, M., Wray, J., Meloche, S., and Smith, A. (2007). FGF stimulation of the Erk1/2 signalling cascade triggers transition of pluripotent embryonic stem

cells from self-renewal to lineage commitment. *Development* *134*, 2895–2902.

Kurek, D., Neagu, A., Tastemel, M., Tüysüz, N., Lehmann, J., Van De Werken, H.J.G., Philipsen, S., Van Der Linden, R., Maas, A., Van Ijcken, W.F.J., *et al.* (2015). Endogenous WNT signals mediate BMP-induced and spontaneous differentiation of epiblast stem cells and human embryonic stem cells. *Stem Cell Reports* *4*, 114–128.

Lanner, F., Lee, K.L., Sohl, M., Holmborn, K., Yang, H., Wilbertz, J., Poellinger, L., Rossant, J., and Farnebo, F. (2010). Heparan sulfation-dependent fibroblast growth factor signaling maintains embryonic stem cells primed for differentiation in a heterogeneous state. *Stem Cells* *28*, 191–200.

Laschak, M., Bechtel, M., Spindler, K.D., and Hessenauer, A. (2011). Inability of NCoR/SMRT to repress androgen receptor transcriptional activity in prostate cancer cell lines. *Int. J. Mol. Med.* *28*, 645–651.

Li, J., and Wang, C.Y. (2008). TBL1-TBLR1 and beta-catenin recruit each other to Wnt target-gene promoter for transcription activation and oncogenesis. *Nat. Cell Biol.* *10*, 160–169.

Li, L., Lyu, X., Hou, C., Takenaka, N., Nguyen, H.Q., Ong, C.T., Cubeñas-Potts, C., Hu, M., Lei, E.P., Bosco, G., *et al.* (2015). Widespread Rearrangement of 3D Chromatin Organization Underlies Polycomb-Mediated Stress-Induced Silencing. *Mol. Cell* *58*, 216–231.

Li, T.W.-H., Ting, J.-H.T., Yokoyama, N.N., Bernstein, A., van de Wetering, M., and Waterman, M.L. (2006). Wnt activation and alternative promoter repression of LEF1 in colon cancer. *Mol. Cell. Biol.* *26*, 5284–5299.

Li, V.S.W., Ng, S.S., Boersema, P.J., Low, T.Y., Karthaus, W.R., Gerlach, J.P., Mohammed, S., Heck, A.J.R., Maurice, M.M., Mahmoudi, T., *et al.* (2012). Wnt Signaling through Inhibition of β -Catenin Degradation in an Intact Axin1 Complex. *Cell* *149*, 1245–1256.

Lien, W.-H., Polak, L., Lin, M., Lay, K., Zheng, D., and Fuchs, E. (2014). In vivo transcriptional governance of hair follicle stem cells by canonical Wnt regulators. *Nat. Cell Biol.* *16*, 179–190.

Lim, C.Y., Tam, W.L., Zhang, J., Ang, H.S., Jia, H., Lipovich, L., Ng, H.H., Wei, C.L., Sung, W.K., Robson, P., *et al.* (2008). Sall4 Regulates Distinct Transcription Circuitries in Different Blastocyst-Derived Stem Cell Lineages. *Cell Stem Cell* *3*, 543–554.

Liu, C., Li, Y., Semenov, M., Han, C., Baeg, G.H., Tan, Y., Zhang, Z., Lin, X., and He, X. (2002). Control of beta-catenin phosphorylation/degradation by a dual-kinase mechanism. *Cell* *108*, 837–

847.

Liu, F., van den Broek, O., Destrée, O., and Hoppler, S. (2005). Distinct roles for *Xenopus* Tcf/Lef genes in mediating specific responses to Wnt/beta-catenin signalling in mesoderm development. *Development* *132*, 5375–5385.

Liu, P., Wakamiya, M., Shea, M.J., Albrecht, U., Behringer, R.R., and Bradley, A. (1999). Requirement for Wnt3 in vertebrate axis formation. *Nat. Genet.* *22*, 361–365.

Loh, Y.-H., Wu, Q., Chew, J.-L., Vega, V.B., Zhang, W., Chen, X., Bourque, G., George, J., Leong, B., Liu, J., *et al.* (2006). The Oct4 and Nanog transcription network regulates pluripotency in mouse embryonic stem cells. *Nat. Genet.* *38*, 431–440.

Love, J.J., Li, X., Case, D.A., Giese, K., Grosschedl, R., and Wright, P.E. (1995). Structural basis for DNA bending by the architectural transcription factor LEF-1. *Nature* *376*, 791–795.

Lustig, B., Jerchow, B., Sachs, M., Weiler, S., Pietsch, T., Karsten, U., van de Wetering, M., Clevers, H., Schlag, P.M., Birchmeier, W., *et al.* (2002). Negative feedback loop of Wnt signaling through upregulation of conductin/axin2 in colorectal and liver tumors. *Mol. Cell. Biol.* *22*, 1184–1193.

Lyashenko, N., Winter, M., Migliorini, D., Biechele, T., Moon, R.T., and Hartmann, C. (2011). Differential requirement for the dual functions of β -catenin in embryonic stem cell self-renewal and germ layer formation. *Nat. Cell Biol.* *13*, 753–761.

Ma, Y., Cui, W., Yang, J., Qu, J., Di, C., Amin, H.M., Lai, R., Ritz, J., Krause, D.S., and Chai, L. (2006). SALL4, a novel oncogene, is constitutively expressed in human acute myeloid leukemia (AML) and induces AML in transgenic mice. *Blood* *108*, 2726–2735.

Maretto, S., Cordenonsi, M., Dupont, S., Braghetta, P., Broccoli, V., Hassan, A.B., Volpin, D., Bressan, G.M., and Piccolo, S. (2003). Mapping Wnt/beta-catenin signaling during mouse development and in colorectal tumors. *Proc. Natl. Acad. Sci. U. S. A.* *100*, 3299–3304.

Marks, H., Kalkan, T., Menafra, R., Denissov, S., Jones, K., Hofemeister, H., Nichols, J., Kranz, A., Francis Stewart, A., Smith, A., *et al.* (2012). The transcriptional and epigenomic foundations of ground state pluripotency. *Cell* *149*, 590–604.

Marson, A., Levine, S.S., Cole, M.F., Frampton, G.M., Brambrink, T., Johnstone, S., Guenther, M.G., Johnston, W.K., Wernig, M., Newman, J., *et al.* (2008). Connecting microRNA Genes to

the Core Transcriptional Regulatory Circuitry of Embryonic Stem Cells. *Cell* *134*, 521–533.

Martello, G., Sugimoto, T., Diamanti, E., Joshi, A., Hannah, R., Ohtsuka, S., Göttgens, B., Niwa, H., and Smith, A. (2012). Esrrb is a pivotal target of the Gsk3/Tcf3 axis regulating embryonic stem cell self-renewal. *Cell Stem Cell* *11*, 491–504.

Martello, G., Bertone, P., and Smith, A. (2013). Identification of the missing pluripotency mediator downstream of leukaemia inhibitory factor. *EMBO J.* *32*, 2561–2574.

Martin, G.R. (1981). Isolation of a pluripotent cell line from early mouse embryos cultured in medium conditioned by teratocarcinoma stem cells. *Proc. Natl. Acad. Sci. U. S. A.* *78*, 7634–7638.

Masui, S., Nakatake, Y., Toyooka, Y., Shimosato, D., Yagi, R., Takahashi, K., Okochi, H., Okuda, A., Matoba, R., Sharov, A.A., *et al.* (2007). Pluripotency governed by Sox2 via regulation of Oct3/4 expression in mouse embryonic stem cells. *Nat. Cell Biol.* *9*, 625–635.

McDonald, A.C.H., Biechele, S., Rossant, J., and Stanford, W.L. (2014). Sox17-mediated XEN cell conversion identifies dynamic networks controlling cell-fate decisions in embryo-derived stem cells. *Cell Rep.* *9*, 780–793.

McMahon, A.P., and Bradley, A. (1990). The Wnt-1 (int-1) proto-oncogene is required for development of a large region of the mouse brain. *Cell* *62*, 1073–1085.

Merrill, B.J., Gat, U., DasGupta, R., and Fuchs, E. (2001). Tcf3 and Lef1 regulate lineage differentiation of multipotent stem cells in skin. *Genes Dev.* *15*, 1688–1705.

Merrill, B.J., Pasolli, H.A., Polak, L., Rendl, M., García-García, M.J., Anderson, K. V, and Fuchs, E. (2004). Tcf3: a transcriptional regulator of axis induction in the early embryo. *Development* *131*, 263–274.

Mitsui, K., Tokuzawa, Y., Itoh, H., Segawa, K., Murakami, M., Takahashi, K., Maruyama, M., Maeda, M., and Yamanaka, S. (2003). The homeoprotein Nanog is required for maintenance of pluripotency in mouse epiblast and ES cells. *Cell* *113*, 631–642.

Molenaar, M., Van De Wetering, M., Oosterwegel, M., Peterson-Maduro, J., Godsave, S., Korinek, V., Roose, J., Destree, O., and Clevers, H. (1996). XTcf-3 transcription factor mediates β -catenin-induced axis formation in xenopus embryos. *Cell* *86*, 391–399.

Morrison, G., Scognamiglio, R., Trumpp, A., and Smith, A. (2016). Convergence of cMyc and β -catenin on Tcf711 enables endoderm specification. *EMBO J.* *35*, 356–368.

- Mosimann, C., Hausmann, G., and Basler, K. (2009). Beta-catenin hits chromatin: regulation of Wnt target gene activation. *Nat. Rev. Mol. Cell Biol.* *10*, 276–286.
- Nagy, A., Rossant, J., Nagy, R., Abramow-Newerly, W., and Roder, J.C. (1993). Derivation of completely cell culture-derived mice from early-passage embryonic stem cells. *Proc. Natl. Acad. Sci. U. S. A.* *90*, 8424–8428.
- Najm, F.J., Chenoweth, J.G., Anderson, P.D., Nadeau, J.H., Redline, R.W., McKay, R.D.G., and Tesar, P.J. (2011). Isolation of epiblast stem cells from preimplantation mouse embryos. *Cell Stem Cell* *8*, 318–325.
- Nguyen, H., Merrill, B.J., Polak, L., Nikolova, M., Rendl, M., Shaver, T.M., Pasolli, H.A., and Fuchs, E. (2009). Tcf3 and Tcf4 are essential for long-term homeostasis of skin epithelia. *Nat. Genet.* *41*, 1068–1075.
- Nichols, J., and Smith, A. (2009). Naive and Primed Pluripotent States. *Cell Stem Cell* *4*, 487–492.
- Nichols, J., Zevnik, B., Anastassiadis, K., Niwa, H., Klewe-Nebenius, D., Chambers, I., Scholer, H., and Smith, A. (1998). Formation of pluripotent stem cells in the mammalian embryo depends on the POU transcription factor Oct4. *Cell* *95*, 379–391.
- Niwa, H., Burdon, T., Chambers, I., and Smith, A. (1998). Self-renewal of pluripotent embryonic stem cells is mediated via activation of STAT3. *Genes Dev.* *12*, 2048–2060.
- Niwa, H., Miyazaki, J., and Smith, A.G. (2000). Quantitative expression of Oct-3/4 defines differentiation, dedifferentiation or self-renewal of ES cells. *Nat. Genet.* *24*, 372–376.
- Novo, C.L., Tang, C., Ahmed, K., Djuric, U., Fussner, E., Mullin, N.P., Morgan, N.P., Hayre, J., Sienerth, A.R., Elderkin, S., *et al.* (2016). The pluripotency factor Nanogregulates pericentromeric heterochromatin organization in mouse embryonic stem cells. *Genes Dev.* *30*, 1101–1115.
- Nusse, R., and Clevers, H. (2017). Wnt/ β -Catenin Signaling, Disease, and Emerging Therapeutic Modalities. *Cell* *169*, 985–999.
- Nusse, R., and Varmus, H. (2012). Three decades of Wnts: A personal perspective on how a scientific field developed. *EMBO J.* *31*, 2670–2684.
- Nusse, R., and Varmus, H.E. (1982). Many tumors induced by the mouse mammary tumor virus contain a provirus integrated in the same region of the host genome. *Cell* *31*, 99–109.

- Ogawa, K., Nishinakamura, R., Iwamatsu, Y., Shimosato, D., and Niwa, H. (2006). Synergistic action of Wnt and LIF in maintaining pluripotency of mouse ES cells. *Biochem. Biophys. Res. Commun.* *343*, 159–166.
- Ogawa, S., Lozach, J., Jepsen, K., Sawka-Verhelle, D., Perissi, V., Sasik, R., Rose, D.W., Johnson, R.S., Rosenfeld, M.G., and Glass, C.K. (2004). A nuclear receptor corepressor transcriptional checkpoint controlling activator protein 1-dependent gene networks required for macrophage activation. *Proc. Natl. Acad. Sci.* *101*, 14461–14466.
- Okamura, R.M., Sigvardsson, M., Galceran, J., Verbeek, S., Clevers, H., and Grosschedl, R. (1998). Redundant Regulation of T Cell Differentiation and TCR α Gene Expression by the Transcription Factors LEF-1 and TCF-1. *J. Biol. Chem.* *273*, 11–20.
- Oosterwegel, M., van de Wetering, M., Timmerman, J., Kruisbeek, a, Destree, O., Meijlink, F., and Clevers, H. (1993). Differential expression of the HMG box factors TCF-1 and LEF-1 during murine embryogenesis. *Development* *118*, 439–448.
- Palstra, R.J., and Grosveld, F. (2012). Transcription factor binding at enhancers: Shaping a genomic regulatory landscape in flux. *Front. Genet.* *3*, 1–12.
- Panne, D., Maniatis, T., and Harrison, S.C. (2007). An Atomic Model of the Interferon- β Enhanceosome. *Cell* *129*, 1111–1123.
- Park, M.S., Kausar, R., Kim, M.W., Cho, S.Y., Lee, Y.S., and Lee, M.A. (2015). Tcf7l1-mediated transcriptional regulation of Krüppel-like factor 4 gene. *Animal Cells Syst. (Seoul)*. *19*, 16–29.
- Parker, D.S., Ni, Y.Y., Chang, J.L., Li, J., and Cadigan, K.M. (2008). Wingless Signaling Induces Widespread Chromatin Remodeling of Target Loci. *Mol. Cell. Biol.* *28*, 1815–1828.
- Peifer, M., McCrea, P.D., Green, K.J., Wieschaus, E., and Gumbiner, B.M. (1992). The vertebrate adhesive junction proteins beta-catenin and plakoglobin and the Drosophila segment polarity gene armadillo form a multigene family with similar properties. *J. Cell Biol.* *118*, 681–691.
- Pereira, L., Yi, F., and Merrill, B.J. (2006). Repression of Nanog gene transcription by Tcf3 limits embryonic stem cell self-renewal. *Mol Cell Biol* *26*, 7479–7491.
- Perissi, V., Aggarwal, A., Glass, C.K., Rose, D.W., and Rosenfeld, M.G. (2004). A Corepressor/Coactivator Exchange Complex Required for Transcriptional Activation by Nuclear Receptors and Other Regulated Transcription Factors. *Cell* *116*, 511–526.

- Perissi, V., Scafoglio, C., Zhang, J., Ohgi, K.A., Rose, D.W., Glass, C.K., and Rosenfeld, M.G. (2008). TBL1 and TBLR1 Phosphorylation on Regulated Gene Promoters Overcomes Dual CtBP and NCoR/SMRT Transcriptional Repression Checkpoints. *Mol. Cell* *29*, 755–766.
- Pistocchi, A., Fazio, G., Cereda, A., Ferrari, L., Bettini, L.R., Messina, G., Cotelli, F., Biondi, A., Selicorni, A., and Massa, V. (2013). Cornelia de Lange Syndrome : NIPBL haploinsufficiency downregulates canonical Wnt pathway in zebrafish embryos and patients fibroblasts. *Cell Death Dis.* *4*, e866-9.
- Pomerantz, M.M., Ahmadiyeh, N., Jia, L., Herman, P., Verzi, M.P., Doddapaneni, H., Beckwith, C.A., Chan, J.A., Hills, A., Davis, M., *et al.* (2009). The 8q24 cancer risk variant rs6983267 shows long-range interaction with MYC in colorectal cancer. *Nat. Genet.* *41*, 882–884.
- Porter, A.H., Johnson, N.A., and Tulchinsky, A.Y. (2017). A new mechanism for mendelian dominance in regulatory genetic pathways: Competitive binding by transcription factors. *Genetics* *205*, 101–112.
- Price, F.D., Yin, H., Jones, A., Van Ijcken, W., Grosveld, F., and Rudnicki, M.A. (2013). Canonical Wnt signaling induces a primitive endoderm metastable state in mouse embryonic stem cells. *Stem Cells* *31*, 752–764.
- Ramakrishnan, A.B., Sinha, A., Fan, V.B., and Cadigan, K.M. (2018). The Wnt Transcriptional Switch: TLE Removal or Inactivation? *BioEssays* *40*, 1–6.
- Rao, S.S.P., Huntley, M.H., Durand, N.C., Stamenova, E.K., Bochkov, I.D., Robinson, J.T., Sanborn, A.L., Machol, I., Omer, A.D., Lander, E.S., *et al.* (2014). A 3D map of the human genome at kilobase resolution reveals principles of chromatin looping. *Cell* *159*, 1665–1680.
- Ravindranath, A., and Cadigan, K.M. (2014). Structure-function analysis of the C-clamp of TCF/Pangolin in Wnt/ β -catenin signaling. *PLoS One* *9*, e86180.
- Reya, T., O’Riordan, M., Okamura, R., Devaney, E., Willert, K., Nusse, R., and Grosschedl, R. (2000). Wnt signaling regulates B lymphocyte proliferation through a LEF-1 dependent mechanism. *Immunity* *13*, 15–24.
- Rijsewijk, F., Schuermann, M., Wagenaar, E., Parren, P., Weigel, D., and Nusse, R. (1987). The *Drosophila* homology of the mouse mammary oncogene *int-1* is identical to the segment polarity gene *wingless*. *Cell* *50*, 649–657.

- Rivera-pérez, J.A., Hadjantonakis, A., Wu, D.K., Kelley, M.W., Nichols, J., and Smith, A. (2014). The Dynamics of Morphogenesis in the Early Mouse Embryo. 1–18.
- Rodda, D.J., Chew, J.-L., Lim, L.-H., Loh, Y.-H., Wang, B., Ng, H.-H., and Robson, P. (2005). Transcriptional regulation of *nanog* by OCT4 and SOX2. *J. Biol. Chem.* *280*, 24731–24737.
- Roose, J., Huls, G., van Beest, M., Moerer, P., van der Horn, K., Goldschmeding, R., Logtenberg, T., and Clevers, H. (1999). Synergy between tumor suppressor APC and the beta-catenin-Tcf4 target Tcf1. *Science* *285*, 1923–1926.
- Roux, K.J., Kim, D.I., Raida, M., and Burke, B. (2012). A promiscuous biotin ligase fusion protein identifies proximal and interacting proteins in mammalian cells. *J. Cell Biol.* *196*, 801–810.
- Saj, A., Chatterjee, S.S., Zhu, B., Cukuroglu, E., Gocha, T., Zhang, X., Göke, J., and Dasgupta, R. (2017). Disrupting Interactions Between β -Catenin and Activating TCFs Reconstitutes Ground State Pluripotency in Mouse Embryonic Stem Cells. *Stem Cells*.
- Salomonis, N., Schlieve, C.R., Pereira, L., Wahlquist, C., Colas, A., Zambon, A.C., Vranizan, K., Spindler, M.J., Pico, A.R., Cline, M.S., *et al.* (2010). Alternative splicing regulates mouse embryonic stem cell pluripotency and differentiation. *Proc Natl Acad Sci U S A* *107*, 10514–10519.
- Sato, A., Kishida, S., Tanaka, T., Kikuchi, A., Kodama, T., Asashima, M., and Nishinakamura, R. (2004a). *Sall1*, a causative gene for Townes-Brocks syndrome, enhances the canonical Wnt signaling by localizing to heterochromatin. *Biochem. Biophys. Res. Commun.* *319*, 103–113.
- Sato, N., Meijer, L., Skaltsounis, L., Greengard, P., and Brivanlou, A.H. (2004b). Maintenance of pluripotency in human and mouse embryonic stem cells through activation of Wnt signaling by a pharmacological GSK-3-specific inhibitor. *Nat. Med.* *10*, 55–63.
- Schaniel, C., Ang, Y.S., Ratnakumar, K., Cormier, C., James, T., Bernstein, E., Lemischka, I.R., and Paddison, P.J. (2009). *Smarcc1/Baf155* couples self-renewal gene repression with changes in chromatin structure in mouse embryonic stem cells. *Stem Cells* *27*, 2979–2991.
- Schmitt, A.D., Hu, M., and Ren, B. (2016). Genome-wide mapping and analysis of chromosome architecture. *Nat. Rev. Mol. Cell Biol.* *17*, 743–755.
- Schuijers, J., Junker, J.P., Mokry, M., Hatzis, P., Koo, B.K., Sasselli, V., Van Der Flier, L.G., Cuppen, E., Van Oudenaarden, A., and Clevers, H. (2015). *Ascl2* acts as an R-spondin/wnt-

- responsive switch to control stemness in intestinal crypts. *Cell Stem Cell* *16*, 158–170.
- Shy, B.R., Wu, C.I., Khramtsova, G.F., Zhang, J.Y., Olopade, O.I., Goss, K.H., and Merrill, B.J. (2013). Regulation of Tcf711 DNA Binding and Protein Stability as Principal Mechanisms of Wnt/ β -Catenin Signaling. *Cell Rep.* *4*, 1–9.
- Sierra, J., Yoshida, T., Joazeiro, C. a, and Jones, K. a (2006). The APC tumor suppressor counteracts beta-catenin activation and H 3 K 4 methylation at Wnt target genes. *Genes Dev.* *20*, 586.
- Sierra, R.A., Hoverter, N.P., Ramirez, R.N., Vuong, L.M., Mortazavi, A., Merrill, B.J., Waterman, M.L., and Donovan, P.J. (2018). *TCF7L1* suppresses primitive streak gene expression to support human embryonic stem cell pluripotency. *Development* dev.161075.
- Silva, J., Nichols, J., Theunissen, T.W., Guo, G., van Oosten, A.L., Barrandon, O., Wray, J., Yamanaka, S., Chambers, I., and Smith, A. (2009). Nanog is the gateway to the pluripotent ground state. *Cell* *138*, 722–737.
- Sinner, D., Rankin, S., Lee, M., and Zorn, A.M. (2004). Sox17 and beta-catenin cooperate to regulate the transcription of endodermal genes. *Development* *131*, 3069–3080.
- Slyper, M., Shahar, A., Bar-Ziv, A., Granit, R.Z., Hamburger, T., Maly, B., Peretz, T., and Ben-Porath, I. (2012). Control of breast cancer growth and initiation by the stem cell-associated transcription factor TCF3. *Cancer Res.* *72*, 5613–5624.
- Smith, A.G., Heath, J.K., Donaldson, D.D., Wong, G.G., Moreau, J., Stahl, M., and Rogers, D. (1988). Inhibition of pluripotential embryonic stem cell differentiation by purified polypeptides. *Nature* *336*, 688–690.
- Solberg, N., MacHon, O., and Krauss, S. (2012). Characterization and functional analysis of the 5'-flanking promoter region of the mouse Tcf3 gene. *Mol. Cell. Biochem.* *360*, 289–299.
- Stavridis, M.P., Lunn, J.S., Collins, B.J., and Storey, K.G. (2007). A discrete period of FGF-induced Erk1/2 signalling is required for vertebrate neural specification. *Development* *134*, 2889–2894.
- Sumi, T., Oki, S., Kitajima, K., and Meno, C. (2013). Epiblast Ground State Is Controlled by Canonical Wnt/ β -Catenin Signaling in the Postimplantation Mouse Embryo and Epiblast Stem Cells. *PLoS One* *8*.

- Takada, S., Stark, K.L., Shea, M.J., Vassileva, G., McMahon, J.A., and McMahon, A.P. (1994). Wnt-3a regulates somite and tailbud formation in the mouse embryo. *Genes Dev.* 8, 174–189.
- Takashima, Y., Guo, G., Loos, R., Nichols, J., Ficz, G., Krueger, F., Oxley, D., Santos, F., Clarke, J., Mansfield, W., *et al.* (2015). Erratum: Resetting Transcription Factor Control Circuitry toward Ground-State Pluripotency in Human (*Cell* (2014) 158 (1254-1269)). *Cell* 162, 452–453.
- Takemaru, K.-I., and Moon, R.T. (2000). The Transcriptional Coactivator Cbp Interacts with β -Catenin to Activate Gene Expression. *J. Cell Biol.* 149, 249–254.
- Tam, W.-L., Lim, C.Y., Han, J., Zhang, J., Ang, Y.-S., Ng, H.-H., Yang, H., and Lim, B. (2008). Tcf3 Regulates Embryonic Stem Cell Pluripotency and Self-Renewal by the Transcriptional Control of Multiple Lineage Pathways. *Stem Cells Day. Ohio* 26, 2019–2031.
- Tesar, P.J., Chenoweth, J.G., Brook, F. a, Davies, T.J., Evans, E.P., Mack, D.L., Gardner, R.L., and McKay, R.D. (2007). New cell lines from mouse epiblast share defining features with human embryonic stem cells. *Nature* 448, 196–199.
- Theunissen, T.W., Powell, B.E., Wang, H., Mitalipova, M., Faddah, D.A., Reddy, J., Fan, Z.P., Maetzel, D., Ganz, K., Shi, L., *et al.* (2014). Systematic identification of culture conditions for induction and maintenance of naive human pluripotency. *Cell Stem Cell* 15, 471–487.
- Thomson, J.A., Itskovitz-Eldor, J., Shapiro, S.S., Waknitz, M.A., Swiergiel, J.J., Marshall, V.S., and Jones, J.M. (1998). Embryonic stem cell lines derived from human blastocysts. *Science* 282, 1145–1147.
- Thomson, M., Liu, S.J., Zou, L.N., Smith, Z., Meissner, A., and Ramanathan, S. (2011). Pluripotency factors in embryonic stem cells regulate differentiation into germ layers. *Cell* 145, 875–889.
- van Tienen, L.M., Mieszczanek, J., Fiedler, M., Rutherford, T.J., and Bienz, M. (2017). Constitutive scaffolding of multiple Wnt enhanceosome components by legless/BCL9. *Elife* 6, 1–23.
- Torres-Padilla, M.-E., and Chambers, I. (2014). Transcription factor heterogeneity in pluripotent stem cells: a stochastic advantage. *Development* 141, 2173–2181.
- Travis, A., Amsterdam, A., Belanger, C., and Grosschedl, R. (1991). LEF-1, a gene encoding a lymphoid-specific with protein, an HMG domain, regulates T-cell receptor α enhancer function.

Genes Dev. 5, 880–894.

Trott, J., and Arias, A.M. (2013). Single cell lineage analysis of mouse embryonic stem cells at the exit from pluripotency TL - 2. *Biol. Open* 2 *VN-re*, 1049–1056.

Tsakiridis, A., Huang, Y., Blin, G., Skylaki, S., Wymeersch, F., Osorno, R.R., Economou, C., Karagianni, E., Zhao, S., Lowell, S., *et al.* (2014). Distinct Wnt-driven primitive streak-like populations reflect in vivo lineage precursors. *Development* 141, 1209–1221.

Tsedensodnom, O., Koga, H., Rosenberg, S.A., Nambotin, S.B., Carroll, J.J., Wands, J.R., and Kim, M. (2011). Identification of T-cell factor-4 isoforms that contribute to the malignant phenotype of hepatocellular carcinoma cells. *Exp. Cell Res.* 317, 920–931.

Vacik, T., Stubbs, J.L., and Lemke, G. (2011). A novel mechanism for the transcriptional regulation of Wnt signaling in development. *Genes Dev.* 25, 1783–1795.

Valenta, T., Gay, M., Steiner, S., Draganova, K., Zemke, M., Hoffmans, R., Cinelli, P., Aguet, M., Sommer, L., and Basler, K. (2011). Probing transcription-specific outputs of β -catenin in vivo. *Genes Dev.* 25, 2631–2643.

Vallier, L., Alexander, M., and Pedersen, R. a (2005). Activin/Nodal and FGF pathways cooperate to maintain pluripotency of human embryonic stem cells. *J. Cell Sci.* 118, 4495–4509.

Verbeek, S., Izon, D., Hofhuis, F., Robanus-Maandag, E., te Riele, H., van de Wetering, M., Oosterwegel, M., Wilson, A., MacDonald, H.R., and Clevers, H. (1995). An HMG-box-containing T-cell factor required for thymocyte differentiation. *Nature* 374, 70–74.

Vietri Rudan, M., Barrington, C., Henderson, S., Ernst, C., Odom, D.T., Tanay, A., and Hadjur, S. (2015). Comparative Hi-C Reveals that CTCF Underlies Evolution of Chromosomal Domain Architecture. *Cell Rep.* 10, 1297–1309.

Wagner, R.T., Xu, X., Yi, F., Merrill, B.J., and Cooney, A.J. (2010). Canonical Wnt/ β -catenin regulation of liver receptor homolog-1 mediates pluripotency gene expression. *Stem Cells* 28, 1794–1804.

Wallmen, B., Schrempp, M., and Hecht, A. (2012). Intrinsic properties of Tcf1 and Tcf4 splice variants determine cell-type-specific Wnt/ β -catenin target gene expression. *Nucleic Acids Res.* 40, 9455–9469.

Wang, Q., Zou, Y., Nowotschin, S., Kim, S.Y., Li, Q. V., Soh, C.L., Su, J., Zhang, C., Shu, W.,

- Xi, Q., *et al.* (2017). The p53 Family Coordinates Wnt and Nodal Inputs in Mesendodermal Differentiation of Embryonic Stem Cells. *Cell Stem Cell* *20*, 70–86.
- Ware, C.B., Nelson, A.M., Mecham, B., Hesson, J., Zhou, W., Jonlin, E.C., Jimenez-Caliani, A.J., Deng, X., Cavanaugh, C., Cook, S., *et al.* (2014). Derivation of naive human embryonic stem cells. *Proc. Natl. Acad. Sci. U. S. A.* *111*, 4484–4489.
- Waterman, M., Fischer, W., and Jones, K.A. (1991). A thymus-specific member of the HMG protein family regulates the human T cell receptor C alpha enhancer. *Genes Dev.* *5*, 656–669.
- Weber, B.N., Chi, A.W.-S., Chavez, A., Yashiro-Ohtani, Y., Yang, Q., Shestova, O., and Bhandoola, A. (2011). A critical role for TCF-1 in T-lineage specification and differentiation. *Nature* *476*, 63–68.
- Weise, A., Bruser, K., Elfert, S., Wallmen, B., Wittel, Y., Wohrle, S., and Hecht, A. (2010). Alternative splicing of Tcf7l2 transcripts generates protein variants with differential promoter-binding and transcriptional activation properties at Wnt/beta-catenin targets. *Nucleic Acids Res.* *38*, 1964–1981.
- van de Wetering, M., and Clevers, H. (1992). Sequence-specific interaction of the HMG box proteins TCF-1 and SRY occurs within the minor groove of a Watson-Crick double helix. *EMBO J.* *11*, 3039–3044.
- van de Wetering, M., Oosterwegel, M., Dooijes, D., and Clevers, H. (1991). Identification and cloning of TCF-1, a T lymphocyte-specific transcription factor containing a sequence-specific HMG box. *EMBO J.* *10*, 123–132.
- Van de Wetering, M., Castrop, J., Korinek, V., and Clevers, H. (1996). Extensive alternative splicing and dual promoter usage generate Tcf-1 protein isoforms with differential transcription control properties. *Mol. Cell. Biol.* *16*, 745–752.
- Van de Wetering, M., Cavallo, R., Dooijes, D., Van Beest, M., Van Es, J., Loureiro, J., Ypma, A., Hursh, D., Jones, T., Bejsovec, A., *et al.* (1997). Armadillo coactivates transcription driven by the product of the *Drosophila* segment polarity gene dTCF. *Cell* *88*, 789–799.
- Van De Wetering, M., Oosterwegel, M., Dooijes, D., and Clevers, H. (1991). Identification and cloning of TCF-1, a T lymphocyte-specific transcription factor containing a sequence-specific HMG box. *EMBO J.* *10*, 23–132.

- Willert, J., Epping, M., Pollack, J.R., Brown, P.O., and Nusse, R. (2002). A transcriptional response to Wnt protein in human embryonic carcinoma cells. *BMC Dev. Biol.* 2, 8.
- Willert, K., Brown, J.D., Danenberg, E., Duncan, A.W., Weissman, I.L., Reya, T., Yates 3rd, J.R., and Nusse, R. (2003). Wnt proteins are lipid-modified and can act as stem cell growth factors. *Nature* 423, 448–452.
- Wöhrle, S., Wallmen, B., and Hecht, A. (2007). Differential control of Wnt target genes involves epigenetic mechanisms and selective promoter occupancy by T-cell factors. *Mol. Cell. Biol.* 27, 8164–8177.
- Wood, S.A., Allen, N.D., Rossant, J., Auerbach, A., and Nagy, A. (1993). Non-injection methods for the production of embryonic stem cell-embryo chimaeras. *Nature* 365, 87–89.
- Wray, J., Kalkan, T., and Smith, A.G. (2010). The ground state of pluripotency. *Biochem Soc Trans* 38, 1027–1032.
- Wray, J., Kalkan, T., Gomez-Lopez, S., Eckardt, D., Cook, A., Kemler, R., and Smith, A. (2011). Inhibition of glycogen synthase kinase-3 alleviates Tcf3 repression of the pluripotency network and increases embryonic stem cell resistance to differentiation. *Nat. Cell Biol.*
- Wu, C.-I., Hoffman, J. a, Shy, B.R., Ford, E.M., Fuchs, E., Nguyen, H., and Merrill, B.J. (2012). Function of Wnt/ β -catenin in counteracting Tcf3 repression through the Tcf3- β -catenin interaction. *Development* 139, 2118–2129.
- Wu, H., D'Alessio, A.C., Ito, S., Xia, K., Wang, Z., Cui, K., Zhao, K., Eve Sun, Y., and Zhang, Y. (2011). Dual functions of Tet1 in transcriptional regulation in mouse embryonic stem cells. *Nature* 473, 389–394.
- Wu, J., Okamura, D., Li, M., Suzuki, K., Luo, C., Ma, L., He, Y., Li, Z., Benner, C., Tamura, I., *et al.* (2015). An alternative pluripotent state confers interspecies chimaeric competency. *Nature* 521, 316–321.
- Xiao, F., Liao, B., Hu, J., Li, S., Zhao, H., Sun, M., Gu, J., and Jin, Y. (2017). JMJD1C Ensures Mouse Embryonic Stem Cell Self-Renewal and Somatic Cell Reprogramming through Controlling MicroRNA Expression. *Stem Cell Reports* 9, 927–942.
- Xing, S., Li, F., Zeng, Z., Zhao, Y., Yu, S., Shan, Q., Li, Y., Phillips, F.C., Maina, P.K., Qi, H.H., *et al.* (2016). Tcf1 and Lef1 transcription factors establish CD8(+) T cell identity through intrinsic

HDAC activity. *Nat. Immunol.* *17*, 695–703.

Xu, C., Rosler, E., Jiang, J., Lebkowski, J.S., Gold, J.D., O’Sullivan, C., Delavan-Boorsma, K., Mok, M., Bronstein, A., and Carpenter, M.K. (2005a). Basic Fibroblast Growth Factor Supports Undifferentiated Human Embryonic Stem Cell Growth Without Conditioned Medium. *Stem Cells* *23*, 315–323.

Xu, R.-H., Peck, R.M., Li, D.S., Feng, X., Ludwig, T., and Thomson, J. a (2005b). Basic FGF and suppression of BMP signaling sustain undifferentiated proliferation of human ES cells. *Nat. Methods* *2*, 185–190.

Xu, R.H., Sampsel-Barron, T.L., Gu, F., Root, S., Peck, R.M., Pan, G., Yu, J., Antosiewicz-Bourget, J., Tian, S., Stewart, R., *et al.* (2008). NANOG Is a Direct Target of TGF β /Activin-Mediated SMAD Signaling in Human ESCs. *Cell Stem Cell* *3*, 196–206.

Xu, Z., Robitaille, A.M., Berndt, J.D., Davidson, K.C., Fischer, K.A., Mathieu, J., Potter, J.C., Ruohola-Baker, H., and Moon, R.T. (2016). Wnt/ β -catenin signaling promotes self-renewal and inhibits the primed state transition in naïve human embryonic stem cells. *Proc. Natl. Acad. Sci. U. S. A.* 201613849.

Yamaguchi, T.P., Takada, S., Yoshikawa, Y., Wu, N., and McMahon, A.P. (1999). T (Brachyury) is a direct target of Wnt3a during paraxial mesoderm specification. *Genes Dev.* *13*, 3185–3190.

Yan, D., Wiesmann, M., Rohan, M., Chan, V., Jefferson, A.B., Guo, L., Sakamoto, D., Caothien, R.H., Fuller, J.H., Reinhard, C., *et al.* (2001). Elevated expression of axin2 and hnk2 mRNA provides evidence that Wnt/beta -catenin signaling is activated in human colon tumors. *Proc. Natl. Acad. Sci. U. S. A.* *98*, 14973–14978.

Ye, S., Zhang, T., Tong, C., Zhou, X., He, K., Ban, Q., Liu, D., and Ying, Q.-L. (2017). Depletion of Tcf3 and Lef1 maintains mouse embryonic stem cell self-renewal. *Biol. Open* *1*, 511–517.

Yeo, J.C., Jiang, J., Tan, Z.Y., Yim, G.R., Ng, J.H., Göke, J., Kraus, P., Liang, H., Gonzales, K.A.U., Chong, H.C., *et al.* (2014). Klf2 is an essential factor that sustains ground state pluripotency. *Cell Stem Cell* *14*, 864–872.

Yi, F., Pereira, L., and Merrill, B.J. (2008). Tcf3 Functions as a Steady-State Limiter of Transcriptional Programs of Mouse Embryonic Stem Cell Self-Renewal. *Stem Cells* *26*, 1951–1960.

- Yi, F., Pereira, L., Hoffman, J.A., Shy, B.R., Yuen, C.M., Liu, D.R., and Merrill, B.J. (2011). Opposing effects of Tcf3 and Tcf1 control Wnt stimulation of embryonic stem cell self-renewal. *Nat. Cell Biol.* *13*, 762–770.
- Ying, Q.-L., Wray, J., Nichols, J., Battle-Morera, L., Doble, B., Woodgett, J., Cohen, P., and Smith, A. (2008). The ground state of embryonic stem cell self-renewal. *Nature* *453*, 519–523.
- Ying, Q.L., Nichols, J., Chambers, I., and Smith, A. (2003). BMP induction of Id proteins suppresses differentiation and sustains embryonic stem cell self-renewal in collaboration with STAT3. *Cell* *115*, 281–292.
- Yochum, G.S., Sherrick, C.M., Macpartlin, M., and Goodman, R.H. (2010). A beta-catenin/TCF-coordinated chromatin loop at MYC integrates 5' and 3' Wnt responsive enhancers. *Proc. Natl. Acad. Sci. U. S. A.* *107*, 145–150.
- Yu, S., Zhou, X., Steinke, F.C., Liu, C., Chen, S.C., Zagorodna, O., Jing, X., Yokota, Y., Meyerholz, D.K., Mullighan, C.G., *et al.* (2012). The TCF-1 and LEF-1 Transcription Factors Have Cooperative and Opposing Roles in T Cell Development and Malignancy. *Immunity* *37*, 813–826.
- Zhang, J.Q., Tam, W.L., Tong, G.Q., Wu, Q., Chan, H.Y., Soh, B.S., Lou, Y.F., Yang, J.C., Ma, Y.P., Chai, L., *et al.* (2006). Sall4 modulates embryonic stem cell pluripotency and early embryonic development by the transcriptional regulation of Pou5f1. *Nat. Cell Biol.* *8*, 1114-U125.
- Zhao, C., Deng, Y., Liu, L., Yu, K., Zhang, L., Wang, H., He, X., Wang, J., Lu, C., Wu, L.N., *et al.* (2016). Dual regulatory switch through interactions of Tcf712/Tcf4 with stage-specific partners propels oligodendroglial maturation. *Nat. Commun.* *7*, 10883.
- Zhao, S., Nichols, J., Smith, A.G., and Li, M. (2004). SoxB transcription factors specify neuroectodermal lineage choice in ES cells. *Mol. Cell. Neurosci.* *27*, 332–342.
- Zuin, J., Dixon, J.R., van der Reijden, M.I.J.A., Ye, Z., Kolovos, P., Brouwer, R.W.W., van de Corput, M.P.C., van de Werken, H.J.G., Knoch, T.A., van IJcken, W.F.J., *et al.* (2014). Cohesin and CTCF differentially affect chromatin architecture and gene expression in human cells. *Proc. Natl. Acad. Sci.* *111*, 996–1001.

APPENDICES

Appendix I: BioID performed on endogenous single copy BirA* tagged TCF7

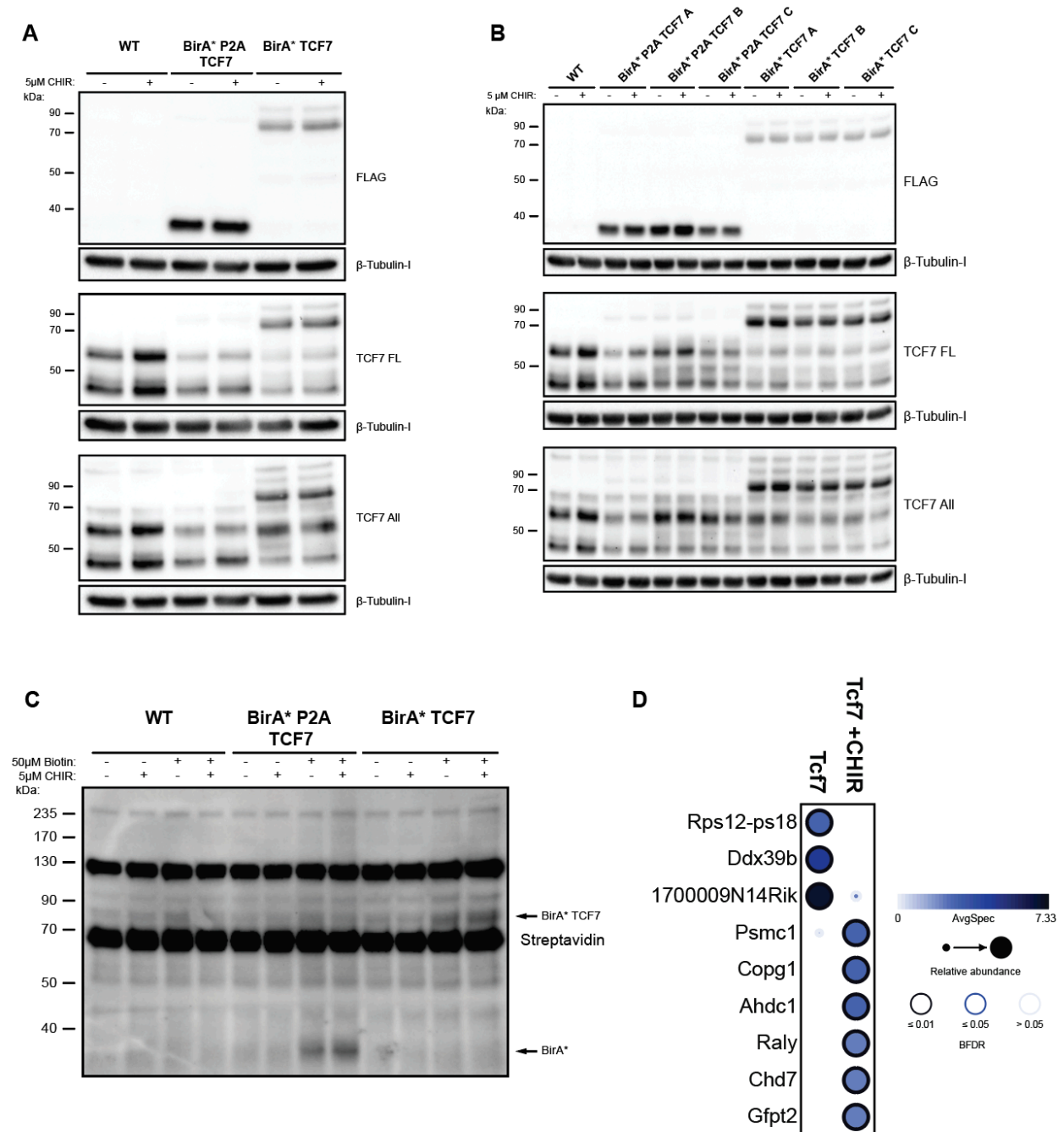


Figure 1. BioID performed on endogenous single copy BirA* tagged TCF7.

(A) Western blots assessing lysates from a single clone of BirA*-P2A-TCF7, BirA*-TCF7 and WT cells maintained in 15% serum for 48h and then treated with $\pm 5\mu\text{M}$ CHIR, for 24h. Lysates were probed with antibodies against FLAG, TCF7 FL, TCF7 ALL and β -Tubulin-I, as indicated. (B) Western blot analysis of WT, BirA*-P2A-TCF7 and BirA*-TCF7 independent clones maintained in 15% serum for 48h, followed by supplementation with $\pm 5\mu\text{M}$ CHIR, for 24h. Lysates were probed with antibodies against FLAG, TCF7 FL, TCF7 All and β -Tubulin-I, as indicated. (C) Western blot analysis of biotinylated proteins in a single clone of BirA*-P2A-TCF7, BirA*-TCF7 and WT cells maintained in 15% serum for 48h, followed by supplementation with $5\mu\text{M}$ CHIR or $50\mu\text{M}$ biotin, for 24h. Lysates were probed with streptavidin-HRP. Arrows point to 3xFLAG-BirA* fusion proteins. (D) Dot plot of TCF7-proximal proteins identified by performing BioID in 15% serum cultures for 48h and then treated with $50\mu\text{M}$ biotin and $5\mu\text{M}$ CHIR for 24h. Biotinylated proteins identified demonstrated a BFDR ≤ 0.05 and a SAINT score > 0.8 in at least one of the 2 conditions. Spectral counts were capped at 50. *Notably few TCF7 peptides were identified.*

Appendix II: Generation of endogenous single copy fluorescent protein tagged TCF7L1 and TCF7

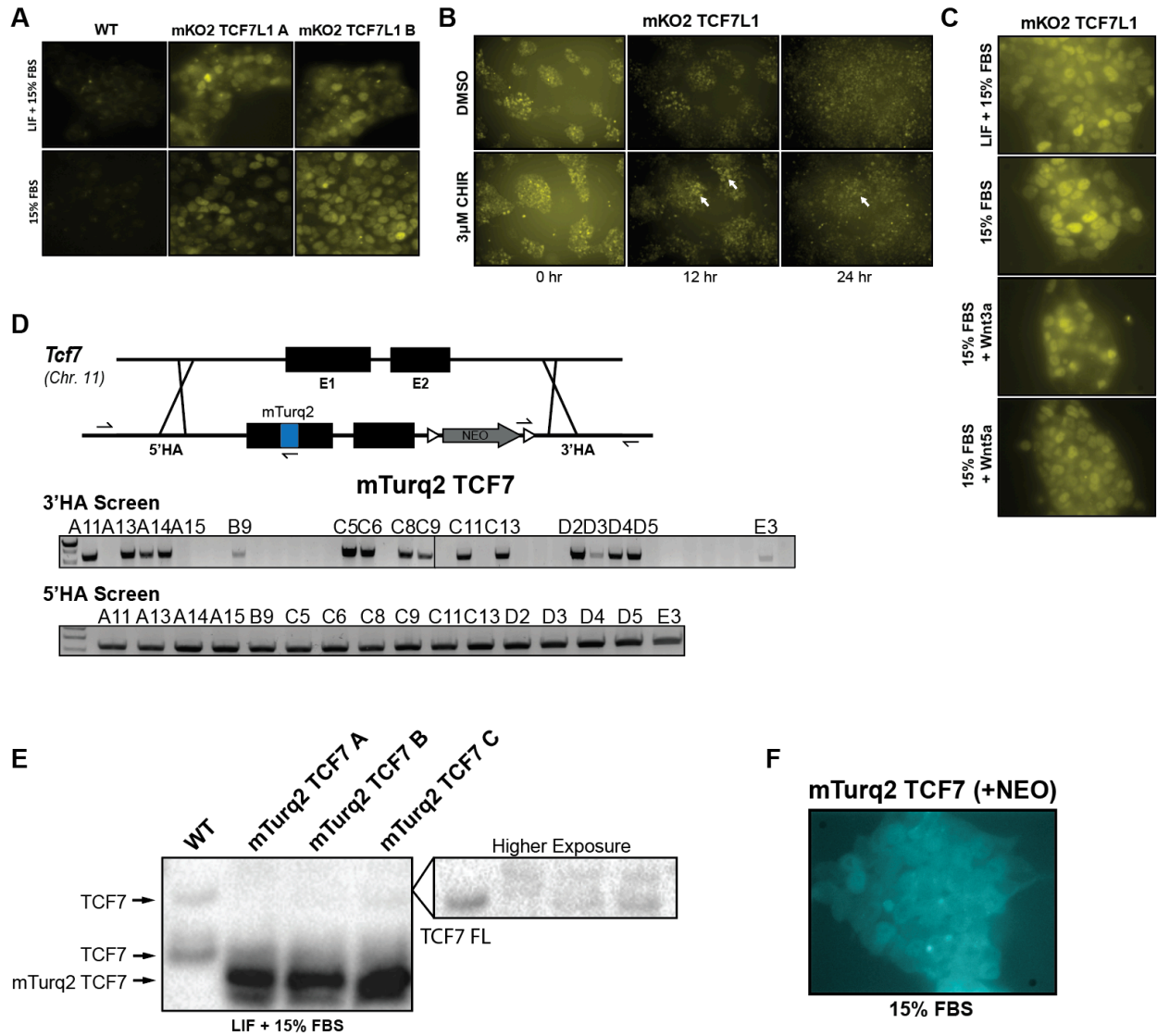


Figure 2. Generation of endogenous single copy fluorescent protein tagged TCF7L1 and TCF7.

(A) Fluorescence imaging of mKO2 in WT and mKO2-TCF7L1 mESCs cultured in maintained in serum \pm LIF for 48h. (B) Live cell imaging of mKO2-TCF7L1 mESCs maintained in serum + LIF, supplemented \pm 3 μ M CHIR for 24h. Images were acquired at the indicated timepoints. White arrows represent pockets of cells with sustained elevated TCF7L1 levels. (C) Fluorescence imaging of mKO2 in WT and mKO2-TCF7L1 mESCs cultured in serum + LIF and serum alone \pm Wnt3a or Wnt5a for 24h. (D) TOP: Schematic representation of the TALEN strategy used to introduce an N-terminal mTurquoise2 fluorescent-tag at endogenous TCF7 in mESCs. BOT: PCR based homology arm screens on putative mTurq2-TCF7 clones using primers binding just outside the homology arms and within mTurquoise2 or the NEO cassette, as indicated in the schematic. (E) Western blots assessing lysates from independent clones of mTurq2-TCF7 and WT cells maintained in serum + LIF for 48h. Lysates were probed with antibodies against TCF7 FL. ***Note the majority of mTurq2-TCF7 is not the correct molecular weight due to the presence of the NEO cassette (known to affect splicing in our system before excision), which has not yet been excised.*** (F) Fluorescence imaging of mTurq2 in WT and mTurq2-TCF7 before NEO excision mESCs cultured in maintained in serum alone for 48h.